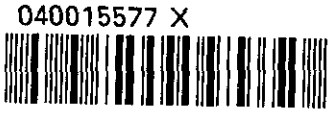

MODELLING OF SERVO-CONTROLLED PNEUMATIC DRIVES - A GENERALISED APPROACH TO PNEUMATIC MODELLING AND APPLICATIONS IN SERVO-DRIVE DESIGN

BY

Pud Tai John MO

A Doctoral Thesis
Submitted in partial fulfilment of the
requirements for the award of
Doctor of Philosophy
of the
Loughborough University of Technology

February 1989

DECLARATION

No part of the work described in this Thesis has been submitted in support of an application for any other degree or qualification of this or any other University or Institution of learning.

CONTENTS

LIST OF FIGURES

LIST OF TABLES

ACKNOWLEDGEMENT

The author wishes to thank:

Professor R.H. Weston, Project Supervisor, for his guidance and advice to carry out the research and the preparation of this thesis, and his patience to provide continuous support during the research.

Professor R.J. Sury, Research Director, for his kind arrangement, advice and support throughout the project.

Professor A.P. Jeary, Local Supervisor, for his guidance and arrangement of equipment support to carry out the research, and his invaluable comments on the preparation of papers and this thesis.

Dr. P.R. Moore for his support and supplying valuable information to the research.

Dr. P.G. Leaney for his kind advice on the philosophy and methodology of the modelling work.

Mr. D. Walters, Mr. G. Charles and Mr. N. Carpenter for their help for starting the research in Loughborough.

Martonair (UK) Ltd. for their allowing to use the proportional valve.

SUMMARY

The primary objective of this research is to develop a general modelling facility for modular pneumatic servo-drives. The component oriented approach has been adopted as the modelling technique to provide the flexibility of modelling a wide variety of components and the segmentation of the non-linear system to less complex uncoupled component modules.

A significant part of the research work has been devoted to identify a series of component modules of the single axis linear pneumatic servomechanism with standardised linking variables. The mathematical models have been implemented in a simulation software which produces time domain responses for design evaluation purposes. Alternative components for different servomechanism design were modelled as mutually exclusive modules which could be selected for assembly as if they were real physical entities. The philosophy of the approach was validated by tests on prototype servo-drives with matching components. Design analysis could be performed by simulating and comparing the performance of alternative system structures.

The research also contributes to the knowledge in the analysis of the pneumatic system by:

(a) Extension of the one-dimensional adiabatic flow to include the dynamic upstream flow head;

(b) Establishment of the flow node model for the valve component;

(c) Study of the phenomenon of pressure drop in pipe and its influence to the pneumatic system.

It is anticipated that by slight modification of the user interface and improvement in the implementation of the mathematical algorithm, the simulation software can be used as a computer-aided-configuration tool for pneumatic servomechanism design.

NOTATION

A	Area of air flow path (with or without subscript), m^2
A_{vp}	Cross-sectional flow path area of valve land, m^2
A_{v1}	Area of valve opened due to positive spool displacement, m^2
A_{v2}	Area of valve opened due to negative spool displacement, m^2
A_p	Cross-sectional flow path area of at valve ports, m^2
A_{pc}	Cross-sectional area of tubing restriction, m^2
A_{R2}	Cross-sectional area of piston rod, m^2
C_v	Specific heat capacity of air at constant volume
C_p	Specific heat capacity of air at constant pressure
C_{Fin}	Dimensionless flow induced force for in valve flow
C_{Fout}	Dimensionless flow induced force for out valve flow
C_d	Coefficient of discharge
C_{ds}	Coefficient of discharge from source
C_{de}	Coefficient of discharge from exhaust
D	Diameter of tubing, m^2
D_s	Diameter of valve sleeve, mm
D_{sp}	Diameter of spool rod, mm
E_1	Flow energy function to cylinder chamber 1, J s^{-1}
E_2	Flow energy function to cylinder chamber 2, J s^{-1}
f	Friction factor of tubing
F	Cross-sectional area of leakage gap, m^2

F_g	Gravitational force if the drive is placed upright, N
F_i	Initial compression of spool spring, N
F_{ind}	Flow induced force on spool, N
F_r	Static or coulomb friction on load, N
F_{sf}	Friction on spool, N
F_s	Static friction on load system, N
F_c	Coulomb friction on load system, N
F_{se}	End load in valve on spool, N
G_s	Solenoid magnetic constant, N/mm
h	Clearance of leakage passage between cylinder chambers, m
i_{prof}	Element number of the gain profile array K_p
K_{sp}	Spool spring constant, N/mm
K_s, K_d	Coefficients of spool dynamics
K_L	Leakage coefficient across cylinder chambers 1 and 2
K_c	Coefficient of viscous friction
K_e	End stop stiffness, N m^{-1}
K_p	Position gain profile (array)
K_v	Gain on velocity value
K_a	Gain on acceleration value
K_{dr}	Coefficient of pressure drop regression line
l	Length of valve land along spool axis, m
L	Length of actuator, m
L^*	Critical frictional length through pipe flow, m
L_1	Frictional length through pipe flow from point 1, m
L_2	Frictional length through pipe flow from point 2, m
L_e	End stop force on load system, N

L_{prof}	Span of application of each K_p profile point
L_{DAC}	Sizing factor on the test rig software for DAC output
L_{nh}	Dimensionless resistance coefficient independent of compressible fluid properties
m	Mass of air (with or without subscript), kg
$\dot{m}$	Mass flow rate (with or without subscripts), kg s^{-1}
$\dot{m}_L$	Leakage mass flow rate, kg s^{-1}
M	Mach number (with or without subscripts)
M_s	Mass of spool, kg
M_p	Mass of moving parts, kg
n	Adiabatic gas flow constant, 1.4
n_p	Quantised position error
n_v	Quantised velocity value determined by the vary mode position difference scheme
n_a	Quantised acceleration value determined by the vary mode velocity difference scheme
n_{DAC1}	Raw DAC value calculated from gain algorithm
n_{DAC2}	Adjusted DAC value due to valve operator characteristics
n_{STPVAL}	Desired spool location for stepper motor valve operator
n_{SPLCOM}	Spool command output value
n_{SPLLOC}	Spool location record on controller
n_{pg}	Position gain value determined by the spool command processor
n_{vg}	Velocity gain value determined by the spool command processor

n_{ag}	Acceleration gain value determined by the spool command processor
n_{xmax}	Maximum one side stepper motor valve operator steps
N_{pmax}	Maximum quantised position error beyond which the position gain is saturated
P	Air pressure (with or without subscript), N m^{-2}
P_{drop}	Pressure drop ratio through tubing, N m^{-2}
P_o	Pressure at source for leakage, Nm^{-2}
r_L	Pressure ratio for leakage formula
R_{ch}	Channel resistance coefficient for leakage
R	Universal gas constant, 286.76 J-kg/s
s	Length of leakage passage (across piston), m
T	Air temperature (with or without subscript), K
T_v	Valve land temperature, K
T_o	Temperature at source for leakage, K
u	Velocity of air (with or without subscript), m s^{-1}
u_v	Velocity of air in valve land, m s^{-1}
V	Volume in cylinder chamber (with or without subscript), m^3
V_{R1}	Residual volume in cylinder chamber 1, m^3
V_{R2}	Residual volume in cylinder chamber 2, m^3
X_c	Commanded location of spool, mm
X_{max}	Maximum one side spool displacement, mm
X_s	Current location of spool, mm
y_e	Penetration of ram to cylinder end, m
y	Position of ram, m
δ	Density of air, kg m^{-3}

σ	Dimensionless mass flow rate
Γ	One dimensional adiabatic flow function with dynamic upstream condition
Ω	Flow node temperature function
H	Enthalpy, J
Q	Heat, J
U	Internal energy, J
W	Work, J
$\dot{m}_{ref}$	Mass flow rate for pressure drop at value K_{dr}, kg s^{-1}

SUBSCRIPTS

1	Cylinder chamber 1
2	Cylinder chamber 2
s1	Between supply and cylinder chamber 1
s2	Between supply and cylinder chamber 2
e1	Between exhaust and cylinder chamber 1
e2	Between exhaust and cylinder chamber 2
n1	Flow node 1
n2	Flow node 2
sv	Valve port to supply
1v	Valve port to cylinder chamber 1
2v	Valve port to cylinder chamber 2

GLOSSARY OF TERMS

"Dynamic upstream flow head" means the flow pressure due to velocity in the air stream ahead of the path restrictions such as valve openings or ports. The unit is in Nm^{-2} and represented by

$$\frac{1}{2} \text{ X (density) X (flow velocity)}^2$$

The word "head" in the report is taken as synonymous with pressure.

CHAPTER 1

INTRODUCTION

The aim of the research work is to establish a general mathematical model for a series of modular linear pneumatic servomechanisms and to implement the model in a simulation software for design analysis. The modelling work has to take into account the need to cope with a wide variety of components and the flexibility necessary to cater for new designs in future.

The design of the modelling method and the choice of research tools involves a number of related activities including electronic, mechanical, computer system and pneumatic functions. It requires an understanding of the thermodynamics of compressible flow, the use of microprocessor and interfacing techniques, the mathematical evaluation process, computer systems and graphics. Wherever possible, the models are validated by experimental tests under comparable test conditions.

This thesis has been arranged in ten chapters:

(a) Chapter 1 introduces to the reader the background of the research, the objectives expected to be achieved and possible extensions which can be projected at the planning stage of the project. Reference to previous work in Loughborough University of Technology is made to provide a concise picture

of the project.

(b) Chapter 2 reviews the current trend of flexible automation and the role of the modelling of pneumatic servomechanisms in such flexible systems.

(c) Chapter 3 deals with the methodologies and tools for the analysis. The various techniques for modelling have been compared and the philosophy of the component oriented approach adopted in this research is discussed. The computational tool for simulation and model validation is outlined.

(d) A generic model in block diagram format is established with the component oriented approach in Chapter 4. The model development starts from the synthesis of the simple open loop bang-bang pneumatic system and finally arrives at the model of servo-controlled pneumatic drives.

(e) The generic model is validated by specific hardware described in Chapter 5. The characteristics of the hardware components are subsequently modelled in Chapter 6. The generality and flexibility of the modelling approach is then demonstrated by the construction of three pneumatic servo-drives which are assembled from a change of basic pneumatic components and simulated by the corresponding change of the component modules of the system model.

(f) Chapter 7 outlines the tests for ascertaining the values and accuracy of the model parameters. Supplementary tests performed for validation purposes are discussed. Using the results of parameter tests the total system responses of the test rigs are compared with the simulated responses.

(g) Chapter 8 highlights typical application examples by adopting

the generalised modelling technique. The capability of the software as a configuration aid is readily seen from the flexibility of the philosophy of the method.

(g) Chapter 9 recommends for possible future research topics and Chapter 10 concludes the thesis.

1.1 Background of research

The application of microprocessors to the control of pneumatic devices in Loughborough University of Technology (LUT) started at the beginning of 1980's when the Department of Engineering Production (now renamed as Manufacturing Engineering) was engaged with a famous pneumatic components supplier in the United Kingdom, Martonair Limited, in an SERC sponsored project. The project was aimed at developing a series of modular pneumatic linear axes [1.1] which were programmable for point-to-point movement in the same manner as the numerically controlled electrical servo-drives [1.2]. The linear axes were so designed both mechanically and software-wise [1.3] that they could be assembled in piecemeal fashion. The concept was extended to form a multiple axes flexible work handling system [1.4].

The control strategy developed in the project was successfully implemented on a Texas Instrument 990 processor controller incorporating digital minor loop compensation and variable gain for the position feedback loop [1.5]. Continual improvements were made in the control algorithm and strategy

including the use of front-end control methods [1.6] and dynamic adjustment of valve null point [1.7]. The performance of the pneumatic test devices in these researches was satisfactory.

On the other hand, there was considerable difficulty to examine the transportability of the control software on different species of pneumatic device. Moore [1.8] had attempted to implement the real-time control system on pneumatic linear axes of a different make and mechanical design, but the results were not always encouraging. It was generally felt that since the previous researches were carried out based on the trial and error philosophy, there was a lack of understanding of the behaviour of the pneumatics in the system. Any design of control algorithm to suit a particular piece of hardware was therefore not immediately transferrable to a new hardware platform due to incompatibilities between the two platforms. A vigorous study to derive a model which describes mathematically the pneumatic phenomenon in the system would improve the understanding of the influences of individual components and help to identify critical factors involved in the physical environment.

1.2 Objectives

The fundamental objective of the project is to investigate the nature of pneumatic systems and to derive a general model of the pneumatic drives commonly used in industrial environment. Through accurate and generalised modelling techniques, it is anticipated that the knowledge can be extended to aid the design

of pneumatic drives: linear, rotary or any physical configuration, without actually building a prototype for evaluation. The behaviour of the newly designed system can be determined based solely on the dimensional data at design stage. Various control algorithms can then be tried on different "software emulated hardware" to check the functionality of the design concepts.

It is obviously impossible to derive a model to describe unlimited combinations of pneumatic components. The analyses in this research are therefore restricted to the modelling of modular pneumatic drives which can be extended to multiple axes constructs by piecemeal fashion.

The objectives of the research are summarised as follows:

(a) To analyse the behaviour of the pneumatic phenomenon in relation to modular pneumatic actuators.

(b) To derive a mathematical model of the pneumatic system with generalised parameters attributable to identifiable and measurable quantities.

(c) To develop a design aid which can provide accurate predicting information of the performance of pneumatic components either in single unit or combination mode. The design aid can function as configuration tool for the design of flexible automation systems.

(d) To discover critical factors and components in the pneumatic servomechanism affecting the performance and transportability of the control software.

The project is expected to be a revolving, on-going exercise to enhance the knowledge in the area of pneumatic servomechanisms which can be used to form the basis of pneumatic numerically controlled machines and robots. The generalised methodology and the generic model in this research can then become a starting point for extensions in the field of flexible automation.

CHAPTER 2

REVIEW OF FLEXIBLE AUTOMATION SYSTEMS

The advancement of computer technology especially in the category of microprocessors and microcontrollers has led to the possibility of implementing automation in a cost effective and flexible way. This chapter reviews the latest technology of computer integrated manufacture and focuses on its implication along the line to the most basic elements at the device level. In particular, the opportunity is taken to review the detailed operation of servo-controlled units and of pneumatic servomechanisms in their complete working range including critical regions such as end stops. The need for a satisfactory method to evaluate new design concepts of pneumatic servo-drives is discussed and the use of computer-aided simulation tool is proposed.

2.1 Overview of computer integrated manufacture

The concept of computer-integrated-manufacturing (CIM) comes as a consequence of developments in computer-aided design [2.1] and factory automation [2.2]. It includes the ability to control all phases of the manufacturing system using computers, from planning through design to shipping [2.3]. It embraces the integration of office automation (OA), computer-aided design and

manufacturing (CAD/CAM), automatic storage and retrieval system (ASRS), distributed data processing, robotics and a wide variety of computers [2.4]. The ultimate aim is to improve manufacturing efficiency, productivity, quality and the ability to cope with rapid marketing demand changes [2.5, 2.6, 2.7].

The key to success in CIM is the systematic approach to integrated systems development. The system engineering method [2.8] has been applied to define the problem and technique for establishing the "architecture" of CIM. The modular approach [2.9], on the other hand, has the advantage of small capital outlay, but brings in the problem of module integration. The need to define clearly the functional blocks in the integrated factory has been recognised [2.10]. All approaches imply the need to communicate between various functional parts of the factory. This demands a mature local area network which can handle information from the factory supervisory level at the top to discrete machine input/output level at the bottom of the hierachy [2.11].

The impact of the design of CIM has been studied in the ESPRIT (European Strategic Program for Research in Information Technology) project [2.12]. It consists of 5 principal topics among which CAM has direct concern with production automation. In essence, CAM is the provision of flexibility in the manufacturing process by computers. The development of flexible manufacturing systems (FMS) nowadays is realised to be an important stepping stone for CIM [2.13]. The following section discusses the recent trend of FMS and the features involved in flexible automation.

2.2 Flexible systems and robots

The major implication of CIM on shop floor machines is the requirement for real time control of manufacturing processes. Two types of flexible machines are available. The more conventional type consists of CNC machines normally designed for materials working and shaping processes. The universal manipulator type, usually known as robot, deals with materials handling and transportation.

2.2.1 Flexible manufacturing systems

Implementation of flexible manufacturing systems (FMS) started in the late 1970's on the conventional mechanical engineering shop-floor. Since then the number of installation kept increasing at a constant rate. It was predicted that the number would double in 1990 [2.14]. The definition of FMS, according to Kief [2.15], is "a group of numerically controlled machine tools linked by a common material handling system and a central control system". The main purpose is to increase productivity and reduce costs by introducing flexibility in the production systems to produce different workpieces simultaneously in an unbroken sequence without interruption [2.16].

Initially, many FMS were developed as national supported projects some of which provided a basis for commercialisation

[2.17, 2.18]. Experience shows that the scale of integration imposed heavy demand on computers and software. A building block approach and a distributed processor system must be adopted [2.19]. Various techniques to aid the design and planning of FMS are eventually available. Rathmill et al [2.20] reviewed the simulation approaches and concluded that it could form a useful second opinion for FMS designer. Ranky [2.21] compiled a FMS software library package using a modular software approach. The technology to fabricate a working FMS is readily available but the complication of integration has still to be investigated to improve the system design efficiency. Likewise, Heinonen et al [2.22] introduced the systems concept which would facilitate the system design in a more systematic way.

2.2.2 Robots and flexible position systems

The Robot Institute of America has defined a robot as "a programmable multi-functional manipulator designed to move materials, parts, tools or specialised devices through variable programmed motions to accomplish a variety of tasks" [2.15]. In general, the anatomy of robot can be categorised as articulated, cylindrical coordinate, radial polar coordinate and cartesian coordinate [2.23].

The most extensive user of robots is the car industry [2.24] in which the main tasks are spot welding and materials handling. Other applications were reported including arc welding [2.25], assembly, spray painting [2.26, 2.27] and keyboard playing [2.28].

In addition to these standalone usage, the versatility offered in the handling of parts by robots has proved to enhance the capability of FMS [2.29]. The need to automate parts handling in a flexible way becomes an essential constituent in modern unmanned manufacturing environments [2.30].

To achieve the objective of flexible manufacturing, provision of an unrestricted flexible positioning environment particularly in assembly type operations, is vital to successful implementation [2.31]. It is not difficult to imagine the large amount of effort required to establish such system and software tools to aid a control system design are available [2.32]. However, these systems are expensive and not readily adaptable to small and medium sized factories [2.33]. Some form of simplication on the user point of view is required such that the flexible automation system is most effective.

2.2.3 Modular units

Control of a robot arm requires the accurate dynamic modelling of the mechanism using a Lagrange-Euler or Newton-Euler formulation on a dedicated mini-computer which inevitably constitutes a high cost product [2.34, 2.35]. Despite the flexibility inherent in the general nature of industrial robots, their mechanical structure and control features are normally over-provided [2.36]. In other words, the total cost would become well above the acceptable capital outlay level of the project. In

fact, Brown reported that problems existed with the general purpose robots and there was a need to custom design robots for small, light, but stiff application [2.37]. These suggest that standardisation of the components in modular form is more beneficial in many cases. Commerical availability of such modules started in early 1980's for hard-wired type automation [2.38, 2.39]. Subsequent developments allowed that the modular units can be strategically located in a distributed fashion to best suit the production environment [2.40]. The advantage offered by modularising the flexible positioning system is justifiable on the basis of cost, simplication and flexibility in configuration.

The implication of modularisation also affects the software control system on individual modules. Surnin et al [2.41] found serious kinematic link problems with an electromechanical modular robot built on 10 basic modules. The computational system for such a modular robot had to take care of the variations in configuration and operating parameters. It was suggested that the complication in control could be tackled by the block oriented approach which was effectively building the control system as modules [2.42]. Extending the concept along the same line, Thatcher et al [2.43] defined the software structure required to effectively operate individual as well as linked modules into 4 task levels. The linking of modules was then possible through the rather slow serial interface under a supervisory control software [2.44]. Research is continuing in the direction of investigating the possibility of achieving contouring control.

The essence of modularisation is the localised control of "single degree of freedom" manipulators. The effect of such decoupled control approach had been studied by Vukobratovic et al [2.45]. In many applications it had been assumed that local control was stable and accurate, and this relied on the good design of the drive system as well as the servo-controller.

2.3 Drive systems

The choice of drive components is a critical decision in the design of industrial robots. While industry is looking for fast, accurate systems for high quality production, manufacturers are also striving for low cost, efficiency and versatility. Basically, mechanical drives suffer from the lack of flexibility to adapt to space limitations. The linkages between the power element and the work-head are often too rigid to be properly located on the machine. Typical examples of mechanical automation systems have been published in various literature [2.46, 2.47].

On the contrary, hydraulic and electric drives are less sensitive to space constraints. Power to drives are passed with flexible wiring or tubing. There is no need to extend linkages in rigid solid form between component locations. The use of hydraulic and electric drive systems was reviewed by Archer et al [2.48] but there was no definite conclusion on which is more desirable for modular unit application.

2.3.1 Hydraulic drives

The theoretical background of using hydraulic drives in servomechanism applications has been studied by Conway [2.49] and Neal [2.50]. Many applications were recorded including the control of the propellant feed system on a space shuttle [2.51].

Hydraulic servo-control relies on the good design of flow control valves. The proper valve configuration has been investigated by Lee [2.52] in conjunction with the study on flow induced forces. The importance of proportional valve to the closed loop servo-controlled hydraulic system is generally recognised [2.53]. The fundamental research work in hydraulic servomechansim has been well recorded. Various aspects of hydraulic drives including load sensitivity [2.54], hydraulic stiffness of spool valve [2.55], pressure transients [2.56] and flow oscillation [2.57] had been studied. Research having direct relation with modern servo-control technique such as model reference adaptive control has been adopted to cater for the inherent non-linearity [2.58].

2.3.2 Electric drives

Although hydraulic systems offer great flexibility in the design and location of drive mechanism, they suffer from other penalties in terms of cost, reliability and power consumption. For high accuracy, fast response and moderate power systems, electric drives have been used as an alternative [2.59].

In small payload cases, small electric servomotors provide a better power to weight ratio [2.60]. Electric drives can be classified into two types: direct current motors and stepping motors [2.61], each of which has its merits in speed, design simplicity or positioning accuracy. With proper amplifier circuits, the electric drives usually possess better linear behaviour. Interfacing and control by microprocessors is also much easier than for hydraulic drives [2.62]. It is due to these favourable characteristics that the design of a zero error contouring system can be done with simple velocity feed forward loop technique [2.63]. These show that electric drives have definite advantages over fluid power systems.

2.4 Pneumatic drives and their controls

Unlike hydraulic systems, the distribution of pneumatic power is simple and less hazardous to the environment. The compressed air can be vented to the atmosphere without any special return path requirements.

Unfortunately, the main drawback for pneumatic system is the relatively small power available due to the low pressure in the line. The compressibility of the fluid makes it difficult to be controlled. The use of pneumatic power is therefore limited to applications less demanding in power, accuracy and rigidity [2.64].

2.4.1 End-stop drives

Pneumatic end-stop drives have been used for many years in the context of low-cost-automation. A typical example is the construction of a "pick and place" device using a purely pneumatic logic controller [2.65]. The major disadvantage of the system is the hardwired nature of the controller and the difficulties in designing the circuit [2.66]. Although it is possible to incorporate flexibility by microprocessor [2.67] or programmable logic controller [2.68], there are circumstances demanding a sophisticated design methodology to deal with the varying sequential nature of the drives [2.69]. In order to automate the circuit design process, individual researchers have developed design programs for the "bang-bang" pneumatic systems [2.70]. However, due to the hardwired limitation and the inflexibility of the drives in positional adjustment, the progress to enhance the usage was not satisfactory.

2.4.2 Servo-drive with on-off valve

Servo-drives undoubtedly provide more flexibility in positional control. An early example of servo-drive in the form of a simple pneumatic position table using an on-off pneumatic circuit was investigated by Cheng et al [2.71]. Positional control was achieved by a slot sensor mounted at the desired location of the table.

By incorporating a microprocessor in the controller, Drazan et al [2.72] designed a pneumatic manipulator arm using on-off logic control circuits. The major problem to construct pneumatic servo-drive with on-off valve is the instability introduced as a result of the compressibility of air. Special arithmetic processing hardware is required to undertake on-line computation of the robot dynamics [2.73]. It was reported that with a low friction piston and a cascaded on-off valve controlled system, accuracy at 0.01 mm level can be achieved [2.74]. Nevertheless, the sophistication needed in such system is a barrier for efficient operation and ease of design.

2.4.3 Servo-drive with proportional valve

Due to the compressibility of air and the non-linearity in the pneumatic system, it is more desirable to have a control element which can produce an output of higher resolution than the 2-state on-off devices. In earlier researches, instead of the proportional valves, flapper valves were commonly used as the proportional component [2.75]. The static and dynamic behaviour of the flapper valves have been studied by Hayashi et al [2.76] in terms of stream function and vorticity. However, it was reported that considerable deviations were found between the static and dynamic characteristics which prevented the flapper valve to be used effectively as a proportional control device [2.77].

The convenience and better linearity obtained in spool type

hydraulic valve controlled systems suggested that pneumatic spool valves could equally be used as the servo-control element. The dynamic behaviour has been investigated by Schwenzer on an analogue servo-controlled system [2.78] and found satisfactory in terms of cost, stability and speed. The practical use of servo-pneumatic components on multi-axle CNC machines and robots was reviewed by Backe [2.79]. Application of the proportionally controlled pneumatic servomechanism was enhanced with microprocessor controller as single axis units [2.80]. A family of such modules were developed by Weston et al [2.81]. It has been shown that with carefully designed supervisory control on top of the single axis modules, a modular robot could be applied for general assembly processes [2.82]. Therefore, the use of pneumatic power in servo-drive with proportional valve has a great potential in the field of flexible automation.

2.4.4 Servo-controllers

The servo-controller is the brain of the servomechanism and has direct influence on its performance. The behaviour of a servo-controller for a pneumatic mechanism was synthesised by Dinerstein [2.83] for controlling the pitch and yaw flaps of a guided missile. A series of describing functions was obtained on frequency response analysis. Reethof [2.84], on the same basis, analysed a high pressure pneumatic servomotor. The design of the servo-controller for a pneumatic system was often complicated by the non-linearity due to compressibility of the medium. Different designs including the choice of working conditions to compensate

for frictions [2.85] and the use of differential pressure feedback were proposed [2.86].

With the advent of microprocessor technology, it has become feasible to implement more complex control algorithms. Based on the concept of the classical three term control algorithm [2.87], control strategy involving position, velocity, acceleration and integral feedback was investigated on a commercial symmetrical cylinder [2.88]. The successful implementation of a compensation scheme on a modular pneumatic servo-drive [2.89] illustrated that microprocessor based servo-controller is most effective in adapting to the non-linearity in pneumatic systems.

2.5 Computer-aided servo-system design

The trend of the requirement for servomechanisms has been heading towards complication in the last decade. Sophisticated control strategies can be programmed into digital controllers with reducing difficulties when the high level languages such as C and Pascal can be used for real-time control programming [2.90]. However, no matter how powerful the controller is, it has to react with external devices which require careful selection, mechanical design and construction.

Analysis tools are available nowadays on digital computers to aid the design of control systems. General purpose analysis algorithm such as time domain simulation, root locus analysis,

frequency responses and so forth are adopted in various packages [2.91, 2.92]. Special modelling packages consisting of module libraries are developed to cater for applications in process controls [2.93]. The need for computer-aided configuration tools to aid in the design of servomechanisms is increasing.

A few analysis packages for hydraulic systems were reported ranging from the more primitive hydraulic transmission simulation programs [2.94] to the highly flexible component oriented CAD facilities [2.95]. Unfortunately, there is no similar computer aided configuration aids for the case of pneumatic servomechanism and this is taken as a primary aim for this research work.

2.6 Summary of servomechanisms and configuration tools

The current situation of computer applications in industry in terms of CIM, FMS, robotics has been reviewed in this chapter. It is clear that due to the increasing demand for product variety, highly flexible, accurate, reliable but low cost servomechanisms are desirable. In view of the control problem of the complex CIM systems, the modular approach has been adopted to provide the capability for easily adapting to a different levels of system configuration. With the latest powerful microprocessor controllers, highly non-linear physical entities like pneumatic components can be controlled by implementing specially designed control algorithms and constructed in compact single axis form.

The increasing sophistication of servo-controller and

associated devices demands the use of computers as a configuration design aid. Modelling and analysis software are available for general applications and hydraulic servo-system design. However, no such configuration design tool is available for pneumatic servomechanisms.

CHAPTER 3

METHODOLOGY OF THE RESEARCH PROJECT

The methodology employed in the analysis of pneumatic servo-drives is outlined in the terms of practical and theoretical facets. The theoretical facet includes a discussion of the modelling techniques commonly used by other researchers and the problems associated with these techniques are highlighted. The component oriented approach is then outlined as a modelling technique which offers great flexibility in software design and ease of validation. Coupled with the component oriented approach, the mathematical and programming tools used in the synthesis of the component and system model are also described.

The model established by the component oriented approach is a generic model applicable to a wide range of pneumatic components and systems. Validation of the generic model requires some degree of materialisation to specific hardware. The practical facet described in this chapter outlines the specification of the project in more precise terms. A choice of hardware for practical investigation and the development of control software are discussed. The test rig then forms the basis for comparison with the theoretical simulated results.

3.1 Modelling techniques for pneumatic systems

The methods of modelling has been classified by Wellstead into 3 categories [3.1]. The methods are established procedures to guide the system analyst to determine mathematical models of different complexity. However, due to the diversity of applications, a purely scientific approach of system identification may not be sufficient [3.2]. Adequacy of the models often relies on the judgement of the engineers and subsequent analysis on the non-linear model would better be carried out with graphical techniques rather than mathematical solving [3.3].

Unlike hydraulic or electric systems, pneumatic systems generally have more non-linear elements the majority of which are due to the compressibility of air and the complication of adiabatic fluid flow. The models derived from the governing laws of thermodynamics preclude the direct use of analytical techniques commonly used in linear system analysis. To circumvent this problem it has become standard practice to replace a detailed non-linear model of the pneumatic system by a linearised version which provides a reasonable description of the system dynamics in the vicinity of an equilibrium condition [3.4]. However, the approach cannot predict global behaviour which in many servo-positioning occasions are as important as the particular solution at specific points within the stroke of the pneumatic mechanism.

The following sections examine the techniques normally employed in the analysis of servomechanisms. The assumptions made in the course of model simplification for analytical solution are highlighted such that the problem of global accuracy of the models is revealed.

3.1.1 Empirical curve fitting

The easiest method to obtain a mathematical description of a system is probably by approximating it in the form of a polynomial or some algebraic form. Clarke [3.5] examined the different algorithms for the identification of discrete systems from input/output data. The basic operation of the methods is to treat the physical system as a "black-box" with the input and output variables defined from the parameters which can be measured in an experiment on the system. A sufficient number of data points is required in order to obtain a smooth curve.

The method has been employed as part of the modelling work of a pneumatic robot by Drazan [3.6]. The empirical model was generated as a 10 degree polynomial by a Numerical Algorithm Group routine.

The disadvantage of the method is the need to obtain experimental test data of the system which may not exist at a design stage. The ignorance of how the coefficients of the polynomial change with the dimensional modification of the actuator prohibits adoption of the method as a general analysis or

configuration tool for modular pneumatic servo-system design.

3.1.2 Linearisation of non-linear model

The linearisation technique for modelling a non-linear system is based on the Taylor series expansion to formulate a systematic procedure for obtaining a linear model [3.7]. Simply speaking, a function $w = f(y)$ can be approximated at a reference point (w_o, y_o) by neglecting the second or higher terms in the Taylor series:

$$w = f(y) \approx f(y_o) + \left(\frac{df}{dy}\right)_{y_o} (y - y_o) \qquad (3.1)$$

When the relation of the input and output variables is not available in analytical form, the operating curves of the physical system can be used instead. The system with non-linear relationships are linearised to obtain a set of linear algebraic equations which can be solved readily.

The major drawback of the linearisation method is its reference to an initial point. For operations far away from the reference point, the linear relationship Eqn (3.1) is no longer valid. This presents large errors and the value of the first order differential have to be updated continuously throughout the range. In addition, if the higher derivatives of the function are significant, the approximation by instantaneous slope is no longer valid.

3.1.3 Small perturbation analysis

The technique of small perturbation anlaysis was developed on the analysis of hydraulic servomechanisms [3.8, 3.9, 3.10]. Subsequently, extensions were made by Rausch [3.11], Bell [3.12], Watton [3.13] and many others for analysing hydraulic phenomena of wide variety. A detail treatment of the subject is presented by Liepmann et al [3.14] with reference to the study of aerodynamics. The basic operation starts with an identification of the exact steady state equation of the physical system. A small perturbation about the stable point is made on the independent variables to obtain the expressions for the perturbation dependent variables.

After eliminating the equalities due to the steady state conditions, the equations are then simplified by neglecting terms of smaller orders of magnitude. The final set of equations, which is normally linear, can be solved by Laplace transform or other simple differential equation methods. The earliest application of small perturbation technique to analysing pneumatic system can be traced back to the work of the research team in MIT [3.15]. Later researches, such as Mariuzzo et al [3.16] and Araki [3.17] followed much the same line.

The major drawback of the small perturbation technique is the uniqueness of the method in tackling problems. It demands a thorough understanding of the physical system in question and the

relationship of the perturbations to the steady state parameters. In addition, the technique only leads to particular solution of the hardware system being modelled [3.18] and requires special mathematical manipulating techniques. Therefore, a slight change of part of the physical system will require a completely new mathematical derivation to be made from scratch.

3.1.4 Non-linear system identification methods

While these methods are not found in any pneumatic system modelling work it is worthwhile to outline them here for the purpose of providing another scope for future research of fast modelling. The methods are classified by Billings [3.19] as 3 basic approaches, namely, functional series methods, block structured systems and difference equation models. These identification approaches are essentially the regression methodology applied to a data set which is obtained from tests of the system of interest. The quantity of data values varies from thousands in the case of functional series methods to the order of 10 for the difference equation models.

The methods offer the advantage of producing a "describing function" for the non-linear systems which can then be analysed in terms of stability, limit cycles and harmonic analysis [3.20]. Variation of parameters can subsequently be made under the restrictions of the fundamental design of the physical systems to achieve optimal performance. Problems are still present particularly in the computational difficulties of the methods and

the validity tests. It is anticipated that if a simpler algorithm can be devised the methods can be used to generate first hand empirical models of pneumatic components for initial evaluation purposes.

3.1.5 Other modelling techniques

In hydraulic analysis, it is possible to reduce the amount of computation time by the lumped parameter theory [3.21]. The method is effectively a simplification technique to absorb small variations in the hydraulic system into bulk variables such as flow rates. The resulting equations can then be solved by simpler and faster routines.

Another modelling technique presented by Iyengar et al [3.22] is addressed to large systems including electrical, mechanical and hydraulic mechanisms. With this technique, the system is organised in canonical form for hierarchical buildup. The method is similar to the lumped parameter theory with special methodology for complex, large systems.

3.2 The generalised approach

From the foregoing discussion, it is readily seen that there is a need for a generalised approach which can provide the following characteristics for pneumatic modelling:

(a) The model to be established with the general modelling scheme

is valid over the whole working range of the device.

(b) Non-linearity phenomena must be included without the need to obtain simplified solution by linearisation. Future extension capability which can include more complicated irregularities like drift is also required to cater for the increasing demand for higher prediction accuracy.

(c) Any component changes in the real system can be reflected easily on the model. In other words, the system must be segmentable into smaller sub-systems to provide flexibility of choice of configuration and direct interpretation.

(d) The scheme must be capable of modelling non-linearities of a wide variety of machine.

(e) The generalised model should be able to handle different types of pneumatic devices, such as end-stop actuators, apart from servo-drives.

(f) A choice of pneumatic models of varying complexity must be present in order to allow for variations in future. The addition of new devices should be simple and take negligible time.

3.2.1 The component oriented approach

With the advancement in computer software technology in the late 1970's, the application of computer simulation to analyse high pressure hydraulic systems was possible, and eventually become a basis for computer-aided-design of fluid power systems. The method of power flow modelling has been summarised by Dransfield et al [3.23] as an extension of the bond graph

technique originally postulated by Rosenberg and Karnopp [3.24]. Bowns et al [3.25] applied the technique as a simple component oriented block diagram method to formulate a system model for a helicopter hydraulic handling system. The system was separated into smaller systems each of which represented the configuration of the circuit for a given direction of operation. It was reported that the simulation results agreed closely during transient stages but deviated significantly at steady state. The inaccuracy was thought to be associated with the difficulties of obtaining practical measurements of the component characteristics.

The power flow modelling approach was further developed into a computer software package which was capable of simulating the dynamic and steady state behaviour of hydraulic circuits [3.26]. An automatic procedure to aid the hydraulic designer to gain the required computational skill was incorporated. It was concluded that by providing a library of the component models and a component model generator in the package, the user could quickly investigate the performance of many different circuit configurations. A similar approach was adopted to develop on small computers a program system consisting of any connection of individual hydraulic elements to form complex hydraulic systems [3.27]. The models described were based on Kirchoff's nodal law applied to an oil volume as a node and was different from the power bond principle adopted by Hull and Bowns. The hydraulic elements were presented to the system in the form of an experimental data file.

Working on the principle of equivalent pressures and volume flow rates, Leaney modelled an electro-hydraulic test rig based on the dimensional characteristics of components [3.28]. The need to include electronic controller as part of the system necessitates modification to describe the non-hydraulic functions. By the component oriented approach, the test rig was modelled as four components. System linking was achieved by power bonding for hydraulic components and electro-mechanical signals for the valve, solenoid and controller.

A direct implementation of the bond graph technique was applied by Tan et al [3.29] to develop a model for describing a rotary on-off pneumatic servodrive. Unfortunately, the modelling was restricted to the explanation of pneumatic phenomena and was not intended to be expanded for design analysis. There was no direct relationship of the bond graph elements to the physical components and hence restricted its interpretation to real life components.

The current research aims at establishing, from the basic compressible flow laws, the mathematical equivalent of the physical components. The application of the component oriented approach to pneumatic servo-drives has been outlined by Mo [3.30]. The essence lies on the process of identifying the elements within the physical system, and of determining the bonding linkage between the elements when several of them are connected together. Due to the variety of principles employed in the modelling of the

basic elements, there is no fixed rule for model linking in this approach and a more flexible way was taken similar to the techniques developed in hydraulic simulation.

3.2.2 Digital simulation

In the study of non-linearity in hydraulic servomechanism, Shearer [3.31] concluded that a more sophisticated model of the coulomb type friction was required to produce simulation results agreeing to experimental results quantitatively. With pneumatic systems, which are highly non-linear, an analysis tool with the capability for predicting the system behaviour by numerical integration is definitely needed. It is anticipated that the model can be simulated with respect to time so that data in the time domain can be compared directly [3.32] (which is usually the case for real time experimental results). This is normally the most efficient comparison methods for experimental results evaluation.

Continuous System Simulation Language (CSSL) [3.33] has been widely used since the 1960's due to its ease of programming. Modifications to the language were reported by Lucas et al [3.34] as a result of changes in computing hardware. Other languages are available and presented by Korn [3.35], Barthelmes et al [3.36]. In choosing these software packages for the simulation of non-linear pneumatic systems, Atherton [3.37] pointed out that the capability to handle discontinuous features was decisive.

Packages including those with discrete system handling are reviewed by Cellier [3.38] and Araki [3.39]. The mathematical tool used in this research has been chosen bearing in mind the need to deal with the discrete system controller in reality. During the modelling stage, it is necessary that the package can provide interactive entry and editing of parameters. Graphics display of the simulated data must be available and tabulated output for fine inspection is sometimes necessary.

3.2.3 Computational tool

The simulation package used for the project is known as "Communication Mode Simulation for Continuous and Discrete Systems" (CMS2) which was developed in UMIST (University of Manchester Institute of Science and Technology) [3.40]. The original version runs on PRIME linked with GINO (Graphical-Input-aNd-Output) Library.

The package is written in FORTRAN and is organised in a modular structure as shown in Fig. 3.1. The user is required to supply his model in the form of a subroutine named EQNS with pre-defined state and algebraic variables structures. The model file is compiled separately and linked to the object codes of the package to form an executable image. The integration method used in the simulation package is the Merson's version of the Runge-Kutta integration algorithm [3.41]. It is a self-starting initial value fourth order algorithm. In fact, this self-starting capability allows the implementation of variable integration step

length required for the management of interrupts which simulate the sampling or digitisation effect of digital controller.

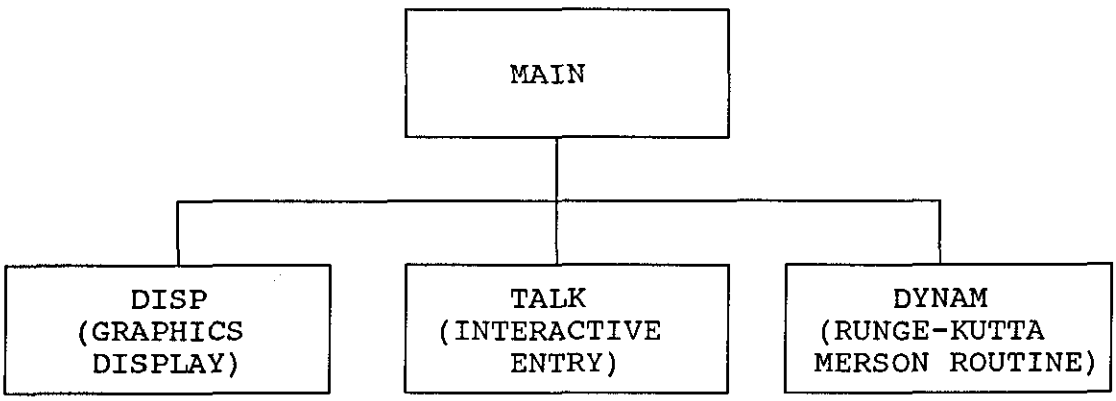

Fig. 3.1 - Modular structure of CMS2

Due to the changes in the availability of computing facilities, the source code of the package was taken to Hong Kong and ported onto several machines. The first version was implemented on a DEC PDP-11/70 which required a lot of manual manipulation of overlays during linking stage due to memory constraints. Some simulation runs were carried out but not much progress was achieved. The second modification was implemented on a VAX-11/750 where the program development tools were more efficient. Some source code debugging was performed on VAX.

The third version was implemented on a Data General MV/10000. A large number of simulation runs were implemented some of which were successful to provide useful information for further

development. Graphic outputs could be obtained on Hewlett Packard HP7585B plotter either as on-line or off-line plots.

The final version of the package runs on SUN-3 graphic workstations using SunCore graphics library [3.42]. A set of software interfacing graphics subroutines is required to link to the basic package during compilation time [3.43]. The size of the package is approximately 1.2 Mbytes. The enhancements on the package are summarised in Appendix I.

3.3 Model verification and system identification

The mathematical model developed in this research is anticipated to be a generic model for pneumatic systems. It entails extension in the theory of compressible air flow and covers the general feature of common industrial pneumatic devices.

3.3.1 Verification studies by specific hardware

Due to the vast variety of pneumatic components in use in industry, it is impossible to verify the generic model with prototypes of all types of components. The scope of study is therefore defined to be related to the single axis modules which are either end-stop or servo-controlled.

The apparatus for verification is made from the commerically available pneumatic components, electronic devices and microprocessor boards. The apparatus is designed as modular unit

which can be further extended to form the kind of modular robots as described by Weston et al [2.81]. The apparatus includes :

(a) Mechanical features are designed and manufactured according to the modularisation concept presented in Section 2.2.3.

(b) A control software running on the test rig is required to control and record the movement of the unit. Facility to upload the data to host computer for analysis purposes should be available.

(c) Other transient capture facilities is to be provided as and when required to obtain useful data for model verification.

3.3.2 Time domain analysis

The model validation is performed by making comparisons between the simulated response and the experimental results. Both responses are output on one graph and hence a direct segment by segment, or point by point comparison can be made.

Having obtained the time series data from both the test rig and the simulation runs, it is then possible to carry out some system identification analysis work. The most fundamental analysis would be the frequency response analysis using the Fast Fourier Transform (FFT) technique. The theory of the analysis can be found in various literature [3.44]. By comparing the frequency responses of the experimental transients with the simulated transients, it is much easier to recognise the basic characteristics of the system including the natural frequency

and damping.

When sufficient starting information is available, test rigs described in published reports and papers are simulated by the component oriented approach using the pneumatic model established in this research to illustrate how the methodology in the project can be applied universally. However, due to the lack of complete information in the abridged literature, the accuracy of such simulation is not anticipated to be high, but the general trend of the simulation should agree with the published results.

3.3.3 Frequency domain analysis

The primary purpose for frequency domain analysis is to obtain cross-correlation data between the simulated and experimental responses. Unfortunately, due to the lack of useful facilities for averaging transformation of the digitised time responses, the frequency domain analysis is limited to obtaining fundamental information about the individual components only.

3.4 Summary of research methodology

The aim of this modelling exercise is to establish a comprehensive mathematical model which can be used to evaluate pneumatic servomechanism at the design stage. The scarcity of real test data at the initial design stage prevents the use of statistical based modelling techniques. Likewise, in the light of the need to predict the performance of the pneumatic systems in

its complete working range, conventional linearisation modelling techniques are inadequate to fulfil the accuracy and flexibility requirements for computer aided design system formulation.

The generalised approach outlined in this chapter leads to the adoption of the component oriented approach which is a natural development of the bond graph technique. It simplifies the complex mechanism into a series of linked component modules. The components are then identified as a physical transformation device with standardised input-output relationships.

The mathematical model is formulated by linking the relevant component modules into a simulation package. Since the servomechanism will be controlled by a digital device, the simulation package is chosen with the capability to simulate discrete events. The integration process has been managed in such a way that the system is evaluated piecewise between the discrete time frames and adjusted at the interrupted moments. The algorithm used in the integration is the Merson's version of Runge-Kutta integration algorithm. The system is implemented on Sun workstations with SunCore graphics facilities.

CHAPTER 4

THE GENERIC PNEUMATIC DRIVE MODEL

The philosophy of the component oriented approach requires that the system should be broken into a series of components which connects to one another via clearly defined linking variables. The linked list of components are formulated in such a way that they can be replaced by alternative components bearing the same linking specification at the component interface or empirical model determined as a result of individual component tests.

There are two important points to be observed in deriving the generic model for the pneumatic drives which can appear in many different forms in industrial automation applications:

(a) The components in the generic model must be traceable to physical entities such that any change in the real world can be reflected by corresponding change (or changes) in the model abstraction. This implies a clear affiliation of the mathematical models of the components to their physical counterparts.

(b) The compressibility of the working medium must be taken into account to include phenomena which may not exist in the other types of servomechanisms.

Owing to the wide variety of pneumatic components used in

industry, it would not be viable to include details of each components at the level of abstraction of the generic model. The system model presented in this chapter is aimed at providing a framework for specific models of the pneumatic components to fit in during the final implementation stage.

The format to segregate the physical system into standard mathematical modules has been compiled by Unruh [4.1] on hydraulic system. Based on the same principle, a simple open loop model can be formulated by synthesising a bang-bang system. The analysis is then extended to include closed loop functions, proportional elements and other features in modern pneumatic servomechanisms.

4.1 The bang-bang open loop system model

In a typical low-cost-automation design, a number of pneumatic actuators are working together under the control of some specially designed pneumatic logic circuit in a coordinated fashion [4.2]. The normal fundamental unit (Fig. 4.1) in the set-up consists of a pneumatic actuator, a 4-way valve which is either manual or solenoid actuated, and the load [4.3]. Design data of such units are obtained from the trade literature [4.4].

From the system point of view, the components of the typical unit can be identified from the physical connections as indicated in Fig. 4.1:

(a) The actuator, which produces mechanical motion as a result of the unbalanced air pressure in the two chambers;

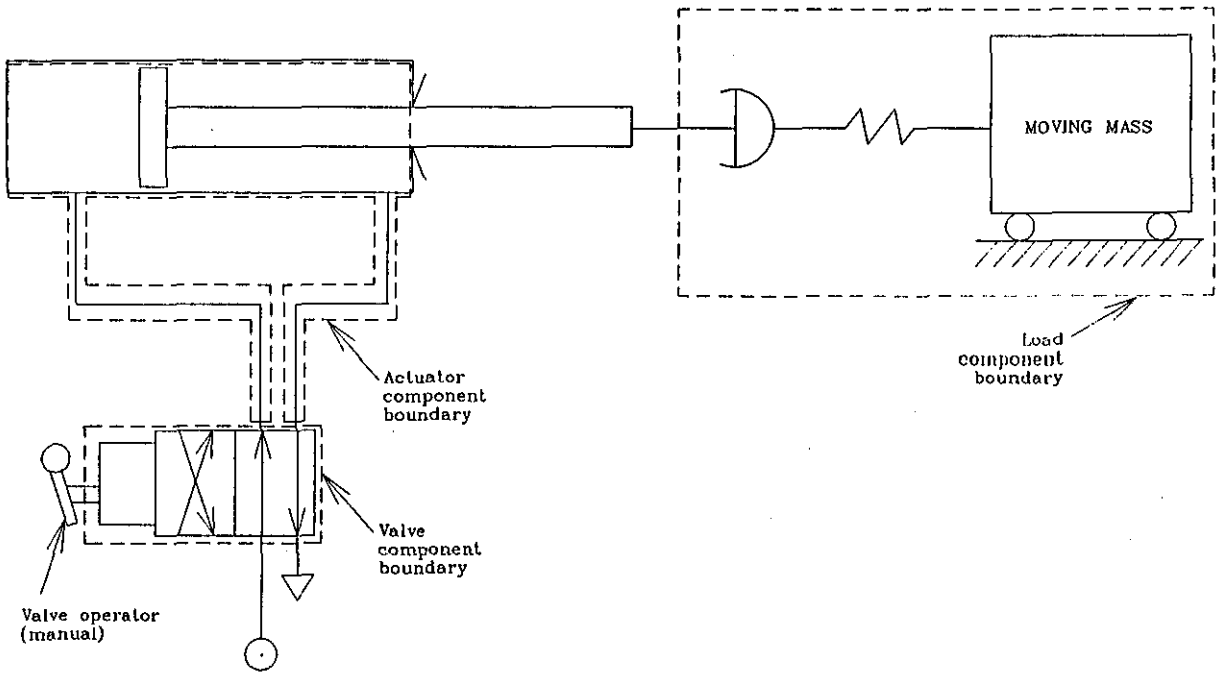

Fig. 4.1 - Fundamental unit of bang-bang system

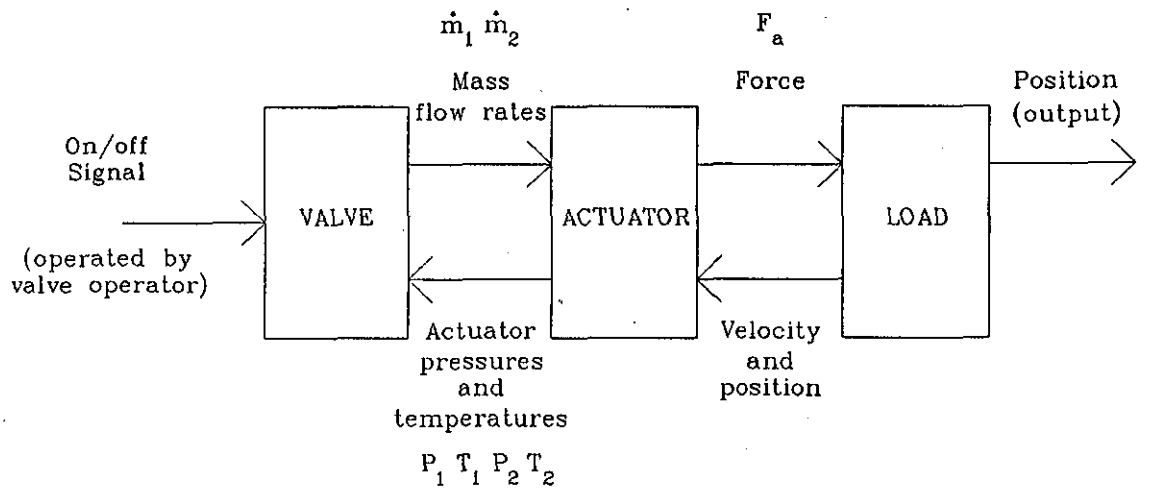

Fig. 4.2 - Abstraction of system

(b) The load, which opposes the actuator due to the mass, friction, spring forces, mechanical stop or forces of other nature;

(c) The valve, which provides a guided passage for the compressed air between the supply, the actuator and exhaust;

(d) The valve operator, which actuates the mechanism in the valve to control the air passage.

An abstraction of the components can be formulated as shown in Fig. 4.2. The connecting signals between the boxes are derived from the inter-relationships of the consecutive components. These consists of:

(a) Pneumatic link in the form of air mass flow rates, pressures and temperatures between the valve body and the actuator;

(b) Mechanical link in terms of force and acceleration between the actuator and load.

4.2 The on-off closed loop system model

A closed loop system using the 2 states on-off pneumatic valve can be constructed using electronic controls [4.5]. The enhancement is primarily based on the traditional closed loop control theory to provide a feedback loop at the load so that the air flow through the valve to the actuator can be regulated according to the position.

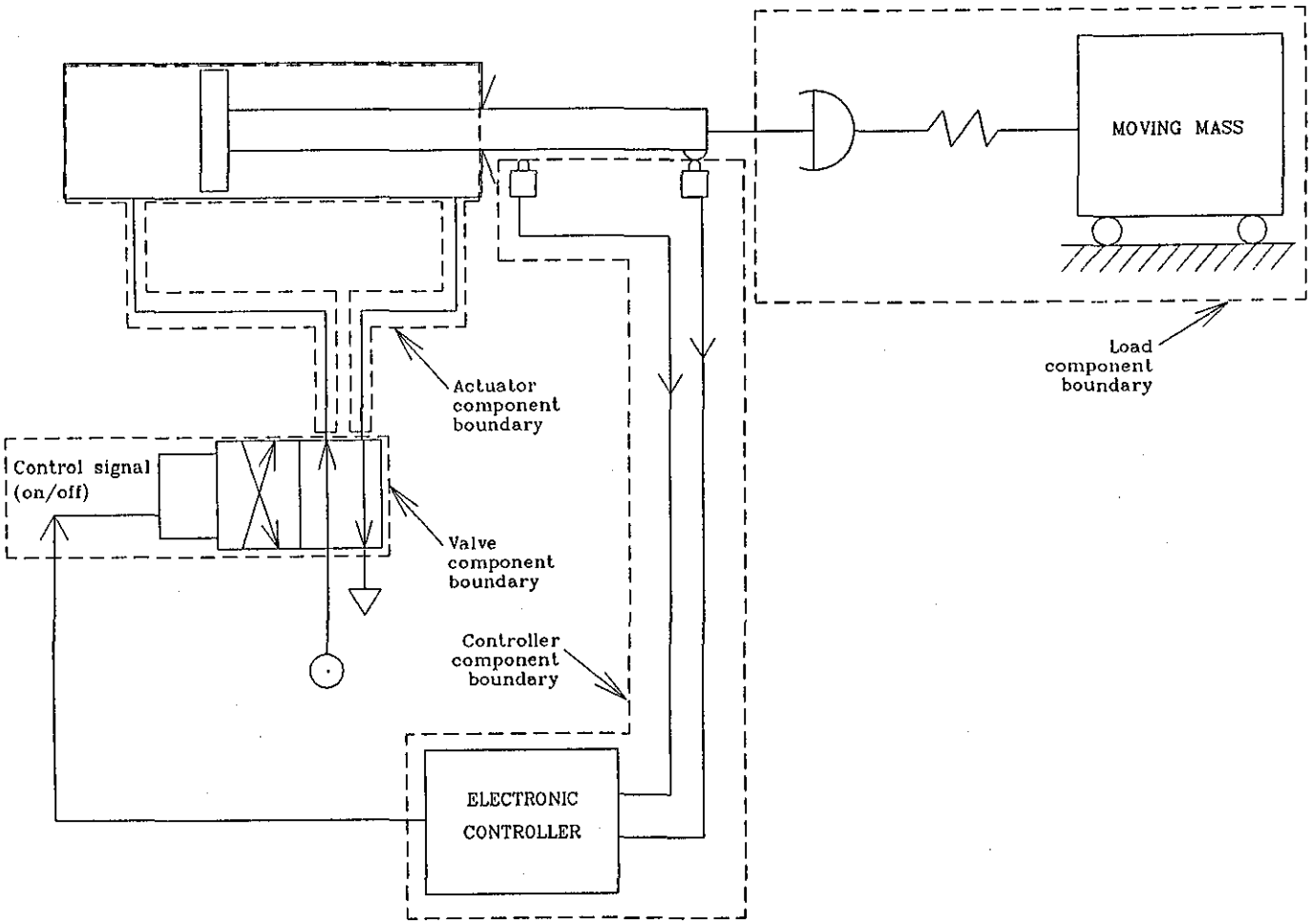

Fig. 4.3 - System with electronic controller

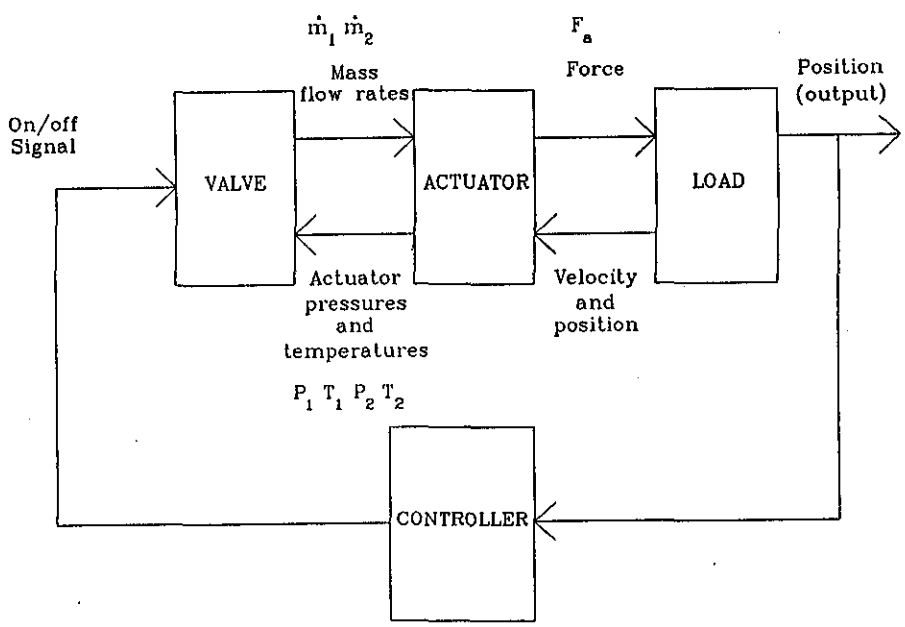

Fig.4.4 - Closed loop system block diagram

The component boundaries can be physically defined for the electronic controller as shown in Fig. 4.3. In contrast to the linkages in Section 4.1, the connection between the load and the controller is an electrical signal indicating the position. Similarly, the connection between the controller and the valve is an amplified electrical current in 2 states.

Extending the block diagram of the open loop system, the controller can be included as the closed loop component between the load and the valve (Fig. 4.4).

4.3 The servo-controlled pneumatic drive model

The accuracy that can be achieved on the on-off pneumatic servomechanisms is inevitably unsatisfactory due to the coarse resolution of the control system. As described in Section 2.4.3, improvement is possible using proportional valve and digital controller. The resolution which is brought into the system by the proportional element at the valve implies that fine breakdown of the component at the valve operating part is required. The valve operator component, which is introduced in Fig. 4.5, represents the electro-mechanical component controlling the amount of air passage opening in the valve component according to the controller command signal.

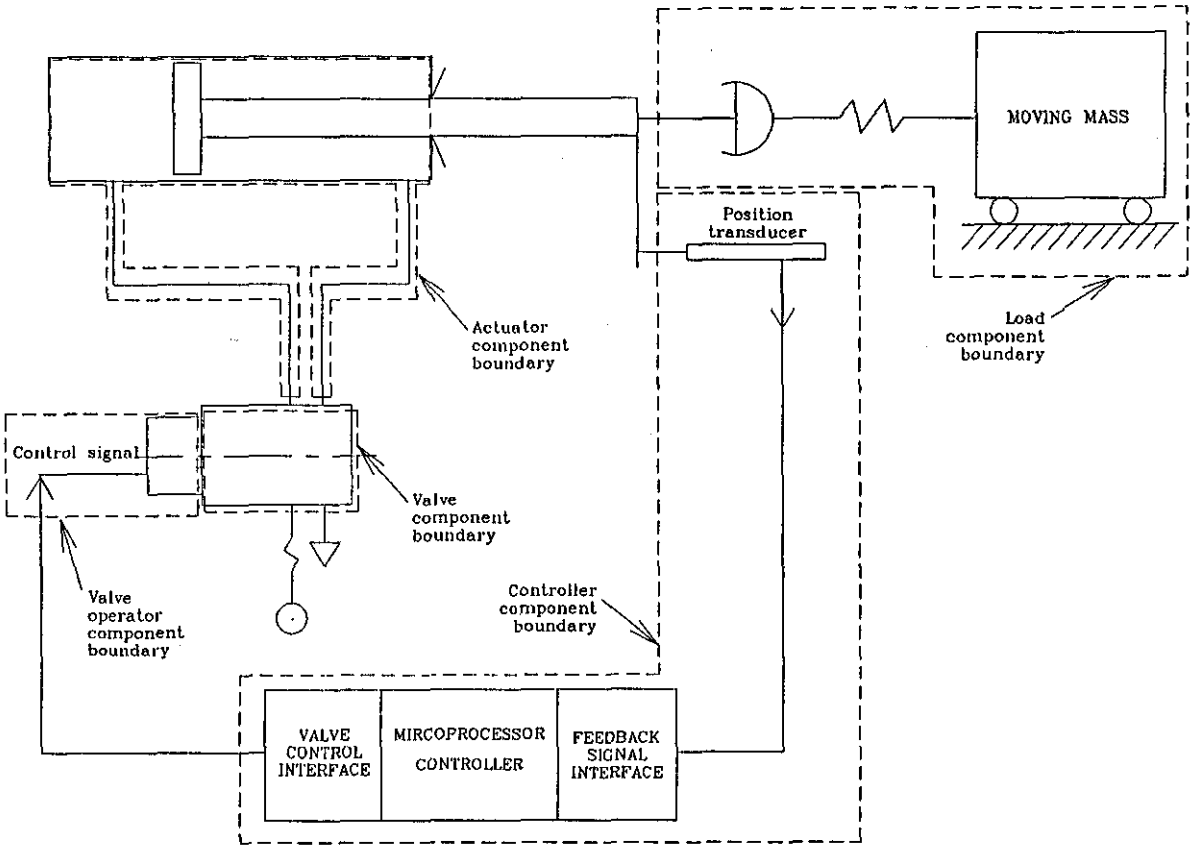

Fig. 4.5 - System with proportional valve element

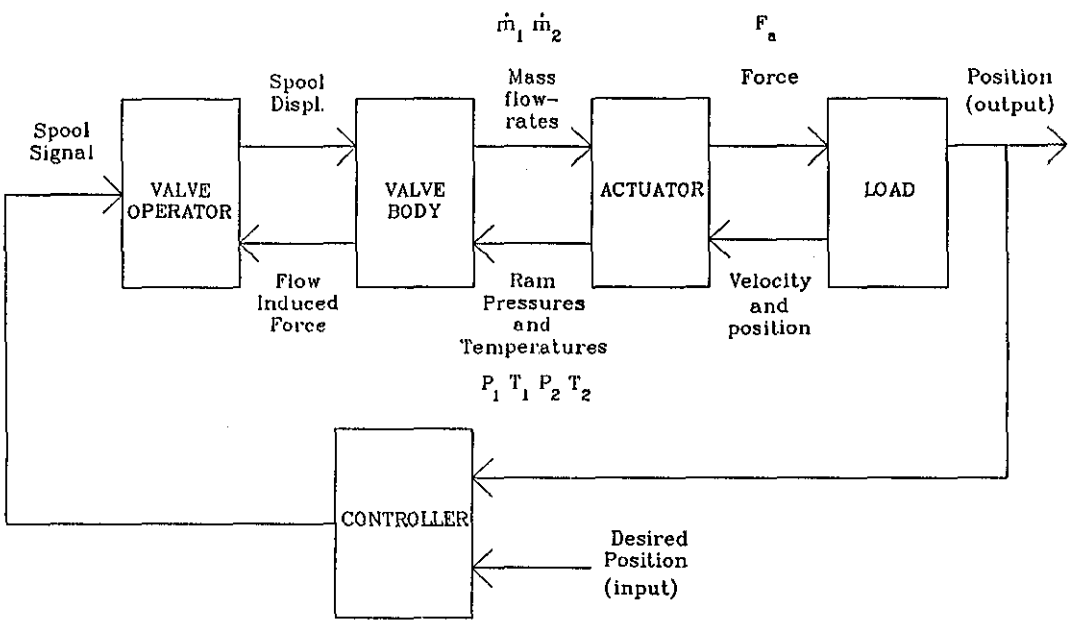

Fig. 4.6 - System block diagram of servo-controlled pneumatic drive

The change in output resolution requires matching at the input side of the controller. The digital controller has the capability to capture suitable proportional signal from the position transducer attached to the load system. The digital controller can be simple logic circuit, programmable logic controller or microprocessor. The block diagram is modified as depicted in Fig. 4.6. The component oriented approach treats the mircoprocessor controller as a black box which, together with the desired set point value, transforms the position information from the load to electrical command signal, amplified to the level suitable for the valve operator device in use. The proportional amplifier and the signal conditioning circuits are amalgamated into the controller because they are similar in nature and tied closely with the microprocessor.

4.4 The effects of tubing in pneumatic systems

One of the influencing factors in pneumatic system is the effect of isentropic expansion due to the compressibility of air. In the confined passages like the tubing in the pneumatic power mechanisms, the pressure and temperature of the air flow will be changed and affect the performance of the system. The problem of compressible flow in tubing has been studied in the analysis of supply of gas in pipe lines [4.6]. Analysis shows that the pressure drop from the inlet to the outlet of the line is significant if the Mach number goes up to 0.7 [4.7]. The phenomenon is therefore not negligible in modelling pneumatic systems.

Apart from the Mach number which is a property of the air flow itself, the pneumatic condition is also affected by parameters which are characteristics of the tubing such as friction, upstream and downstream pressures, length of tubing. Since the tubing connects the valve body and the actuator, both of which are not appropriate to deal with the phenomena, a separate component module is necessary to define the changes. In the real world, the physical boundary can be refined as shown in Fig. 4.7. The corresponding block diagram is defined in Fig. 4.8. The input linking variables are defined to be the mass flow rate, pressure and temperature which provide information for the Mach number at the inlet. The output linking variable is the pressure value at other side of the tubing.

4.5 Models of different complexity

No matter how accurate the component modules are derived, it is inevitable that nature contains more unknowns that the theoretical model can represent. In the compilation of the mathematical model for individual components, the representation can be made at different levels of complexity. For applications demanding very accurate solution, the analysis must take as many influencing factors as possible and very often the outcome is a set of highly non-linear, implicit mathematical expressions. The time required to arrive at a usable solution, either by analytical or computational methods, is also long. On the other hand, if the

accuracy requirement is not stringent, a simple model with the bare minimum number of essential system variables will give the same conclusion in a much shorter time.

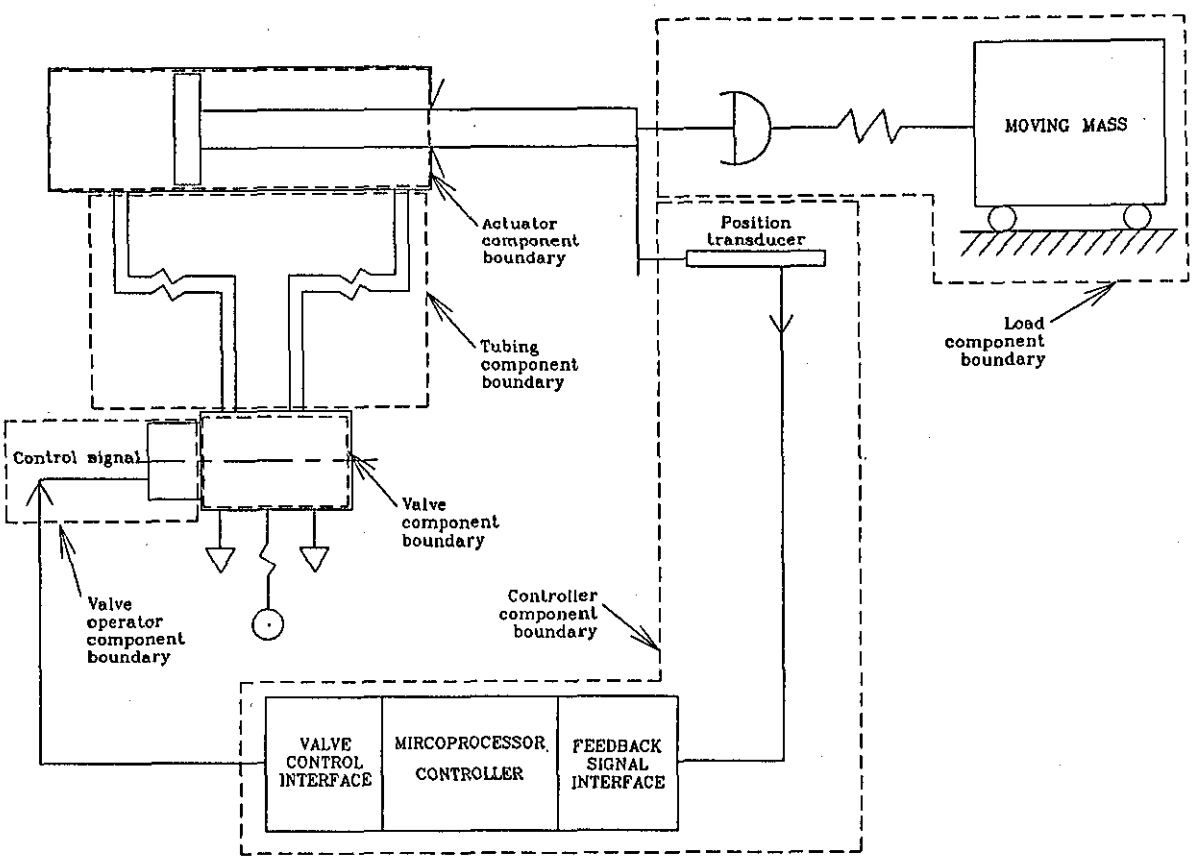

Fig. 4.7 - Refined physical boundary with tubing as component

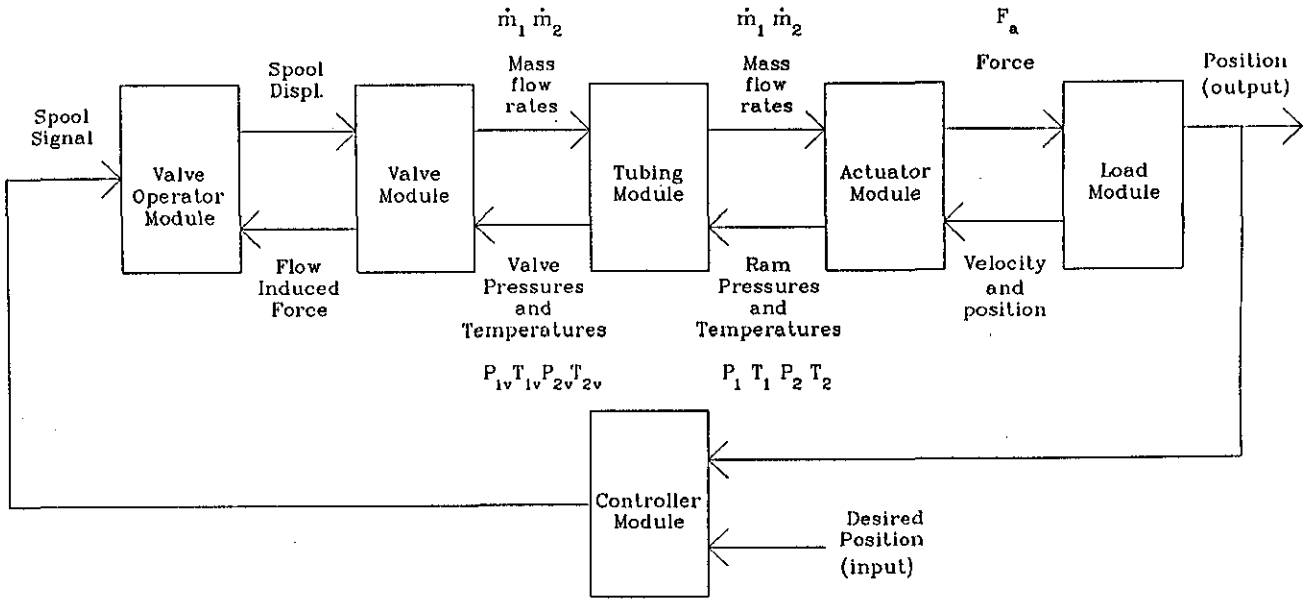

Fig. 4.8 - Modular structure of pneumatic servo-drive

Apart from the primary objective to model the pneumatic mechanism flexibly, there is a second level need to match the modelling efficiency with accuracy requirement. The generalised approach provides a good analytical environment to include any model irrespective of its sophistication. Two features as a consequence of the approach are observed:

(a) Comprehensiveness in a component does not affect the level of complexity of the other components in the system model. In other words, part of the system (often the most critical component) can be modelled as closely as possible to reality while the other components are simplified to reduce the total system evaluation time.

(b) In the absence of theoretical formulation, experimental data, which merely constitute the simplest but empirical model, can be used at initial stages of model development. The representation may be too specific for that particular piece of hardware, but analysis direction can be focussed on more important parts of the system. Generalisation can be made at later stage when sufficient information is collected.

4.6 Summary of generic model

The model presented in Fig. 4.7 has been built by generalising the components and the system construction of pneumatic mechanisms. It possesses the property that the components are actual abstraction of the physical counterpart. Replacement of any component in the model can be affiliated with a corresponding change in the real pneumatic mechanism.

The general nature of the model allows the representation to be valid for a vast number of pneumatic devices. The complete form (Fig 4.8) represents a closed loop mechanism operated either with proportional or on-off valve. The function of the controller is modelled in terms of the linking feedback signals and command output rather than the control algorithm which can vary among different implementations.

Open loop pneumatic mechanism in the applications of low-cost-automation are regarded as special case in the model. This can be done by removing the controller component and leaving the feedback loop open so that the input command on the valve operator is unchanged during the whole working cycle.

The foregoing shows that a generic model has been derived from the synthesis of pneumatic mechanism. The component oriented approach adopted for the model formulation allows choice of components as well as representation complexity. The versatility inherent in the model construction makes it adaptable to most applications in industry employing single axis working modules utilising components of various nature.

CHAPTER 5

THE TEST RIGS

The generic model outlined in Chapter 4 presents a general picture of the pneumatic mechanisms for hardwired as well as flexible automation. Validation of the generic model relies on the verification tests on hardware which is specific in itself. Variations of the hardware to cover as many aspects of the model as possible is desirable but due to the limitations in funding and time, the tests were performed on typical single axis modules specially designed for evaluation purposes. In order to verify the capability of the generic model in dealing with changes in component configuration, alternative components have been arranged to be assembled as variations in system structure to illustrate the philosophy of the approach.

Since the project is aimed at developing a configuration tool for industrial design, the test rig is so designed that it comprises mostly of standard parts. The discussion in this chapter follows the pattern of the generic model for the description of the components. While most components can adapt to any combination of the other parts of the mechanism, there are a few cases in which the characteristics of individual components do not allow cooperative actions between certain consecutive pair of parts. Existence of these restrictions does not affect the

generic nature of the model. It only reflects the reality in actual practice.

5.1 Pneumatic actuators

The scope of interests of the research is the study of low pressure pneumatics with air supply in the range of 0-10 bars. In the current research work, the air pressure is set at 5 bars gauge for all cases. In order to concentrate on the more immediate modelling needs, the tests are confined to linear actuators. It would be possible to extend the same analysis for validation of rotary actuator cases but it is not anticipated to be worthwile for pursual at this stage.

5.1.1 Asymmetric cylinder

Several versions of the pneumatic actuator has been built. The initial test rig [5.1] was built in 1983 consisted of a heavy vertical standing cylinder and a rigid brass bushing. The performance was a nightmare due to the dominant friction in the apparatus. Subsequent versions were designed bearing in mind the stiction problem of the initial rig.

The square rod cylinder designed by Martonair [5.2] showed great improvement. The design allowed 4 rollers, one each side of the cylinder rod to function as bearings on the slideway. The friction of the rig was greatly reduced.

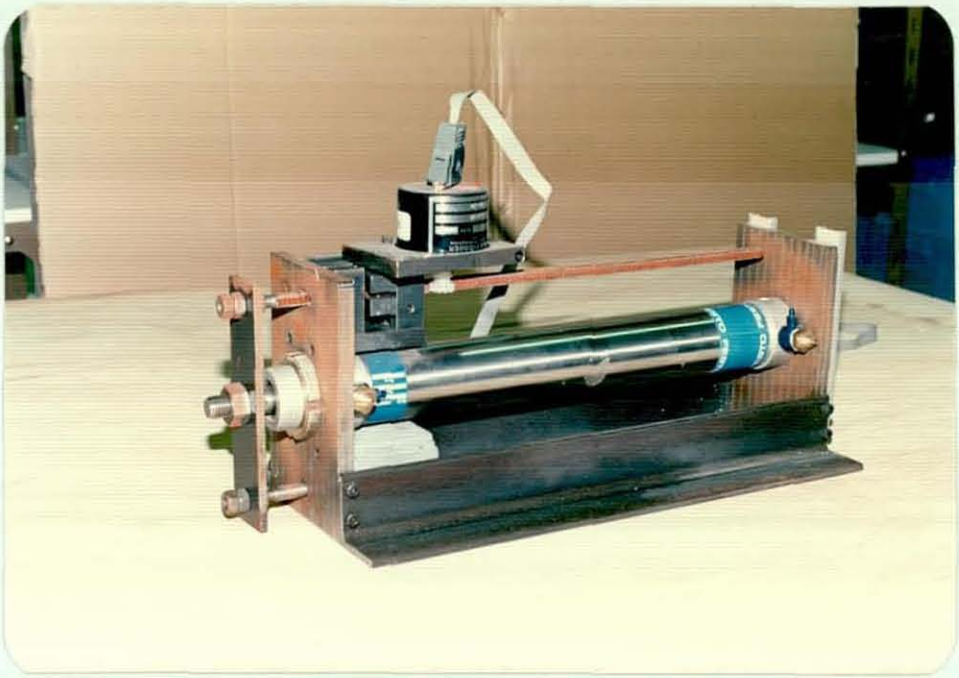

(a) Photograph

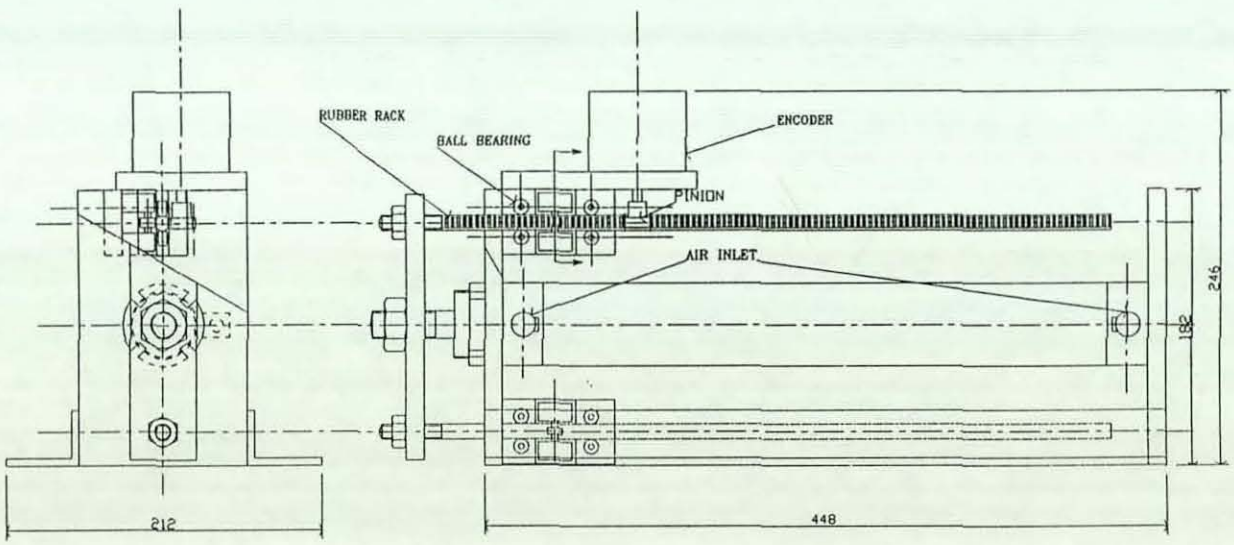

All dimension in mm

CYLINDER DATA :
BORE = 50 MM
STROKE = 300 MM

(b) Drawing

Fig. 5.1 - Drawing and photograph of asymmetric pneumatic actuator

The asymmetric actuator in the research was designed based on the idea of the Martonair modular units. Two guide rods supported by 7 ball bearings on a framework supported the longitudinal movement (Fig. 5.1). An end plate with suitable mounting holes was attached at the end to allow for any attachment to the test rig.

5.1.2 Rodless cylinder

The alternative component of the actuator was a rodless cylinder with two pulleys at both ends through a wire attached to the moving block (Fig. 5.2). The rodless design has the advantage that the area at both sides of the piston are equal. In terms of closed loop control, it is easier to operate symmetrical actuator because if the air pressure can be balanced by the valve at the centre point, the piston will remain at its stopped position.

5.2 Proportional valve

The proportional valve was a 5-port spool valve made of 3 main parts:

(a) An aluminium valve casing;

(b) A brass sleeve tightly fitted in the core of the valve casing;

(c) A spool made of aluminium moving freely in the sleeve.

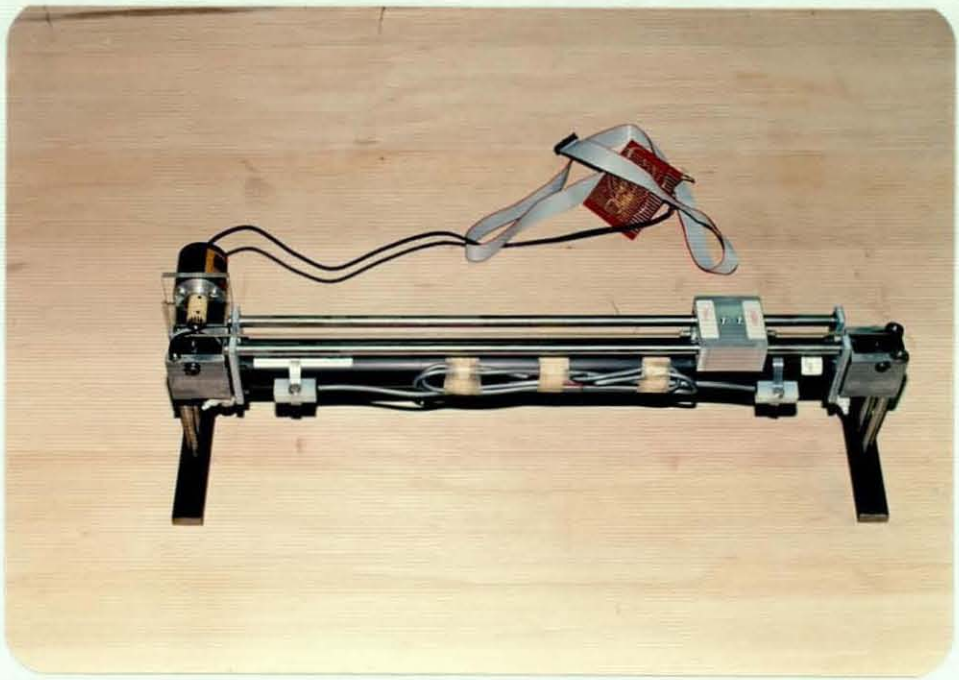

Fig. 5.2 - Photograph of symmetric actuator

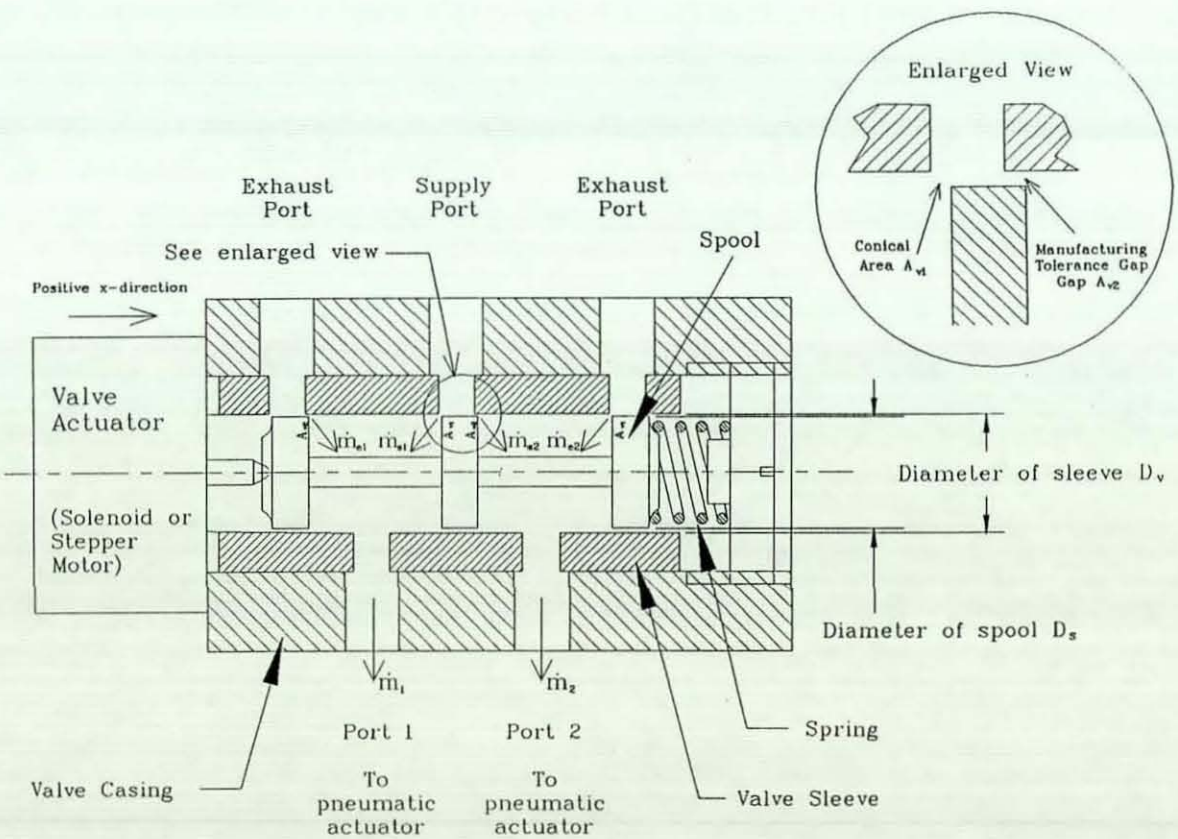

Fig. 5.3 - 5-port proportional valve

Fig. 5.3 shows a drawing of the valve and spool. The valve was designed to be manipulated by a single operator at one end, whereas the other side of the spool was counteracted by a spring.

5.2.1 Solenoid operated valve

A choice of valve operators to manipulate the spool in the proportional valve was available. The initial design was made with a proportional solenoid which reacted to input current of 0-1A to produce 0-50N axial force [5.3]. The spool spring balanced the solenoid force somewhere in the spool displacement range of 0-2mm proportional to the input current.

5.2.2 Stepper motor operated valve

The second choice of spool manipulator was a stepper motor with lead screw mechanism [5.4]. The axial step displacement, upon a half step increment pulse signal of the stepper motor was 0.0125mm. Details of the theory of stepper motor and its circuit can be found in various literature [5.5, 5.6]. The stepper motor valve operator had the advantage that it could position the spool more precisely and the data could be more useful for analysis purpose.

5.3 Controller and associated circuits

The electronic components of the test apparatus included the microprocessor and its interface boards. There were two types of

interfaces to cope with the solenoid or the stepper motor operated valves. For analysis purpose, an analogue signal acquisition board was included and the control software had been tailored to cater for the function.

5.3.1 The microprocessor

The microprocessor was the Motorola MC68000 16-bit processor on a standard MVME110-1 board [5.7]. The 32-bit internal architecture of the processor allowed multiplication, division and data manipulation to be done more efficiently with the data registers. The clock rate of the processor was at 8MHz.

The MVME 110-1 Board was designed to function as a system controller for industrial applications. It had a VME bus extension and an input/output (I/O) adaptor for extending to include peripherals (VME is a standard bus introduced by Motorola). The total configuration of the microprocessor system included (Fig. 5.4):

(a)	MVME110-1	Main board
(b)	MVME201	256K Dynamic RAM board
(c)	MVME410 (2 sets)	2 x 16-bit parallel I/O board
(d)	MVME400	dual serial interface board

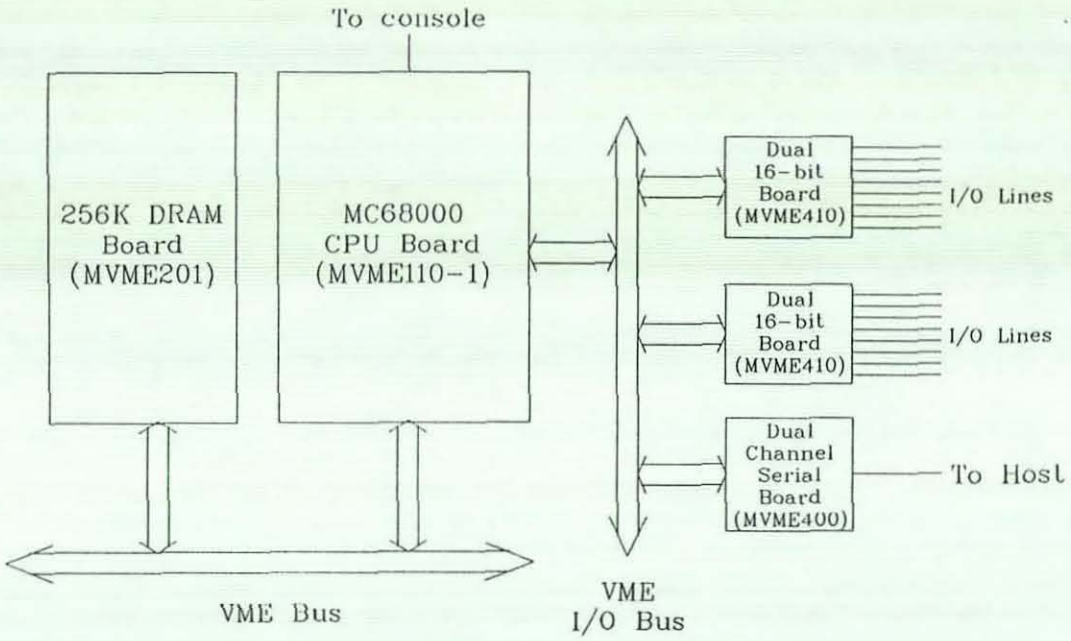

Fig. 5.4 - Microprocessor configuration

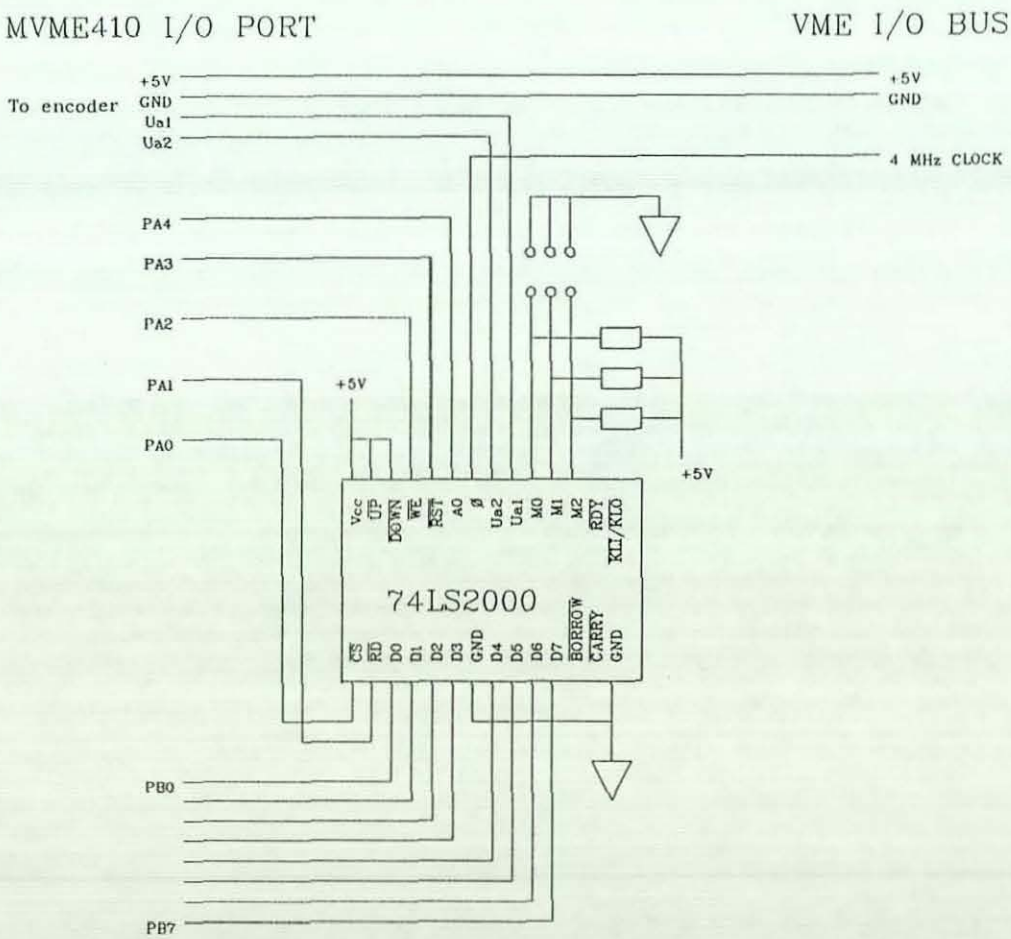

Fig. 5.5 - Encoder interface

The RAM board was used to hold the control software and transient data acquired during tests. The parallel I/O boards were interfaced to the custom-made boards described in subsequent sections. The serial interface board provided a point of communication between the microprocessor and the host (DG MV/10000).

The feedback device was a rotary incremental pulse encoder with 1000 lines/revolution resolution. A Texas Instruments 74LS2000 chip transformed the pulses to counter information [5.8]. The chip automatically counted up or down depending on the phase relationship of the two channels from the encoder. A parallel port circuit (Fig. 5.5) captured the position data in 2 bytes via one of the two MVME410 interface boards.

In order to synchronise the data points with the timer on the microprocessor, the controller was designed with its own data acquisition facility. The analogue-to-digital converter (ADC) board was a custom-made board with one each of the following Burr-Brown chips [5.9]:

(a) 12-bit ADC-85

(b) sample and hold SHC85

(c) 16-channel analogue multiplixer

Three analogue signals: two pressures from pressure transmitters and linear displacement from the short stroke transducer for spool location were detected. The sampling was done consecutively within one sampling cycle. The estimated time

for sampling one signal was approximately 100μs. Fig. 5.6 shows the circuit with connections to the analogue signal lines.

5.3.2 Controller for solenoid operated valve

The solenoid operated valve required a proportional voltage signal of 0 - 10 V from the digital controller through a custom-built digital-to-analogue converter (DAC) circuit. The DAC was controlled via a data latch from a MVME410 port (Fig. 5.7).

The amplifier circuit worked in connection with the DAC circuit to control the proportional solenoid. The amplifier (Fig. 5.8) consisted of 3 stages. The initial prescaling stage amplified the input signal and added a gain to the valve to make it comparable with the other input signals. The second stage mixed the dither signal and input signals from first stage. The final stage converted the voltage signal to driving current through the power transistor 2N3055. A linearity test on the amplifier circuit (Fig. 5.9) showed that the amplifier was practically linear.

According to the findings of previous related researches [1.8], the stiction on the valve spool was significant and it required dither signal to relief the spool from serious hysteresis problems. This provision was adopted in the specific tests to eliminate as much uncertainties as possible during verification.

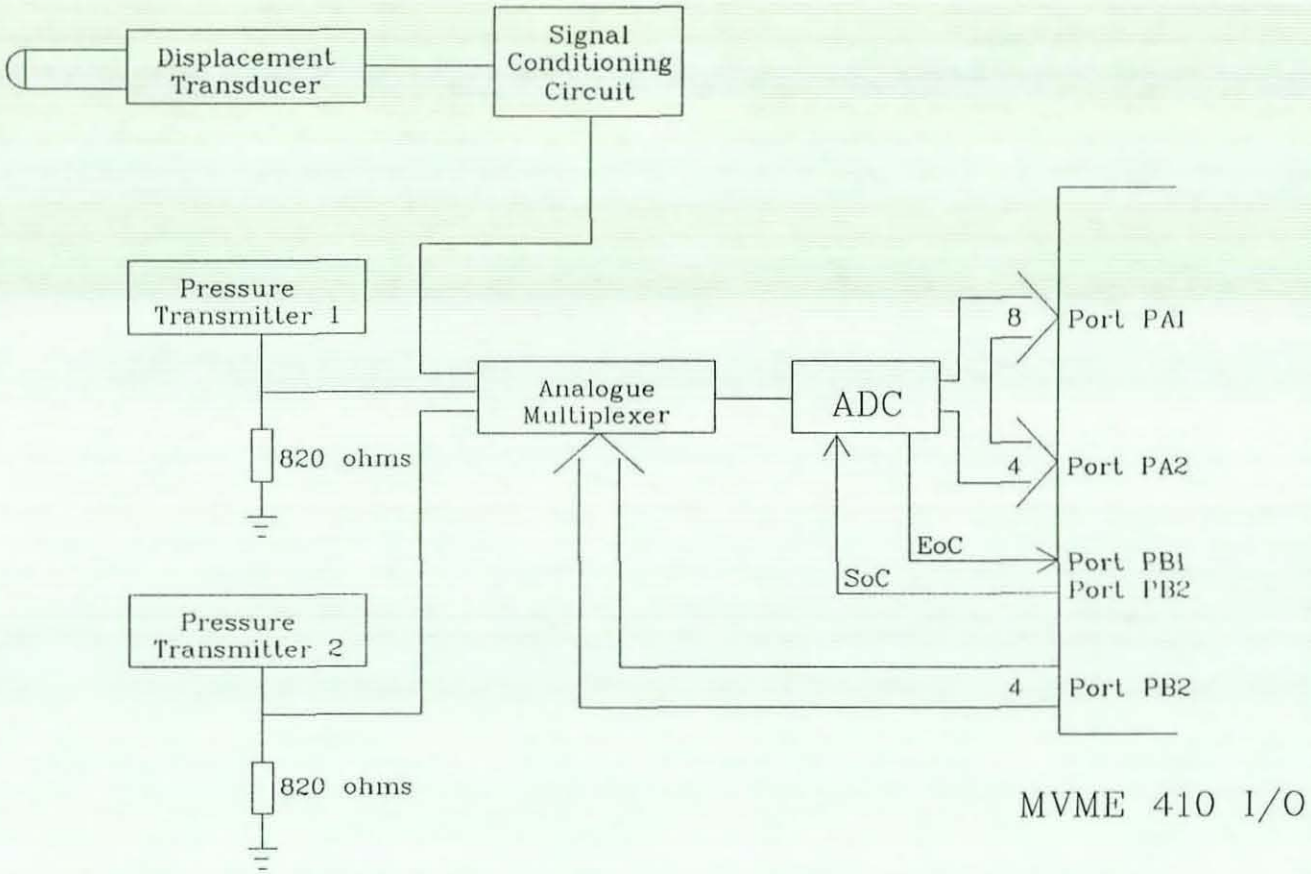

Fig. 5.6 - Analogue-to-digital converter circuit

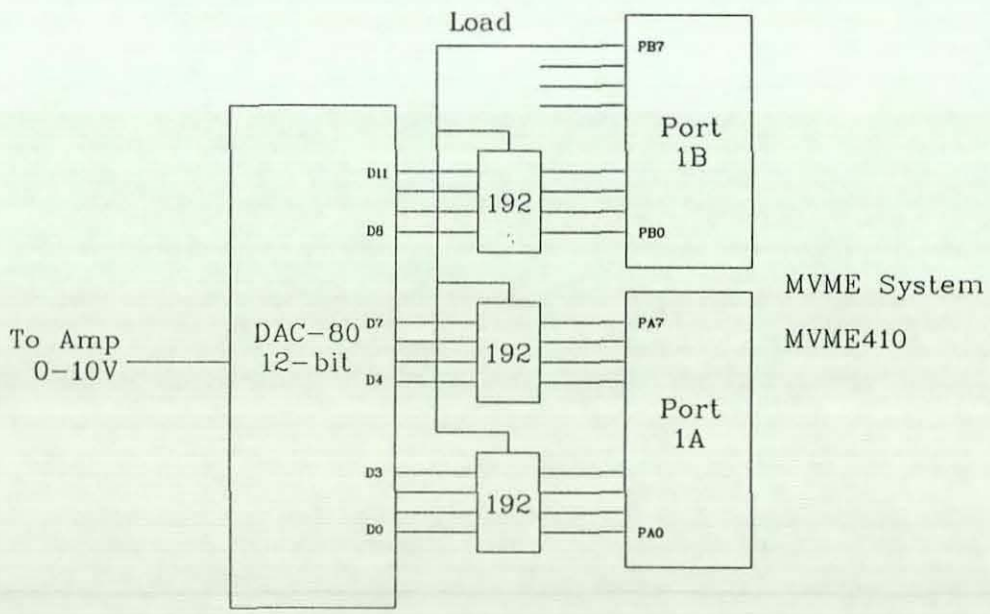

Fig. 5.7 - 12-bit digital-to-analogue converter interface

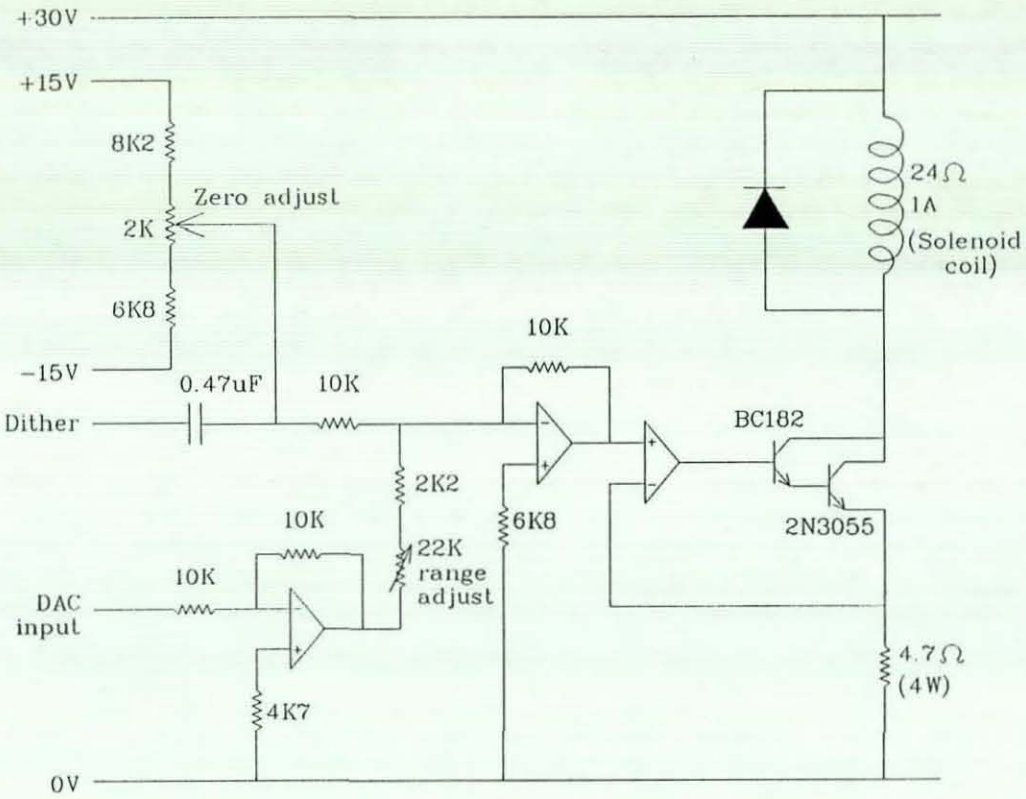

Fig. 5.8 - Solenoid valve amplifier circuit

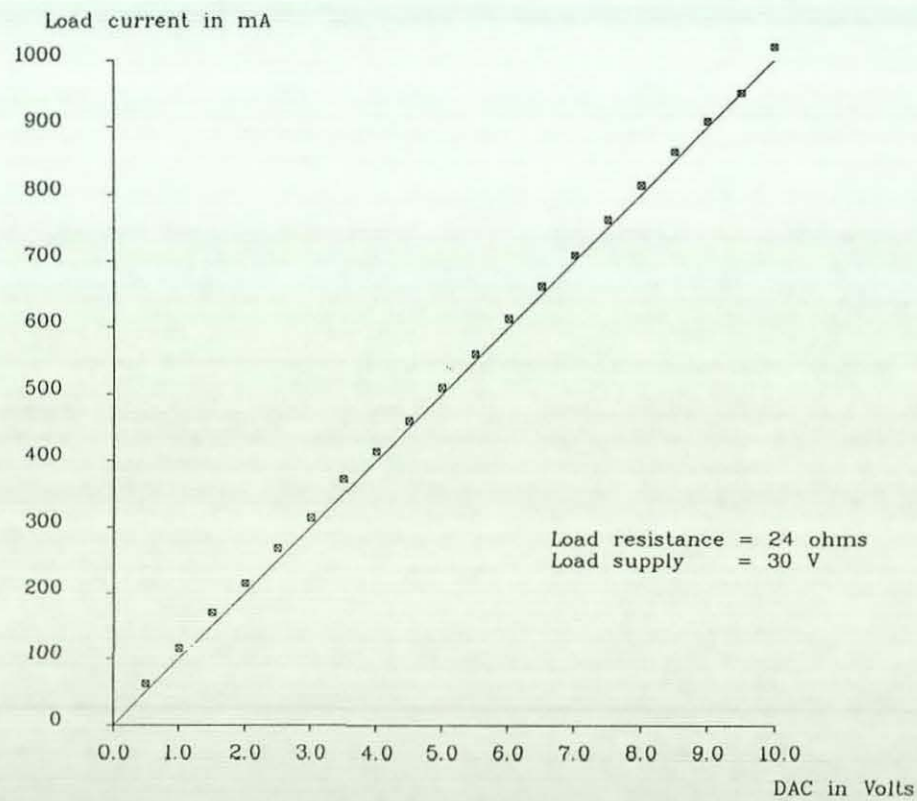

Fig. 5.9 - Linearity check of amplifier circuit

5.3.3 Controller for stepper motor operated valve

The stepper motor valve operator required a series of pulse signals to be passed to the 4 motor coils in specified order. A translator board was used to convert the command signal from the controller to the required sequence. A MVME410 port functioned as the interface as shown in Fig. 5.10.

5.3.4 The control software

The real time control software which was written in Motorola assembly language, has been described with particular emphasis on the illustration of the control and analysis features [5.10]. The design philosophy of the control software was to provide a simple microprocessor control environment with the capability of:

(a) Implementing the variable position gain scheduling algorithm;
(b) Providing testing options such as closed loop, exit conditions and so on;
(c) Providing data acquisition facilities for model validation.

Two versions of the software were available:

(a) The software for solenoid operated valve output the command signal via the DAC board;
(b) The software for stepper motor operated valve sent a pulse to the translator circuit in every sampling time if errors between the commanded spool location and current spool location existed.

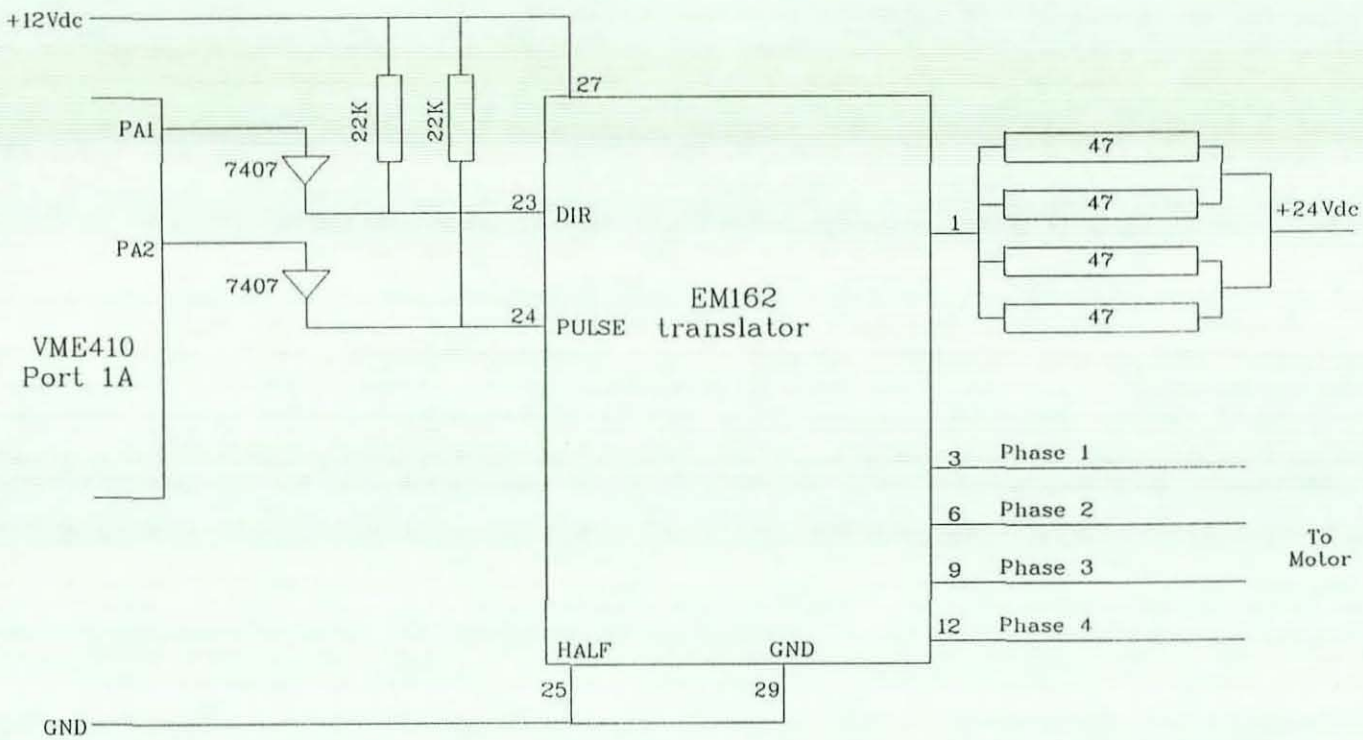

Fig. 5.10 - Stepper motor translator interface circuit

Except for the need to adapt to valve operator characteristics, the two versions of the control software provide exactly the same functions for control and evaluation purposes.

5.4 Assembly of components

The components were assembled to form three combinations as shown in Tab. 5.1. The appropriate control software was loaded to suit the particular hardware configurations. For all combinations, the same length of tubing was kept to ensure a consistent pressure drop relationship to be maintained in order to reduce the amount of uncertainty at this stage. These servo-drives, labelled A, B and C, were represented as specific mathematical models in Chapter 6 and subsequently simulated. The results from testing the servo-drives and simulating the models were compared.

Tab. 5.1 - Assembly of components for servo-drive

Components	Servo-drive		
	A	B	C
Actuator	Asymmetric	Asymmetric	Symmetric
Valve	5-port	5-port	5-port
Valve operator	Stepper motor	Solenoid	Solenoid
Control interface	Translator	12-bit DAC	12-bit DAC
Controller file	ST.AB	M3.AB	M3.AB

5.5 Data acquisition and analysis

The process of data acquisition consisted of 2 parts: the acquisition of data at real time and the transfer of data from target system back to the host. Once the data file was up at the host, the data analysis part could be dealt with later with the simulation software or programs written for special operations.

5.5.1 Transient acquisition

Six sets of transient data were captured in each test. The position data and the two pressure transients were captured directly from the ADC board. The DAC and error transients were captured for the purpose of ascertaining the accuracy of the data.

For the spool location transient, a special memory variable SPLLOC has been kept in the control software to record the current spool location. In the case of stepper motor operated valve, the control software kept track of the spool location value by incrementing or decrementing every time when the controller sent out a pulse to the valve operator.

In the case of solenoid operated valve, since the valve operator/spool mechanism was affected by hysteresis, friction, flow induced force and so forth, the position of the spool was unknown. In order to provide a true position value back to the

system, a miniature displacement transducer, which touched on the spool at the spring end, was installed (Fig. 5.11). The output from the transducer was fed to a signal conditioning circuit (Fig. 5.12) and subsequently acquired by the ADC circuit through the analogue multiplexer.

Due to the limitation of memory on the target system, the velocity and acceleration transients were not stored during test runs. The data were generated by the "EVAL" programme on the host computer instead.

5.5.2 Data transfer to host

Transient data acquired on the target system were transferred to the host (DG MV/10000) via the auxiliary RS232 port. A hand-shaking data recording program "HOST.PR" was written (in FORTRAN) to read the transient data from the line in ASCII format. The files were named as TARGETxx.DAT where xx would be a two-digit number incremented automatically by "HOST.PR" to document the test number.

For the purpose of analysis, supplementary information including run-time settings, timer constants, mean spool location were also transferred. These values could be put into the simulation model as initialising parameters so that both results were generated from the same starting point.

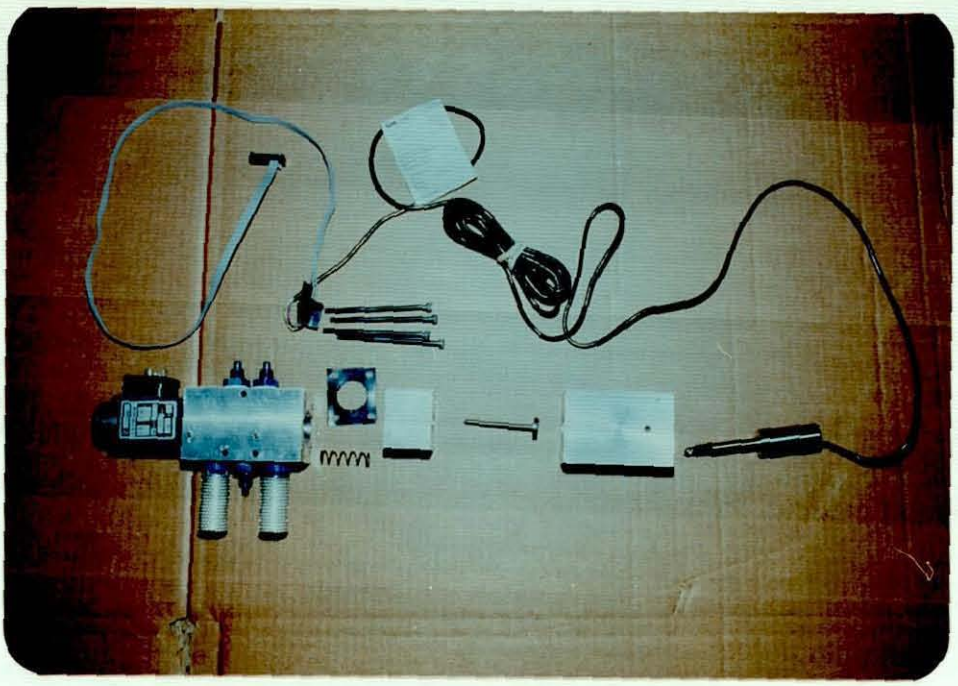

Fig. 5.11 - Photograph of spool location transducer

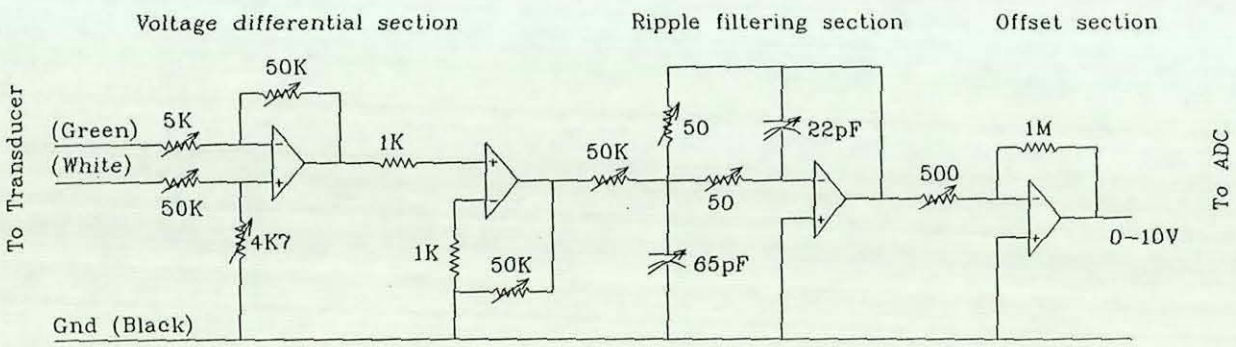

Fig. 5.12 - Signal conditioning circuit for spool transducer

5.5.3 The transient evaluation program (EVAL.PR)

The transient evaluation program extracted the "TARGETxx.DAT" file and transformed the data to numeric format. Two output features were available:

(a) All transients captured on the target system could be plotted with A3 size paper on Hewlett Packard pen plotters. In particular, pressure transients (P_1 and P_2) were put together on one graph which was normally the case to view simulation results. The graphs were made of the same size as those produced by the simulation package CMS2 and could be compared directly.

(b) A text data file could be created containing all the transient data. The file was a formatted ASCII file and can be transferred by "KERMIT" to IBM PC compatibles and then to the Sun workstation.

5.5.4 The response merging program "EVALCMS2"

It was desirable that the results from the test rig could be displayed together with the simulation responses on the same graph. However, due to the different program environment, the data structures on the two systems were different.

In view of the fact that the graphics display utilities on the simulation package were more sophisticated and powerful, it was decided to transform the test rig data to a format suitable for merging with the simulation data file. The merged transient

response file could be manipulated on Sun workstations when the "CMS2" package was executed. The "EVALCMS2" program on Sun accepted an ASCII transient file created by "EVAL.PR" (on DG).

5.6 Summary of test rigs

The main features of the set of test apparatus designed and built specially for this research has been described. The main purpose of these hardware was to provide a specific test environment which would validate part of the generic model of pneumatic mechanisms. Since the components were made from common products available commercially, it was possible to configure several combinations to make up variations in the test rig.

On the software aspects, the control software has been written bearing in mind the need to accumulate and transfer data to host systems for analysis. A series of programs on Data General and Sun machines were written to provide the link between the target system environment and the analysis package. Fig. 5.13 summaries the relationship of the programs in this research. Due to the need to cope with the specific hardware characteristics, two versions of the control software were available. Both versions provided similar features in terms of user interface and control algorithm.

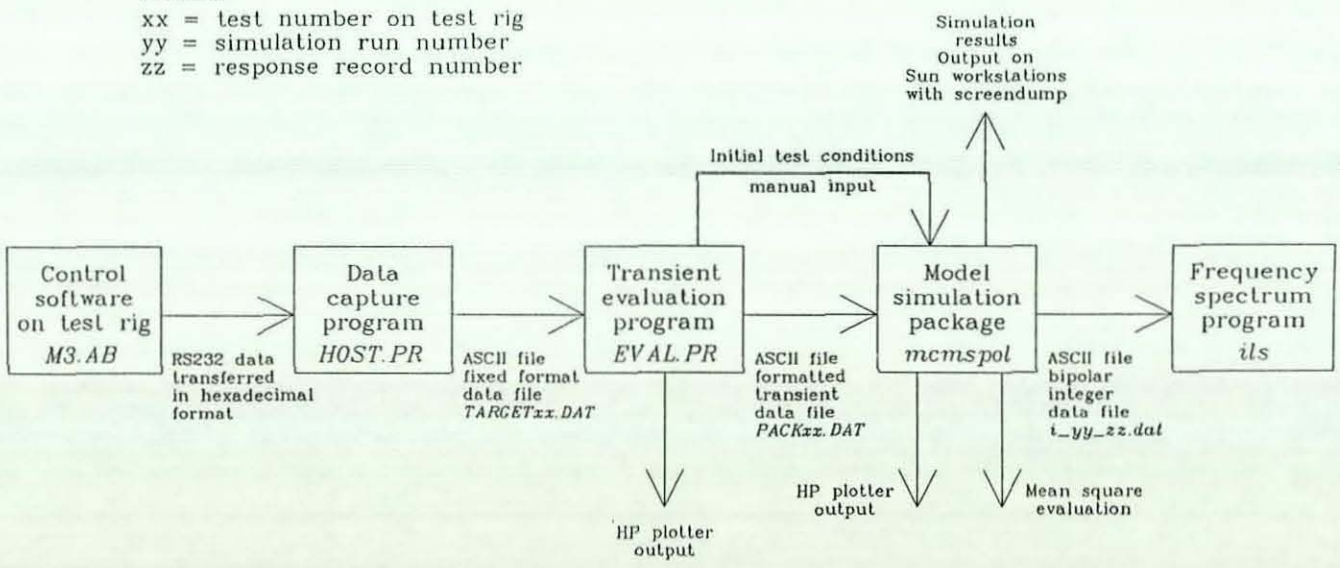

Fig. 5.13 - Relationship of programs

CHAPTER 6

MATHEMATICAL MODEL FOR SPECIFIC COMPONENTS

According to the philosophy of the generic model established in Chapter 4, it is necessary to build the working simulation model of the prototype test rigs in Chapter 5 by modular programming technique. The components were written as independent modules with inter-module linking adapted from the linking variables as defined in the generic model. Auxiliary subroutines and functions in support of the component modules were added but they did not alter the basic structure drastically.

The modularised programme offered the advantage that a change of one module will not affect the operation of the whole model. This approach was proved valuable because during the initial stages of module development, a lot of changes have been made on individual modules but the effect of such changes to the other modules were kept to the minimum.

The differential equations were expressed in state matrix form [6.1] for the purpose of adapting to the Runge-Kutta-Merson integration algorithm. The number of state variables varied between 7 to 9 depending on the configuration of the pneumatic servomechanism.

In addition, alternative component modules were proposed to provide a choice of model complexity. All component modules were programmed as mutually exclusive subroutines if they represented the same component.

6.1 Pneumatic actuator module

Derivation for the equations to describe the behaviour of the pneumatic actuator module relies entirely on the study of charging and discharging processes of air to the controlled volume in the cylinder chambers. The processes are basically polytropic [6.2]. Application of this type of thermodynamic analysis to pneumatic servo-controlled system was initiated by the foundation research of Shearer [6.3] based on the principles of thermodynamics of compressible fluid flow. His work was extended by many authors including Cutland [6.4] and Burrows [6.5] on the study of pneumatic servomechanism with on-off valves, Bowns et al [6.6] on the transient performance of pneumatic actuator valve combination, Chitty et al [6.7] on the loaded double acting actuator. A standard procedure of perturbating the differential equations and then linearising to obtain a transfer function has been established. The analysis method led to characteristic equations ranging from second to fourth order which could be used for devising control algorithms to cope with the non-linearities in the pneumatic system.

However, the assumption made in the perturbation method that the derivation from equilibrium point should be small contains

inherent error if the analysis is extended to cover the full stroke of the actuator. Burrows [6.8] showed that the characteristic equation to describe a symmetric pneumatic servo-actuator was of the fourth order and the coefficients varied with the position of the actuator. It was also noted that the linearised analysis was only valid for small perturbations about the initial position (where the coefficients were determined).

The limitation imposed by the traditional approach on the analysis is not acceptable in this research. The requirement that the model should be valid over the whole stroke range demands a more general approach to derive the describing equations. The forms of pneumatic actuators can vary from the commonly used double acting cylinder to pneumatic motor.

6.1.1 Actuator dynamics

The following analysis refers to the asymmetric actuator component for parameter visualisation purpose and can be generalised to include single acting asymmetric or double acting symmetric cylinders. Fig. 6.1 illustrates diagrammatically the relationship of the chambers and inlet connections. The assumptions made in the derivation are:

(a) The heat loss to the environment including cylinder and tubing walls is ignored;

(b) Kinetic energy of air in cylinder chambers is negligible;

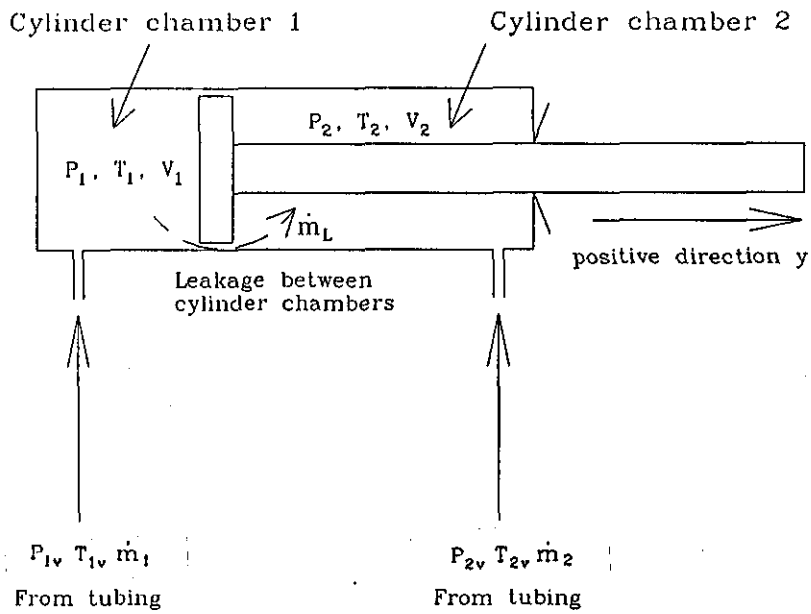

Fig. 6.1 - Schematic diagram of chambers and inlet connections

(c) The polytrope gas model is adopted [6.9]. Unlike the traditional analysis, the effect of air flow at source and leakage through piston gap are included to produce a complete solution;

(d) The state conditions of air, such as pressure and temperature, in the bounded volume are homogeneous. For instance, the pressure at the inlet is the same as that near the piston in the same cylinder chamber.

Consider the control volumes in the cylinder chambers. Applying the adiabatic energy equation $dH - dW = dU$ (with $dQ = 0$) and assuming that $P_1 > P_2$, for chamber 1, if the flow comes from the valve, the equation can be expressed in terms of enthalpy,

$$\dot{m}_1 C_p T_{1v} - \dot{m}_{L1} C_p T_1 - P_1 \frac{dV_1}{dt} = \frac{d}{dt}(C_v \delta_1 V_1 T_1) \qquad (6.1)$$

The first term indicates in flow of energy from supply. The second term denotes leakage mass flow from chamber 1 to chamber 2. The third and right hand side terms represent work and internal energy respectively. The leakage flow will be discussed in more details in Section 6.1.2.

If the flow $\dot{m}_1$ is negative, so that air flows out of the cylinder chamber, the energy source of the first term at left hand side is changed. The enthalpy equation becomes

$$\dot{m}_1 C_p T_1 - \dot{m}_{L1} C_p T_1 - P_1 \frac{dV_1}{dt} = \frac{d}{dt}(C_v \delta_1 T_1 V_1) \qquad (6.2)$$

In either case, the right hand side can be simplified as

$$C_v \delta_1 V_1 T_1 = \frac{C_v}{R} P_1 V_1 = \frac{P_1 V_1}{n - 1} \tag{6.3}$$

Eqn (6.1) and (6.2) become

$$\dot{m}_1 C_p T_{1v} - \dot{m}_{L1} C_p T_1 - P_1 \dot{V}_1 = \frac{d}{dt} \left(\frac{P_1 V_1}{n - 1}\right) \tag{6.4}$$

$$\dot{m}_1 C_p T_1 - \dot{m}_{L1} C_p T_1 - P_1 \dot{V}_1 = \frac{d}{dt} \left(\frac{P_1 V_1}{n - 1}\right) \tag{6.5}$$

Rearranging terms, the equations become

$$\dot{m}_{L1} nRT_1 + \dot{P}_1 V_1 + nP_1 \dot{V}_1 = E_1 \tag{6.6}$$

where $E_1 = \begin{cases} nRT_{1v} \dot{m}_1 & \text{if } \dot{m}_1 \geq 0 \\ nRT_1 \dot{m}_1 & \text{if } \dot{m}_1 < 0 \end{cases}$

The assumption $P_1 > P_2$ in the foregoing derivation is only partially true. If $P_2 > P_1$, the leakage flow direction is reversed. Eqn (6.6) is modified:

$$\dot{m}_{L2} nRT_2 + \dot{P}_1 V_1 + nP_1 \dot{V}_1 = E_1 \tag{6.7}$$

where the first term represents energy flow from chamber 2 to chamber 1 due to the higher pressure P_2. Similarly, for chamber 2, if $P_1 > P_2$

$$\dot{P}_2 V_2 + nP_2 \dot{V}_2 - \dot{m}_{L1} nRT_1 = E_2 \tag{6.8}$$

where $E_2 = \begin{cases} nRT_{2v} \dot{m}_2 & \text{if } \dot{m}_2 \geq 0 \\ nRT_2 \dot{m}_2 & \text{if } \dot{m}_2 < 0 \end{cases}$

If $P_2 > P_1$, Eqn (6.8) becomes

$$\dot{P}_2 V_2 + nP_2 \dot{V}_2 - \dot{m}_{L2} nRT_2 = E_2 \tag{6.9}$$

Eqn (6.6) - (6.9) relate the changes of the air properties in the 2 cylinder chambers to the mass flow rates from the flow control device (the valve). There are 4 unknowns in these equations: P_1, T_1, P_2 and T_2, whereas effectively only two independent equations exist:

$$\dot{P}_1V_1 + nP_1\dot{V}_1 + \dot{m}_L nRT_L = E_1 \tag{6.10}$$

$$\dot{P}_2V_1 + nP_2\dot{V}_2 - \dot{m}_L nRT_L = E_2 \tag{6.11}$$

where $\dot{m}_L$ = effective leakage mass flow rate depending on relative values of P_1 and P_2

T_L = effective temperature of leakage flow source

To find the extra equations, consider the air in control volume of chamber 1,

$$R = \frac{P_1V_1}{m_1T_1}$$

Differentiating

$$\frac{m_1T_1(\dot{P}_1V_1 + P_1\dot{V}_1) - (\dot{m}_1T_1 + m_1\dot{T}_1)P_1V_1}{(m_1T_1)^2} = 0 \tag{6.12}$$

Rearranging,

$$\frac{P_1V_1}{m_1T_1} = \frac{\dot{P}_1V_1 + P_1\dot{V}_1}{\dot{m}_1T_1 + m_1\dot{T}_1} = R$$

$$\text{then} \quad P_1\dot{V}_1 + \dot{P}_1V_1 = R(\dot{m}_1T_1 + \dot{T}_1\frac{P_1V_1}{RT_1}) \tag{6.13}$$

Combining with the energy equations (6.10) and (6.11),

$$E_1 - (n-1)P_1\dot{V}_1 = R(\dot{m}_1T_1 + \dot{T}_1\frac{P_1V_1}{RT_1}) + \dot{m}_L nRT_L \tag{6.14}$$

Expressing in the first order form,

$$\dot{P}_1 = \frac{E_1 - nP_1\dot{V}_1 - \dot{m}_L nRT_L}{V_1} \tag{6.15}$$

$$\text{and} \quad \dot{T}_1 = \frac{T_1}{P_1V_1}(E_1 - R\dot{m}_1T_1 - (n-1)P_1\dot{V}_1 - \dot{m}_L nRT_L) \tag{6.16}$$

Similarly, considering the control volume in chamber 2,

$$\dot{P}_2 = \frac{E_2 - nP_2\dot{V}_2 + \dot{m}_L nRT_L}{V_2} \tag{6.17}$$

$$\dot{T}_2 = \frac{T_2}{P_2V_2}(E_2 - R\dot{m}_2T_2 - (n-1)P_2\dot{V}_2 + \dot{m}_L nRT_L) \tag{6.18}$$

It should be noted that the leakage term is the same in Eqn (6.15) - (6.18). The volumes V_1 and V_2 are calculated from the cylinder geometry:

$$V_1 = A_1\, y \tag{6.19}$$

$$V_2 = A_2\,(L - y) \tag{6.20}$$

Due to the fact that at the end stroke positions, i.e. when

$$y = 0 \text{ or } y = L$$

there still exists some residual volume in the tubing (and perhaps the cylinder inlets), a small constant is added to the Eqn (6.19) and (6.20).

$$V_1 = A_1y + V_{R1} \tag{6.21}$$

$$V_2 = A_2(L - y) + V_{R2} \tag{6.22}$$

The values of V_{R1} and V_{R2} need not be the same. The rate of change of volumes $\dot{V}_1$ and $\dot{V}_2$ are related to the velocity of the actuator y:

$$\dot{V}_1 = A_1\,\dot{y} \tag{6.23}$$

$$\dot{V}_2 = -A_2 \dot{y} \tag{6.24}$$

The actuator module can then be formulated as shown in Fig. 6.2. The force delivered by the actuator is given by

$$F_a = P_1A_1 - P_2A_2 - P_eA_{R2} \tag{6.25}$$

The input variables for the actuator module are identified from Eqn (6.15) - (6.18) as mass flow rates $\dot{m}_1$, $\dot{m}_2$, and from Eqn (6.23) - (6.24) as $\dot{y}$. The air volume conditions such as P_1, P_2, T_1, T_2, T_{1v}, T_{2v} are generated by the actuator as a result of energy input and were passed to connecting components as output variables. In case of symmetrical cylinder, the areas A_1 and A_2 are equal and A_{R2} is zero.

6.1.2 Internal leakage

The internal leakage represents the small amount of air flow from the high pressure chamber to the low pressure chamber of the cylinder through any gap between the piston seal and cylinder. The leakage is always ignored in the derivations of other researchers because it complicates the mathematical model significantly. The component oriented approach adopted in this research introduces the complexity into the actuator module but does not require substantial mathematical manipulation. The term has been included in the derivation of Eqn (6.6) - (6.9).

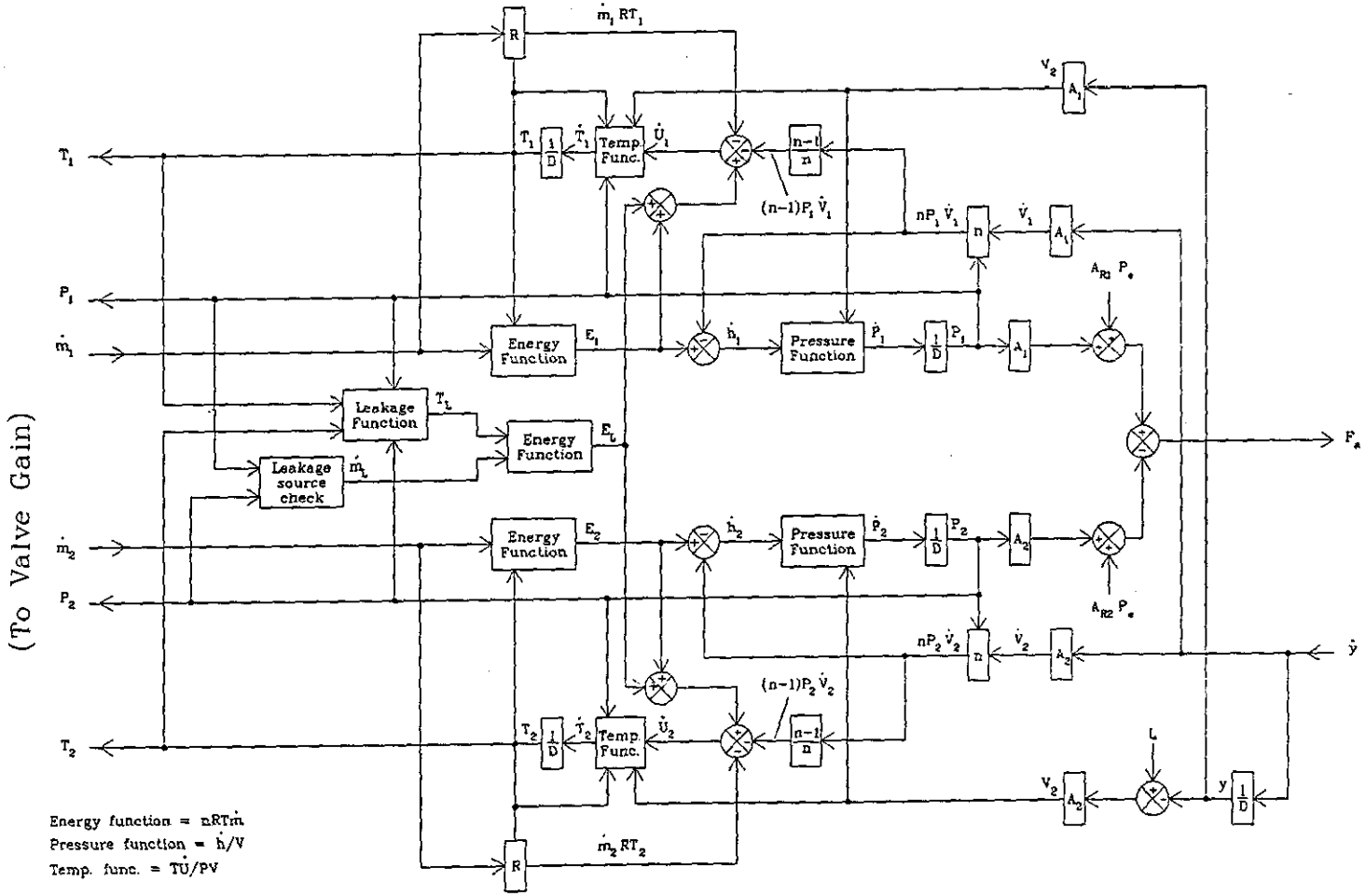

Fig. 6.2 - Actuator module block diagram

Two models have been considered for the internal leakage. As a rule of thumb, the leakage flows from the high pressure chamber to low pressure chamber. The direction is considered positive if it flows from chamber 1 to chamber 2. The choice of model is governed by an integer flag set in the interactive part of the package.

6.1.2.1 Laminar flow model

When the pressure difference between the two cylinder chambers is not significant, the change of density of air from one chamber to another can be regarded as negligible. The leakage flow therefore resembles the flow of hydraulic fluid through journal bearing and the incompressible laminar flow Bernoulli's equation [6.10] can be applied. The equation for leakage from chamber 1 can then be expressed as

$$\dot{m}_{L1} = K_L(P_1 - P_2) \qquad (6.26)$$

where K_L = the coefficient of mass flow leakage which represents a lumped constant for values of viscosity, leakage gap size and passage length

Similarly, if $P_2 > P_1$, leakage comes from chamber 2,

$$\dot{m}_{L2} = K_L(P_2 - P_1)$$

$$= - \dot{m}_{L1} \qquad (6.27)$$

The advantage of this model lies at its simplicity. The only consideration needed to be taken is the direction of flow which is automatically determined in the pressure difference calculation.

On the contrary, the model suffers from not being able to deal with large pressure differences accurately.

6.1.2.2 Adiabatic flow model

The leakage of fluid through narrow channels has been investigated by Egli [6.11]. A general formula derived from the fundamantal principle of one-dimensional adiabatic flow has been formulated to describe the leakage mass flowrate

$$\dot{m}_L = \sigma F P_o / \sqrt{(RT_o)} \qquad (6.28)$$

where σ = dimensionless mass flowrate

$= \sqrt{[(1 - r_L^2)/R_{ch}]}$

F = cross-sectional area of gap

P_o = pressure at source

T_o = temperature at source

R = gas constant

r_L = pressure ratio of destination to source

R_{ch} = channel resistance which is constant for the channel

In the case of leakage from chamber 1 to chamber 2,

$$\sigma_{L1} = \sqrt{\{[1 - (P_2/P_1)^2]/R_{ch}\}}$$

$$\dot{m}_{L1} = \sigma_{L1} F P_1 / \sqrt{(RT_1)} \qquad (6.29)$$

whereas the reverse flow is

$$\sigma_{L2} = \sqrt{\{[1 - (P_1/P_2)^2]/R_{ch}\}}$$

$$\dot{m}_{L2} = -\sigma_{L2} F P_2 / \sqrt{(RT_2)} \qquad (6.30)$$

The negative sign in Eqn (6.30) indicates that the flow goes from

chamber 2 to chamber 1. The value of R_{ch} is given by

$$R_{ch} = L_{nh}(s/h)$$

where L_{nh} = dimensionless resistance coefficient independent of compressibility of fluid

s = length of leakage passage

h = clearance of passage

It is difficult to measure the exact value of R_{ch} because of the uncertainties in determining the clearance "h" and the equivalent length "s" of the passage. However, it can be estimated based on an understanding of the physical dimension of the piston and referencing to the data presented by Egli. According to the dimensions of the actuator, a reasonable estimation of the values is:

$$s = 0.010 \text{ m}$$

$$h = 0.00001 \text{ m}$$

and from Egli's graphs, $L_{nh} = 0.02$

from which $R_{ch} = 20$

This value is substituted into the appropriate constant in the simulation.

6.1.3 Summary of actuator module

The actuator module is formulated by considering the compressible air flow into the two chambers of a cylinder. The asymmetric cylinder is the general case from which the model equations Eqn (6.15) to (6.18) are derived. The symmetric cylinder is the particular case by setting A_{R2} to zero and therefore does not require any special derivation. The problem of

leakage can be studied by two models: the laminar and adiabatic flow. Tab. 6.1 summaries the special features of the actuator module being modelled. The digital simulation evaluation procedure is most helpful in this respect.

Tab. 6.1 - Features included in the actuator module

Feature	Modelled by	Eqn No.
Source of air flow to control volume	$E_i = \begin{cases} nRT_{iv}\dot{m}_i & \text{if } \dot{m}_i \geq 0 \\ nRT_i\dot{m}_i & \text{if } \dot{m}_i < 0 \end{cases}$ where i=1,2	(6.6) to (6.9)
Leakage across chamber	$\dot{m}_L nRT_L$	(6.10) and (6.11)
Residual volume	V_{R1}, V_{R2}	(6.21) and (6.22)
Laminar leakage model	$\dot{m}_L = K_L(P_1-P_2)$	(6.10) and (6.11)
Adiabatic leakage model	$\dot{m}_L = \sigma F P_o/\sqrt{(RT_o)}$	(6.28)

6.2 Load module

The load module describes the behaviour of the drive mechanism, including the slideway, ram and attaching mass, under the influence of actuator force F_a. The total mass of the load is accelerated by the net force after deducting dry friction, viscous friction and any opposing weight. The mechanism then determines the velocity and position of test rig after integration of the acceleration.

The dynamics of the components can be formulated in the most general case:

$$F_a = M_p\ddot{y} + L_e + F_r + F_g + K_c\dot{y} \qquad (6.31)$$

where

(a) L_e is the end stop force determined in Section 6.2.2.

(b) F_g represents the dead weight of the load system. It is always in the same direction. For most analysis cases in this research, the cylinder is placed horizontally and hence F_g is zero.

(c) F_r represents the dry friction as discussed in Section 6.2.1

(d) $K_c\dot{y}$ represents the viscous friction due to lubricating oil. The value of K_c is estimated based on the published viscosity data of the oil [6.12].

Eqn (6.31) is transformed to the load module as shown on Fig. 6.3.

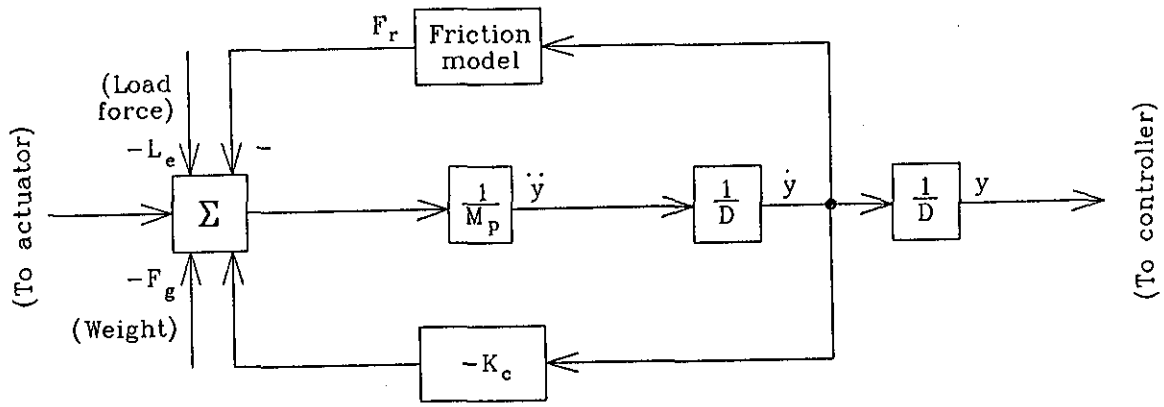

Fig. 6.3 - Load module block diagram

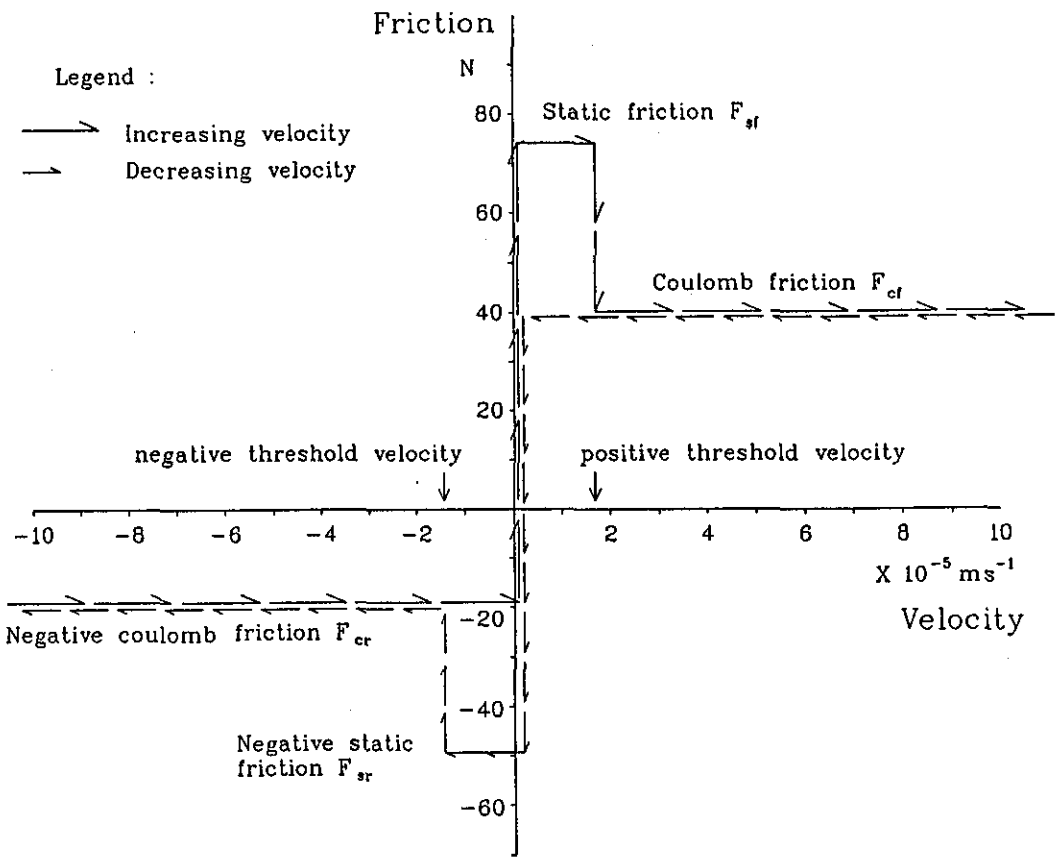

Fig. 6.4 - Graphical description of friction model

6.2.1 Static and coulomb frictions

The effect of seal friction in pneumatic actuators has been studied by Bowns et al [6.13] and an empirical formula was proposed for analytical purposes. Working on electro-hydraulic servo-systems, Chiappalini [6.14] summarised friction phenomenon in several friction models for a variety of contact materials and surfaces. For the pneumatic cylinder in this resarch, the boundary friction model which is suitable for the 'O'-seal of the cylinder and standard lubricating oil has been adopted. The model is simplified to obtain the more commonly used threshold model for ease of programming and visualisation [6.15]. However, friction tests on the test rig showed that the frictional values during actuator extend was larger than when it retracted (see Section 7.1.3.1). This is mainly due to the design of the piston seal which adheres more tightly to the cylinder bore during forward movements. The phenomenon requires a modification of Coulomb's model to allow for a different set of friction coefficients at positive (extend) and negative (retract) actuator velocity.

Fig. 6.4 is a graphical description of the friction model used in the research. The static and coulomb friction values for forward and reverse moves are entered independently at interactive mode. A supplementary routine implementing the model returns the current friction value according to the magnitude of input force, direction of movement and the immediate past friction. The subroutine is also used by the spool operator module (Section 6.4.3) to determine the friction on spool in the pneumatic valve.

6.2.2 End-stop problems

In the traditional pneumatic system analysis, the fundamental assumption made due to small perturbation analysis method was that all moves were small. Such move limitation assumption does not apply to the simulation in this research. The model must be able to deal with all movements in the physically possible stroke of the cylinder so that the pneumatic servomechanism designer can investigate extreme and even open loop cases.

In order to ensure that the actuator will not go beyond its end positions during the computer simulation, it is necessary to devise a means to keep its position value within the stroke length. However, it is forbidden in the package to change the value of state variables (X) within the model equation call because of the tracking requirement within the simulation package. In other words, the limit checking feature cannot be done by simple mathematical restriction. The problem is tackled by considering the mechanics when the actuator reaches its end. The physical boundary of the cylinder has a high stiffness equivalent to the material elastic modulus and delivers a large force which rebounces the piston. The phenomenon is then programmed as part of the load module to introduce a large opposing force for any penetration action of the piston into the ends.

Unfortunately, it was found that if the actuator moves at a

high speed towards the end-stop, the large end stiffness cannot stop the actuator fast enough to prevent further movement. Further penetration of the actuator into the cylinder end increases the end stop force to an unjustified level leading to data handling problem. This imposes large error in the integration routine and sometimes leads to a failure of the system. On the contrary, if the actuator moves slowly near the end, the reaction stiffness stops it immediately just at the end. In this case, the reaction stiffness value still applies resulting in an unnecessary re-bounce.

The problem is tackled by putting additional velocity and acceleration checks of the load module. The concept behind is to provide the end stop elastic force if the actuator is moving into the cylinder body. If the actuator retreats from the penetration, end stiffness is not applied. The routine is implemented as follows:

At the cylinder extended state,

(a) If $\dot{y} > 0$, $L_e = K_e y_e$

(b) If $\dot{y} = 0$, and if $\ddot{y} \geq 0$, $L_e = K_e y_e$

if $\ddot{y} < 0$, $L_e = 0$

(c) If $\dot{y} < 0$, $L_e = 0$

where $\dot{y}$ = Actuator velocity

$\ddot{y}$ = Actuator acceleration

K_e = End stop stiffness

y_e = Penetration to cylinder body

L_e = End stop force

The same concept is applied to the case when the actuator is at the retracted end. The direction of velocity, acceleration and forces are taken care by the sign of the values.

6.3 Controller module

The component oriented approach separates the controller from the pneumatic system and allows a more accurate functional matching to be done. The following analysis differs from the traditional methods [6.16, 6.17] by which the controller signals were mixed in the final transfer function and did not allow variable gain schemes to be modelled.

The controller module deals with the functions of processing and sampling of data within the model. It consists of the main routine "CTRL" and several supporting subroutines. The module has been written along with the establishment of the testing hardware and a consistency of the functions on the software module with those on the test rig has been maintained. Direct comparison can then be made on the position, velocity, spool location, pressure and actuator force responses obtained from actual experiments and simulations.

Three controller component modules are available each of which is mutually exclusive and selectable by a flag before starting the simulation run. The components describe different

types of systems which may exist by a substitution of physical components. The linking of the controller module to the system model is defined with reference to the electronic signal flow within the microprocessor kernel.

6.3.1 Continuous system

The continuous system controller module simulates the use of analogue or high speed digital controllers. In the latter case, the module regards the system to be continuous if the sampling time is less than 1 micro-second. It can also be used by setting an integer flag which forces slower digital controllers to be assumed as continuous for quick model reference or simplification.

The module takes in position information and feeds the values directly to the gain calculation routine to determine the spool signal, viz, controller information is updated continuously. No interrupt is required except that if the closed loop forced exit condition is enabled, an interrupt is serviced at time out and a new desired position is put into the working variable.

6.3.2 Discrete system

The discrete mode is generated by 2 interrupts in the simulation package. The first interrupt simulates the sampling effect of a digital controller, whereas the second interrupt is aimed at producing a time lag simulating the time required for the

controller to determine appropriate command signal output.

At first interrupt time, the position value (X_4 in the programme) is recorded. Subsequent codings are added to produce other information including position error, gain values, velocity and acceleration are also generated in the same way as on the physical system. Two arrays each of 80 elements are maintained to match the operation on the target software.

At second interrupt time, the position dead band and forced loop exit condition are checked. If one of the exit conditions is met, a new desired position is placed into the working command position variable which will be in effect at the next interrupt moment. Fig. 6.5 illustrates the timing relationship of the two interrupts. Otherwise, the spool command signal is determined from the position error calculated in the last interrupt time.

Subsequent processing for the spool signal output depends on the hardware to be controlled. There are fundamental differences in the control method of a stepper motor valve operator and a solenoid valve operator as described in subsequent sections.

6.3.2.1 Discrete controller for stepper motor operator valve

The discrete controller for stepper motor operated valve simulates the action of the microprocessor controller with the software for stepper motor valve operator.

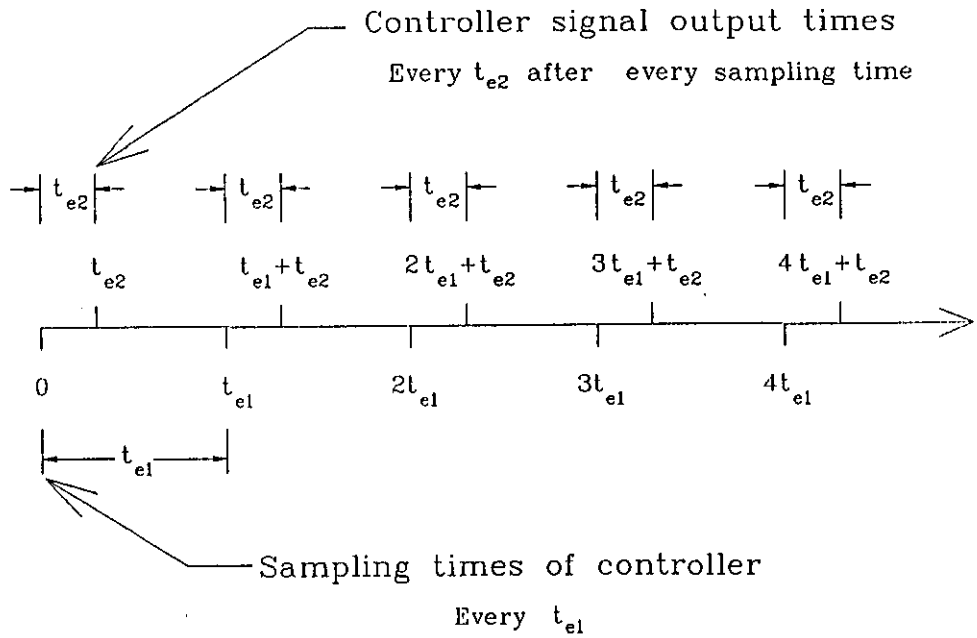

Fig. 6.5 - Timing relationship of controller interrupts

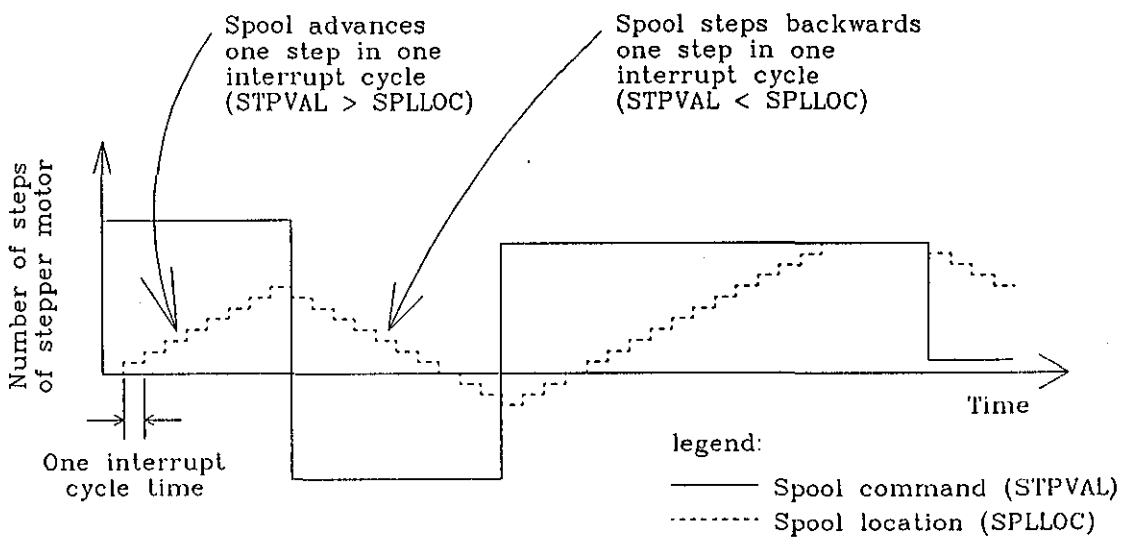

Fig. 6.6 - Diagram of stepper motor valve in open loop mode

At second interrupt time, the appropriate spool command is determined according to the control algorithm implemented on the target system. The desired spool location is governed by the maximum spool displacement attainable in the valve (n_{xmax}).

$$n_{STPVAL} = \min (|n_{SPLCOM}|, n_{xmax}) * \text{sign} (n_{SPLCOM})$$

where n_{SPLCOM} = spool command generated from control algorithm

n_{STPVAL} = the desired spool location to be achieved as a result of the spool command.

The difference between the commanded spool location (n_{STPVAL}) and the current spool location (n_{SPLLOC}) then indicates the direction of the required spool movement.

In addition, due to the difficulty to match the timing of motor in the simulation, the target software has been programmed to set only one pulse to the stepper motor at each sampling cycle. This action is simulated in the module by passing a spool signal of only one step change at the second interrupt time. The direction of the step change spool signal depends on the sign of the difference between n_{STPVAL} and n_{SPLLOC}.

The relationship of spool command and spool location is illustrated in Fig. 6.6

6.3.2.2 Discrete controller for solenoid spool operator

The discrete controller for solenoid spool operator simulates

the action of the microprocessor controller with the software for solenoid spool operator.

At second interrupt time, the appropriate spool command is determined in the same way as the stepper motor valve operator module. Since the target hardware can output the signal value through the digital-to-analogue converter almost instantaneously, the module emulates the action by simply passing command value to the succeeding component module.

The spool command value is checked against 2048 which corresponds to the range of the 12 bit digital-to-analogue converter. The spool signal output is:

$$X_C = \min(|n_{SPLCOM}|, 2048)/2048 * X_{max} * \text{sign}(n_{SPLCOM})$$

where X_{max} = maximum one side spool displacement in valve.

6.3.3 The control functions

The spool command processors are the supporting routines for the three controller modules. They are written as separate routines in order to cater for any changes in the control algorithm in the control software on the test rig. The interfaces between the controller modules and these routines are standardised to be position error, velocity and acceleration as input, and un-conditioned gain values returned from the routines as output. The gains are then manipulated in the calling modules to suit specific requirements of the component.

Four gain algorithms have been programmed including proportional control, variable dead band gain, positional gain contour and minor loop compensation. In the continuous system module, the current actuator velocity and acceleration are used. In the discrete controller module, the velocity values are derived from the difference of position samples and subsequently acceleration values as derived from the velocity values.

The final spool command value is determined by the equation:

$$n_{SPLCOM} = (n_{pg} - n_v * K_v - n_a * K_a)/L_{DAC}$$

where n_{pg} = positional gain

n_v, n_a = velocity and acceleration values

K_v, K_a = velocity and acceleration gain coefficients

The denominator L_{DAC} is a sizing factor introduced to reduce the spool command value to a reasonable level so that sufficient portion of the cylinder stroke is influenced by the gain algorithm. This value is decided by trial and error on the test rig to be:

(a) 65536 (equivalent to shifting 16 bits) on the controller for stepper motor spool operator

(b) 256 (equivalent to shifting 8 bits) on the controller for solenoid spool operator.

In addition, in order to investigate the pure pneumatic responses, an open loop mode selection flag is maintained to simulate the same feature on the test rig control software. The coding was done by simply disabling the position error information

to be passed to the gain calculation routine "KPPROF". The open loop function is available for all controller modules.

6.3.4 Summary of controller

Two major classes of controller are identified. The continuous system controller module is simple and fast to evaluate. It does not have any digitisation action on the information of position, velocity and so on. The discrete system controller makes use of two interrupts in the CMS2 software. The first interrupt facilitates sampling of position and calculation of position error. The second interrupt performs the command output to the spool operator.

Due to the difference of the nature, the discrete controller is further sub-divided into the controller for solenoid and that for stepper motor operated valves. Choice of these modules are done by setting a module flag. Tab. 6.2 summaries the features of the controller being implemented as separate modules.

Tab. 6.2 - Summary of controller module features modelled

Feature	Modelled by	Described in Section
Continuous controller simulating fast or analogue controller	Continuous position feedback from actuator module	6.3.1
Discrete controller with solenoid valve operator	Two event interrupt with second step simulating time delay for output due to computation	6.3.2.2
Discrete controller with stepper motor valve operator	Two event interrupt with second event as single pulse output time control	6.3.2.1
Minor loop compensation control algorithm	Use of K_v, K_a	6.3.3
Gain scheduling control algorithm	Use of gain profile K_p with 256 elements	Appendix IX
Proportional position gain control algorithm	K_p use as a constant (array disabled)	6.3.3
Open loop control for testing of pure pneumatic responses	Position error value in controller disabled to be passed to gain calculation routine	6.3.3

6.4 Valve operator module

The valve consists of two parts. The valve body comprising of the spool and sleeve is modelled in terms of valve gain characteristics which is part of the pneumatic system. The valve operator is the device controlling the position of the spool. It receives signal command information from the control module and produces spool displacement proportional to the command signal.

Three valve operator modules are available: two for the solenoid operated valve and one for the stepper motor operated valve. In the former case, the solenoid accepts electrical signal in 0 - 1A to produce a total core displacement of 2 mm. For simplification purpose, the electrical signal is referenced as a proportional spool location signal in the range of ±1 mm.

On the contrary, the stepper motor takes in pulses which are transformed to rotary steps by the motor. A lead screw which is fixed on the motor shaft moves with a step length of 0.0125mm.

6.4.1 Stepper motor valve operator model

The stepper motor valve operator module simulates the action of the stepper motor when a step signal is received. The current implementation assumes that the stepper responds to the input signal immediately. Other physical phenomena specific to stepper motor actuator such as acceleration and deceleration ramp are not incorporated both on the test rig and the model.

6.4.2 Empirical solenoid valve operator model

Due to the new design of the valve, literature on the dynamic response of the solenoid operated valve is not available. Reference to similar servo-controlled systems [6.18] reveals that a first order lag would be appropriate for each of the solenoid and spool response. The product of the two parts then forms a second order dynamics. It was also pointed out that for servo-valve with frequency higher than 50 Hz, a third order response is more desirable [3.28]. A preliminary test on another valve of the same make indicates that the natural frequency of the solenoid-spool mechanism lies in the range of 20-50 Hz [6.19].

Based on these considerations and a second order model suggested by Bell et al [6.20], the empirical model is evolved as a damped spring-mass mechanism. If X_s represents the spool displacement from the null (or neutral) position, and X_c is the command in force at that moment, the acceleration of the spool from the current displacement to the commanded position should be proportional to the spool error. The motion of the spool is damped by the viscous lubrication proportional to spool velocity. Thus,

$$\ddot{X}_s = K_s (X_c - X_s) - K_d * \dot{X}_s \qquad (6.32)$$

where K_s and K_d are coefficients to be determined experimentally. The value of X_c will vary according to the actuator position and changes as a function of the position error when the actuator

moves.

The non-linearities in the servo-valve mechanism have been studied with reference to servomotor control systems by Hattori et al [6.21]. It was concluded that such non-linearities comprising mainly of coulomb friction and hysteresis could be suppressed with dither superimposed on the system input. The dither signal is modelled as superposition on the spool displacement output from Eqn (6.32). Similarly, a hysteresis (Section 6.4.5) routine which deals with the magnetic hysteresis is included to modify the computed spool displacement X_s. Both superposition modifies a variable local to the model rather than the state variable X_s which affects the operation of the integration routine.

6.4.3 Analytical solenoid spool manipulator model

The analytical solenoid spool operator model is evolved by looking at the fundamental force elements acting on the spool. Using the same spool displacement notation as in Section 6.4.2 and referring to the force diagram on Fig. 6.7, the equation of motion of the spool is given by:

$$G_s X_c = M_s \ddot{X}_s + K_d \dot{X}_s + K_{sp} X_s + F_i + F_{ind} + F_{sf} + F_{se} \qquad (6.33)$$

The values of the solenoid constant G_s, spring constant K_{sp}, initial spring compression F_i are found by actual measurements on the valve.

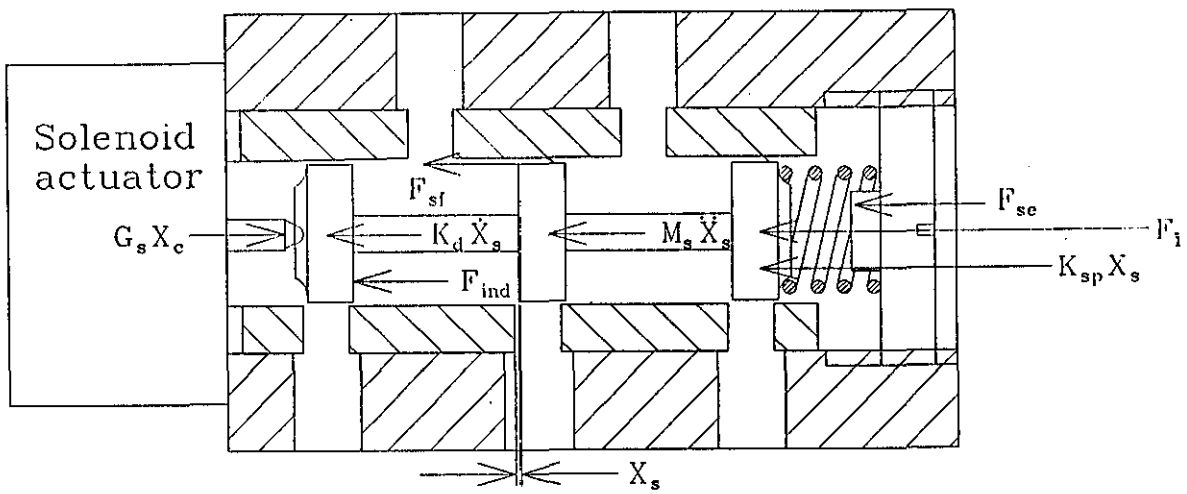

Fig. 6.7 - Force diagram in solenoid valve

The spool end stop load F_{se} is given as a reasonably large number to stop the spool in the same way as described in Section 6.2.2. In fact, the same set of coding is used with all parameters referring to the spool instead.

The flow induced force F_{ind} is the resultant flow induced force on the spool due to air flowing through the valve lands. Two models, which are selectable by a choice of model flag, are available as discussed in Section 6.4.4.

The dither signal is modelled as a superimposed modification of the value of X_c which represents the total input to the valve. Similarly, the hysteresis routine modifies X_c to reflect the magnetic force reduction due to material property. The variable X_s and its derivative are programmed as two state variables to be integrated by the package.

The coulomb friction model used in Section 6.2.1 is adopted to describe the dry friction in the valve. The values of static and coulomb frictions are found from simple pull test on the spool-sleeve assembly.

6.4.4 Flow induced forces

Flow induced forces arise from the change in momentum of the fluid in the valve lands. Its direction is always trying to close the valve. Two models are proposed. Due to the rigidity of the

lead screw mechanism of the stepper motor valve operator, flow induced forces only affects the solenoid valve.

6.4.4.1 Experimental formulae

Louis and Logan [6.22] studied the in-valve and out-valve flow forces and expressed the forces as two 12 term-polynomials dimensionless flow force with the dimensionless spool displacement as the independent variable. The action of the forces depend on the direction of the flows. Referring to Fig. 6.8, if C_{Fin} and C_{Fout} represent the dimensionless flow forces for in-valve and out-valve flows respectively, the flow induced force for the whole spool is:

$$F_{ind} = [(C_{Fin}(P_{sv}-P_{n1})-C_{Fin}(P_{sv}-P_{n2})]A_{vp} \quad \text{if } \dot{m}_1 \geq 0 \text{ and } \dot{m}_2 \geq 0$$

$$F_{ind} = [(C_{Fin}(P_{sv}-P_{n1})+C_{Fout}(P_{n2}-P_{2v})]A_{vp} \quad \text{if } \dot{m}_1 \geq 0 \text{ and } \dot{m}_2 < 0$$

$$F_{ind} = [(C_{Fout}(P_{n1}-P_{1v})-C_{Fin}(P_{sv}-P_{n2})]A_{vp} \quad \text{if } \dot{m}_1 < 0 \text{ and } \dot{m}_2 \geq 0$$

$$F_{ind} = [(C_{Fout}(P_{n1}-P_{1v})+C_{Fout}(P_{n2}-P_{2v})]A_{vp} \quad \text{if } \dot{m}_1 < 0 \text{ and } \dot{m}_2 < 0 \qquad (6.34)$$

where A_{vp} respresents the flow path area in valve $= \frac{\pi}{4}(D^2_s - D^2_{sp})$

P_{n1}, P_{n2} are the air pressures in flow nodes 1, 2

P_{1v}, P_{2v} are the air pressure at valve port 1, 2

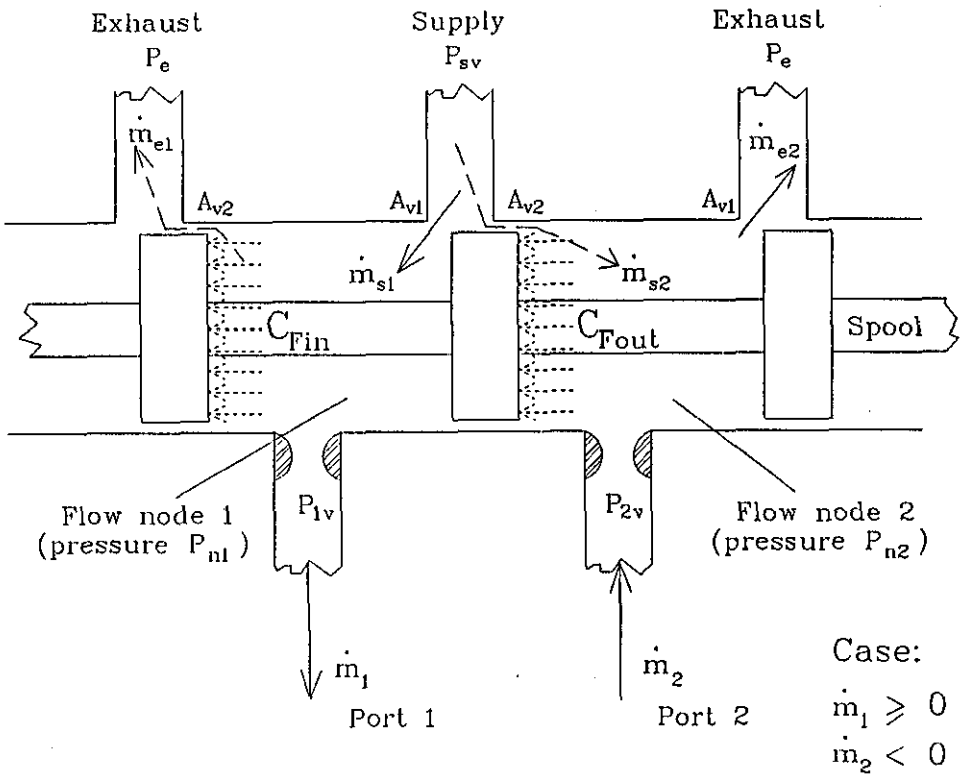

Fig 6.8 - Flow force coefficient due to Louis and Logan

6.4.4.2 Theoretical formulae

Flow induced forces had been a serious error source for hydraulic servomechanisms. Lee and Blackburn [6.23] derived the theoretical formula for hydraulic spool valve based on the momentum changes of oil flow through spool land. The analysis in Appendix III is an extension of the hydraulic derivation to take care of the compressibility of air. For chamber 1 , the flow induced force is given by

$$F_{ind1} = \dot{m}_{s1}u_{s1} + \dot{m}_{e1}u_{e1} - \dot{m}_1u_1 + \frac{1}{2}(\ddot{m}_{s1} - \ddot{m}_{e1}) \qquad (6.35)$$

where $$u_{s1} = \frac{\dot{m}_{s1}RT_s}{P_{sv}A_{v1}}$$

$$u_{e1} = \frac{\dot{m}_{e1}RT_e}{P_e\ A_{v2}}$$

$$u_1 = \frac{\dot{m}_1RT_{1v}}{P_{n1}\ A_p}$$

Similarly,

$$F_{ind2} = \dot{m}_{s2}u_{s2} + \dot{m}_{e2}u_{e2} - \dot{m}_2u_2 + \frac{1}{2}(\ddot{m}_{s2} - \ddot{m}_{e2}) \qquad (6.36)$$

where $$u_{s2} = \frac{\dot{m}_{s2}RT_s}{P_{sv}A_{v2}}$$

$$u_{e2} = \frac{\dot{m}_{e2}RT_e}{P_eA_{v1}}$$

$$u_2 = \frac{\dot{m}_2RT_{2v}}{P_{n2}\ A_p}$$

The total flow induced force is given by

$$F_{ind} = F_{ind1} - F_{ind2} \tag{6.37}$$

In the simulation programme, the rates of change of mass flow rates:

$$\dot{\dot{m}}_{s1},\ \dot{\dot{m}}_{e1},\ \dot{\dot{m}}_{s2},\ \dot{\dot{m}}_{e2}$$

are determined at the conclusion of an integration step.

6.4.5 Hysteresis modelling

Hysteresis exists at the solenoid valve operator and tends to reduce the effect of the input signal. The source of hysteresis includes magnetic saturation, backlash, valve contamination. The effect of hysteresis on stability of servo system has been studied by Stone on a theoretical basis [6.24]. Particular investigation was carried out by Arafa et al [6.25] on electro-hydraulic servo-valve. In this modelling work, the description by Leaney [3.28] is adopted to produce a subroutine which gives a characteristic diagram as shown in Fig. 6.9.

The output signal represents the magnetic force that would be produced from the input signal. The diagram indicates that the force will depend on the history of the input variations. For simplicity of mathematical description, the boundary is formed by straight lines.

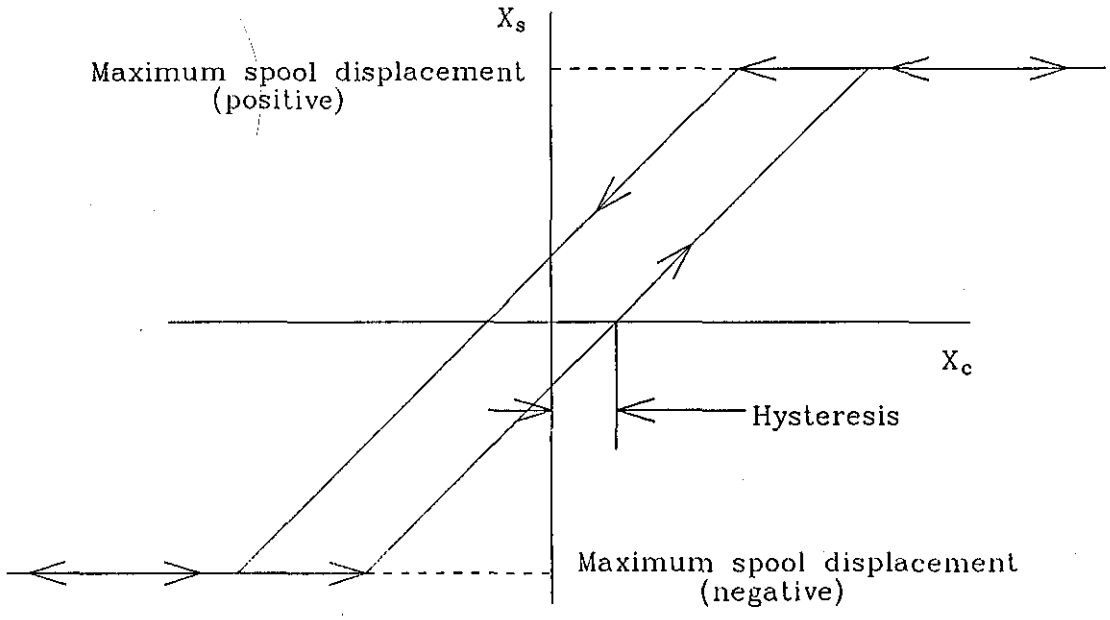

Fig. 6.9 - Characteristics of hysteresis subroutine

The hysteresis effect is only valid for solenoid valve operator. With the stepper motor valve operator, it is assumed that the linear movement effected by a step pulse signal should be large enough to overcome any minor opposing forces such as hysteresis, friction and flow induced forces.

6.5 Valve module

The valve module describes the pneumatic part of the valve and provides the mass flow rates for the actuator module. The input variable to the module is spool displacement determined in the valve operator module. Three models which are mutually exclusive to each other and selectable by a model type flag are investigated.

6.5.1 Spool opening area function

The amount of fluid flowing through the spool valve depends on a number of factors one of which is flow passage area opened. Considering geometrical relationship within the spool valve (Fig. 6.10), the flow area against spool displacement will depend on the valve lap situation. For an ideal valve, the area opened is zero at negative spool displacement and proportionally increases at positive spool displacement. The effects of underlap and overlap are shifting the ideal line to the left or right respectively.

Andersen [6.26] pointed out the due to manufacturing

tolerances, leakage due to rounded seat, fit clearance and underlaps is always present in the actual valve. The effects of these tolerances on hydraulic servo-valve had been simulated by Shearer [6.27]. On the study of pneumatic valve configuration, Araki [6.28] reported that valve laps affected the pneumatic responses seriously. Similarly, Bowns and Ballard [6.29] reported the simulated response of the pneumatic actuator due to valve changes. Unfortunately, there is no standardised way of determining the area function in terms of spool displacement. Individual valve requires independent area function derived directly from the valve design specification.

Assuming that the valve spool is made slightly smaller than the valve sleeve in order that the spool can "float" in the sleeve core, the area between the corner of the spool and the sleeve will be a truncated cone of area A_o (Appendix IV)

$$A_o = \frac{\pi(D_v+D_s)}{2}.\sqrt{[z^2 + \frac{(D_v-D_s)^2}{4}]} \qquad \text{if } z \geq 0$$

$$\text{and} \quad A_o = \frac{\pi(D_v^2-D_s^2)}{4} \qquad \text{if } z < 0 \qquad (6.38)$$

Fig. 6.11 shows the plot of spool area opened (in m^2) of the actual valve used against spool displacement (in mm). Underlaps are shown as negative values whereas positive underlap means overlap. The non-zero valve opening when the spool is at negative displacement indicates leakage area.

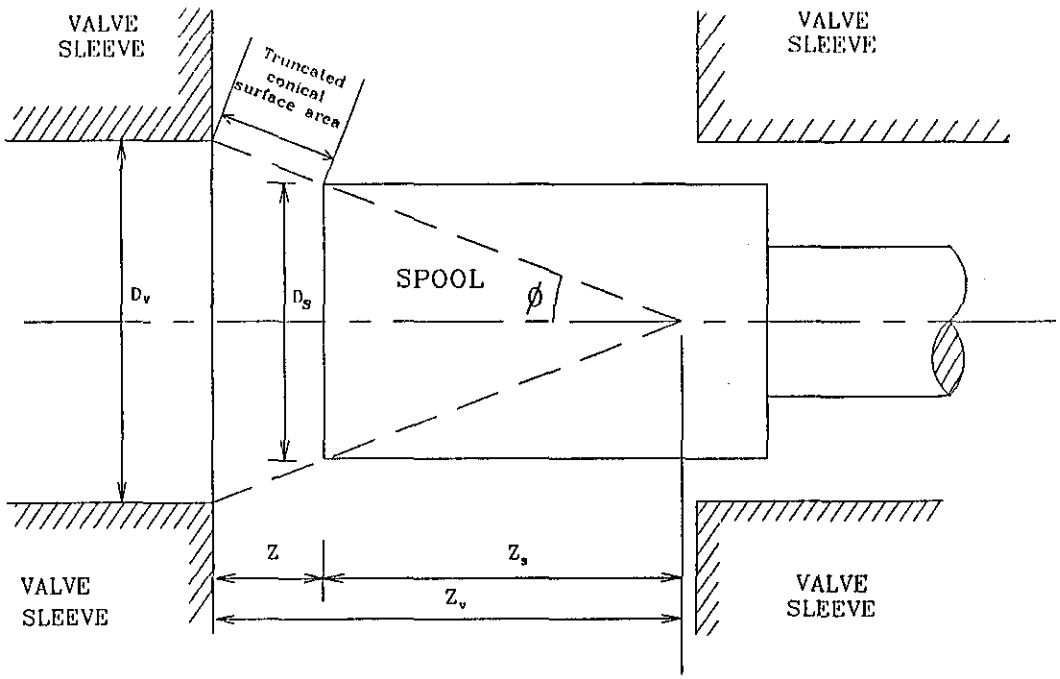

Fig. 6.10 - Geometry of valve and spool

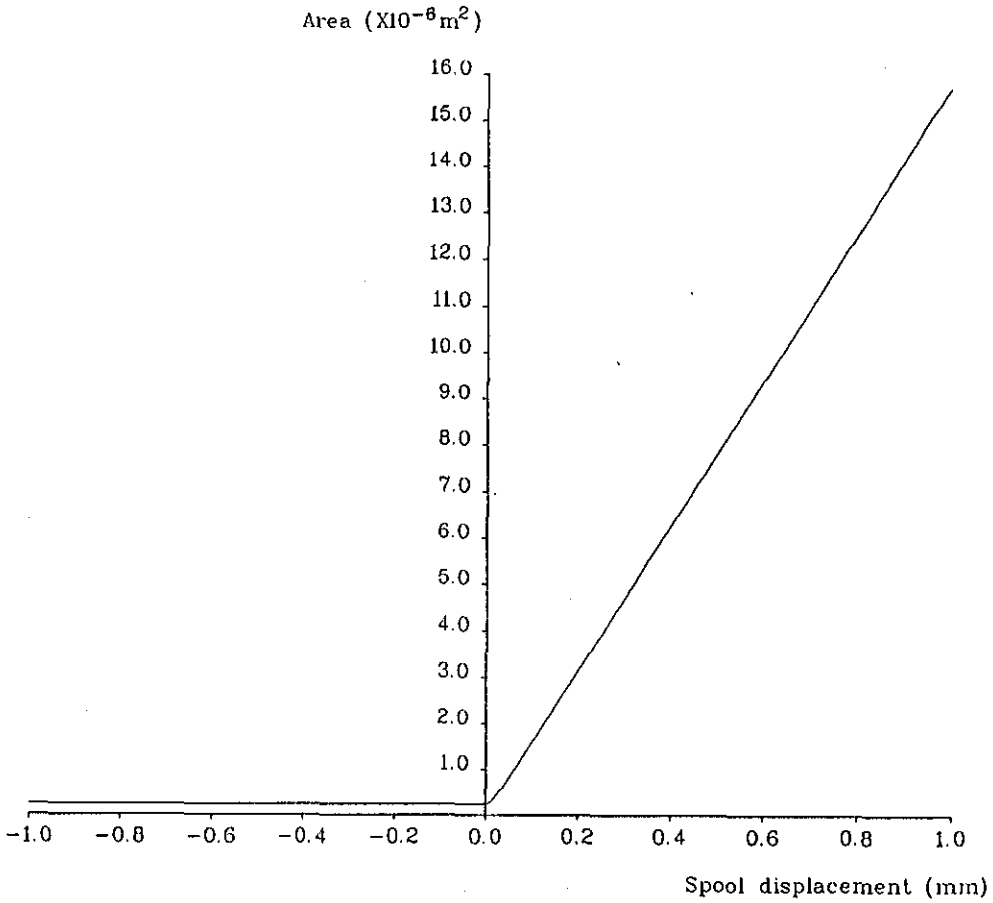

Fig. 6.11 - Plot of area function A_o vs. spool displacements

6.5.2 Single restriction model

The original research by Shearer on the valve-actuator air volume relationship assumes that the valve opening due to spool displacement constitutes an orifice restriction to the flow from supply to the control volume, or from the control volume to exhaust [6.30]. The one-dimensional adiabatic compressible flow equation has been applied to analyse the thermodynamics of the air in the two cylinder chambers. The method has formed the theortical basis for many analyses such as Burrows [6.31] and Bowns et al [6.29] both on the response of an on-off pneumatic servomechanism, Nazarczuk [6.32] on the modelling of a rectilinear moving pneumatic actuator, Eun et al [6.33] on the stability and positioning accuracy and Araki [6.34] on the effect of valve underlap on the frequency response.

The following derivation is made based on the traditional approach with slight modification in the convention of reverse flow to produce the equations in more generalised form. The formulae are incoporated as one of the 5 valve models and can be selected by a valve model flag. Referring to Fig. 6.12, assuming a symmetrical valve, and adopting the nozzle flow formula [6.35] the mass flow rates through the spool openings are given by:

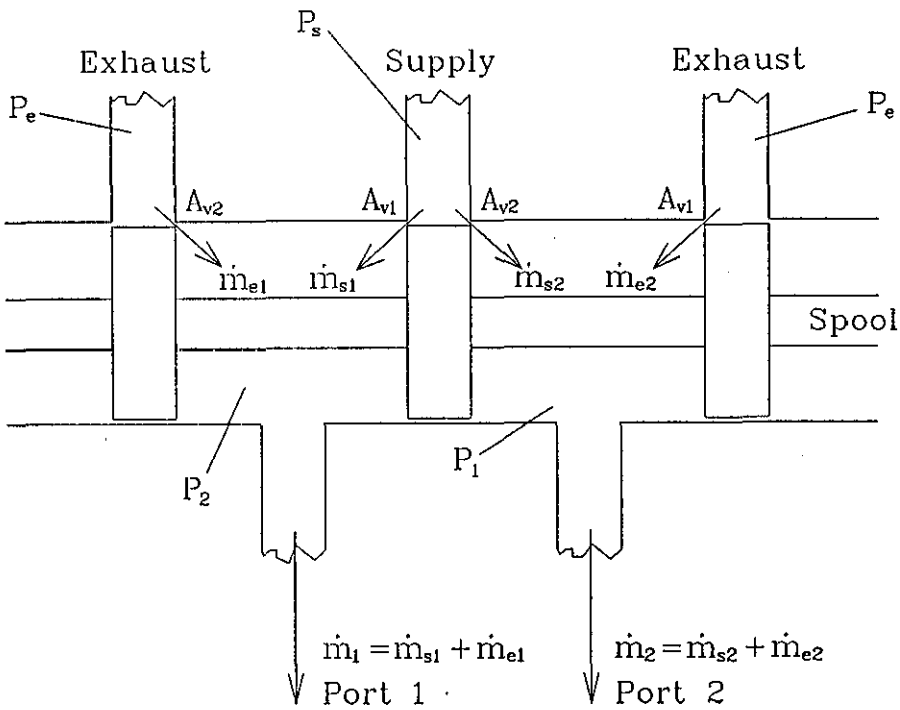

Fig. 6.12 - Single restriction valve model

$$\dot{m}_{s1} = C_{ds} \frac{A_{v1} P_s}{\sqrt{T_s}} \left(\frac{1}{r_{s1}}\right)^{\frac{1}{n}} \cdot \sqrt{\left[\left(\frac{n}{R}\right) \cdot \left(\frac{2}{n-1}\right) \cdot \left(1 - r_{s1}^{\frac{n-1}{n}}\right)\right]} \quad \text{if } r_{s1} > r_{crit}$$

$$= C_{ds} \frac{A_{v1} P_s}{\sqrt{T_s}} \sqrt{\left(\frac{n}{R}\right) \cdot \left(\frac{2}{n+1}\right)^{\frac{n+1}{2(n-1)}}} \quad \text{if } r_{s1} \leq r_{crit} \qquad (6.39)$$

$$\dot{m}_{e1} = -C_{de} \frac{A_{v2} P_1}{\sqrt{T_1}} \left(\frac{1}{r_{1e}}\right)^{\frac{1}{n}} \cdot \sqrt{\left[\left(\frac{n}{R}\right) \cdot \left(\frac{2}{n-1}\right) \cdot \left(1 - r_{1e}^{\frac{n-1}{n}}\right)\right]} \quad \text{if } r_{1e} > r_{crit}$$

$$= -C_{de} \frac{A_{v2} P_1}{\sqrt{T_1}} \cdot \sqrt{\left(\frac{n}{R}\right) \cdot \left(\frac{2}{n+1}\right)^{\frac{n+1}{2(n-1)}}} \quad \text{if } r_{1e} \leq r_{crit} \qquad (6.40)$$

$$\dot{m}_1 = \dot{m}_{s1} + \dot{m}_{e1} \qquad (6.41)$$

$$\dot{m}_{s2} = C_{ds} \frac{A_{v2} P_s}{\sqrt{T_s}} \left(\frac{1}{r_{s2}}\right)^{\frac{1}{n}} \sqrt{\left[\left(\frac{n}{R}\right) \cdot \left(\frac{2}{n-1}\right) \cdot \left(1 - r_{s2}^{\frac{n-1}{n}}\right)\right]} \quad \text{if } r_{s2} > r_{crit}$$

$$= C_{ds} \frac{A_{v2} P_s}{\sqrt{T_s}} \sqrt{\left(\frac{n}{R}\right) \cdot \left(\frac{2}{n+1}\right)^{\frac{n+1}{2(n-1)}}} \quad \text{if } r_{s2} \leq r_{crit} \qquad (6.42)$$

$$\dot{m}_{e2} = -C_{de} \frac{A_{v1} P_2}{\sqrt{T_2}} \left(\frac{1}{r_{2e}}\right)^{\frac{1}{n}} \cdot \sqrt{\left[\left(\frac{n}{R}\right) \cdot \left(\frac{2}{n-1}\right) \cdot \left(1 - r_{2e}^{\frac{n-1}{n}}\right)\right]} \quad \text{if } r_{2e} > r_{crit}$$

$$= -C_{de} \frac{A_{v1} P_2}{\sqrt{T_2}} \cdot \sqrt{\left(\frac{n}{R}\right) \cdot \left(\frac{2}{n+1}\right)^{\frac{n+1}{2(n-1)}}} \quad \text{if } r_{2e} \leq r_{crit} \qquad (6.43)$$

$$\dot{m}_2 = \dot{m}_{s2} + \dot{m}_{e2} \qquad (6.44)$$

where the areas A_{v1} and A_{v2} are determined in Eqn (6.38).

$$r_{crit} = \left(\frac{2}{n+1}\right)^{\frac{n}{n-1}}$$

$$r_{s1} = \left(\frac{P_1}{P_s}\right) \qquad r_{1e} = \left(\frac{P_e}{P_1}\right)$$

$$r_{s2} = \left(\frac{P_2}{P_s}\right) \qquad r_{2e} = \left(\frac{P_e}{P_2}\right)$$

and assuming $P_s > P_1 > P_e$, $P_s > P_2 > P_e$.

In the operation cycle of the pneumatic actuator, it is possible to have circumstances in which the control volume is compressed seriously such that P_1 or P_2 is higher than P_s, the mass flow rates are modified:

$$\dot{m}_{s1} = -C_{de} \frac{A_{v1}P_1}{\sqrt{T_1}} \cdot \left(\frac{1}{r_{1s}}\right)^{\frac{1}{n}} \cdot \sqrt{\left[\left(\frac{n}{R}\right) \cdot \left(\frac{2}{n-1}\right) \cdot \left(1 - r_{1s}^{\frac{n-1}{n}}\right)\right]} \quad \text{if } r_{1s} > r_{crit}$$

$$= -C_{de} \frac{A_{v1}P_1}{\sqrt{T_1}} \cdot \sqrt{\left(\frac{n}{R}\right) \cdot \left(\frac{2}{n+1}\right)^{\frac{n+1}{2(n-1)}}} \quad \text{if } r_{1s} \leq r_{crit} \qquad (6.45)$$

$$\dot{m}_{s2} = -C_{de} \frac{A_{v2}P_2}{\sqrt{T_2}} \cdot \left(\frac{1}{r_{2s}}\right)^{\frac{1}{n}} \cdot \sqrt{\left[\left(\frac{n}{R}\right) \cdot \left(\frac{2}{n-1}\right) \cdot \left(1 - r_{2s}^{\frac{n-1}{n}}\right)\right]} \quad \text{if } r_{2s} > r_{crit}$$

$$= -C_{de} \frac{A_{v2}P_2}{\sqrt{T_2}} \cdot \sqrt{\left(\frac{n}{R}\right) \cdot \left(\frac{2}{n+1}\right)^{\frac{n+1}{2(n-1)}}} \quad \text{if } r_{2s} \leq r_{crit} \qquad (6.46)$$

where $r_{s1} = \frac{P_1}{P_s}$ and $r_{s2} = \frac{P_2}{P_s}$

The negative sign indicates that the flow direction is opposite to that indicated on Fig. 6.12.

Similarly, hypothetical reverse flow equations for $\dot{m}_{e1}$ and $\dot{m}_{e2}$ for circumstances of $P_e > P_1$ and $P_e > P_2$ can be formulated to provide numerical return during simulation runs. The inputs to the valve module are spool displacement which affects A_{v1} and A_{v2}, whereas the air conditions (pressures and temperatures) are passed through state variable common block. Fig. 6.13 illustrates a mass flow rate plot against spool displacement. From flow measurement tests (Section 7.1.1):

(a) The upstream kinetic energy of the air stream expressed in terms of Mach number was significant for large spool openings. At high flow rate, a level of 0.035kg/s which corresponded to Mach number equal to 0.35 had been recorded. The subsonic upsteam condition pushed the mass flow rate function nearer to the critical point.

(b) There was saturation effect at high flow rate. However, the flow rate functions in Eqn (6.39) - (6.46) do not describe such flow saturation phenomenon.

These observations suggest that a new formula is required to derive the mass flow rate function more accurately.

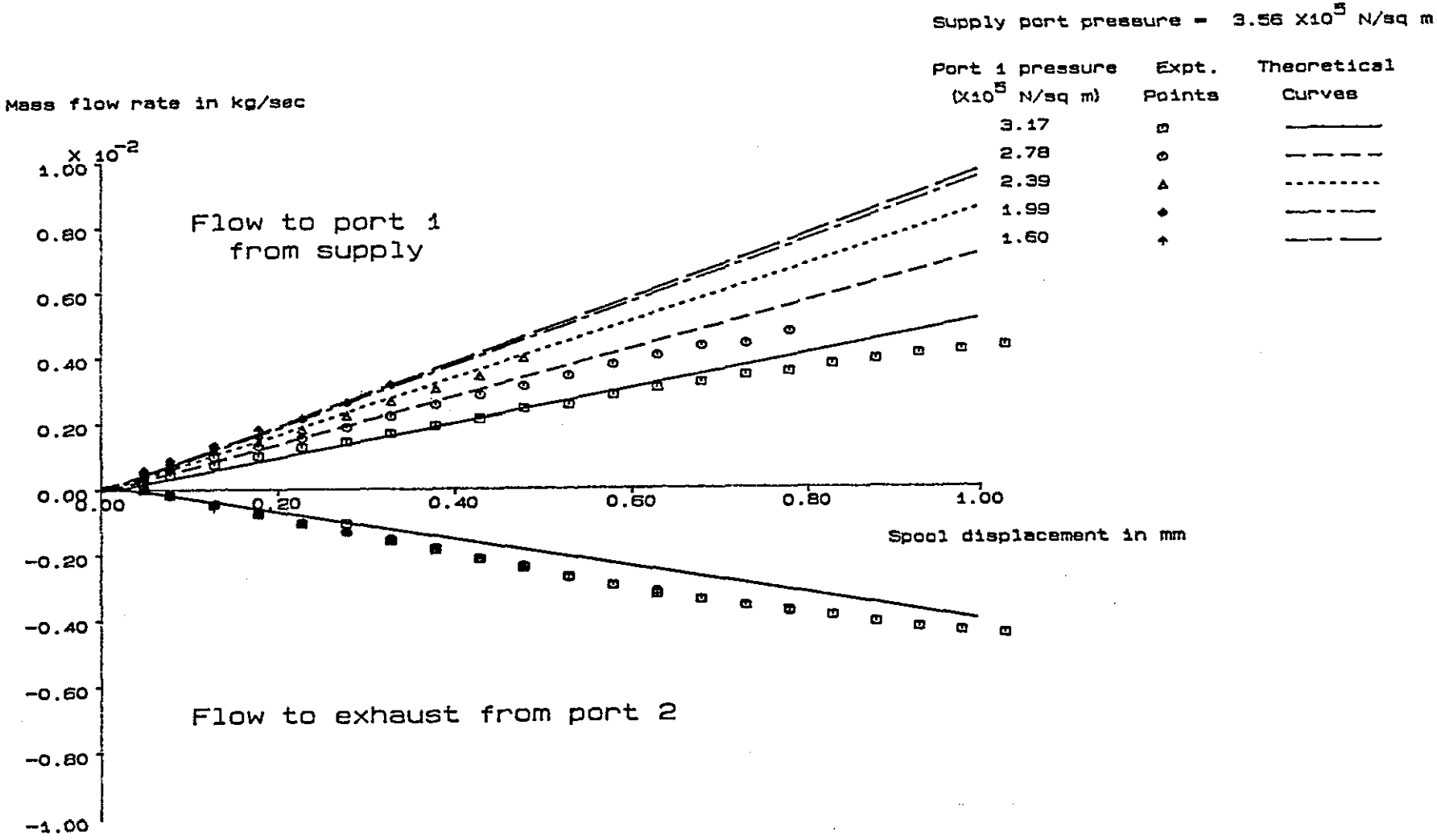

Fig. 6.13 - Mass flow rate vs. spool displacements (single restriction model)

As discussed in Section 3.1.1, it is possible to obtain an empirical model by fitting the data to some polynomials. Unfortunately, the limitation to such approach is inherent in itself that the valve is basically unknown. Any new valve of slightly modified configuration will require another set of experiments to ascertain the flow gain. In other words, there is no fundamental law built within the model which can generally be applied to predict the flow gain if the valve is to be designed from scratch.

6.5.3 Flow function Γ

In all pneumatic valve derivations, the one-dimensional adiabatic flow equation is used. Variations to this fundamental form were made due to various reasons. For instance, Sanville [6.36] simplified the function for analytical use based on the approximation around the critical pressure ratio. Zalmanzon et al [6.37] proposed that an incompressible version of the flow function can be used if there is no significant pressure drop across the restriction. An independent study on the performance of conical diffuser due to variations of inlet Mach number indicated that deterioration of pressure recovery would exist at Mach numbers higher than 0.8 [6.38]. The compressible flow was mostly influenced by the growth of the turbulent boundary layer [6.39]. Unfortunately, there is no literature found to extend the function to deal with the mass flow rate influenced by upstream subsonic Mach numbers.

In order to obtain an adequate model of the pneumatics, the one-dimensional adiabatic flow function with up-stream flow (non-zero up-stream Mach number) different from the conventional function has been derived to calculate the mass flow rate through the valve. It is perceived that the flow head is significant when the valve opens sufficiently within a short time (say 0.1 sec), the sudden pressure drop between the two sides of the restriction will give rise to a high mass flow rate.

Derivation of the mass flow rate with kinetic upstream flow has been presented in Appendix V. The flow function Γ is introduced to simplify the notation of mass flow rate Eqn (V.13).

The direction of the flow depends on the pressures at both sides of the restriction. Air always flows from high pressure to low pressure. One of the two Mach number independent variables in the routine will become the influencing upstream kinetic head value. The flow function used in the simulation therefore looks at the pressure ratio as well as the Mach numbers of the two sides of the restriction. Two separate sequence of codes are provided to deal with normal and reverse flow situations. The function is plotted in Fig. 6.14.

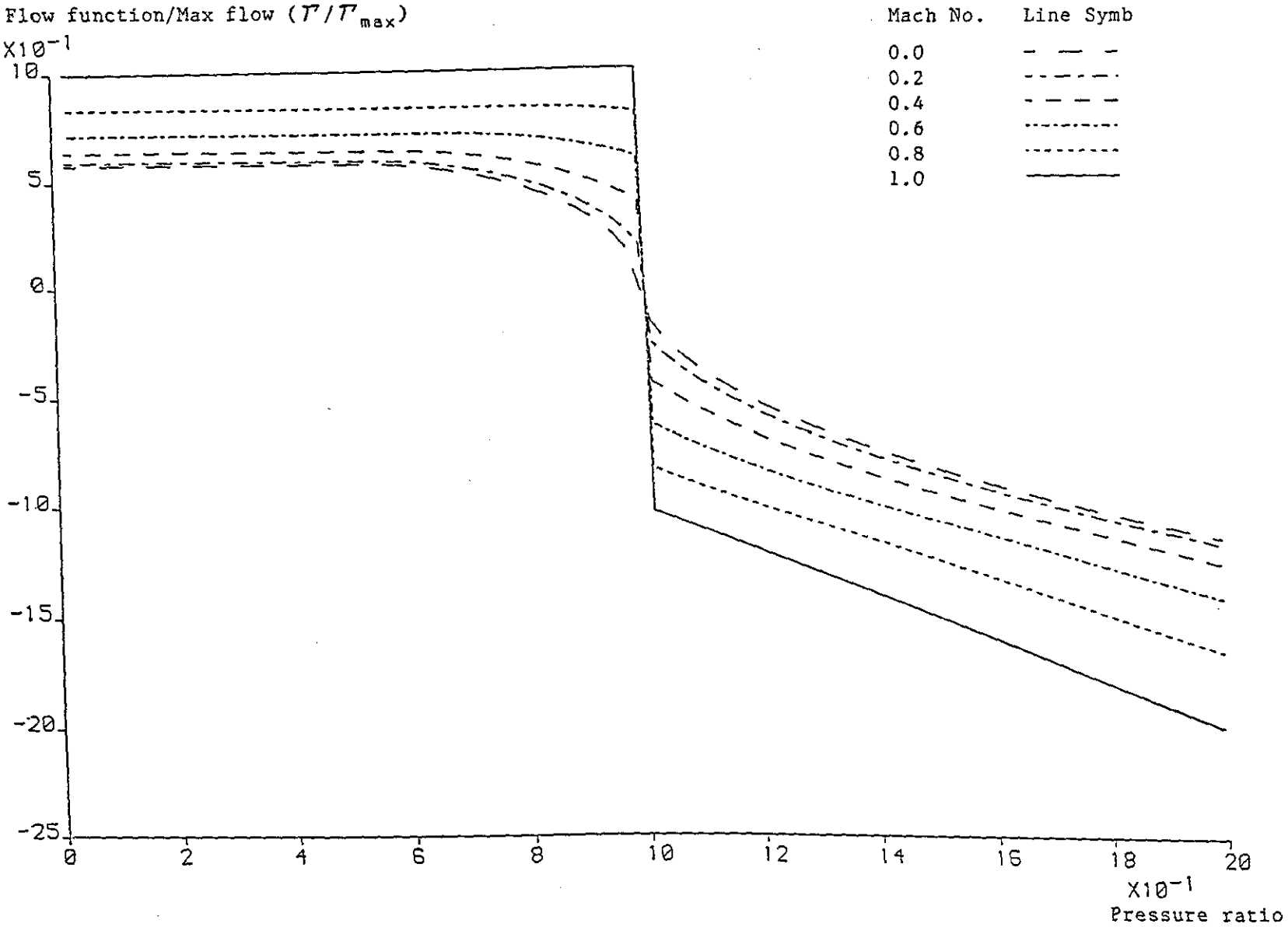

Fig. 6.14 - The flow function Γ

6.5.4 Flow node model

Examination of the geometry of the air flow path through the valve showed that a buffer volume could exist in the valve cavity and generated the effect of saturation in the flow gain characteristics. Huber [6.40] in an analysis of a rotary actuator, included the buffer volume as the inlet port of the actuator. The analysis highlighted some of the problems of the pneumatic servo-system but did not show how the buffer volume might affect the performance.

The effect of the buffer volume on the compressed air flow has been investigated in this research. The flow node model has been postulated by Mo [6.41] and can be illustrated in Fig. 6.15. The two chambers of the cylinder are each leading to one of the valve ports which in turn has access to the corresponding valve land through some port restrictions. If the valve land is regarded as being a small air volume functioning as a buffer or reservoir, the pressure and temperature of air inside the valve land volume should be different from those at the inlets of the valve. A set of valve land pressure and temperature values must be determined in order to calculate the mass flow rate between the valve and the cylinder chamber. In other words, a flow node is anticipated at the valve land to re-arrange the flow. Calculation of a pair of unknowns (P_{n1}, T_{n1}) for flow node 1 is required such that (Appendix V):

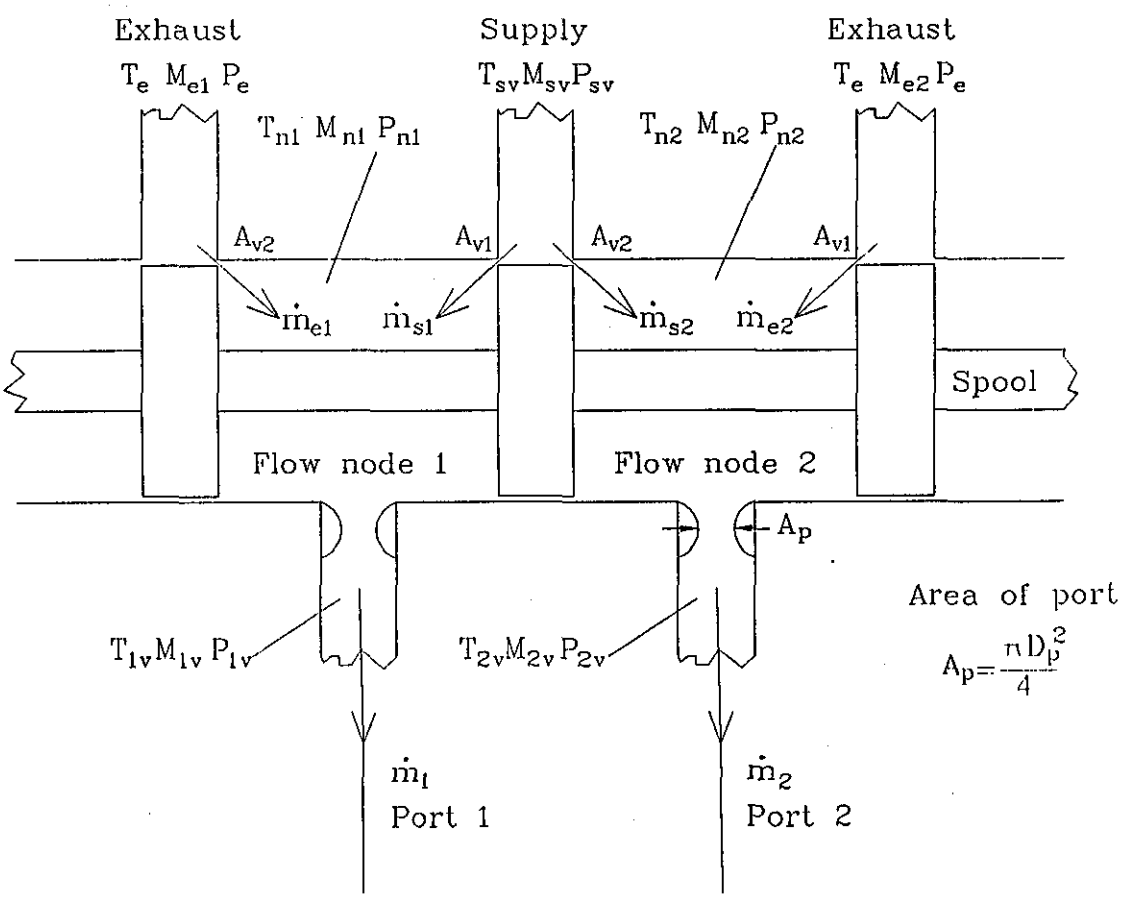

Fig. 6.15 - Flow node model

$$\dot{m}_{s1} = C_d \cdot A_{v1} \cdot \Gamma(P_{sv}, T_{sv}, M_{sv}, P_{n1}, T_{n1}, M_{n1}) \cdot \sqrt{\left(\frac{n}{R}\right)} \quad (6.47)$$

$$\dot{m}_{e1} = C_d \cdot A_{v2} \cdot \Gamma(P_e, T_e, M_e, P_{n1}, T_{n1}, M_{n1}) \cdot \sqrt{\left(\frac{n}{R}\right)} \quad (6.48)$$

$$\dot{m}_1 = C_d \cdot A_p \cdot \Gamma(P_{n1}, T_{n1}, M_{n1}, P_{1v}, T_{1v}, M_{1v}) \cdot \sqrt{\left(\frac{n}{R}\right)} \quad (6.50)$$

and $$\dot{m}_1 = \dot{m}_{s1} + \dot{m}_{e1} \quad (6.51)$$

The additional equation required is determined by assuming that the valve land volume is relatively small compared with the other volumes and the net energy gained by in-flow and out-flow of air will not be kept by the volume. In terms of enthalpy,

$$H_{n1} = H_{s1} + H_{e1} - H_1 = 0 \quad (6.52)$$

Furthermore, to expand Eqn (6.52), it is assumed that the air in the flow node is turbulent and any dynamic head in the air will not be able to affect the flow through the small restrictions. The enthalpy equation is transformed to Eqn (6.53) in 8 combinations of H_{s1}, H_{e1} and H_1 to solve for the flow node temperature in Appendix VI :

$$T_{n1} = \Omega(\dot{m}_{s1}, \dot{m}_{e1}, \dot{m}_{1v}, M_{s1}, M_{e1}, M_{1v}, T_{s1}, T_e, T_{1v}) \quad (6.53)$$

The Mach numbers at the input points (M_{s1}, M_{e1}, M_1) are calculated according to the mass flow rate and stream conditions:

$$M = \frac{\dot{m}}{A\ P} \cdot \sqrt{\left(\frac{R\ T}{n}\right)} \quad (6.54)$$

A default check is built in to restrict that only sub-sonic flow

should exist at these points because:

(a) If it was supersonic (M > 1), it would change to sub-sonic immediately by shock within the tubing before going to the restriction;

(b) If it was sub-sonic, it would remain subsonic up to the restriction.

The Mach number information is fed to the supplementary valve flow subroutine "VFLOW" which determines the flow node parameters according to Eqn (6.47)-(6.51). This calculation is repeated for cylinder chamber 2.

6.5.5 Multiple flow node model

It was found that the pressure drop in tubing is significant and affects the input pressure to the valve and cylinder chambers. The multiple flow node model is postulated as an extension of the flow node model to include adiabatic fluid flow in tubing. Additional restrictions are imposed between the valve ports and the tubings, and between the tubings and the cylinder inlet points (Fig. 6.16).

The equations of flow dynamics become:

$$\dot{m}_{s1} = C_d \cdot A_{v1} \cdot \Gamma(P_{sv}, T_{sv}, M_{sv}, P_{n1}, T_{n1}, M_{n1}) \cdot \sqrt{\left(\frac{n}{R}\right)} \qquad (6.55)$$

$$\dot{m}_{e1} = C_d \cdot A_e \cdot \Gamma(P_e, T_e, M_{e1}, P_{n1}, T_{n1}, M_{n1}) \cdot \sqrt{\left(\frac{n}{R}\right)} \qquad (6.56)$$

$$\dot{m}_{n1} = C_d \cdot A_p \cdot \Gamma(P_{n1}, T_{n1}, M_{n1}, P_{1v}, T_{1v}, M_{1v}) \cdot \sqrt{\left(\frac{n}{R}\right)} \qquad (6.57)$$

$$\dot{m}_1 = C_d \cdot A_{pc} \cdot \Gamma(P_{1v}, T_{1v}, M_{1v}, P_1, T_1, M_1) \cdot \sqrt{\left(\frac{n}{R}\right)} \qquad (6.58)$$

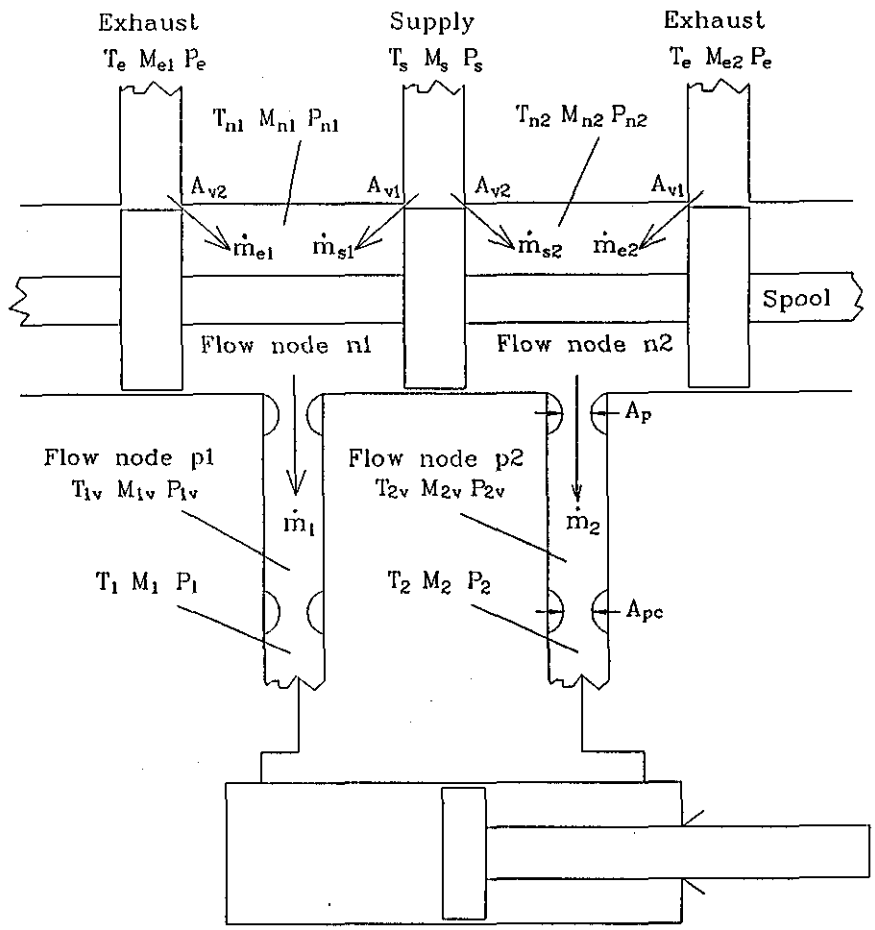

Fig. 6.16 - Multiple flow node model

and

$$\dot{m}_{s1} + \dot{m}_{e1} = \dot{m}_{n1} \tag{6.59}$$

$$\dot{m}_{n1} = \dot{m}_{1} \tag{6.60}$$

The values of P_{n1}, T_{n1}, P_{1v} and T_{1v} are found by the same principle as in Section 6.5.4. Since the model lumps the tubing flow effect into Eqn (6.57) and (5.58), the tubing module described in Section 6.6 is not used with this model. The output from this valve model is fed directly to the actuator and valve operator.

Due to the increased complexity of Eqn (6.55) to (6.60), the number of iterations in the routine to solve the algebraic equations for T_{n1} and T_1 substantially increased. The time required to solve the solution is normally 3 times as much time as that in Section 6.5.4. Therefore, no substantial investigation has been done with this model. It is anticipated that it will require a super-computer with array processing capability in order to achieve reasonable result.

6.5.6 The IMSL routines

Part of the model requires the calculation of a set of valve land pressures and temperatures which are determined as result of the flow and energy between the supply, exhaust and port conditions. This balance is formulated as a set of two algebraic equations with the two unknowns of valve land pressure and temperature.

Initial attempt to use the C05NAF routine in the Numerical Algorithm Group (NAG) Library [6.42] was unsuccessful. The difficulties were understood to be associated with:

(a) Some of the parameters before entering the numerical routine were not properly initialised.

(b) The call procedure was difficult to follow and involved significant user interaction during in the intermediate returns from the NAG routine. The trial programme was unable to handle the procedure returns well.

In City Polytechnic, the International Mathematical and Science Library (IMSL) routines are available. The routine "ZSPOW" [6.43] which solves a set of non-linear equations was used to perform the root determination process. Application of the routine was simpler than the NAG routine in that there was no need for user interaction between intermediate steps. The user needed only to supply a subroutine (must be named FCN) which evaluated the set of equations. The user equations were formulated to find an error vector whose norm was minimised to zero. The routine is based on Powell's hybrid method [6.44] for non-linear algebraic equations.

6.6 Tubing module

During the measurement of mass flow rate delivered through the valve, it was found that there was significant pressure drop

in the tubing. Experiments showed that the pressure drop varied according to the mass flow rate. There are many factors contributing to the effect. The major contribution to the pressure drop is the isentropic expansion of fluid in the tubing. The pressure drop will vary according to a span ratio L/D [6.45] where L is the length of tubing and D is the diameter of tubing.

The maximum pressure drop possible in the tubing is governed by the choked flow condition [6.46]. For flow from stagnation point, the maximum pressure drop is 0.528 which corresponds to a Mach number of 1 at the downstream point. Further pressure drop is not possible as shock will occur beyond the critical point and pressure is resumed as an energy recovery in shock wave. This perception of the pressure drop phenomenon led to a modification of the model description of the pressure drop function in the simulation.

Two models are postulated. The empirical model demands less computing power but has to depend on the experimental data to provide a regression line relationship. The analytical approach is independent of any test data but is more complicated to be computed.

6.6.1 Empirical approach

The empirical approach to model the pressure drop effect is by determining the regression line to the experimental points. During the flow gain test, a straight line relationship was found.

It is tentatively designed that the tubing leading to and from the pneumatic cylinder is kept constant so that the same empirical formula can be applied throughout the pneumatic system.

The formula is of the form:

$$P_{drop} = 1 - (1 - K_{dr})\dot{m}/\dot{m}_{ref} \qquad (6.61)$$

where P_{drop} is the pressure drop ratio from inlet to outlet.

If the flow is negative, the value of P_{drop} is reciprocated so that P_{outlet} is greater than P_{inlet}.

6.6.2 Analytical approach

The analytical approach is based on the normal shock model of compressible fluid flow through ducts [6.47]. Due to the isentropic expansion of the fluid, the flow resolves to shock in the flow passage when it reaches supersonic condition. A detail mathematical treatment covering flows of all Reynolds number is given by Ward Smith [6.48]. An expanded version of the theoretical representation with particular reference to one-dimensional turbulent flow through ducts of constant cross-section is found with Anderson [6.49]. Starting from the standard relationships which relate the pressure at any point in the tube to Mach number, the downstream pressure can be determined by the equation derived in Appendix VIII:

Assuming all flow rates defined in Section 6.5.4 are

positive, for flow from valve port 1 to actuator chamber 1, the down stream pressure P_{1v} is formed by:

$$P_{1v} = P_1 \frac{M_1}{M_{1v}} ./ [\frac{2 + (n-1)M_1^2}{2 + (n-1)M_{1v}^2}] \tag{6.62}$$

where the downstream Mach number M_{1v} is found by solving

$$\frac{4fL_{1v}^*}{D} = \frac{4fL_{1v}}{D} + \frac{4fL}{D} \tag{6.63}$$

Similarly, for flow from valve port 2 to actuator chamber 2,

$$P_{2v} = P_2 \frac{M_2}{M_{2v}} ./ [\frac{2 + (n-1)M_2^2}{2 + (n-1)M_{2v}^2}] \tag{6.64}$$

and for flow from supply to valve,

$$P_{sv} = P_s \frac{M_{sv}}{M_s} ./ [\frac{2 + (n-1)M_{sv}^2}{2 + (n-1)M_s^2}] \tag{6.65}$$

If the flow is negative, i.e. reverse flow, the alternative equations in Appendix VIII apply.

6.7 Component modules assembly

The assembly of the components to a total system is straight forward in the software side. The initialisation must be done before the simulation takes place. The appropriate component module flags are set and the rest relies on the information collected for that particular test rig to be simulated.

The flexibility of the generic model allows that the test rig models can be mathematical formulated by enabling the component modules. Tab. 6.3 illustrates the sequence of component modules necessary for the assembly of the specific hardware alternatives A, B and C as described in Chapter 5.

Tab. 6.3 - Assembly of specific test rig models

Flag value	Choice of models	Mechanism		
		A	B	C
	CONTROLLER: Flag L(22)			
1	Continous controller, LUT algorithm			
2	Continous controller, Burrow's test			
11	Discrete controller for solenoid operated valve		*	*
12	Discrete controller for stepper motor operated valve	*		
13	Discrete controller, solenoid operated valve, Moore's proportional algorithm			
	VALVE OPERATOR: Flag L(2)			
0	Empirical valve			
1	Analytical valve		*	*
2	Stepper motor valve operator	*		
3	On-off valve			
	VALVE: Flag L(16)			
1	Flow node model	*	*	*
2	Single restriction model			
3	Multiple flow node model			
4	Flow node model with experimental flow forces			
5	Flow node model with analytical flow forces			
	TUBING: Flag L(11)			
0	Empirical model	*	*	*
1	Analytical model			
	ACTUATOR: Flag L(18)			
0	Asymmetric cylinder with laminar leakage function	*	*	
0	Symmetric cylinder (special case of asymmetric above)			*
1	Asymmetric cylinder with adiabatic leakage function			
	LOAD: Flag L(21)			
0	Spring-mass, viscous friction model	*	*	*

Note: An asterisk indicates the module choice

6.8 Summary for models of test rigs for validation

In general, the components can be modelled with empirical or simplified approach which gives an approximate solution. Often the approach requires some form of initialisation from experimental data and hence restricts itself to the generalisation to other variety of the component. On the contrary, the analytical approach is postulated to cater for new designs and substantial component variations. The analytical models are normally more complex and computational intensive.

Both the empirical and analytical models are written under the same set of linking criteria. They are mutually exclusive if they are modelling the same component and selectable by the appropriate module flag.

CHAPTER 7

VALIDATION OF SPECIFIC MODELS

The specific models formulated in Chapter 6 for the evaluation test rigs required a number of parameters to be measured. These parameters were represented as numerical constants or coefficients of algebraic expressions in the components models and were most vital to the accurate interpretation of the simulation result. Apart from the dimensional parameters, which could be measured by the vernier or micrometer, separate measurements were performed in experiments specially designed to ascertain the parameters of the component models.

The data collected in the measurement tests were substituted into the "C" (for real numbers) and "L" (for integers) array of the simulation package. The initial conditions of the test rigs were determined from the corresponding transient file. By inserting the same initial conditions and operating parameters into the simulation model, the results could be compared directly by magnitudes. In addition to visual comparison on the same graph, by using the enhanced feature of the simulation software, the standard deviations between corresponding experimental and simulated responses could be calculated thereby providing additional indicators on the closeness of the model to reality.

7.1 Component tests

The measurements on components mainly concentrated on the valve, cylinder, load and tubing. These concerned the mechanical and pneumatic parameters which were normally highly uncertain. The controller was the most predictable component but one calibration test on timing was still required.

7.1.1 Valve characteristics

There were two sets of valve tests:

(a) The flow gain test was carried out to determine the volume flow rates (and hence the mass flow rates) through the valve at all possible spool displacements.

(b) The pressure gain test was carried out to determine the change of pressures at the service ports at blocked port situation in the vicinity of the valve null position.

The results were analysed to determine relevant parameters which were later entered into the "C" array elements concerning the valve dimensions and coefficients.

7.1.1.1 The flow gain test

The valve was connected to an air cylinder which moved in either direction. During the moving of the cylinder, air was fed to the cylinder chamber in one port from the supply, but the air

in the other chamber was compressed so that air passed back to the valve in the other port. The experimental arrangement (Fig. 7.1) was made to simulate the bi-directional flow situation.

The flow from the supply at pressure P_{ss} passed through the tubing connection to the supply port of the valve. The pressure at the supply port was measured by the gauge "P_s". Similarly, the pressure gauge "P_1" measured the air pressure immediately at port 1 and the gauge "P_{f1}" measured the air pressure after the tubing connection at port 1. A separate source was connected at port 2 to provide an inflow of air back to the valve.

While the micrometer pushed the spool into the valve, the dial indicator recorded the spool location. The indicator provided both spring force on the spool against the micrometer as well as maintaining a clear indication of where the spool was. The flow restrictor at port 1 in the experimental was installed to produce a back pressure which resembled the back pressure of air inside a cylinder chamber.

7.1.1.2 The blocked port test

The primary aim of the blocked port test was to locate the null position of the valve with reference to the micrometer readings (Fig. 7.2). Due to manufacturing tolerance, air leakage was inevitable even if the spool was located at the position where the valve was expected to be totally closed. Leakage flow also existed between the valve lands and the exhaust ports.

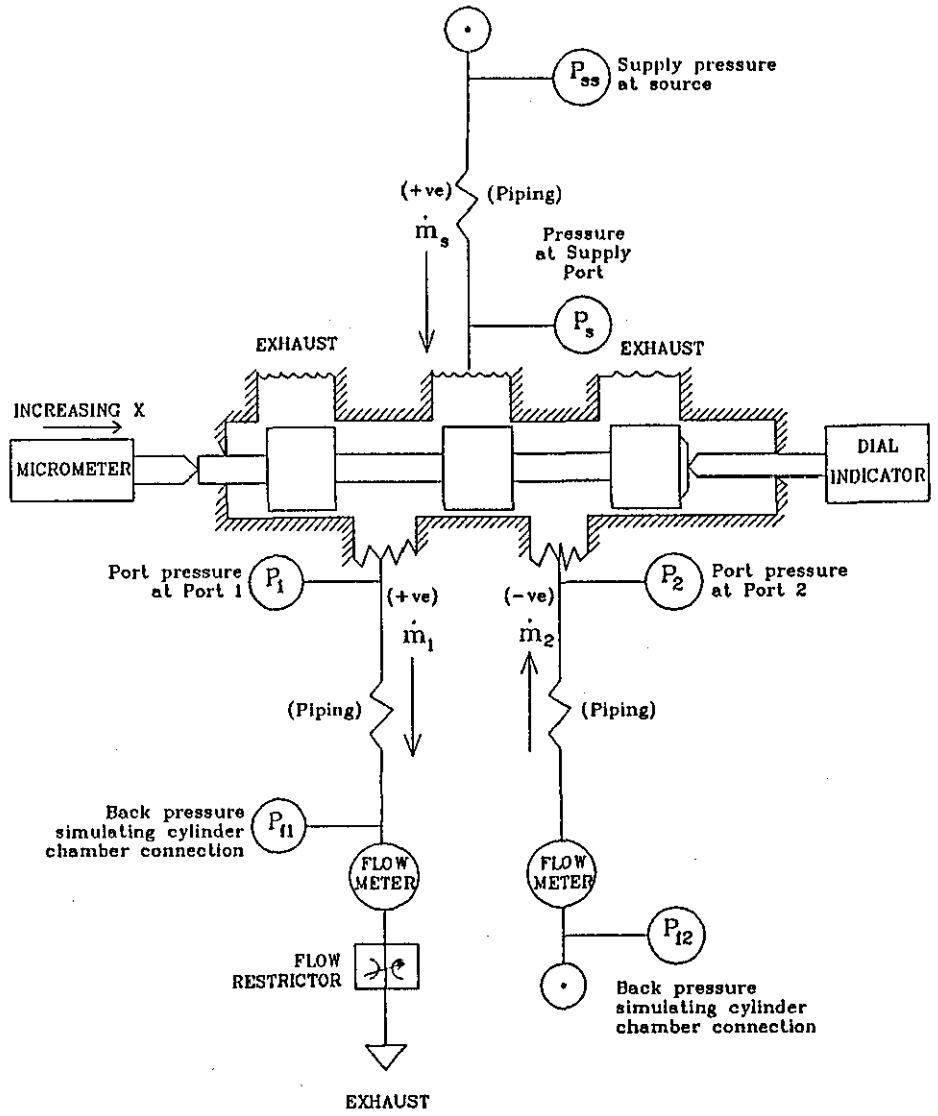

Fig. 7.1 - Experimental set-up for flow gain test

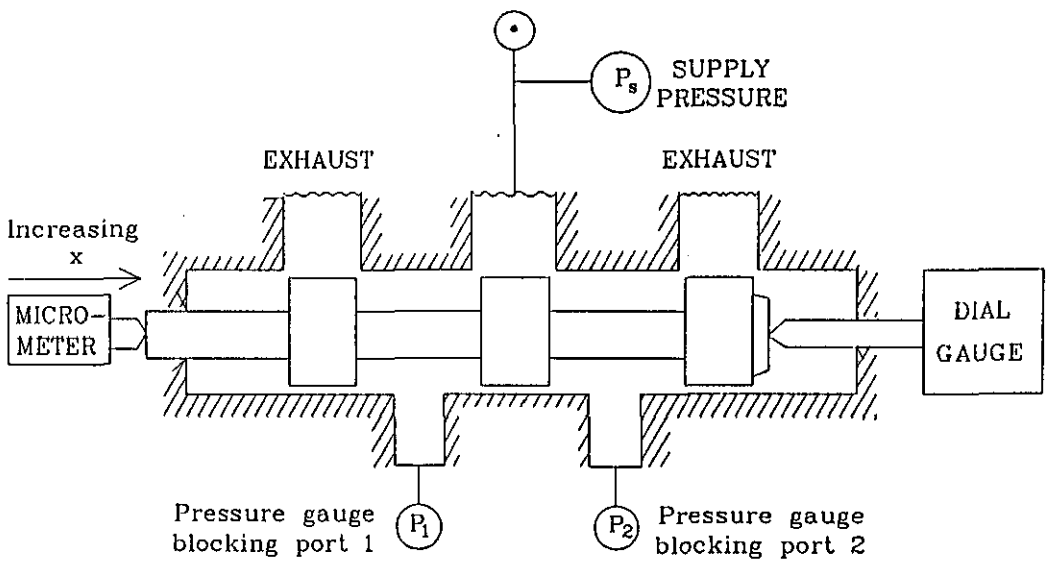

Fig. 7.2 - Experimental set-up for blocked port test

It was logical to define that the valve null point should be at the point where there was no pressure difference between the two ports. The null point then implied a spool reference location where the valve openings to both ports were equal. When the leakage flow from the supply to the respective valve lands was equal to that from the valve lands to exhaust, that is,

$$\dot{m}_{s1} + \dot{m}_{e1} = 0$$

$$\dot{m}_{s2} + \dot{m}_{e2} = 0$$

and $\dot{m}_{s1} = \dot{m}_{s2}$

The intermediate pressures in the two valve lands should be equal. This condition then reflected that the spool was at the null position.

7.1.1.3 The theoretical characteristics

There were two theoretical characteristics: pressure gain and flow gain characteristics. The pressure gain characteristics is defined as a series of pressure gain curves, at different supply pressures, being put together to present a full picture of pressure variations due to spool displacements. Likewise, the flow gain characteristics is defined as a series of flow gain curves, at different supply pressures, being put together to present a full picture of flow rate variations due to spool displacements.

The pressure gain characteristics were plotted in Fig. 7.3.

The theoretical curves were determined based on the flow node valve model described in Section 6.5.4. A general discussion of the nature of area factor in pneumatic flow capacities can be found with Tsai et al [7.1] and it was specifically referred as coefficient of discharge in the case of orifice meter or nozzle flows. Experimental values of the coefficient of discharge could be found in the work of Perry [7.2], Stenning [7.3] and Logan et al [7.4]. Although the data were organised in varying fashions, the values presented in these experiments were quite similar. Perry's values were more precisely presented in tabular form and was adopted in this calculation.

The null point of the pressure gain characteristics was determined by a trial and error process. An initial guess micrometer value was made to start calculation. A sum square error was then calculated by which the computer program adjusted the guess point in both directions until a minimum error was reached. The same iteration process was repeated for all 5 pressure gain curves. The null points were summarised in Tab. 7.1.

The pressure gain characteristics were determined using the mode reading (i.e. 9.572 mm) as the zero micrometer setting for all 5 curves. The fitting errors for the curves 4 and 5 were slightly higher but the whole characteristic plot was made consistent at a unique null point.

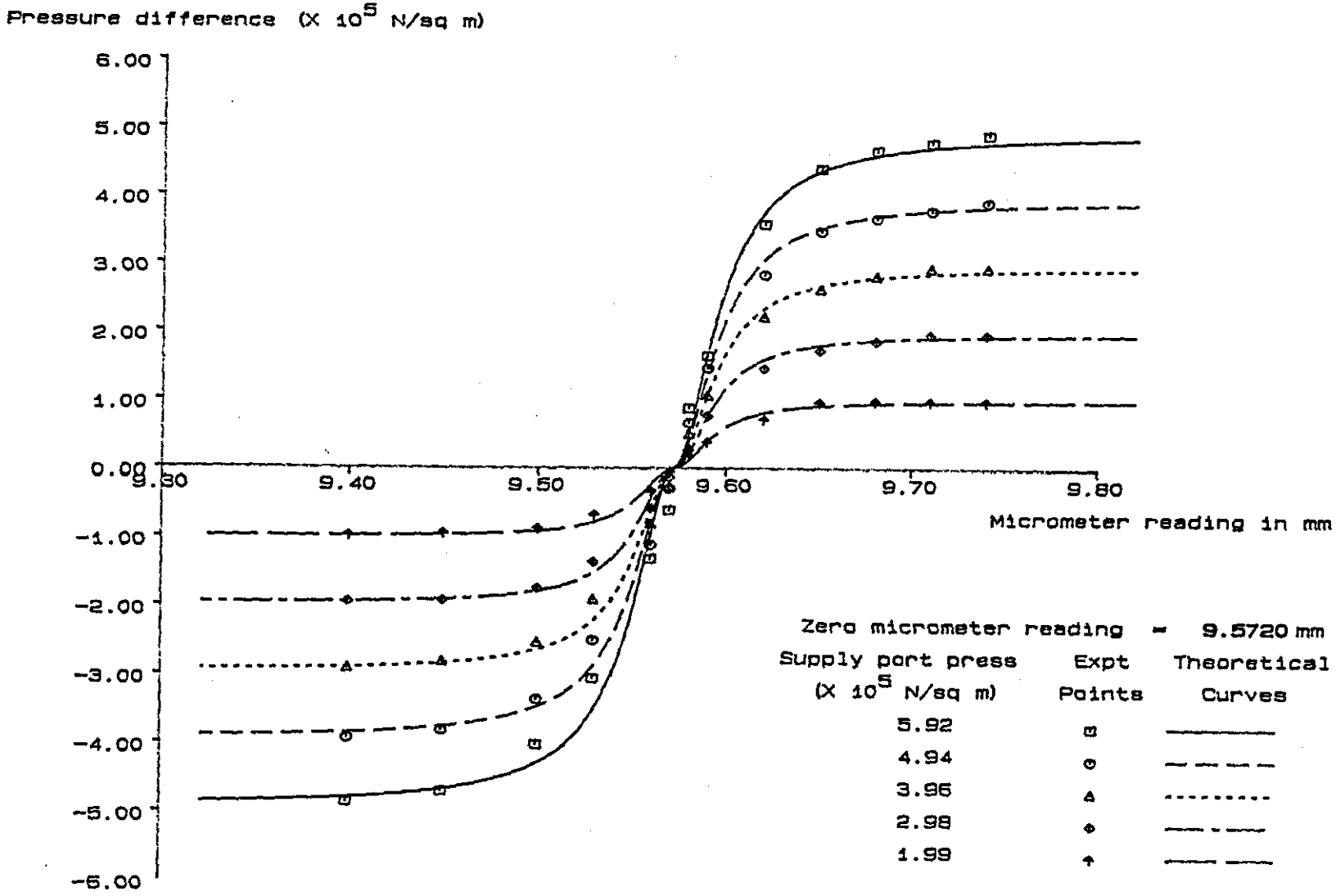

Fig. 7.3 - Pressure gain characteristics

Tab. 7.1 - Null positions determined in pressure gain test

Curve No.	Supply Pressure MNm^{-2}	Null Position as indicated on micrometer (mm)
1	0.5065	9.572
2	0.4052	9.572
3	0.3039	9.572
4	0.2026	9.573
5	0.1013	9.570

Based on the null point value determined from the pressure gain characteristics, the flow gain characteristics could be calculated with the spool displacement adjusted about the micrometer reading 9.572. The flow gain characteristics curves in Fig. 7.4 were determined using the same set of physical parameters as in the pressure gain characteristics. The density of air was taken as 1.2 kg m^{-3} [7.5].

The flow gain characteristics showed a saturation effect of the flow when the spool was displaced significantly. The saturation effect could not be derived from the conventional single restriction model. A comparison of the flow gain characteristics of the two theoretical models was made in Fig. 7.5. The flow saturation was attributable to the presence of an

intermediate volume in the valve land where the dynamic flow head to the associated channels was absorbed by the turbulence. The pressure difference to the other ports was subsequently reduced so that a relatively smaller total flow than that expected was generated.

The effect of upstream dynamic flow head was investigated by putting all the upstream Mach numbers in Eqn (6.51) to zero. The results are also depicted on Fig. 7.5. No substantial variations were found at small flow rates. However, at large flow rates (Mach Number > 0.5), the traditional adiabatic flow function falls short of the modified function Γ. This calculation showed that the upstream flow head was significant when the valve was more than half-open.

From Eqn (6.47) - (6.51), the reverse flow is given by the conditions at point 2 of the valve where the flow rate is independent of P_1 and T_1. This was confirmed by the phenomenon that the reverse flow curves, which were plotted at the fourth quadrant of Fig. 7.4, coincided for all values of P_1. Both experimental and theoretical results arrived at the same conclusion. This substantiated the validity of the flow function Eqn (V.13) and the flow node model for all flow situations through the 5-port valve.

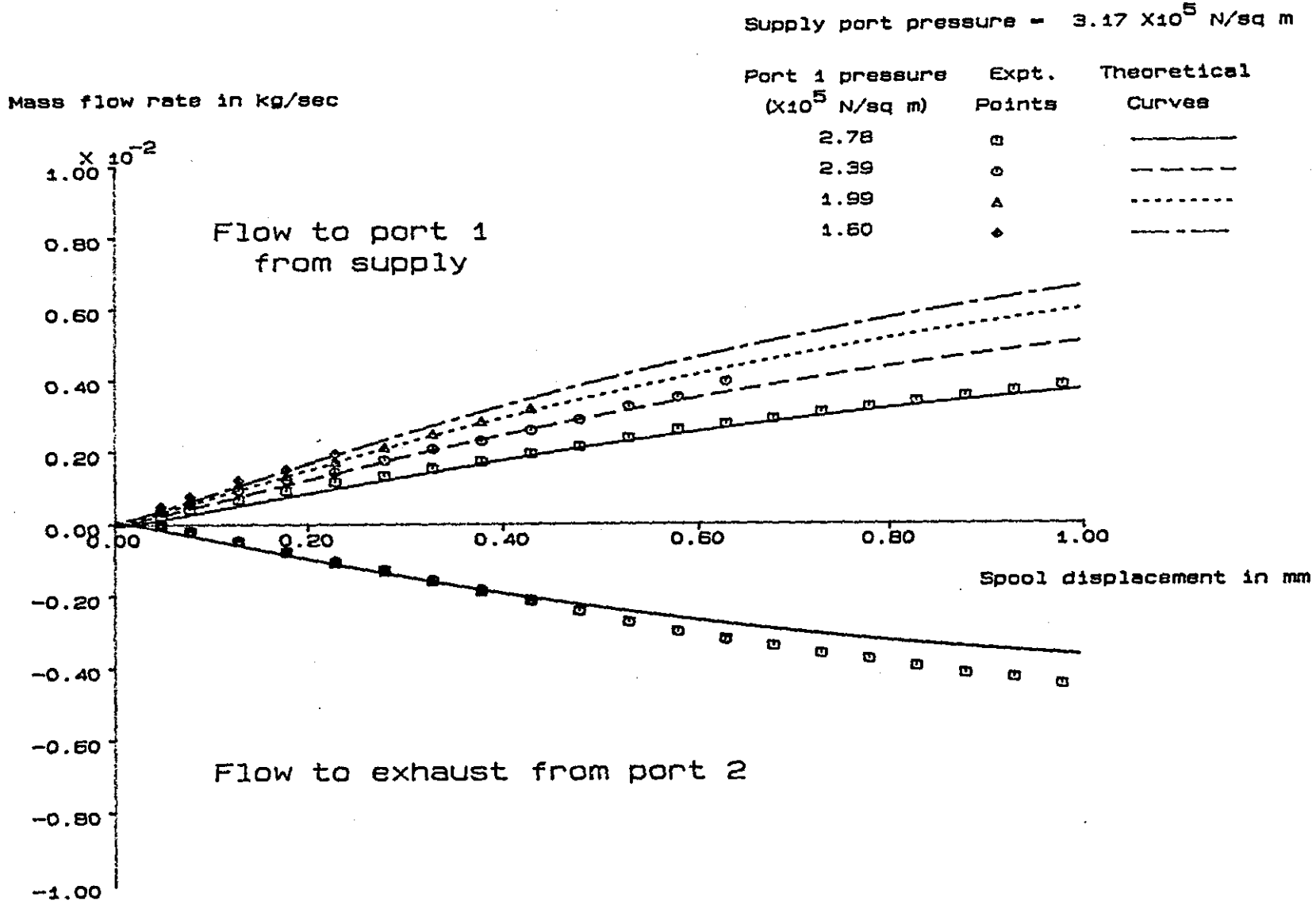

Fig. 7.4 - Flow gain characteristics

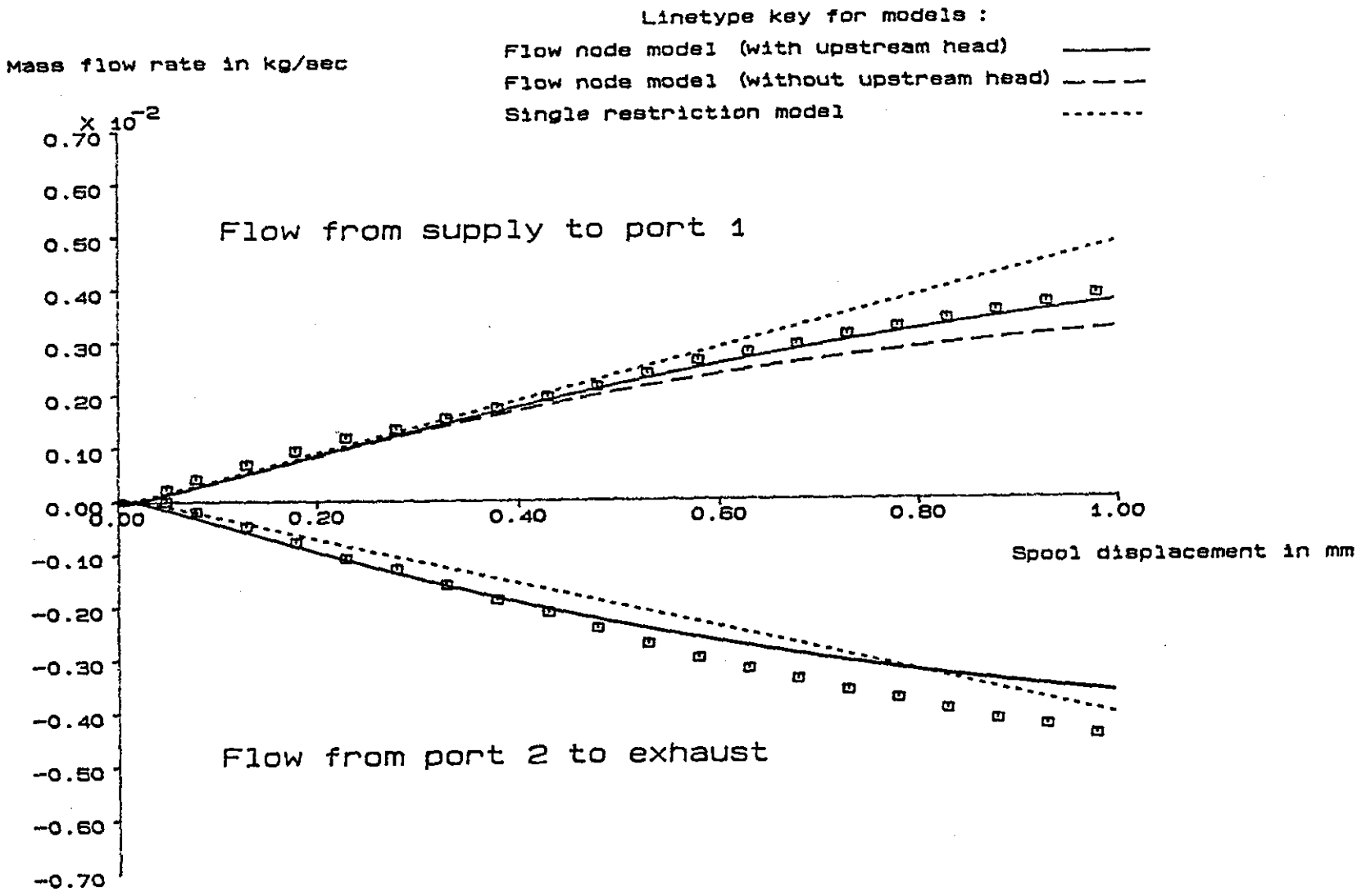

Fig. 7.5 - Flow gain comparison of valve models

7.1.1.4 The intermediate pressures

It was not possible to obtain any intermediate pressure values from the conventional approach in which the whole flow stream was lumped together in the formula. There was no way to segregate from Eqn (6.39) - (6.44) the type of pressure values pertinent to the description of pressure gain characteristics.

On the other hand, the proposed valve model suggested that an intermediate region existed between the supply, exhaust and output port. The pressure gain characteristics were the variations of the intermediate pressures due to spool displacements and could be deduced from the physical mensuration as well as the support data from other researchers. The theoretical intermediate pressures were obtained as the roots of the set of non-linear equations. The close agreement between the theoretical intermediate pressure curves and the experimental pressure gain curves therfore proved that the proposed flow node model is a good representation of the flow of compressed air through the valve.

7.1.2 Solenoid operated spool responses

It was difficult to measure the response of spool due to input signals because of the much smaller dimensions and forces involved in the valve. Some tests were carried out to assess the influencing factors but uncertainty of the actual values was large. The parameters which were put into the simulation model

were estimated to the most logical values from experimental as well as independent data sources.

7.1.2.1 Hysteresis

The hysteresis of the solenoid was checked by the short stroke displacement transducer. Fig. 7.6 shows a plot of the spool displacement against input current signal. Since the input current to the coil was proportional to the voltage which in turn was proportional to the DAC value, total hysteresis of the solenoid valve operator component could be estimated. In the absence of air flow and dynamic variations, Eqn (6.33) could be reduced to:

$$G_s X_c = K_{sp} X_s + F_i + F_{sf} \qquad (7.1)$$

Taking away the portion of input signal which would produce the proportional spool displacement X_s and initial compression F_i, Eqn (7.1) could be transformed as:

$$I_h = I_{sf} + I_{coil} \qquad (7.2)$$

where I_{sf} = signal attributed to friction force

I_h = input current (excluding portion for producing F_i and proportional force $K_{sp}X_s$)

I_{coil} = current signal utilised by the coil for overcoming magnetic hysteresis

That is, the total hysteresis measured in this test consisted of two parts, viz, magnetic hysteresis of solenoid and mechanical hysteresis due to stiction in valve.

From Fig. 7.6, the total hysteresis was 0.21A. The magnetic hysteresis was estimated to be 3.8% from consideration of the polarisation of the magnetic material of the core [7.6]. This corresponds to a current value of 0.038A. The stiction on spool could be estimated as:

Solenoid constant x (0.21/2 - 0.0375)

= 50 NA^{-1} x 0.067

= 3.35N

This stiction value was entered as the static friction constant F_{sf} in the analytical solenoid valve operator model Eqn (6.33).

7.1.2.2 *Effect of dither*

It is impossible to measure the spool location statically when the dither signal is switched on. However, the effect was determined indirectly by a test similar to the block port test (Fig. 7.7). The pressure at port 1 (P_1) was taken as the indicator of the hysteresis effect.

A series of tests up to 60 Hz input dither signal (all signals at 4 V peak-to-peak) were taken. The results are plotted on Fig. 7.8. The hysteresis was found to be minimum around dither frequencies 40 - 50 Hz.

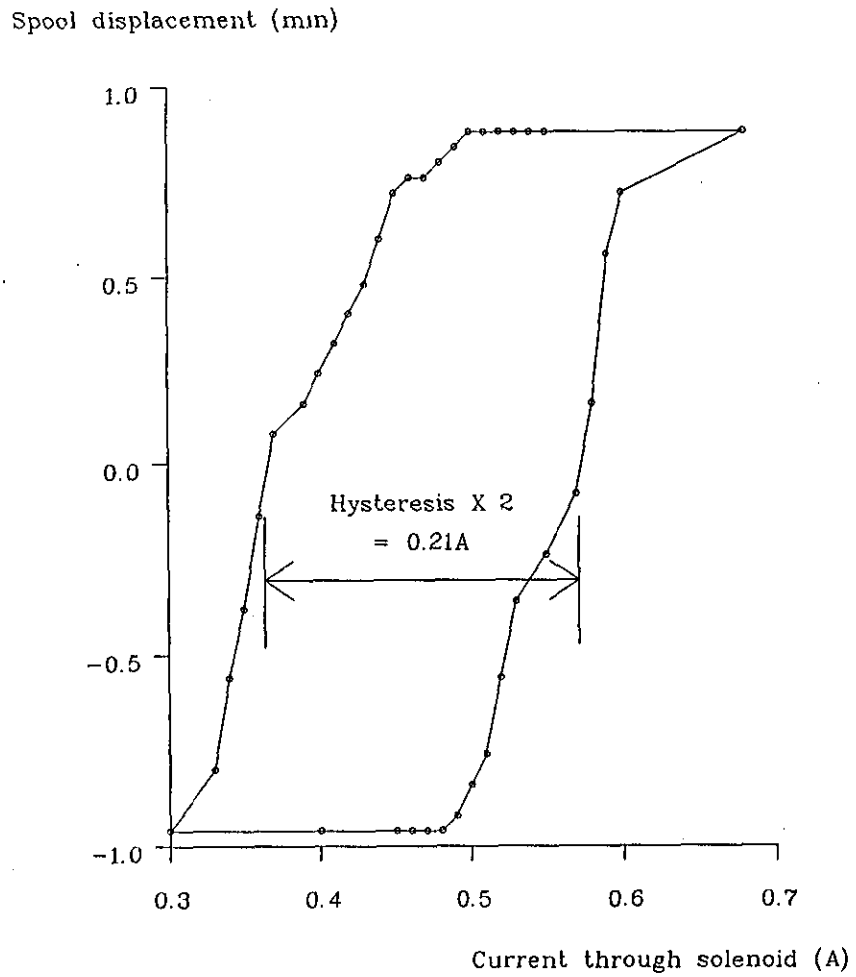

Fig. 7.6 - Hysteresis effect of solenoid

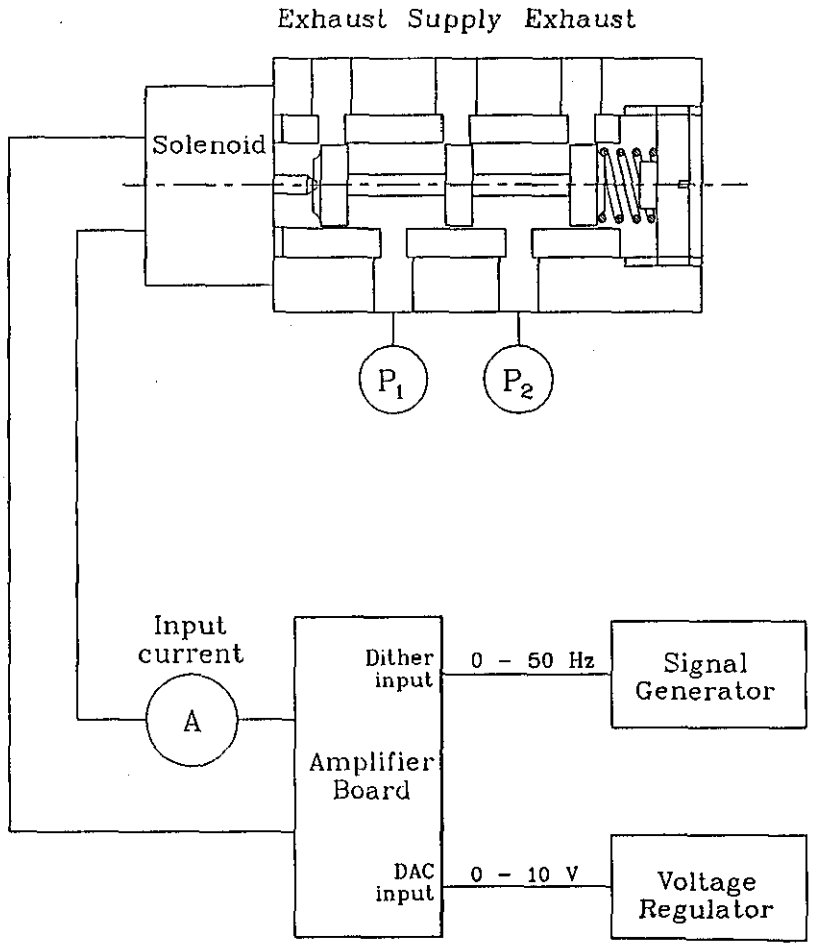

Fig. 7.7 - Measurement of dither effect

Fig. 7.8 - Tests with dither

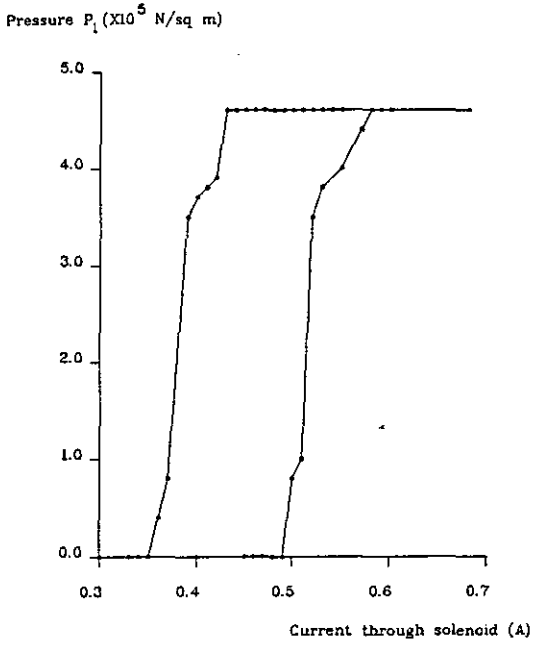

(a) - Dither frequency 20 Hz

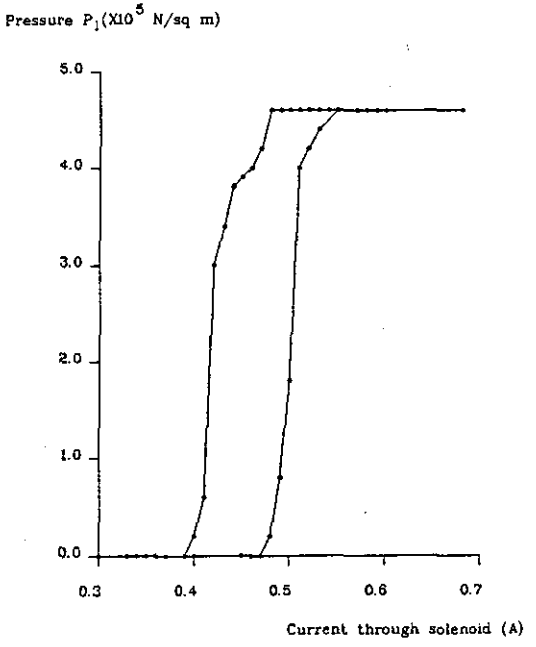

(b) - Dither frequency 30 Hz

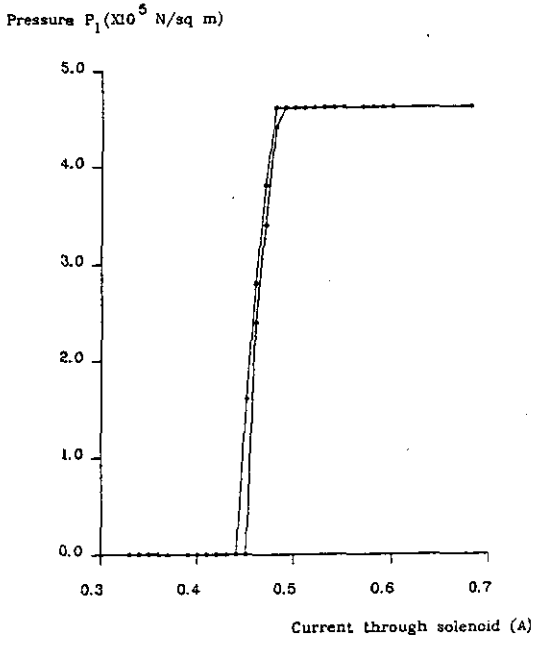

(c) - Dither frequency 40 Hz

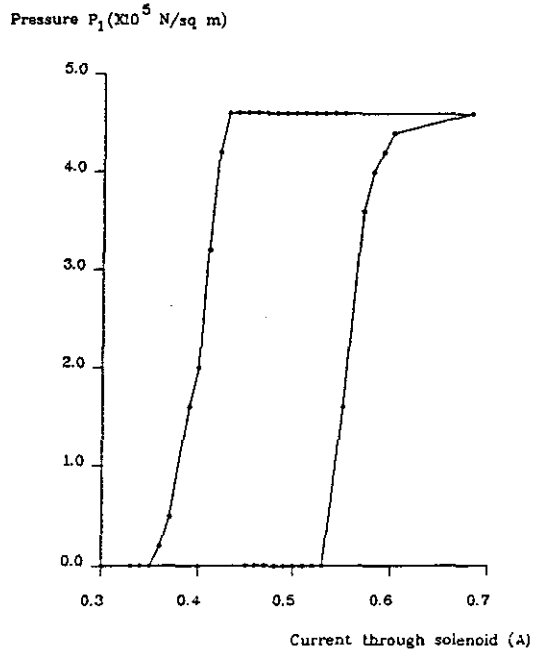

(e) - Dither frequency 60 Hz

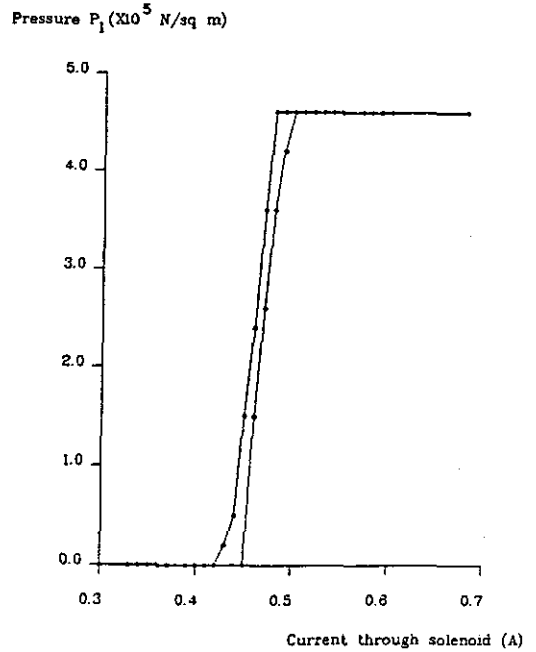

(d) - Dither frequency 50 Hz

7.1.2.3 Inertia and viscous damping

The inertia and viscous damping information was required by the analytical solenoid valve operator component module to determine the acceleration and velocity of the spool.

There were two moving parts in the solenoid valve: the spool and the solenoid core. The mass of the spool was 23 gm whereas the solenoid core was estimated to be 2 gm.

The viscous damping coefficient was estimated from the published viscosity data of the oil [6.12] used to lubricate the pneumatic circuit.

The frequency response of the spool-valve operator mechanism was investigated by a frequency spectrum analysis package "ils" [7.7]. The data file of spool location transients was transferred from the Sun workstation via an ASCII file containing bi-polar integer data to IBM PC. By the same facility, the simulated response of the analytical valve operator was transferred similarly. Both responses were analysed by the Fast Fourier Transform (FFT) techniques [7.8]. The result was depicted in Fig. 7.9. Both the actual and simulated frequency spectra showed that similar resonance frequency around 8 Hz and several harmonics in the 50 Hz spectrum. The component model of the solenoid valve operator is therefore regarded as a good representation of the real solenoid-spool mechanism.

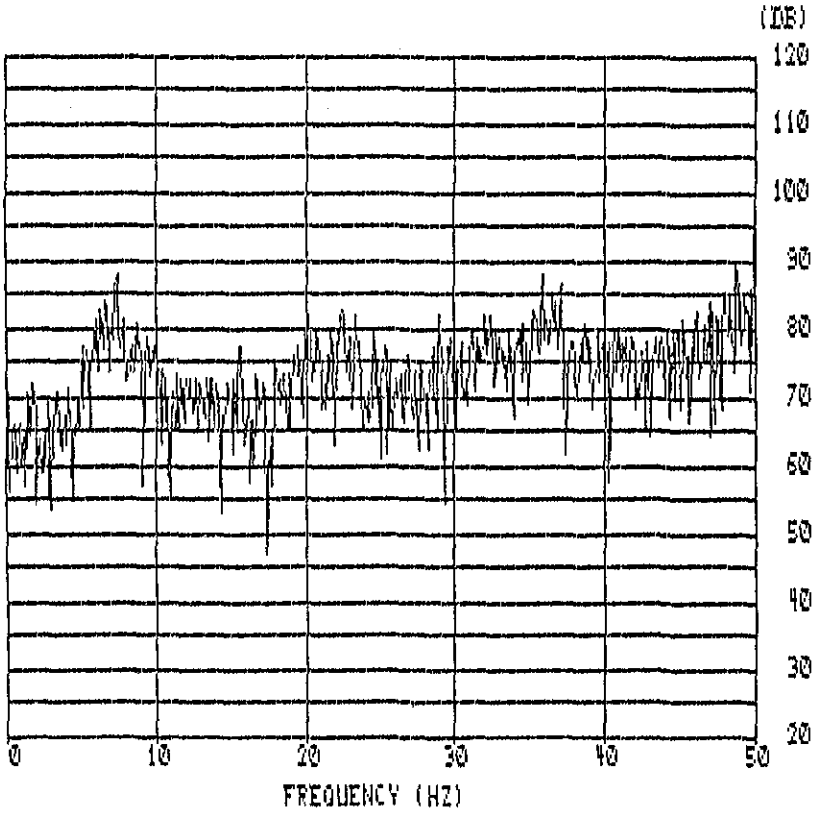

(b) Simulated spool location frequency spectrum

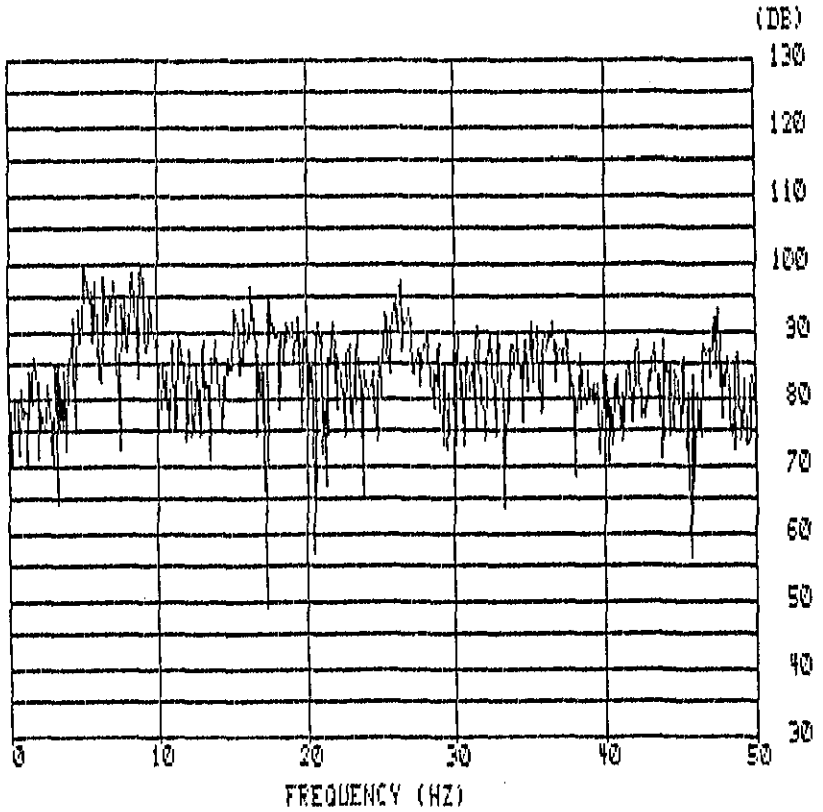

(a) Experimental spool location frequency spectrum

Fig. 7.9 - Frequency spectra of spool location responses

7.1.3 Actuator parameters

Two types of actuator parameters were identified:

(a) The dimensional parameters including the stroke length, bore diameter, piston rod and so on were measured directly on the actuator. The dimensions and their appropriate "C" parameters are depicted in Appendix VII.

(b) The estimated parameters which could not be measured directly. These include frictions, residual volume leakage, etc. The parameters were determined from various tests and related dimensions.

7.1.3.1 Static and coulomb frictions

The frictional forces in the test rig were determined by operating in open loop mode and measuring the pressures in the cylinder chambers. Two sets of tests were done - extending and retracting circumstances.

The air pressure to the test rig was initially adjusted to nearly zero. Using the open loop mode, the valve was opened to about 1/4 of the full opening. The transient recording feature was then enabled.

The air pressure was increased slowly until the test rig started to move. The movement continued for a while to ascertain that it extended (or retracted) at constant speed. Transients

were recorded until the buffer was exhausted. The data were subsequently transferred to DG machine and analysed.

Fig. 7.10 and 7.11 depicts the transient plots when the test rig was retracting and extending. Static friction was effective immediately before the piston started to move and was calculated at points where the velocity changed to non-zero. The actuator force was determined by Eqn (6.25). In the same way, the frictional force calculated at points where the velocity was constant was dynamic (coulomb) friction.

It was found that the frictional forces at extend and retract circumstances were different. The values estimated from the above test on the asymmetric actuator were:

Tab. 7.2 - Static and coulomb frictions

Circumstances	Static	Coulomb
Extending cylinder	74.3N	40.6N
Retracting cylinder	40.4N	12.2N

This directional difference has been modelled by a separate routine and the relevant friction values were entered into the corresponding "C" parameters of the load module.

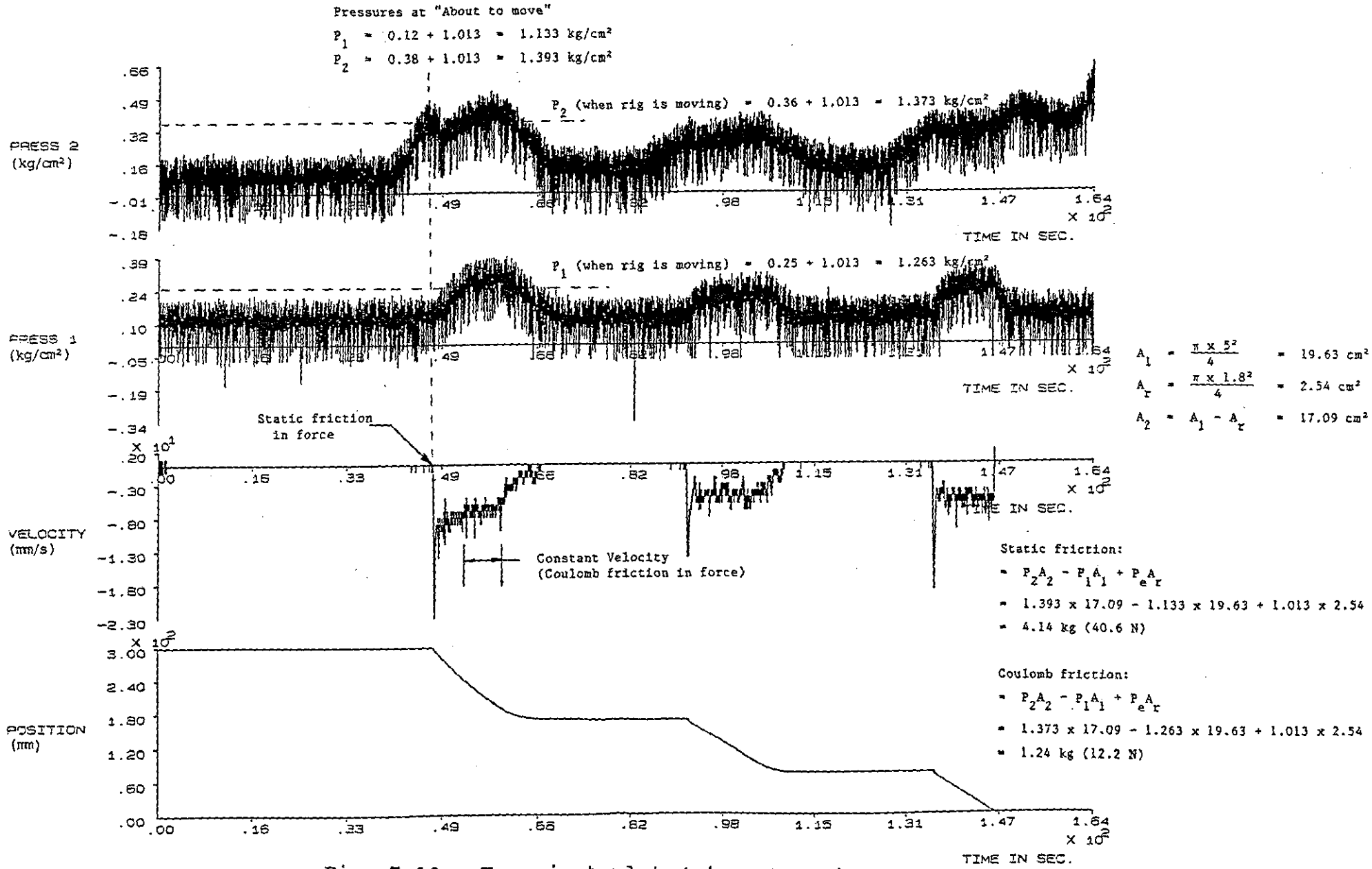

Fig. 7.10 - Transient plot (rig retracting)

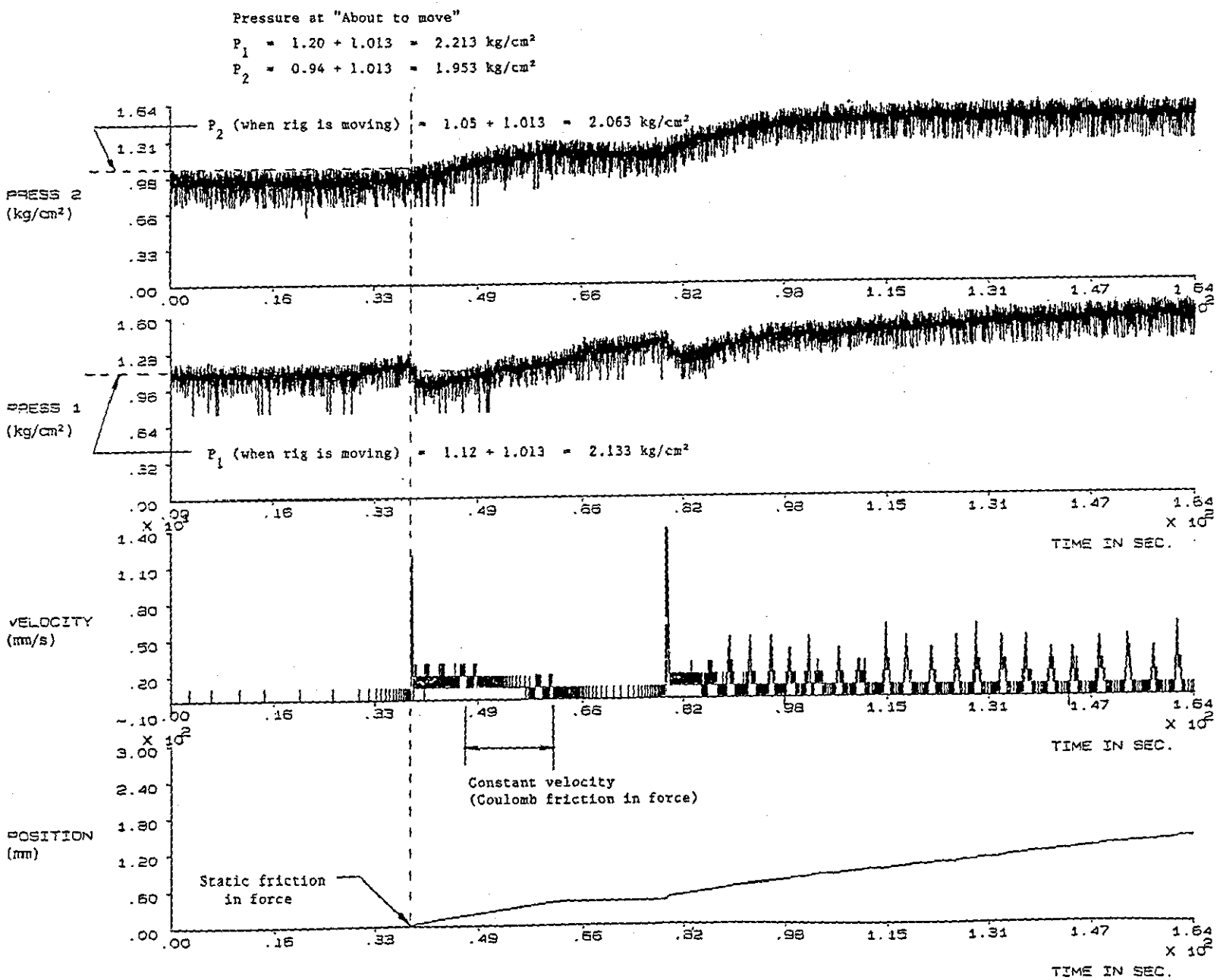

A_1 = 19.63 cm²

A_r = 2.54 cm²

A_2 = 17.09 cm²

Static friction:

= $P_1A_1 - P_2A_2 - P_eA_r$

= 7.57 kg (74.3 N)

Coulomb friction:

= $P_1A_1 - P_2A_2 - P_eA_r$

= 4.11 kg (40.4 N)

Fig. 7.11 - Transient plot (rig extending)

7.1.3.2 Viscous friction

The pneumatic test rigs have been designed to eliminate, as much as possible, any contact type friction. It was inevitable that dry friction existed between the seal and piston as well as at the slideway. A significant reduction has been achieved by mounting the slideway on ball bearings for the asymmetric actuator. Some viscous friction still existed at various locations such as the bearing and the cylinder where traces of oil were left as a result of droplets in the air stream or maintenance lubrication. The viscous friction coefficient was estimated from the technical data of the lubrication oil [6.12].

7.1.3.3 Residual volume

The residual volume was defined as the air volume at the end of the cylinder when the piston stayed at that end. The volume could not be measured due to the irregularity in shape. It was estimated by considering that the gap could be lumped to an annular ring at the end-blocks.

For the sake of simplicity, the residual volumes of the asymmetric actuator and the symmetric actuator were assumed to be similar (Tab. 7.3).

Tab. 7.3 - Estimation of residual volume

Actuator	Asymmetric	Symmetric
Thickness gap (mm)	10	10
Diameter of piston (mm)	50	25
Residual volume (m^3)	0.00002	0.000005

7.1.4 Calibration of pressure drop in tubing

The pressure drop through tubing was investigated in an experiment in conjunction with the measurement of mass flow rates through the 5-port valve. The experimental data were plotted in Fig. 7.12. The trend of the data showed that the pressure drop ratio varies linearly with the mass flow rates. A regression line was drawn on the data points according to Eqn (6.61). The values of K_{dr} and the reference mass flow rate $\dot{m}_{ref}$ were determined to be 0.4 and 0.00465 respectively.

7.1.5 Timer calibration of the microprocessor controller

Due to the uncertainty of the overhead in the time keeping interrupt routine, a calibration facility was built into the control software. The facility directed execution to go through the normal route but the control function was disabled. A loop counter was kept and reported periodically to the console. The

timer could then be calibrated by a stop watch and the time per interrupt cycle was calculated with the reported count number. The intention was to determine, in real time, the interrupt interval time generated by the on board timer.

Fig. 7.13 shows the timer calibration chart. It was clear that due to the execution overheads in the interrupt service routine, a minimum interval time of 0.28 msec was found at very low timer values.

The proportional portion of the chart was also calibrated as a regression line which was used as the function for calculating the time base of the transient responses in the response evaluation program "EVAL.PR".

7.1.6 Constants

The physical constants such as the adiabatic constant (n), the gas constant (R), supply and exhaust conditions (P_s, T_s, P_e, T_e), mechanical dimensions of test rig and pneumatic components were extracted from the relevant literature [7.5]. The meaning of the "C" and "L" parameters are tabulated in Appendix VII. Parameters marked "Not used" were reserved for future use. Parameters marked "Working constant" were used by the model to store data for communication between integration passes.

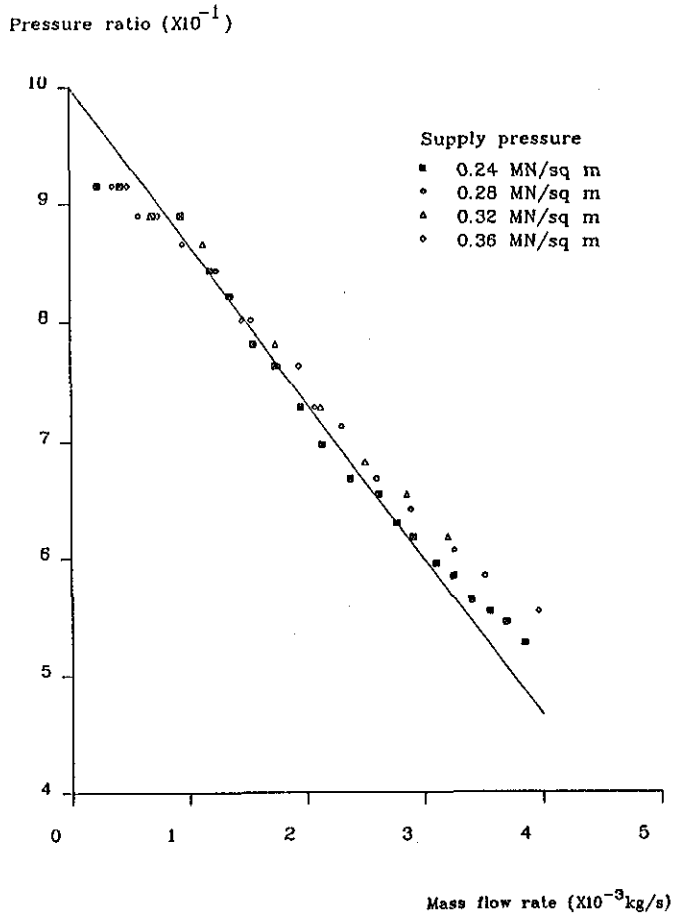

Fig. 7.12 - Regression plot of pressure drop in tubing

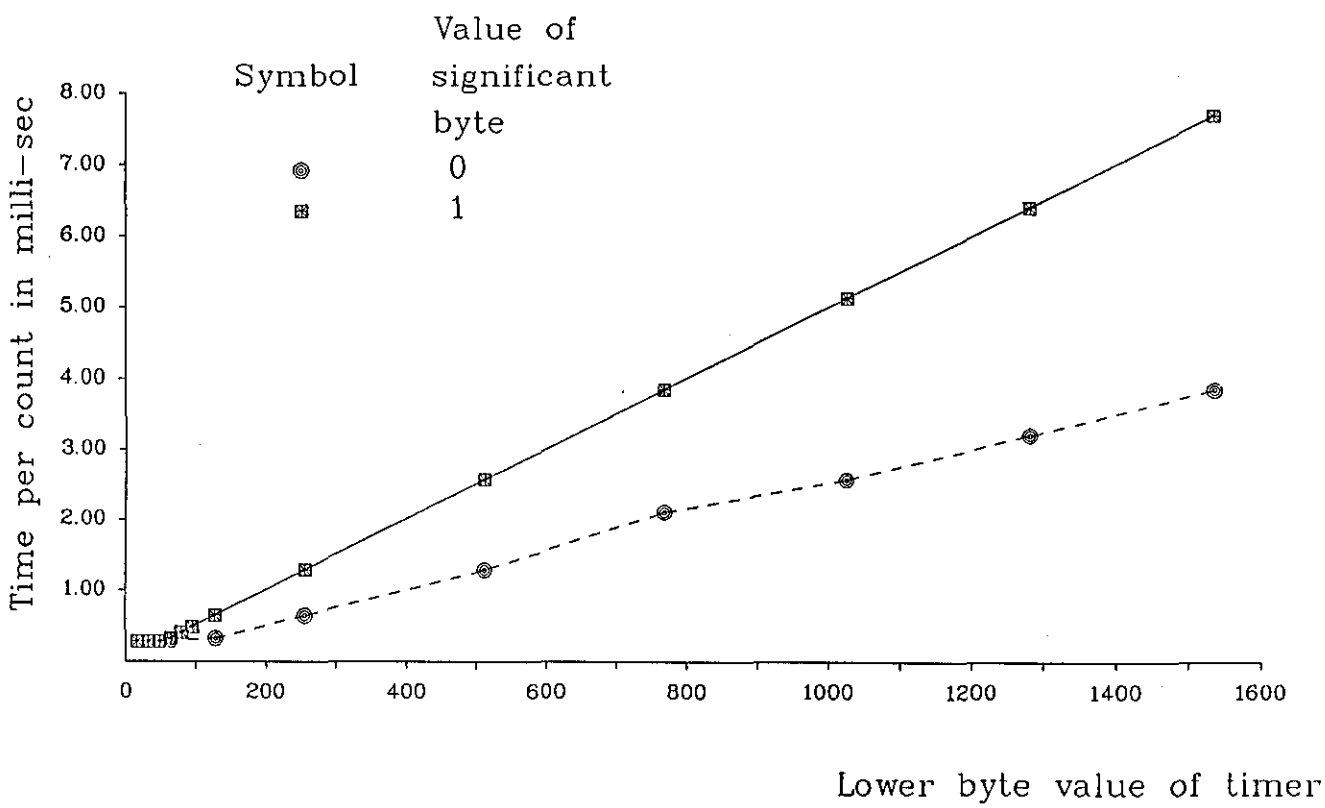

Fig. 7.13 - Calibration of timer

Since there were 3 servo-drives assembled for validation, the default values only indicated typical values to be used for preliminary test runs. Changes to suit the particular component of the real system would be made to refine the parameters in the module during simulation initialisation stage.

7.2 Simulation of specific test rig models

The specific models of the servo-drives A, B and C outlined in Section 6.7 were simulated to obtain the time responses. In order to secure exact comparison of the responses, the initial parameters of the tests such as starting position, pressures and temperatures were entered into the package during the initialisation phase. The experimental responses were merged to the corresponding simulation data by the response merging program "EVALCMS2".

7.2.1 Servo-drive A - Stepper motor operated valve system

The open loop responses of servo-drive A are shown on Fig. 7.14. The theoretical and experimental position curves agreed fairly well. Due to the effect of physical-stop at the end of stroke, both the experimental and simulated curves stopped exactly at the two ends of the cylinder. When the rig was moving, the rate of change of the two position curves (speed) differ slightly and this resulted in time lag at the later part of the simulated position response.

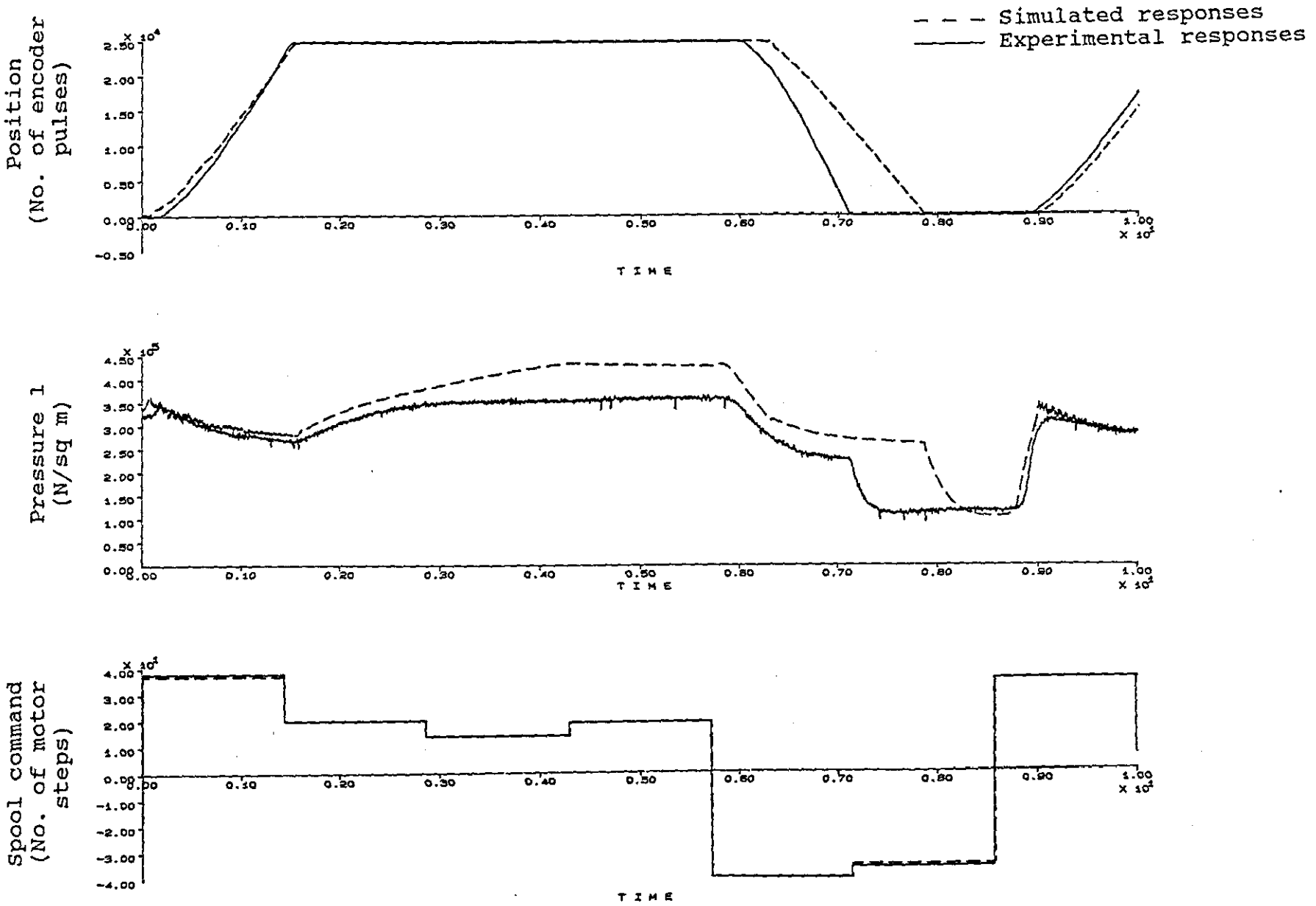

Fig. 7.14 - Open loop responses of servo-drive A

The spool command transients showed that the timing and value for the open loop commands have been simulated exactly by the controller module. This reflected the fact that the controller was the best known component in the system.

The pressure responses did not agree satisfactorily in value. However, agreement of the trend could be seen from both responses. The large difference between the responses could be due to :

(a) There is leakage flow between the two cylinder chambers. The actuator module generating the graph on Fig. 7.14 did not have leakage function enabled. In a trial run with the leakage function and intuitive guess of the necessary parameters, a closer agreement was obtained especially during the retracting motion. However, more thorough tests are required to ascertain the validity of the parameters. As explained in Section 8.3.3, there are instrumentation problems involved in the measurements. Therefore, the trial run results are not presented here as a confirmed record of finding.

(b) The theoretical model assumes that the pressures in the control volumes of the actuator are homogeneous. The simulated values were in fact the pressures inside the cylinder chamber whereas the experimental transmitters connected to the inlet which was outside the cylinder chamber. This would induce deviations due to non-homogeneity of the volume. It could exist eventhough the cylinder was at rest because of the leakage problem discussed in (a) above.

(c) An attempt was made to use the instantaneous pressures P_{1v} and P_{2v} which were simulated pressure values at the valve outlet, where the transmitters were connected, to compare to the experimental responses. Fig. 7.15 shows the comparison graph using P_{1v} and the experimental pressure. It can be seen that the instantaneous values are far too oscillatory.

After careful investigation in the whole integration process, it was found that the high frequency oscillation is a numerical instability due to the immediate backward reference of the mass flow rate in the computational procedure. The fact that the tubing model has been established from steady state flow characteristics effectively implies that the mass flow rate flowing in is exactly the mass flow rate flowing out of the tubing. The tubing model is therefore a stiff model as far as the numerical integration routine is concerned.

In reality, air pressure takes time to build up. A preliminary investigation in the problem has been carried out by introducing a first order time lag for the propagation of the calculated pressure drop values. Trial runs of the simulation showed that oscillations are notably reduced when the time constant is 1 ms and totally removed when the delay is increased to 10 ms.

This is, however, not a formal formulation of the underlying phenomenon. More work is required to determine, from first

principles, the propagation of the pressure wave in tubing so that the proper tubing model can be established without relying much on empirical data or intuitive guesses. Further research in this direction is required to refine the tubing model on the damping effect of the air column on the pressure values at both ends of the tubing.

In the current implementation of the pneumatic system model, there are at least 5 passes required by the integration algorithm before it concludes at an integration step. Therefore, as the integration routine progresses, the effect will be averaged out in time. This trend can be determined from Fig. 7.15 if a smoothing operation is done on the vibrating P_{1v}. In other words, there is a significant bearing on the intermediate numerical values of the variables in the system between consecutive passes of the model, but the effect will be cancelling one another by the integration process. It is for this reason that the P_{1v} and P_{2v} values are not used as the basis for model validation whereas P_1 and P_2 are still valid in the light of the proper theoretical tubing model with time delay is not available.

The closed loop responses of the servo-drive are shown in Fig. 7.16. In general, the theoretical and experimental position curves agreed well. A larger amount of damping was found with the simulated responses and this reflected the indication of the difference in velocity responses in open loop test.

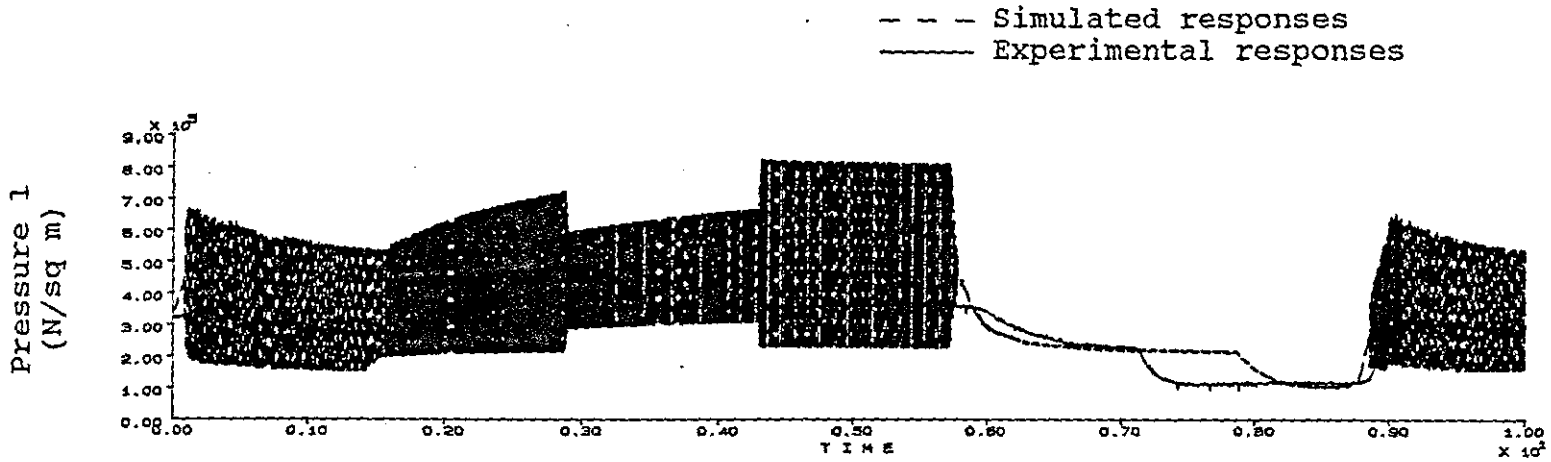

Fig. 7.15 - Pressure responses using P_{1v} as comparison

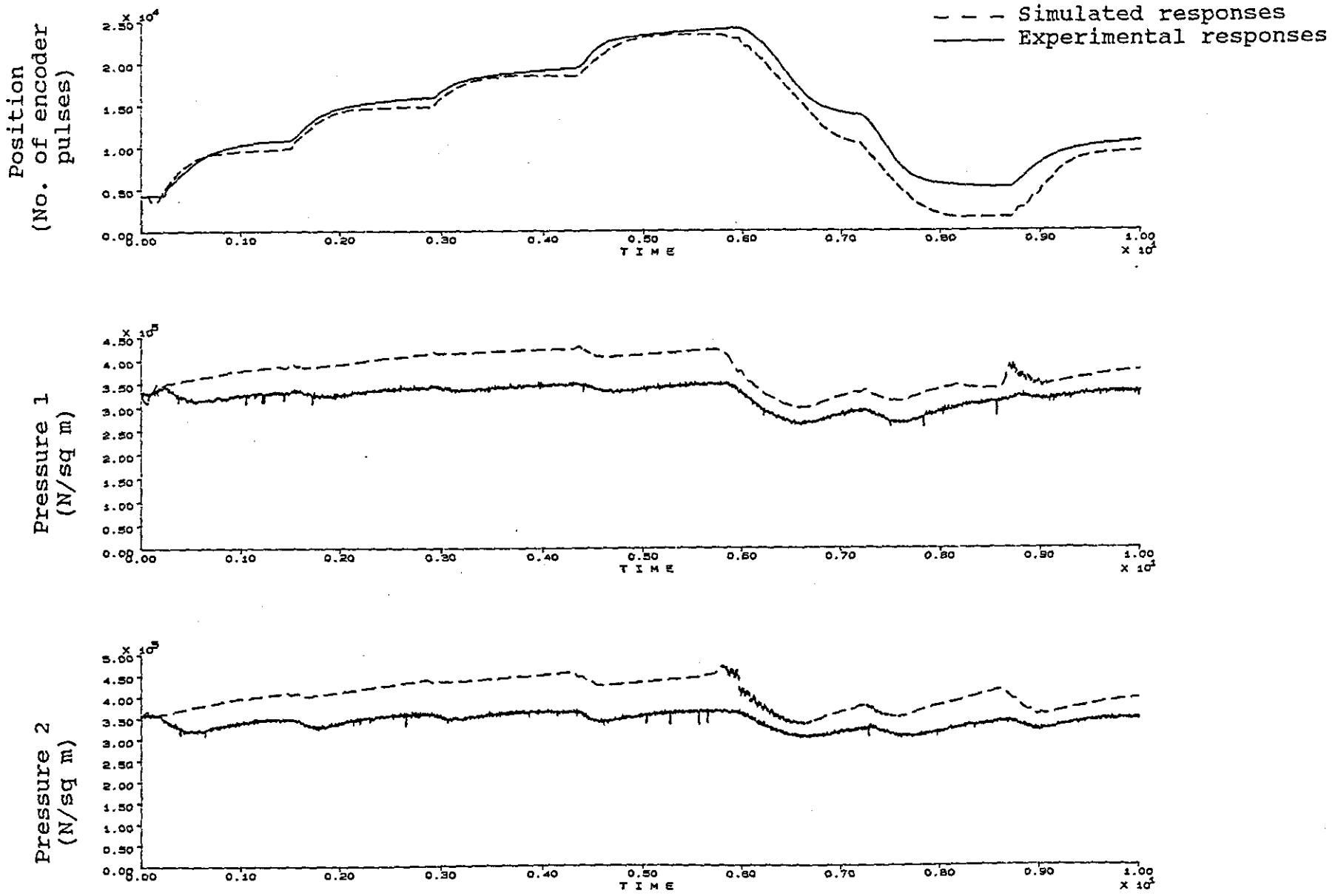

Fig. 7.16 - Closed loop step responses of servo-drive A

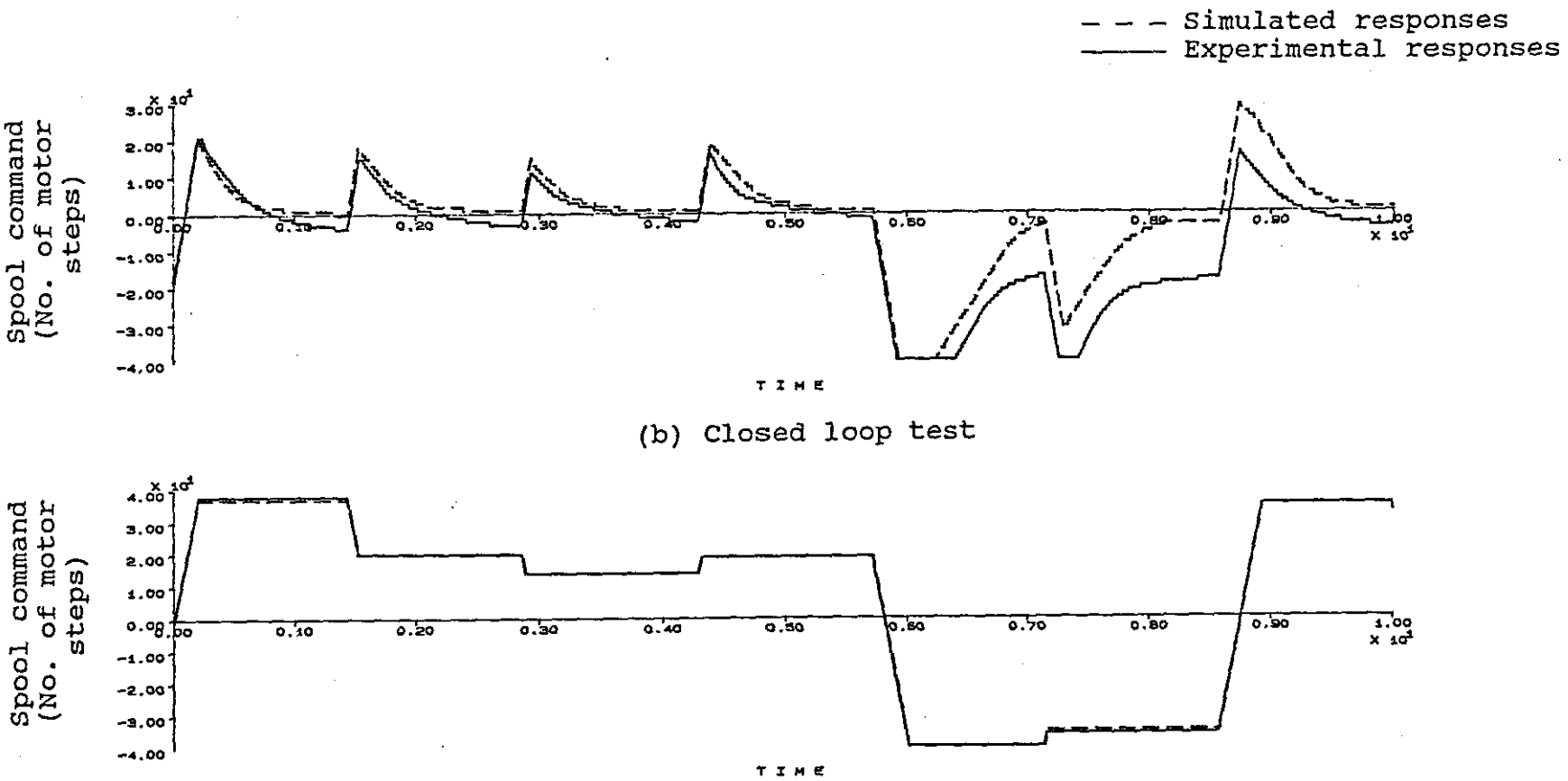

Fig. 7.17 - Spool location responses of open loop and closed loop tests

For the stepper motor valve operator, the spool location responses were readily obtainable from the track-keeping of command output. Fig. 7.17 shows the spool location responses of the open loop and closed loop tests. It is understandable that the discrete nature of the controller and the valve operator allows an accurate modelling of the components.

The model was successful in simulating the stable performance of the servo-drive. Although there were deviations in values of the steady state errors, the prediction was acceptable in terms of dynamic behaviour and timing of moves.

7.2.2 Servo-drive B - Solenoid operated valve system

The closed loop responses of servo-drive B were the result of a step test with the variable positional gain profile control strategy (Fig. 7.18). Detail description of the control algorithm is depicted in Appendix IX. A close agreement was obtained with the position responses with slight deviations in stability, frequency and amplitude of vibration. The pressure responses, however, deviated significantly in magnitude, although there were signs for the simulated responses to agree to the trend of pressure variations during step changes. The large deviation was attributed to the difficulties in predicting the performance of the valve operator/spool mechanism, especially the influence of dither and hysteresis. The error introduced by these parameters affected both actuator chambers and hence only had minor effect on position responses. It is noted that the chamber pressures were

reduced slightly.

Comparing with the servo-drive A, the simulation model for servo-drive B had better agreement with respect to the position responses. This further supported the view that the solenoid valve operator was less accurately modelled than the stepper motor valve operator. The averaging effect of the errors in spool location, pneumatic conditions and load force calculations had outweighted the tolerance of the spool mechanism.

7.2.3 Servo-drive C - Symmetric actuator system

The closed loop responses of the servo-drive C is shown in Fig. 7.19. The reverse motion part agreed well with the experimental data showing that the model basically represented the symmetric actuator system. However, the forward moves did not match closely enough especially on the prediction of damping on the test rig. This deviation was due to the fact that the friction values in Tab. 7.2 was used. The friction test was not performed on the symmetric test rig because of changes in the laboratory environment during later part of the project and the connection to Data General host machine was no longer available. The transfer of test data was difficult though not impossible. It is anticipated that if the correct friction values could be measured, the accuracy of the simulation results would be improved.

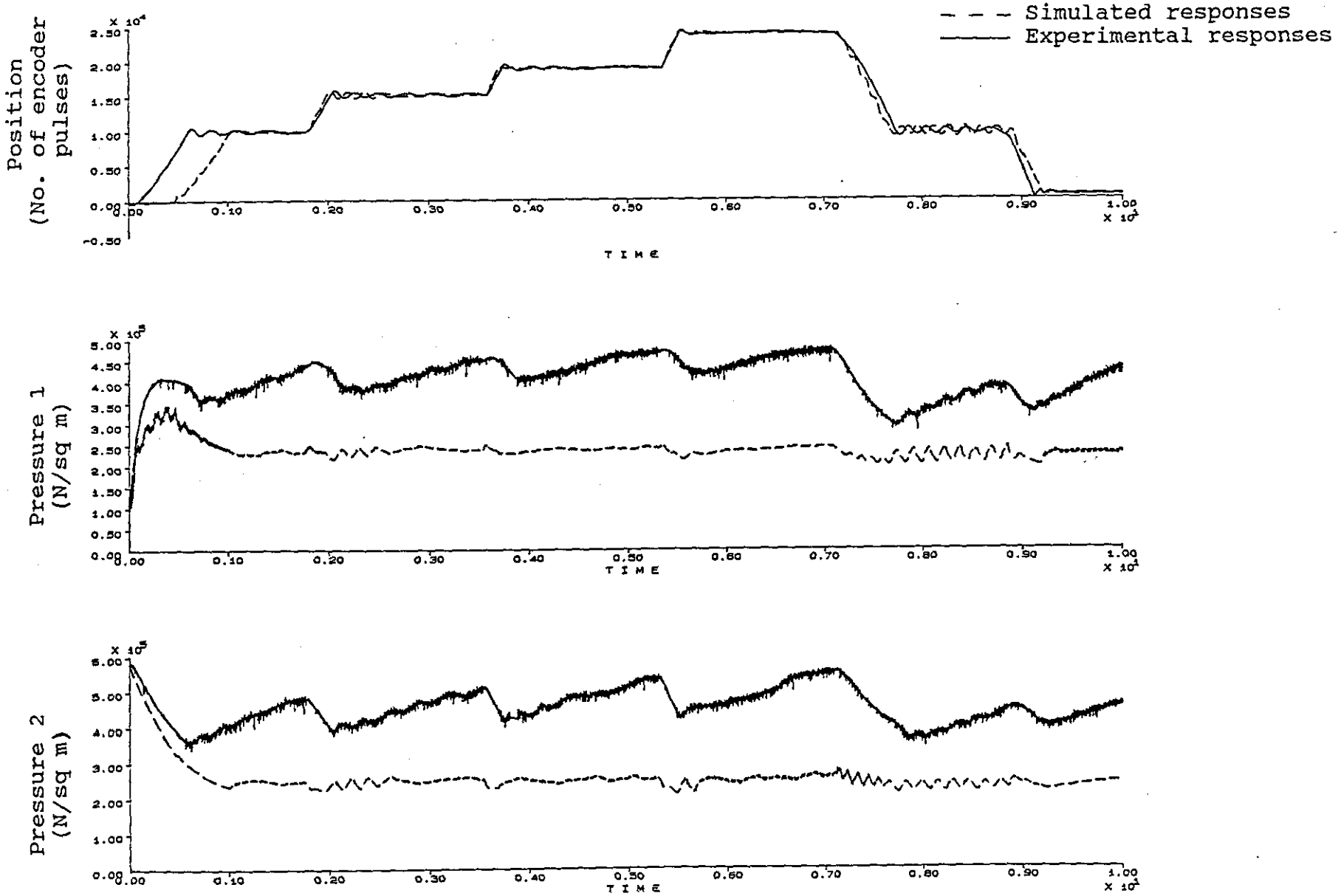

Fig. 7.18 - Step responses with solenoid operated valve system

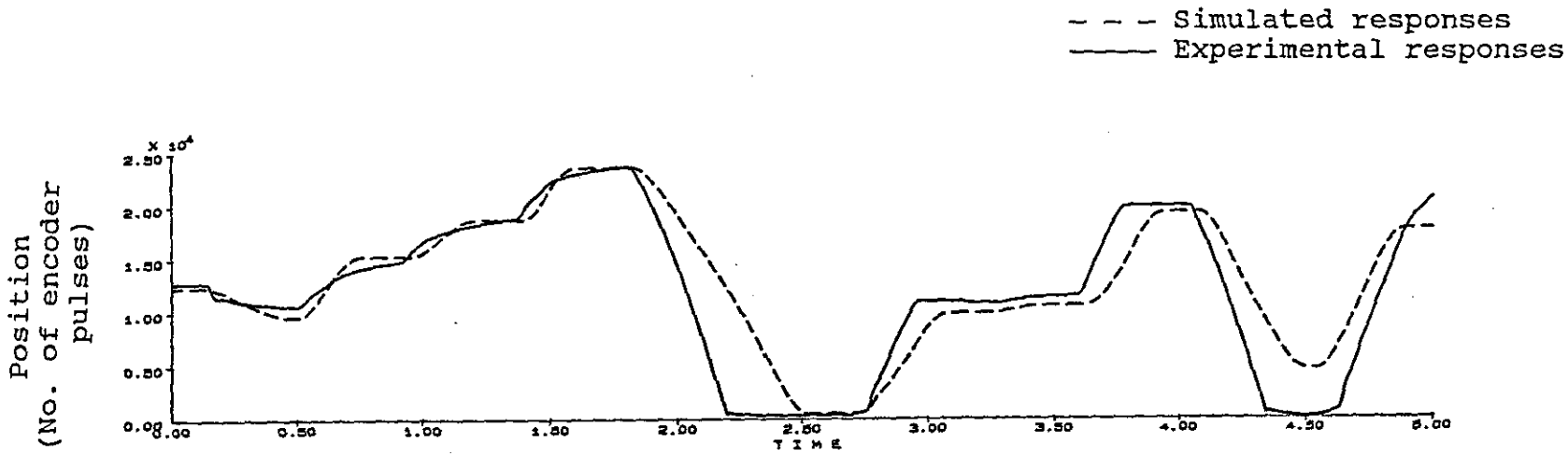

Fig. 7.19 - Step responses with symmetric actuator system

Nevertheless, the test showed that the component oriented approach provide a preliminary picture of the system quickly. Further refinement can be made if the first off results are promising thereby saving the effort to investigate non-viable systems.

7.2.4 System accuracy

By using an enhanced option in the simulation package, the simulated and experimental responses were compared by computing the standard deviations between corresponding responses. The results were shown in Tab. 7.4.

Tab. 7.4 - Tabulated standard deviation of responses

Servo-drive	Responses	Standard deviation	Unit
A	Open loop :		
	Position	3,161	Encoder pulse
	Pressure 1	59,071	N/sq m
	Pressure 2	90,245	N/sq m
	P_{1v} and P_1	212,716	N/sq m
A	Closed loop :		
	Position	1,837	Encoder pulse
	Pressure 1	56,813	N/sq m
	Pressure 2	65,736	N/sq m
B	Position	1,523	Encoder pulse
	Pressure 1	173,470	N/sq m
	Pressure 2	204,023	N/sq m
C	Position	2,637	Encoder pulse
	Pressure 1	186,863	N/sq m
	Pressure 2	225,410	N/sq m
	Spool location	0.0138	mm

It is difficult to assess the results in absolute terms but the values do indicate the relative accuracy of the models for the three servo-drives being simulated. In terms of position responses, the responses with servo-drive B was the best among the three. The length corresponded approximately to 0.8% of the total stroke.

In contrast, the pressure responses were unsatisfactory. The deviations from the actual results were all having a higher value. This requires further investigation into the factors affecting the pressure levels in cylinder chambers, apart from the actuator dynamics described in the actuator dynamics (Section 6.1.1).

7.3 Verification based on published data

In order to check the validity and flexibility of the component modules, data from other selected sources are applied to formulate new components and linked to the package. Due to the lack of detail information of the hardware, certain amount of assumptions were made to the system parameters. High conformity to the transient responses of the published data should not be expected, but a general agreement to the trend of the performance was obtained.

7.3.1 LUT data with stepper motor operated valve

Earlier tests in LUT on control strategies and configuration

of pneumatic servomechanisms were useful to provide additional verification database for the generic model. One of the tests performed on a vertical mounted asymmetric cylinder had been documented by Moore [1.8]. The test rig was heavily loaded and the friction force in the slideway was high. These parameters were estimated and entered into the relevant "C" and "L" arrays in the package. The test run was made with a modified proportional control algorithm. A separate control algorithm routine was written to cater for the modification. The routine was used to compute the appropriate spool command for the controller module. Detail information of the test is reproduced in Fig. 7.20 for reference.

Since the data were not recorded in numerical form, it was only possible to make visual comparison of the corresponding responses. Since the reported responses were shown in different units, the simulated responses were rescaled and labelled to make the two comparable. From Fig. 7.21, the pattern of variations shows remarkable agreement both in the differential pressure and velocity responses. The numerical values of the velocity matched with the range of magnitude. In the case of the differential pressure responses, since the actuator was asymmetric, there should be a pressure difference when the actuator was not moving. The zero pressure difference line was therefore taken as the datum in the simulated response graph where the actuator was stationary. Having made the adjustment, the differential pressure values agreed in magnitude.

7.3.2 LUT data with solenoid operated valve

Later tests in LUT using the same pneumatic actuator and load system but controlled by a solenoid operated valve showed that the system had better response to input signal in terms of start-up delay and stability. The graphs of the test is depicted in Fig. 7.22. The test run was made with positional gain profile, velocity and acceleration feedback.

Only one step's move was recorded and was simulated, as far as possible, with the reported test parameters initialised. The move represented a retraction from 4000 (hex.) back to 2000 (hex.) encoder pulses. The gain profile during the test was used exactly as it was in the actual experiment.

Fig 7.23 shows the simulated responses of the system. Due to the lack of fine detail information of the test, the simulated responses were regarded as sufficiently close to the reported responses. The model therefore provides a fair representation of the LUT system without much modification.

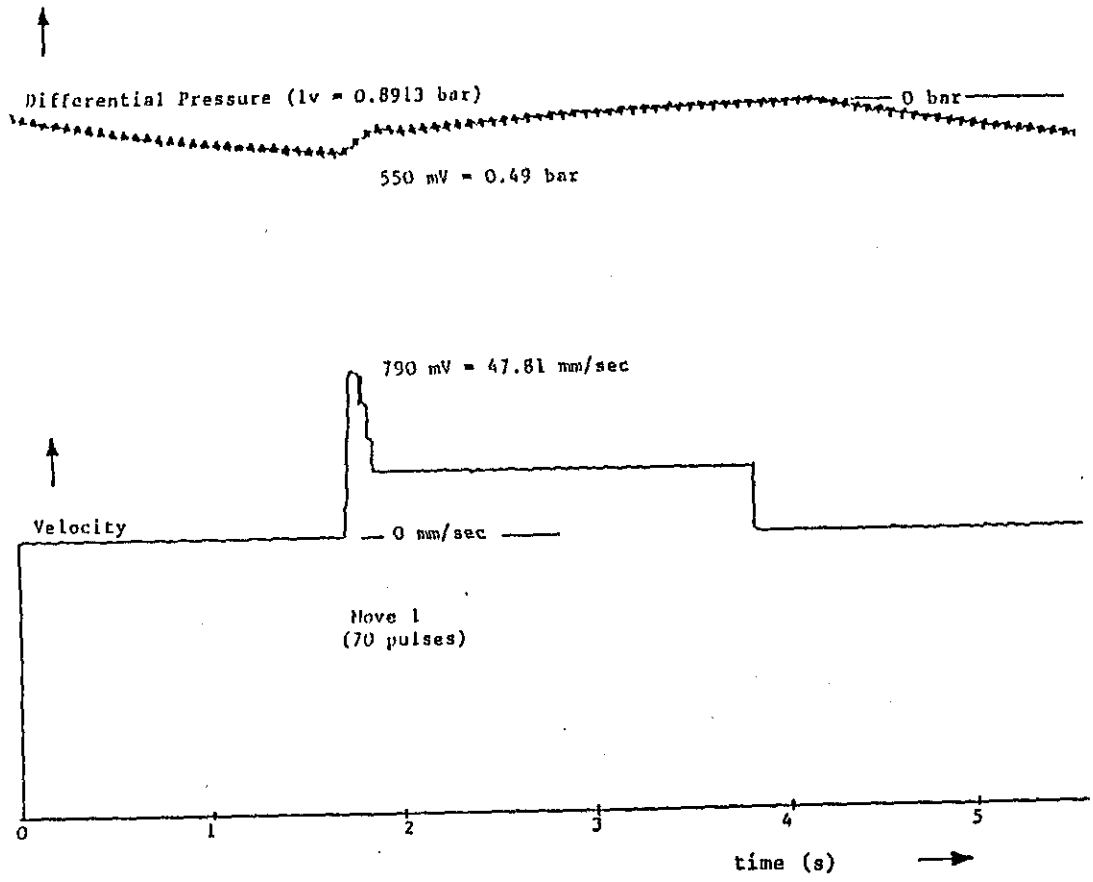

Fig. 7.20 - LUT stepper motor operated valve test

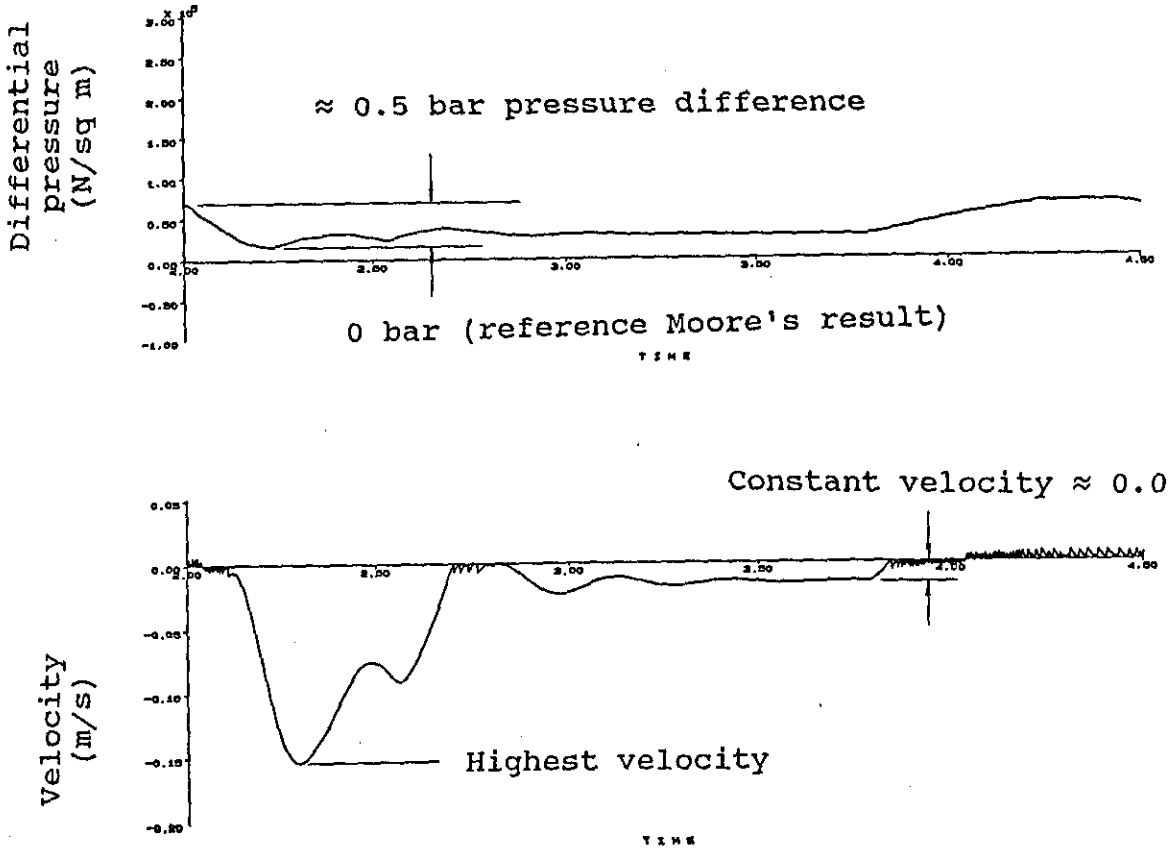

Fig. 7.21 - Simulation of LUT stepper motor operated valve system

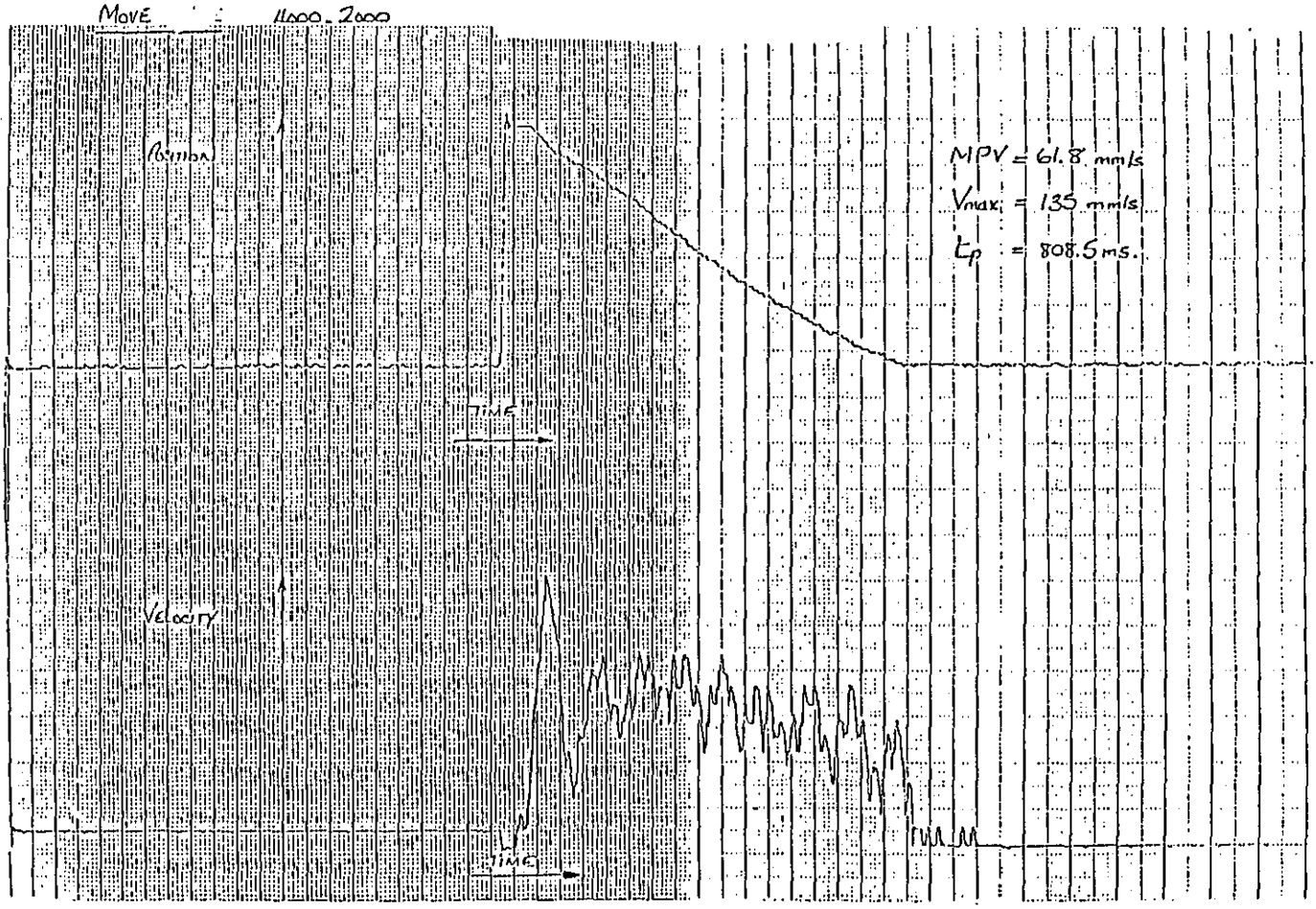

Fig. 7.22 - LUT solenoid operated valve test

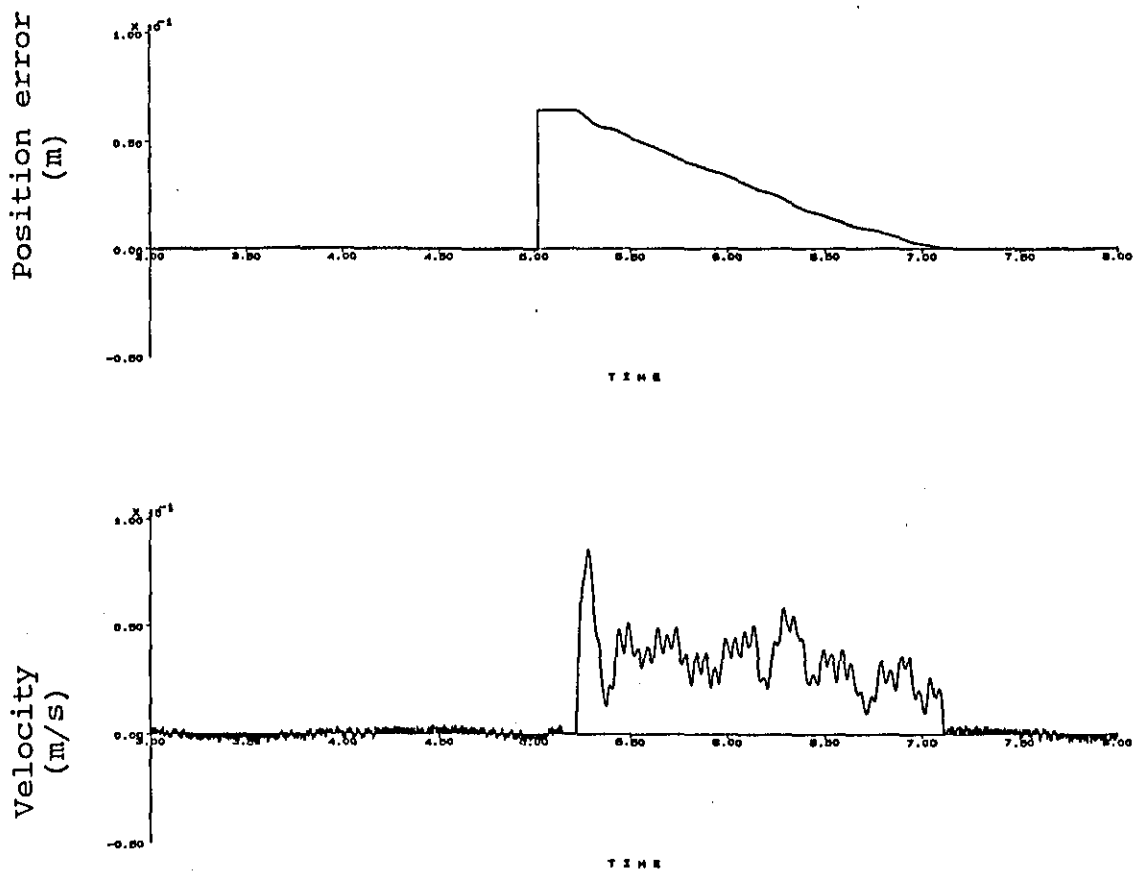

Fig. 7.23 - Simulation of LUT solenoid operated valve system

7.3.3 On-off controlled drives

There are very few published research papers with sufficient experimental data accompanied with the publication to provide information to be put into the model for cross-validation purposes. One of the more complete reported experiments is found with Burrows et al [7.9] in an analysis of on-off pneumatic servomechanism. A separate valve operator module was written to simulate the action of the on-off flapper valve which could function in three states:

(a) Totally closed off

(b) Fully open to chamber 1 only

(c) Fully open to chamber 2 only

The physical dimensions and the amplifier gains of the control circuit were determined from the data furnished in the paper.

The simulated position error responses are shown on Fig. 7.24. Fig. 7.25 shows the corresponding responses reported by Burrows. Due to definition difference, the sign for the position error responses had been inverted to positive. The results generally agreed in the variation fashion but there was not enough data to transform the voltage values in Fig. 7.25 to match with the position error values in the simulation. Since some of the simulation parameters such as friction, mechanical linkage and the controller gains were not totally clear from the paper, they were initialised by intuitive guesses. Consequently, the results are not expected to match exactly numerically but the validity of the

specific mathematical model as an application of the generic model has been illustrated.

7.7 Summary of model validation

The generic model established in Chapter 4 has been applied to derive specific mathematical models of the experimental pneumatic servomechanisms described in Chapter 5. The tests can be classified in two categories. Tests in spool hysteresis, static and coulomb friction, timer and pressure calibration were able to provide information relating to the physical characteristics of the test rig. Other tests including flow gain, blocked port, tubing pressure drop, effect of dither provided supplementary information to validate the model.

The tests on complete system were performed on the three servo-drives. Two modes of operations were examined. The open loop tests were needed to determine the validity of the pneumatic and mechanical parts of the system model. The electronic controller was programmed to hold a fixed input signal throughout the run. The closed loop tests were aimed at simulating the performance of the test rigs at normal working conditions.

Close agreement between the experimental and simulated position responses was obtained in most cases showing that the models represented the real systems well. Deviations in the pressure responses were attributed to the fact that the measurement points of the pressure transmitters were not exactly

the same as the simulated pressures which were the instantaneous values in the course of integration. The over-simplified assumption that pressure in the control volumes was homogeneous also contributed to the difference.

In summary, the specific models have been verified satisfactorily. More refinements can be made with additional tests on the parameters and characteristics of the component models, but in view of the shortage of time, these tests were left in this research and can be picked up again if the need for more accurate modelling arises.

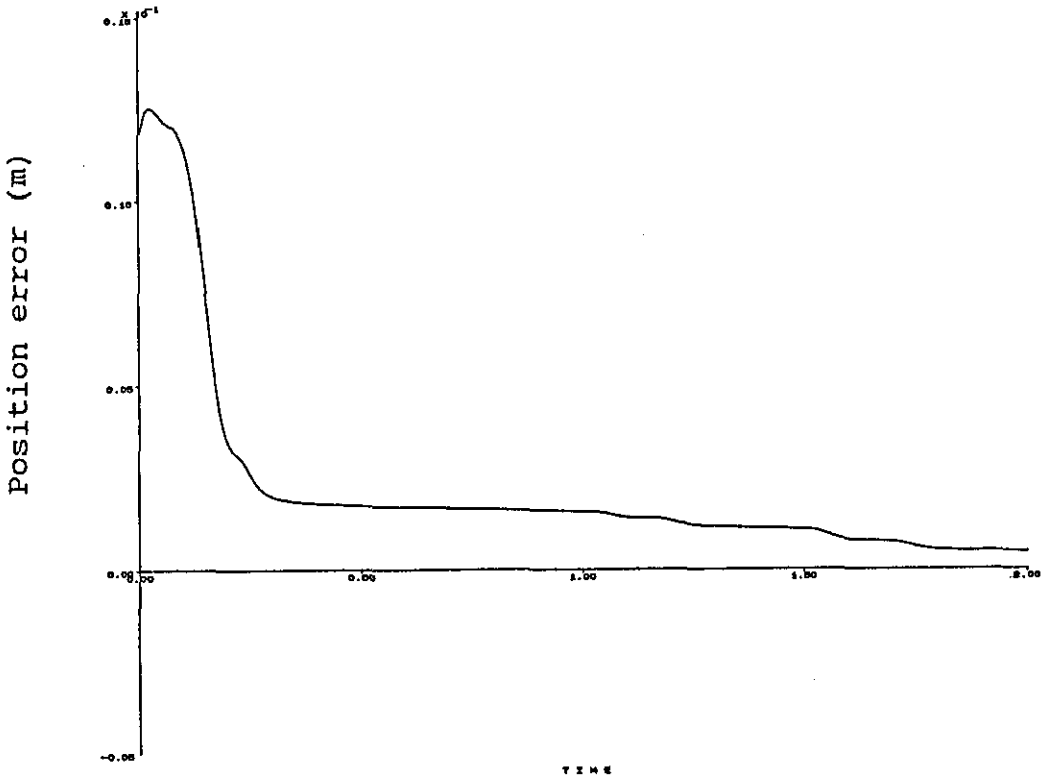

Fig. 7.24 - Simulation based on Burrow's data

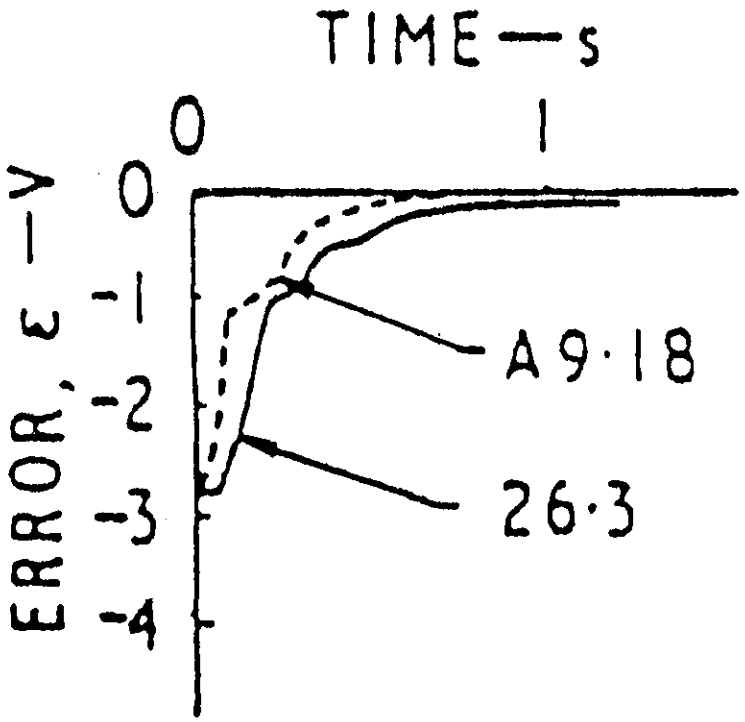

Fig. 7.25 - Reported responses on Burrow's mechanism

CHAPTER 8

APPLICATIONS TO PNEUMATIC MODELLING

The application of the component oriented approach to modelling of specific pneumatic servomechanisms has been successfully demonstrated using the three experimental test rigs and data from published documentation. The versatility of the generic model has been illustrated by the capability of simple replacement of components to form new systems which can be simulated to produce performance data.

The generalised nature of the approach is not limited to the aforementioned applications. In the interest of formation of a computer-aid-configuration tool for pneumatic servo-drives, it is necessary to extend the scope of applications to check the functionality of the generic model as a framework for servo-drive modelling. The following sections describe the investigations by injecting variations in the component models. In most cases, the investigations were coupled with actual tests which provided validation to the generality of the model. However, difficulties existed in a few occasions where the variation could not be controlled on the test rig. The investigations were then limited to theoretical comparison of simulation results of similar runs.

8.1 New design configuration evaluation

The primary objective for a computer-aided-design tool is to predict the variation of performance if the design is changed. The ability of the generic model to cater for changes in component combinations have been verified by the assembly of the component models in Section 6.7.

The changes in design do not restrict to trial at component level. The evaluation study can also be made for changes in part of the component. A study was made on servo-drive B in which the spring in the solenoid operated valve was replaced by a softer spring. The situation was simulated with the same set of parameters as in Section 7.2.2 except that the spring constant K_{sp} was reduced to 60% of that of the original spring. Fig. 8.1 shows the result of the experimental and simulated responses.

Compared with the responses shown in Fig. 7.18, persistent vibration was recorded both on the hardware and the model. There were slight deviations in frequency and amplitude, but the unsteadiness of the system could be predicted readily.

8.2 Variations in operation conditions

One of the methods to illustrate the generic nature of the model is to determine from the model the performance of the mechanism under different operating conditions.

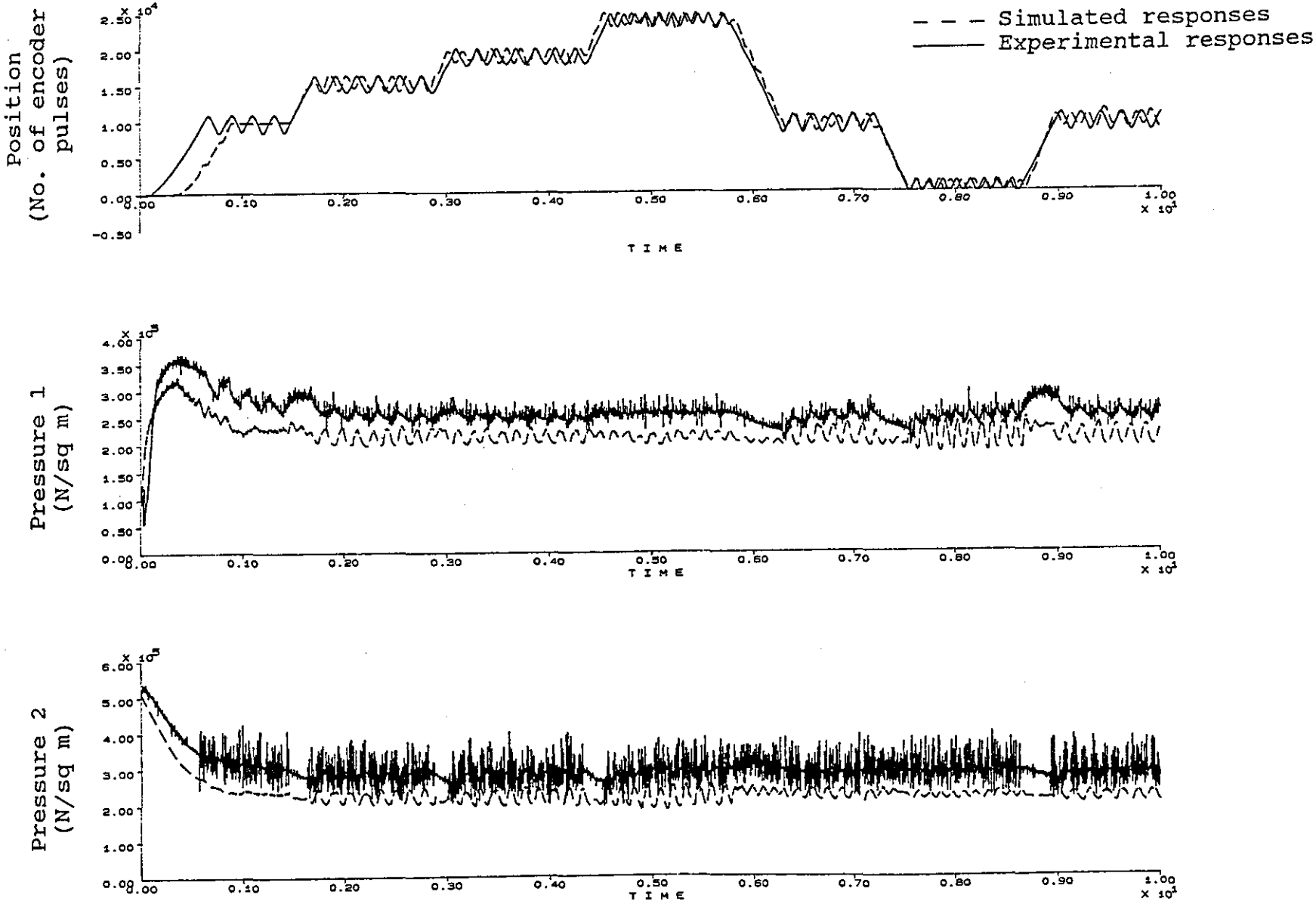

Fig. 8.1 - Step responses of servo-drive B with soft valve spring

The changes in this category may not affect the fundamental design, but the simulation result may highlight associated problems after the design is implemented.

The type of operating condition variations can be simple alteration of resistor setting or more complex re-organisation of control strategies. The following sections examine the issue in five aspects showing the methodology of tackling the problem. In the case of complicated changes, the component oriented approach allows that a separate component module to be established instead of varying the parameters of previously existed modules. The new module can be linked to the simulation software easily by the UNIX make facility.

8.2.1 Impulse test

Instead of the step input signals normally used to investigate the performance of servomechanism, an impulse, which was a strong signal at short duration, was injected into the servo-drive B. Fig. 8.2 shows the responses in the test rig and from the simulation.

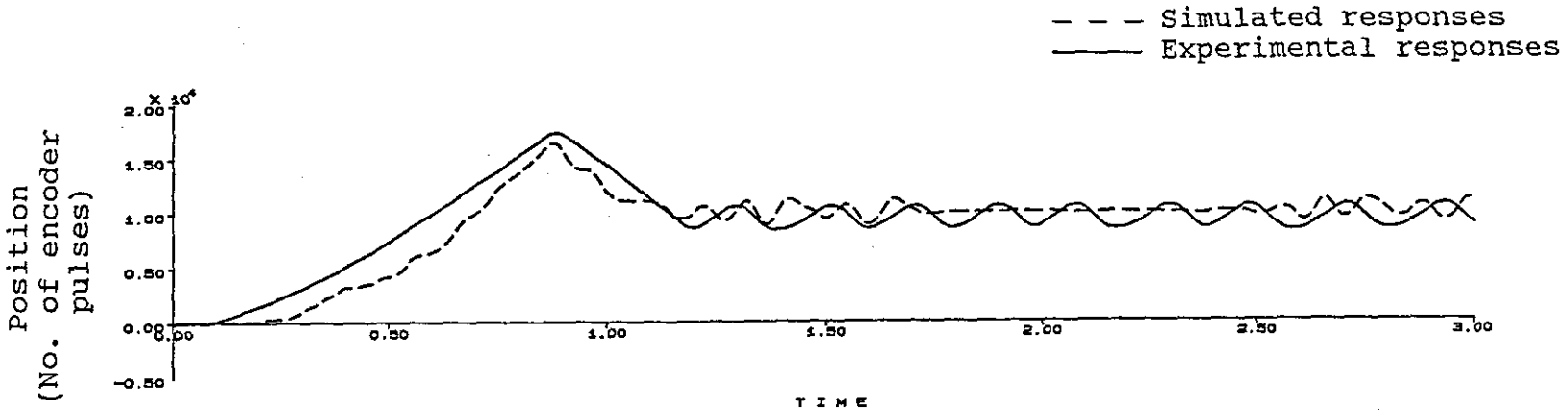

Fig. 8.2 - Impulse test on servo-drive B

It can be seen from the experimental position transients that the system was unstable. Although the simulated responses became stable after 5 ripples, it reverted to vibration after 1.5 sec. The amplitude and frequency of vibration were not matching too closely due to various inaccuracies in the model parameter settings. A time lag was recorded on the simulation result. Apart from these, the model was able to predict the inherent instability in the system.

8.2.2 Effects of gain adjustment

It was found that if the amplifier current gain was reduced by varying the 22K gain adjust in Fig. 5.8, the system became stable at steady state. The spool was in fact displaced slightly from the normal valve null position as indicated by the spool location responses (Fig. 8.3). There was a steady state deviation between the experimental and simulated responses which were attributed to the lack of experimental means of determining the model parameters of the valve operator component module.

The simulated responses were generated by reducing the gain coefficient G_s and keeping the other parameters of the system in Section 8.2.1 unchanged.

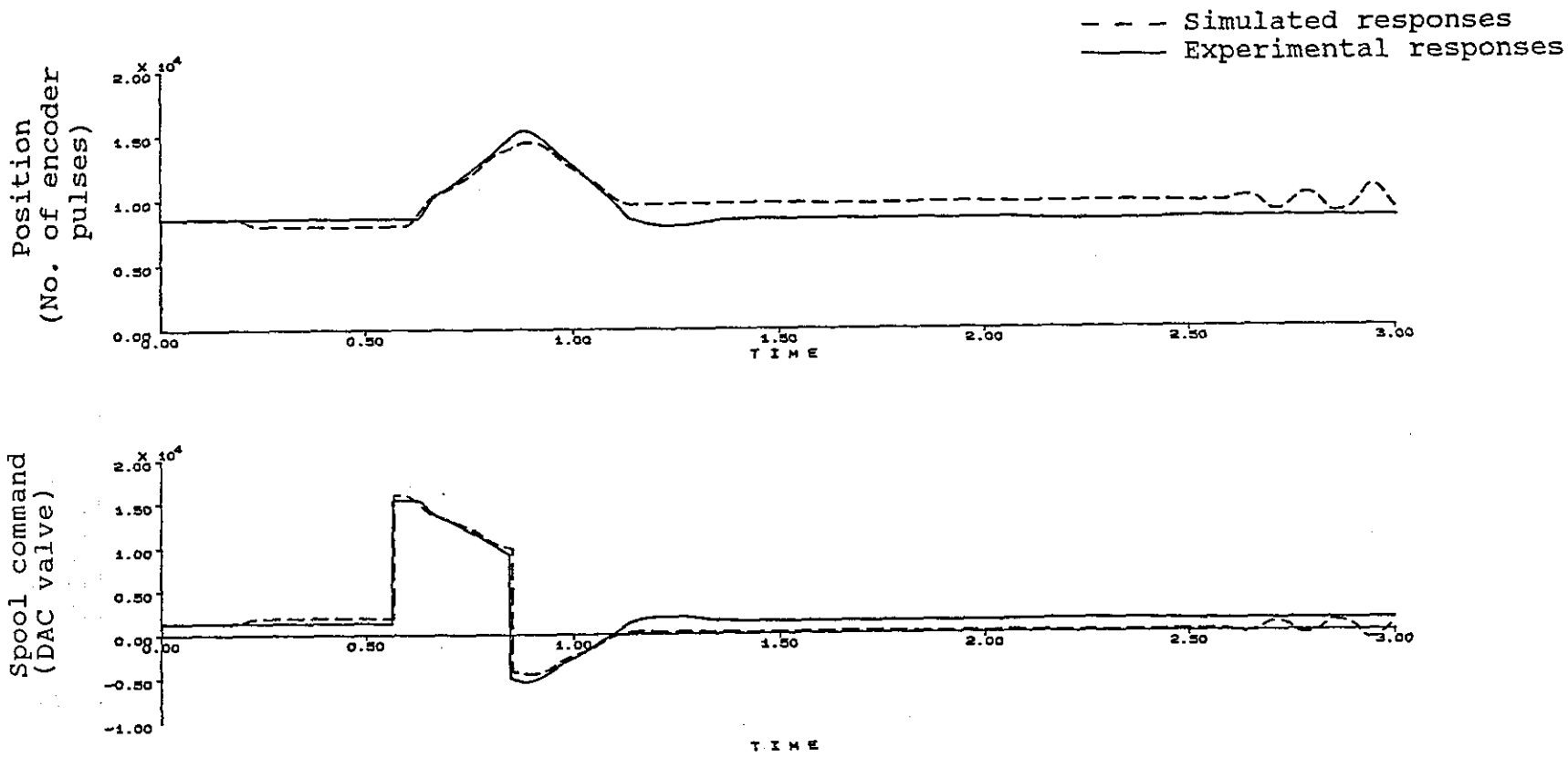

Fig. 8.3 - Impulse test on reduced gain setting

8.2.3 Tests on control strategies

The time to implement a control strategy on a microprocessor controller varies with the complication of the algorithm. For simple proportional control, the programming task is straight forward. However, if the algorithm requires a lot of data manipulation and hardware interrupts (sometimes nested), it can easily occupy a few weeks before the debugged version of the software is ready.

By using the generic model, programming the algorithm into the controller module is made simple. Since the module is written in FORTRAN, the mathematics and logistics of the algorithm can be programmed easily in high level language representation. The time required to examine the difference in control strategies is reduced.

As an example, Pu [8.1] has devised a learning strategy which dynamically adjusts the null offset of the valve. Implementation of the learning strategy required programming at the assembly language level on suitable target hardware. In fact, the formulation and trial of the algorithm had constituted a major portion of Pu's work.

On the generic model, a separate routine to simulate the strategy with the following codes in FORTRAN can be used:

```
      {                                          }
      {In dead band exit control routine}
      {                                          }

       subroutine dbexit(poserr,old_offset,new_offset,new_despos)
C
C -- Dead band exit control subroutine
C
      {                                }
      {Other codes in the routine}
      {                                }
C
C -- Set valve null offset by dead band value
C
       if (poserr.lt.dead_band) then
         new_offset = old_offset + poserr
         new_despos = pos_array(stepno + 1)
       else
         return
       endif

      {                                            }
      {In controller gain calculation routine}
      {                                            }

       subroutine ctrlgain
C
C -- Controller gain calculation subroutine
C
      {                                }
      {Other codes in the routine}
      {                                }
       call dbexit(poserr,old_offset,new_offset,new_despos)
C
C -- Add valve offset to spool command
C
      adj_splcom = splcom + new_offset/scale
      splsig     = adj_splcom/dac_range * max_spldis
      {                                }
      {Other codes in the routine}
      {                                }
```

Since there is not enough quantifiable response data reported (the results were consolidated as null offsets in the run rather than time series data), it is not possible to proceed with meaningfull comparison. Nevetheless, the foregoing discussion serves as an illustrative example of how the model can be used to tackle control strategy problems.

8.2.4 Step time reduction check

It is common practice that during position programming, the dwell time or the duration of each step is changed frequently. A check on the performance of the test rig with changes in step length is always useful to ascertain acceptable stability and response of the system before the design is produced.

Fig. 8.4 shows a reduced step length run on servo-drive B. The graphs should be compared with those on Fig. 8.1. The system behaved exactly in the way as that would exist in a reduced step time situation. Deviations still existed but they were in the same pattern as in Fig. 8.1. As far as the prediction of performance is concerned, the model showed conformance in terms of relative changes. In other words, the model was robust enough to represent proportional variations.

8.2.5 Control software bug

During evaluation stage, it was found that some of the tests could not be simulated satisfactorily. Both the experimental and simulated results were checked. A control software bug was found such that the gain calculation routine could only give positive gains. The spool command responses on the test rig showed jerks whereas those from the simulated responses did not show the phenomenon (Fig. 8.5). Consequently, the relevant part of the control software was examined and the bug was fixed.

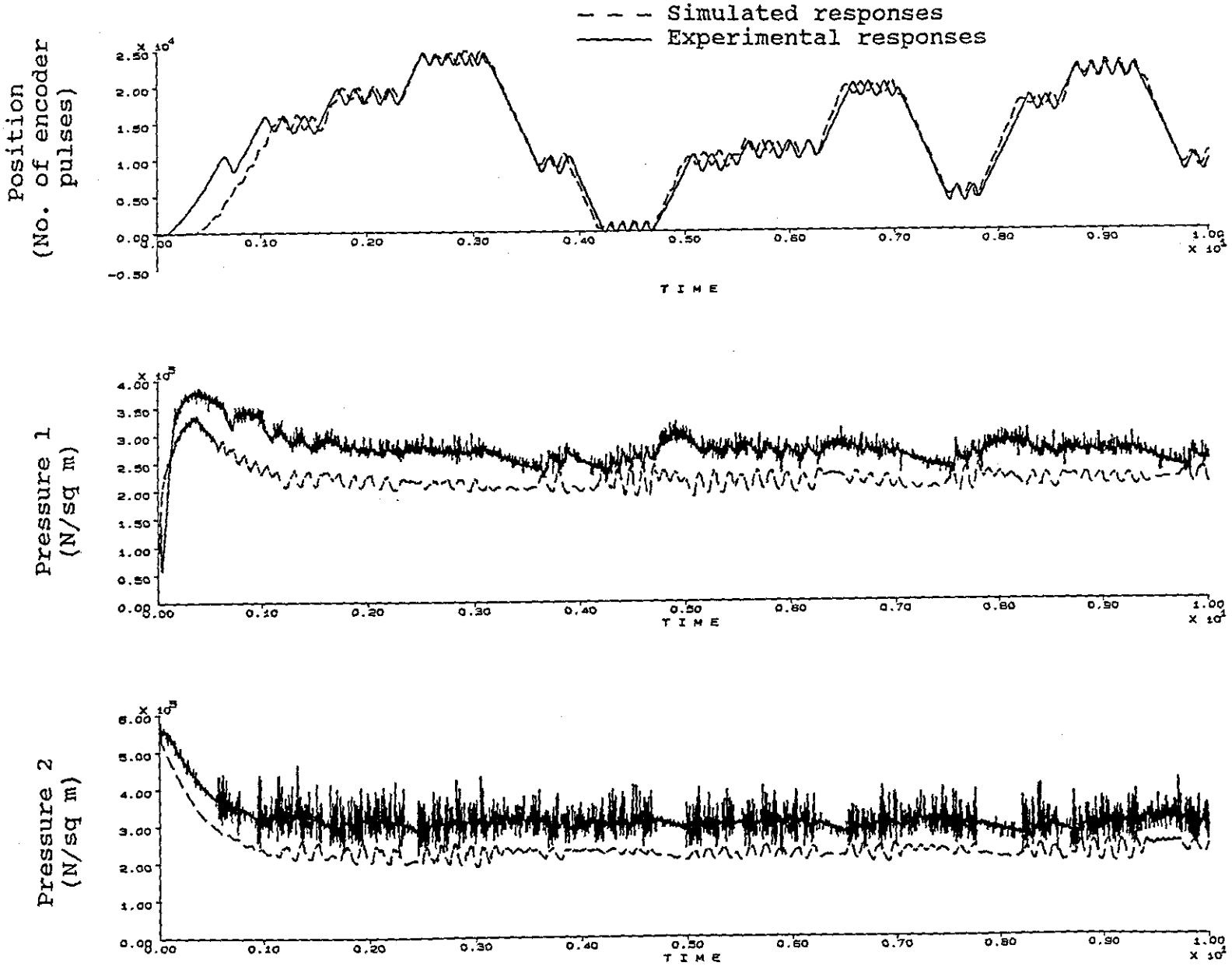

Fig. 8.4 - Step responses on servo-drive B with reduced step time

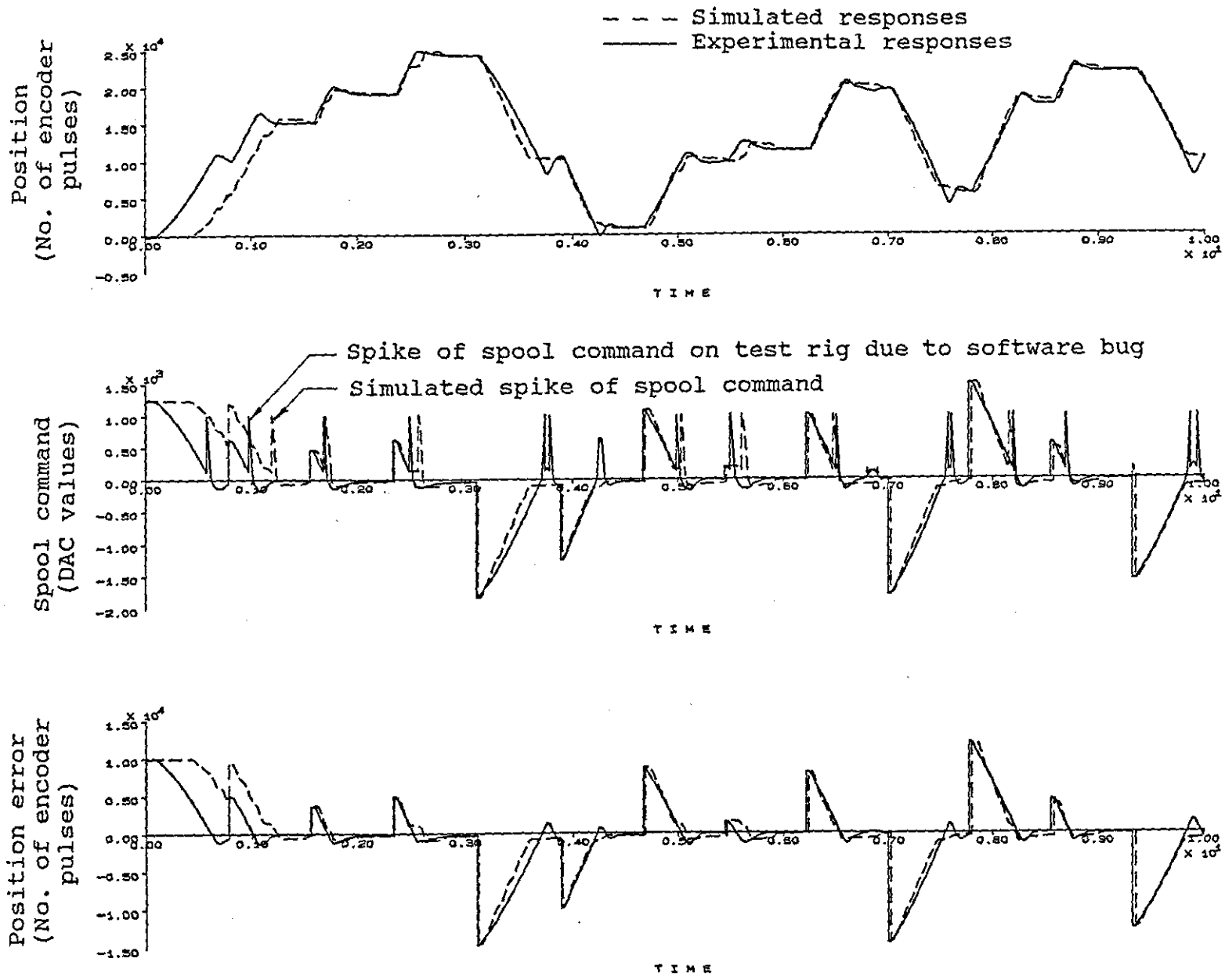

Fig. 8.5 - Step responses with control software bug

8.3 Choice of models of varying complexity

The main reason for supplying simpler models is to reduce the simulation time if the accuracy of the system model is not crucial. The alternative approach is to use empirical model or continuous system mode which avoids the time consuming interrupts for discrete system. The resultant model is then unable to show the digitising effect of the discrete controller. If the controller is fast sampling, the effect is not significant. However, if the sampling time is long, the effect can be detrimental to the gains calculation in simulation.

8.3.1 Step responses with continuous system

The servo-drive B was also simulated as a continuous system as shown in Fig. 8.6. The rather large deviations between the actual and simulated responses especially in the case of position response indicates that the continuous controller model is not appropriate to represent the digital controller. The simulated system generally shows more vibration due to the continuous update of the position feedback rather the sampled position data actually happening on the test rig.

The main advantage for the continuous model is the speed of simulation involved. The simulation time for the continuous system is about half an hour whereas the digital controller models takes at least 5 times longer.

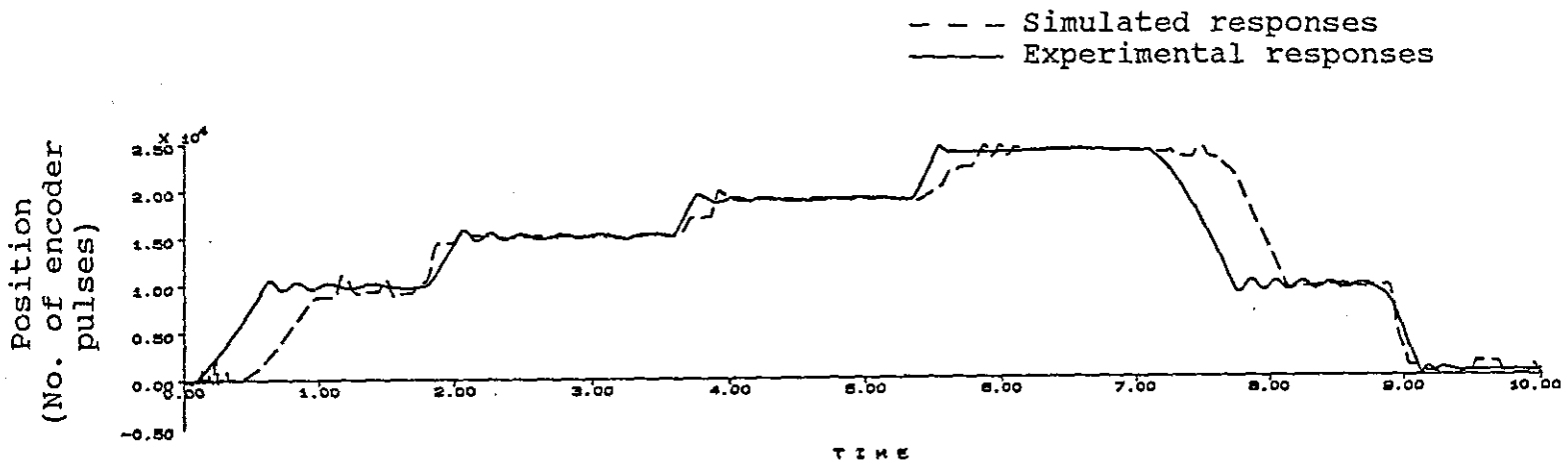

Fig. 8.6 - Simulation as continuous system

8.3.2 Empirical valve operator model

The empirical solenoid valve operator model described in Section 6.4.2 is simulated based on the discussion in Section 7.1.2.3. It is noted that due to the difficulties of estimating the values of K_s and K_d, deviation in the frequency of vibration was found with the position responses (Fig. 8.7). The simulation time is only an hour. The values of K_s and K_d were 36000 (corresponding to 30 Hz) and 500 respectively.

Remarkable agreement was recorded with the pressure transients. This could be due to the reasonable estimation of K_s and K_d from experience on the component. In addition, the oscillation about the set point would facilitate a neutralisation effect of the positive and negative errors. However, since this model relies heavily on the experimental determination of its parameters, there is no guarantee that the same fitness can be obtained if another valve operator is used.

8.3.3 Effect of internal leakage

The effect of leakage across cylinder chambers and its mathematical implication has been discussed in Section 6.1.2. Leakage is inevitable whenever there are moving parts. However, there is no straight forward way to control or measure the exact amount of leakage across the actuator so as to derive an empirical function or to determine the coefficients in some known leakage functions.

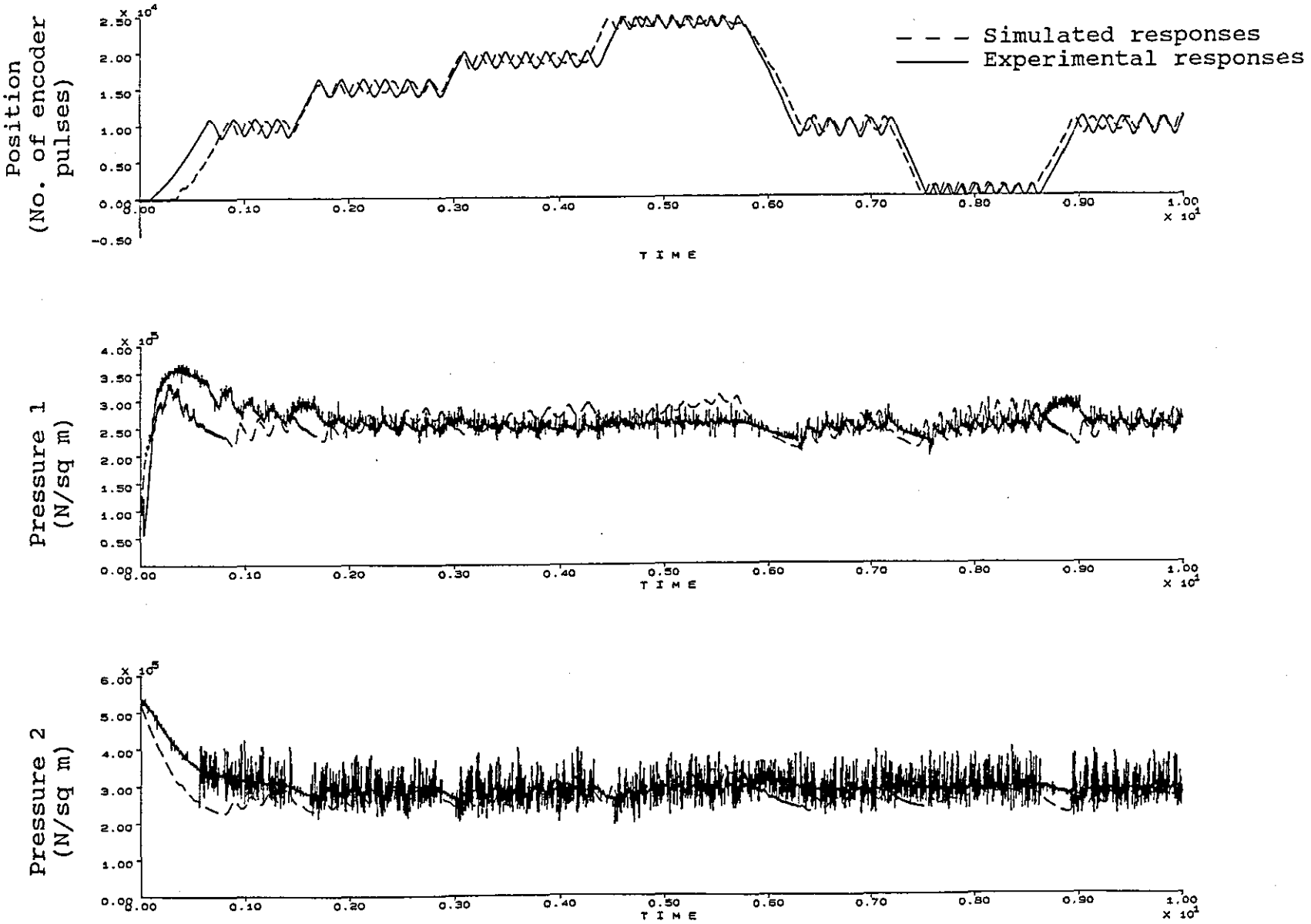

Fig. 8.7 - Simulation with empirical valve model

A test was made with the set-up as shown in Fig. 8.8. The inlets to the cylinder was re-connected in order to direct the compressed air through the cylinder seal. The result was unsatisfactory because the amount of air was too small to be measurable by the available instrument.

One possible interpretation of the leakage problem is as an indication of the performance of the servo-drive after wearing out. This is not a design problem. However, it does show the problem if the design deteriorates quickly. For the purpose of illustrating the application of the generic model in ascertaining the effect of leakage in pneumatic servo-drive, a simulation was carried out based on the adiabatic flow model (Section 6.1.2.2) on servo-drive B.

The amount of leakage in this simulation was obtained by an estimation of the leakage gap and the appropriate coefficients on the test reported by Egli [6.11]. The position responses (Fig. 8.9) showed that the system was slightly less stable than one without leakage (compared with Fig. 7.18). This finding shows that while leakage allows energy to escape from the high pressure chamber to low pressure chamber, it disturbs the balance of compressed air forces in the asymmetric cylinder. In more precise terms, for the asymmetric cylinder, the actuator stops when

$$P_1A_1 = P_2A_2 + P_eA_{R2}$$

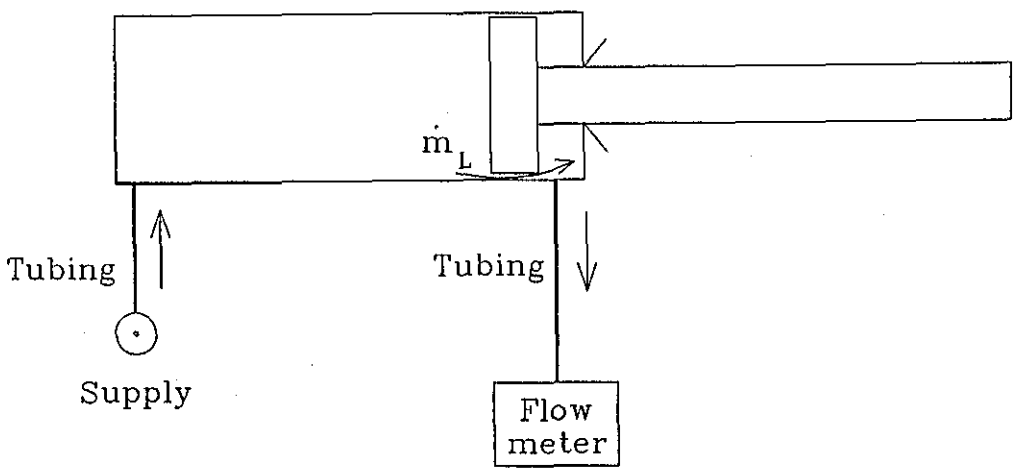

Fig. 8.8 - Experimental set-up for leakage measurement

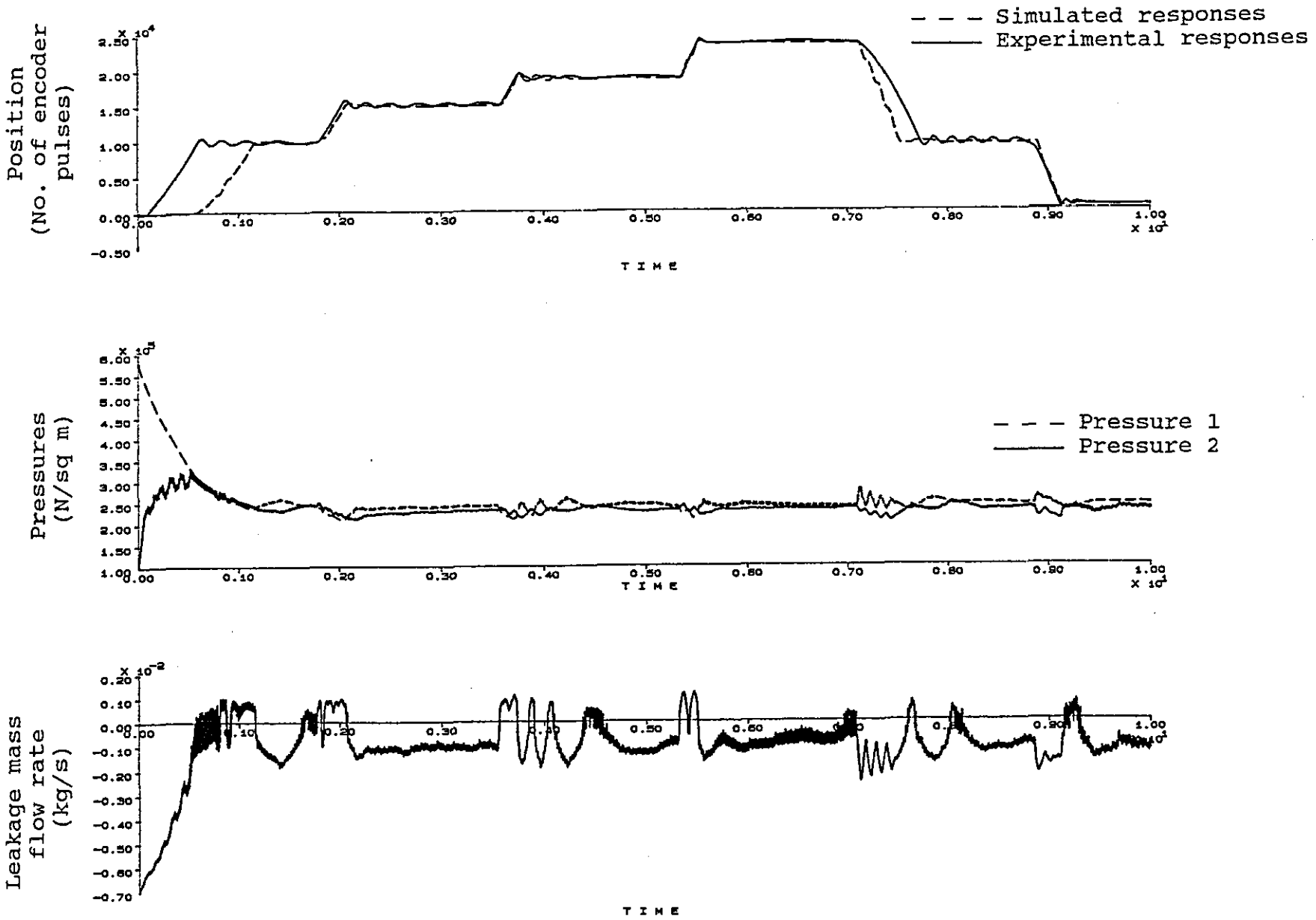

Fig. 8.9 - Simulation of servo-drive B with adiabatic leakage model

The term $P_e A_{R2}$ is normally small compared with the other terms in the equation. This implies $P_1 < P_2$ because $A_1 > A_2$. Leakage therefore reduced P_2 and hence the cylinder moved slower as indicated by the larger deviations during extend or retract of the actuator.

8.4 Summary of applications

With proper information of the physical system, the generic model can provide insight into the performance of the pneumatic servo-drive, existing or non-existing, for various objectives of investigation. Tab. 8.1 summaries the functionality of the generic model as described in the previous sections.

Tab. 8.1 Summary of application studies

Function	Relevant section
Choice of component	7.2
Design of part of component	8.1
On line adjustment effects	8.2.1, 8.2.2, 8.2.4
Design of control strategies	8.2.3
Bug detection and fixing	8.2.5
Investigations on wear out	8.3.3
Choice of model complexity	8.3.1, 8.3.2

The scope of applications, however, is not limited to those described in this chapter. There are certainly other topics of interest. For instance, drift was reported to be a disastrous phenonmenon on the control electronics and the pneumatic components affecting the consistency of the performance of the servo-drive [8.2]. Due to the time limit for completion of this research project, the drift problem was not attempted. However, with the generic model, it is possible that a time-dependent offset function can be programmed into the controller as well as the actuator modules to describe the changes. Obviously, the mathematical representation of this function requires tests on some existing test rigs and this is worth as a separate research project in its own right.

This chapter serves as a guideline for using the generic model as a starting tool for design evaluation. The studies showed that it is simple to use and flexible to adapt to any real life configuration. If the component has been created before or the variations are minor, the evaluation simulations can be done by simple change of parameters. In some cases like the change of controller which is more fundamental in nature, a new component module can be written and linked to the software. In either cases, the adaptation process is straight forward.

CHAPTER 9

RECOMMENDATIONS FOR FUTURE RESEARCH

The results of this study reveal that the research is worthwhile to be pursued further in several directions. The extensions of the ideas are discussed as a natural development to the thinking involved in the project. Possible directions of research include component generalisation, multi-axes control, CAD and real-time performance predictive control.

9.1 Component library

There is no fixed procedure or coding method to generate new components from scratch. Modelling of component therefore depends solely on the understanding of the characteristics of the part itself. Perhaps a prospective method is by describing the pneumatic circuit as a number of volume nodes as in the modelling of a valve gain module, and interconnect the volume to other components by restrictions and tubing. This conception requires further investigation of the pneumatic system and mathematical feasibility.

The current concept on generalisation of components is to classify the components into groups. A general component model for each group is established as a reference model which defines

the essential system linking features. Variations of the components within a group, which are local to the component module, are allowed to generate new components.

9.1.1 Actuators

For the purpose of servo-control, double acting cylinders are always used because of the simplest pneumatic manipulation. However, it is also possible that bang-bang actuators are required to work together so that the generalisation of including such components is necessary.

Rotary components such as air motors and rotary chambers are often used in conjunction with linear components to provide a cylindrical working envelope. The component generalisation requires a describing model which can deal with more than two controlled volumes.

9.1.2 Valve configurations

Valves can vary from the spool valve used in the research to poppet or flapper valves. Several model templates are required for developing the wide variety of valve configurations.

Two valve operators were used in the research and modelled according to their respective characteristics. It has been concluded that due to the slower response of the stepper motor,

the performance of the servo-axis is not satisfactory with the stepper motor actuated valve [1.8].

The generalisation of the valve operator component module should then be concentrated on the modelling of the solenoid operators. It is also noted that pressure feedback has been used by some researchers as a means of imposing damping into the system [9.1]. Flexibility is required in the template model that variations in design are easily incorporated.

9.1.3 Controller

The high flexibility of the microprocessor controller nowadays has presented problems to create a general controller module. It would be relatively easy to describe the hardware portion of the controller in terms of resolution and sampling time, but it is impossible to have one universal gain determination routine to describe all software control algorithms on the physical system.

The current implementation of the controller has included algorithms like gain scheduling, proportional control, and minor loop compensation [9.2]. New algorithms are catered for in separate subroutines which must be compiled and linked together with the whole package. The research work for generalisation of the controller component is anticipated to be the development of a descriptive format which will eliminate the rather technical and clumsy re-compilation procedure.

The model, as it stands now, carries a lot of computing redundant elements which lengthen the simulation time significantly. The computation overhead can be eliminated if the integration program is re-written to avoid excess routine management. There are two possible ways to achieve efficiency:

(a) The management routine for print time data could be re-written to allow interpolation rather than the existing stop and record arrangement;

(b) A faster and perhaps smaller mathematical procedure could be adopted to calculate the nodal conditions in the valve.

9.2 Computer-aided-design package

One of the objectives of this research was to establish a set of procedures to generate a usable model for pneumatic systems quickly. The model can then be evaluated in terms of static and dynamic behaviour. Such an evaluation exercise may occur at the design stage which suggests that the software could function as a computer-aided-design tool for new pneumatic servo-mechanisms.

9.2.1 User Interface

One of the drawbacks of the existing CMS2 package is the universal user interface which is designed for the model builder or very experienced researchers. In order to configure the software for general users, the user interface must be re-written

such that "X", "Y", "C" and "L" variables are replaced by meaningful system parameters. On-line help facilities to explain the system parameters and possible implications are essential for meaningful CAD applications. Before it goes for simulation, a check for all the possible errors in the parameters values is required. This is necessary because when a new component is selected from the module library, the corresponding values of the component should be initialized to the new part, otherwise, computational failure such as division by zero may result.

Since the simulation is a time consuming process, it is worthwhile to put the simulation process to background (batch processing) whilst leaving the front end (user screen) for transient display or data entry.

9.2.2 Modelling of multiple axes constructs

Work is still required to extend the simulation to multi-axes servomechanisms. This extension would include the calculation of tool path, inter-axes co-ordination and the action of the supervisory controller. The amount of work required in this part would probably be worth of a separate research project.

9.3 Real time predictive control

One of the ultimate objectives of closed loop control is the ability to design a self-tuning controller which would adjust itself in response to external changes. In particular, the study

of predictive control theory by Clarke [9.3] shows that the method relies on a good model which predicts changes in the output in terms of known changes in the current input. The current control is subsequently chosen on the basis of its effect on the predicted variable. Alternatively, the set-point can be modified with reference to the prescribed model to achieve ultimate speed in closed loop. The latter scheme has been investigated partially as "front-end control scheme" [1.6] based on the theoretical derivation by Astrom [9.4].

There are problems of implemention of predictive control with the simulation model in the current form due to the prediction speed and data structure. Some suggestions are made in the following sections to simplify the model design to achieve real-time model reference.

It is impossible to incorporate the simulation package on the rather simple and cheap single axis controller. Neither is it possible to predict, with sufficient generality, the performance of the axis for all moving conditions and save it in the memory of the axis controller.

A viable solution to the real time predictive control is to develop a learning strategy which will adjust the system parameter according to the current system information and some quickly retrieved simulation data. A preliminary investigation of such ad hoc artificial intelligence has been tried with a strategy on the

dynamic adjustment of the null point [9.5]. The learning methodology was formulated with the aim of achieving velocity control for applications in contour positioning [9.6].

Due to the implication of the enormous computing power requirement, the real time model reference adaptive control approach on the axis controller will be a challenging problem to be solved if funding for further enhancement of the microprocessor controller is available.

With the recent advent of local area network technology [9.7], it is now more realistic to investigate the possibility of having a remote mainframe computer which possesses the facilities for real-time computation (such as array processing) of the model reference. The resultant action can be communicated back to the individual axis controller via the high speed network. The possible restriction on this approach is the need of the remote processor to respond in real time with the consequent implication for reduced availability of an expensive computer.

Alternatively, a similar, but rather localised approach is to adopt the concept of parallel processing whereby the prediction can be performed on a separate processor and the resultant action is transmitted to the controlling processor through the local data bus. The disadvantage of this approach is mainly due to the less powerful computing engine normally associated with the parallel-processor environment. Additionally, the processor communication can be more complicated.

CHAPTER 10

CONCLUSION

This chapter summaries the findings in the project and the developments as a consequence of the study of the pneumatic servo-controlled linear drives.

The general conclusion can be drawn with reference to the objectives of the research in Section 1.2. With the successful implementation of the concept of component oriented approach and the agreement achieved between the experimental and simulated results outlined in Section 7.2, there is no doubt to conclude that the requirements set forth at the start of the project have been fulfilled and that the formulation of the mathematical model and its component modules has provided a valuable foundation for further refinement to become a configuration tool for pneumatic servomechanism design.

10.1 The generic model and the component oriented approach

The technique of the component oriented approach has been successfully extended to adapt to the non-linear pneumatic system. A number of component modules were established under the criteria of the approach. The components were defined clearly with the linking variables associated with the traceable physical entities

in the pneumatic linear servo-drive. Some of the uncoupled system components were measured in simulated experimental conditions and the theoretical background for the component module was ascertained.

The pneumatic component modules were linked together via the input and output component variables to form a complete mathematical model which was integrated numerically with the corresponding actual test initial conditions. The simulated results showed satisfactory coherence in respect to the performance of the servo-drive in the actual test.

Several components were manufactured and assembled to form a working alternatives for validation of the component oriented approach. The components were designed not only in the variation of dimensions, but also in the actual methods of operation. The large difference in the nature of the components required that new component modules were programmed as mutually exclusive modules and easily selectable by the respective component flags during simulation time.

Apart from the servo-drives A, B and C in Section 7.2, a number of alternative systems were studied. Wherever possible, the studies were supported with associated tests to show the validity of the generic model. It is certain that given more time, a considerable number of components can be accumulated to form a library of components which can be chosen by the pneumatic servomechanism designer at a re-designed CAD interface.

10.2 Pneumatic Modelling

The study of the pneumatic system with reference to specific tests led to enhancement in the understanding of the phenomena of the compressibility of air and the geometrical relationship of the flow path. The theoretical background of the pneumatic properties investigated in the research:

(a) The one-dimensional adiabatic flow equation has been extended to include the dynamic flow head which was found to influence the mass flow rate significantly in high valve opening cases. The extension leads to the definition of a flow function Γ to denote a set of formulae to relate two locations in the flow stream.

(b) The flow node model has been established to describe the existance of a small buffer volume in the valve land where the conditions of the compressed air are different from the connected channels. The flow node model was proved to be able to deduce the pressure gain characteristics and flow saturation phenomena in the compressed air flow through the 5-port pneumatic spool valve.

(c) The analytical model of the solenoid actuator has been established to separate it from the valve gain module so that the mechanical effects of the valve and spool components can be investigated. In particular, the effect of change of spring and reduction of amplifier gain were simulated and the ensuring prediction agreed with the experimental findings.

(d) Two models were proposed to describe the pressure drop phenomena through the tubing connections in the pneumatic system. The study provided the theoretical background for further investigation in the adiabatic flow of air in the flow path.

10.3 Software development

The software development work in the research can be related to two main parts: work on the test rig control program and enhancement of the simulation package.

The control software was written in Motorola 68000 family assembly language and contained the necessary features for controlling the test rig in either open loop or closed loop mode. The software also has the capability to acquire transient data which can be transferred back to the host for analysis.

The simulation package was a modified version of the discrete simulation package from UMIST on Sun, VAX and DG. Improvements were made on:

(a) Adding more optional features in interactive mode for easy operation, better file management and data transfer;
(b) Inclusion of a self-contained graphics driver file for porting on different graphics platform;
(c) Elimination of bugs in the display and integration module;
(d) Minor changes for more efficient use of computing resources.

The current primary version of the software runs on Sun graphics workstations.

10.4 Summary

The generalised approach adopted in this research has successfully formulated a generic model for pneumatic drives. The model has been applied to specific cases to simulate test hardware units as well as published data. The flexibility offered by the approach has been shown to include many other possible usages. It is therefore concluded that the research objectives were achieved and the modelling software can be extended to become a computer-aided-design tool for pneumatic servomechanisms.

APPENDIX I

ENHANCEMENTS ON THE SIMULATION PACKAGE

I.1 The interactive routine (TALK)

The subroutine "TALK" in the package functions as the user interface to allow variables and parameters to be initialised in interactive mode. System variables are referred as state variables "X", which are going to be integrated, and algebraic variables "Y", which records any intermediate values during a simulation run. In addition,there are 3 types of parameter constants:

(a) System parameters such as simulation run time, accuracy, step length and print time interval;

(b) "C" parameters for real constants in the model;

(c) "L" parameters for integer constants in the model.

All parameters must be set before simulation starts.

Enhancements were made in the following areas:

(a) Run number was originally set by the package and incremented by one every time the whole simulation is initialised. This created problem of unnecessary initialisation when high run-numbers are desired. An extra command "rnum" was inserted in the command processor to allow the user to set to any new run-number in one step.

(b) When hard copy of check data was recorded to disk, the date and time of the creation of the check data file was recorded

simultaneously. The date and time are used for documentation produced by the package, including graph plots, so that reference to the same simulation run could be ascertained. This enhancement required change of the binary initialisation file structure.

(c) The transient data file was originally fixed to be "TRANS.DAT" which was overwritten whenever a new run started. It was then impossible to display the transients of any previous runs again. The package was enhanced by creating a set of binary files AABBX.bin and AABB6.TRS such that the status of the simulation run when the package is exited will be automatically saved, where:

AA = two letter identification of the run (entered by user)

BB = two digit run number (incremented by package or set for binary steady state data)

x.bin = extension for current state file

6.TRS = extension for transient file (replacing TRANS.DAT)

This enhancement marked a coherent set of files for each simulation run and allowed retrieving of graphics data any time after the run.

(d) Since UNIX is case-sensitive, the command input processor of the Sun version has been enhanced to include lower case characters.

(e) An additional "stat" option was added to allow mean sum square values of the difference between 2 responses to be computed. This provided a measure of the accuracy of the simulated responses compared with the experimental responses.

(f) An additional "ils" option was added to create an ASCII file to be transferred to the frequency spectrum analysis program "ILS". The ASCII file would contain integer data of 12-bit bi-polar form, i.e., in the range of -2048 to +2048.

I.2 The graphic primitive routines

Since there was no GINO-F (Fortran version of GINO) library or similar graphics software available in the City Polytechnic, part of the display subroutine was modified to cope with a custom-made graphics routine file which emulated the same GINO named routines. The subroutines are listed in Appendix II.

The graphics primitive routines were essentially device drivers for different kinds of graphic devices. They were written bearing in mind the strategy of maintaining minimum modification to the CMS-2 package. The file was later linked to the "EVAL.F77" program on Data General machine (DG MV/10000) for producing transient plots on Hewlett Packard plotters.

I.3 The display routine "DISP"

The enhancements made in the "DISP" routine were:

(a) Adaptation of the display routine to the environment was required to adjust the graphics output sized to the optimum screen display. The initialisation of the database was modified to suit the graphic devices in City Polytechnic of

Hong Kong.

(b) It was found that if the transient file grew to a large size, the time to enter the display routine was terribly long (for 5M byte transient file, it took 20 min.). This was because the display routine had to scan all the transients on the disk to find the maxima and minima which were necessary for graph range generation. The modification was made in the "DYNAM" routine such that the information of the maxima and minima could be passed back to "TALK" routine and subsequently saved on disk. Upon entry to "DISP" routine, the information could then be ready for use.

(c) The original codes only allowed plotting to start from time zero to any user-defined time. Therefore, if a time range of say 1.0 to 2.0 seconds was requested, the package would still start to plot from time zero up to 2.0 seconds. The whole graph was distorted by a time scale of 1 second. In the modified version, it was possible to plot any time range starting and ending at any point without distortion of graph data.

I.4 Output to Hewlett Packard (HP) plotters

Modification necessary to give either on-line or off-line output on a HP plotter was added to the code. In the case of an on-line plot, the plotter should be set to EAVESDROP mode and connected as shown in Fig. I.1. The ASCII terminal was used as a control console. The plotter started in transparent state so that the user could run the programme as usual. When graphics was

required, an escape sequence would be transmitted to start graph plotting.

In the case of an off-line plot, a plot file subfixed ".plt" is created on disk. The user could then use the "type" command to send the plot file to the plotter. The plot files were normally created in a numbered sequence automatically in the package.

I.5 Output to Sun Workstations

The simulation package was ported onto Sun workstations with the support of Suntools - the graphics windowing system. Two windows were opened during display time:

(a) A text window was required to accept commands from the keyboard;

(b) A display window was opened to allow plotting of graphic data.

If hard copy from Sun was required, a third window under C-shell was required to accept "screendump" command which dumped the Sun screen to Hewlett Packard Laser Jet printer. When the windows were on the screen, they can be manipulated freely, including icon, hide, resize, expose and quit operations.

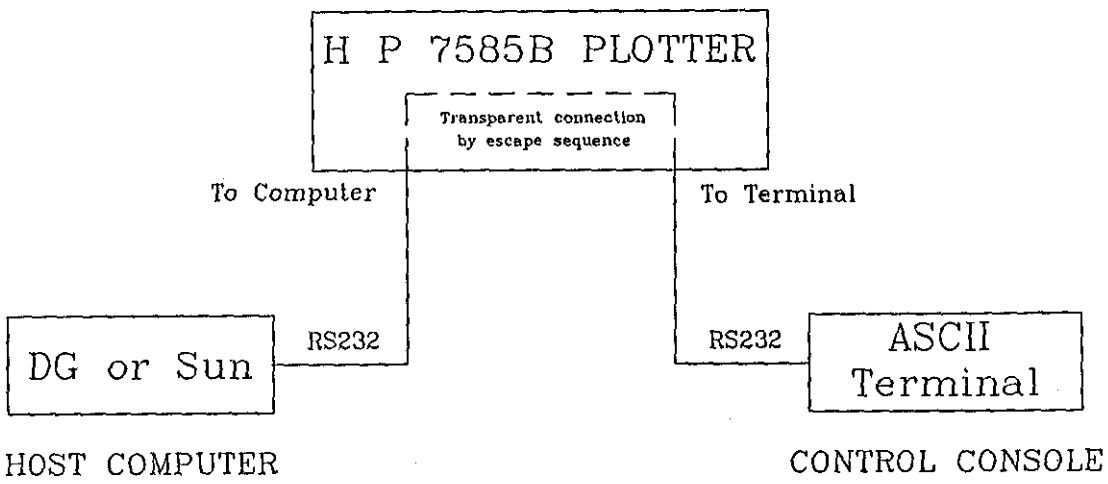

Fig. I.1 - Eavesdrop connection of Hewlett Packard plotter

I.6 The dynamic routine "DYNAM"

The "DYNAM" subroutine controlled the sequence of calling the integration routine and manipulating parameters during the integration phase. It was the master routine handling the checking of step length, interrupt generation and, if on-line graphics was enabled, setting the device to accept graphics data.

There were two minor modifications to "DYNAM":

(a) Some DO loops manipulating state variables "X" were simplified by replacing the number of looping from 200, which was the maximum allowable number of state variables, to NEQN, which is the number of active state variables set by the user-supplied model equations. The pre-requisite for this looping reduction was that all state variables should be grouped together at the lowest elements (from X_1 to X_{neqn}). The reduction saved time in the simulation run.

(b) A major bug which could set the integration step length to zero was found. A step length check was added to ensure that no zero step length could exist.

APPENDIX II

GRAPHIC SUBROUTINES EMULATING GINO SUBROUTINES

II.1 The graphics device driver routines

(a) dummy - an imaginary device without actual graphics output

(b) suncor - the Sun console under Sun's Core graphics library

(c) hp7585 - HP7585 A0 size plotter at the terminal line (on-line plotting) or to a plot file (off-line plotting)

(d) hp7475 - HP7475 A3 size plotter to a plot file. Only off-line plot was allowed.

(e) S6140 - Sigmex S6140 colour terminal

II.2 Graphic primitives

(a) MOVTO2 - emulated GINO MOVTO2 function

(b) LINTO2 - emulated GINO LINTO2 function

(c) MOVBY2 - emulated GINO MOVBY2 function

(d) LINBY2 - emulated GINO LINBY2 function

(e) DRWTO2 - special routine for plotters to function as LINTO2 but without lifting the pen after the line drawn. This reduced the wear of the plotter mechanism due to frequent pen up and down motions.

(f) PICCLE - emulated GINO PICCLE function

(g) DEVEND - emulated GINO DEVEND function

(h) CHAARR - emulated partially GINO CHAARR function. The character array was passed to the routine as a CHARACTER * 255 data instead of the original integer array in GINO.

(i) CHASIZ - emulated GINO CHASIZ function

(j) CHAMOD - emulated GINO CHAMOD function

(k) PENSEL - emulated GINO PENSEL function

(l) PENUP - a complementary routine to DRWTO2 to lift plotter pen when the draw completed

(m) SYMBOL - emulated GINO SYMBOL function. For the HP plotters, the symbols were drawn as alternative character set 5, i.e. 8 characters 'A', 'B', 'C', 'F', 'G', 'D', 'K', 'L' are sent to the plotter which writes the letters in a different form. For the Sun and Sigmex workstations, no alternative character sets were available. The symbols were drawn by programming lines and circles using LINTO2, LINBY2, MOVTO2, MOVBY2 primitives.

(n) AXISET - emulated partially GINO AXIPLO function. The routine was written in a general way but some of the functions of AXIPLO had not been included.

(o) GRAPOL - emulated GINO GRAPOL function

(p) CHAFIX - emulated GINO CHAFIX function

(q) CHAHOL - emulated GINO CHAHOL function

(r) CHAINT - emulated GINO CHAINT function

(s) CHAPOS - emulated GINO CHAPOS function

(t) DEVRSM - an internal routine to resume the device to graphics if it has been previously set to character mode by CHAMOD. A device state variable is always maintained for detection by this routine.

(u) INTCON - an internal routine to convert integers to ASCII strings suitable for Sigmex S6140 terminal

(v) ENCODE - an internal routine to encode computer data into ASCII code. This function is available on PRIME and DEC FORTRAN but is not found on DG and Sun.

APPENDIX III

Derivation for the Flow-induced Force in Spool Type Valve

The following analysis extends from the original analysis by Lee and Blackburn [6.23] to compressible fluid. Consider a control volume of fluid "V" and assume that flow outwards across the boundary of "V" is positive,

$$\bar{M} = \int_V \delta \bar{q} dV$$

where $\bar{q}$ = instantaneous velocity vector

δ = density of air

or $M_x = \int_V \delta u dV \qquad M_y = \int_V \delta v dV \qquad M_z = \int_V \delta w dV$

Consider the surface integral

$$\int_S \delta x \bar{q}.\overline{dS} = \int_S \delta x (u\cos\alpha + v\cos\beta + w\cos\gamma) dS$$

$$= \int_S (\delta x u\cos\alpha + \delta x v\cos\beta + \delta x\cos\gamma) dS$$

$$= \int_V \left(\frac{\partial(\delta u)}{\partial x} + \frac{\partial(\delta v)}{\partial y} + \frac{\partial(\delta w)}{\partial z}\right) x dV + \int_V \delta u dV$$

where α, β, γ are angles between $\bar{q}$ and $\overline{dS}$.

By continuity,

$$\frac{\partial \delta}{\partial t} + \frac{\partial(\delta u)}{\partial x} + \frac{\partial(\delta v)}{\partial y} + \frac{\partial(\delta w)}{\partial z} = 0$$

$$\int_S \delta x \bar{q}.\overline{dS} = \int_V -\left(\frac{\partial \delta}{\partial t}\right) x dV + \int_V \delta u dV$$

so that $M_x = \int_S \delta x \bar{q} . \overline{dS} + \int_V \frac{\partial \delta}{\partial t} \cdot x dV$

Assuming that $\frac{\partial \delta}{\partial t}$ is constant over V,

$$M_x = \int_S \delta x \bar{q} . \overline{dS} + \frac{\partial \delta}{\partial t} \int_V x dV$$

$$= \int_S \delta x \bar{q} . \overline{dS} + \frac{\partial \delta}{\partial t} V \bar{x}$$

where $\bar{x}$ = centroid of volume V

Approximating the surface integral by flow through K holes,

$$M_x = \sum_{k=1}^{N} x_k \dot{m}_k + \frac{\partial \delta}{\partial t} V \bar{x}$$

and the flow induced force

$$F_x = -\left(\frac{\partial M_x}{\partial t}\right) = - \sum_{1}^{N} u_k \dot{m}_k - \sum_{1}^{N} x_k \ddot{m}_k - V \bar{x} \frac{\partial^2 \delta}{\partial t^2}$$

For 3 holes only, as in the case of the spool valve, the flow induced force in the fixed container

$$F_x = \dot{m}_{s1} u_{s1} + \dot{m}_{e1} u_{e1} - \dot{m}_1 u_1 + x_{s1} \ddot{m}_{s1} + x_{e1} \ddot{m}_{e1} - x_1 \ddot{m}_1 - V \bar{x} \frac{\partial^2 \delta}{\partial t^2}$$

But for the control volume, the change of fluid mass

$$\frac{\partial^2}{\partial t^2} \int_V \delta dV = \frac{\partial^2 \delta}{\partial t^2} V = \ddot{m}_V = \ddot{m}_{s1} + \ddot{m}_{e1} - \ddot{m}_1$$

so that $\frac{\partial^2 \delta}{\partial t^2} = \frac{\ddot{m}_{s1} + \ddot{m}_{e1} - \ddot{m}_1}{V}$

Therefore,

$$F_x = \dot{m}_{s1}u_{s1} + \dot{m}_{e1}u_{e1} - \dot{m}_1u_1 + x_{s1}\ddot{m}_{s1} + x_{e1}\ddot{m}_{e1} - x_1\ddot{m}_1 - \bar{x}(\ddot{m}_{s1}+\ddot{m}_{e1}-\ddot{m}_1)$$

$$= \dot{m}_{s1}u_{s1} + \dot{m}_{e1}u_{e1} - \dot{m}_1u_1 + \ddot{m}_{s1}(x_{s1}-\bar{x}) + \ddot{m}_{e1}(x_{e1}-\bar{x}) - \ddot{m}_1(x_1-\bar{x}) \qquad \text{(III.1)}$$

The spatial relationships are shown in Fig. III.1. If the spool displacement is small compared to the axial dimension of the spool, and the service port of the valve is half way between the supply and exhaust ports, then

$$\bar{x}_{s1} - \bar{x} \approx l/2$$

$$\bar{x}_{e1} - \bar{x} \approx l/2$$

$$\bar{x}_1 - \bar{x} \approx 0$$

where l is the length of the controlled volume along the spool axis. Subsequently,

$$F_x = \dot{m}_{s1}u_{s1} + \dot{m}_{e1}u_{e1} - \dot{m}_1u_1 + \frac{1}{2}(\ddot{m}_{s1} - \ddot{m}_{e1}) \qquad \text{(III.2)}$$

It is noted that F_x is always opposing the opening of spool.

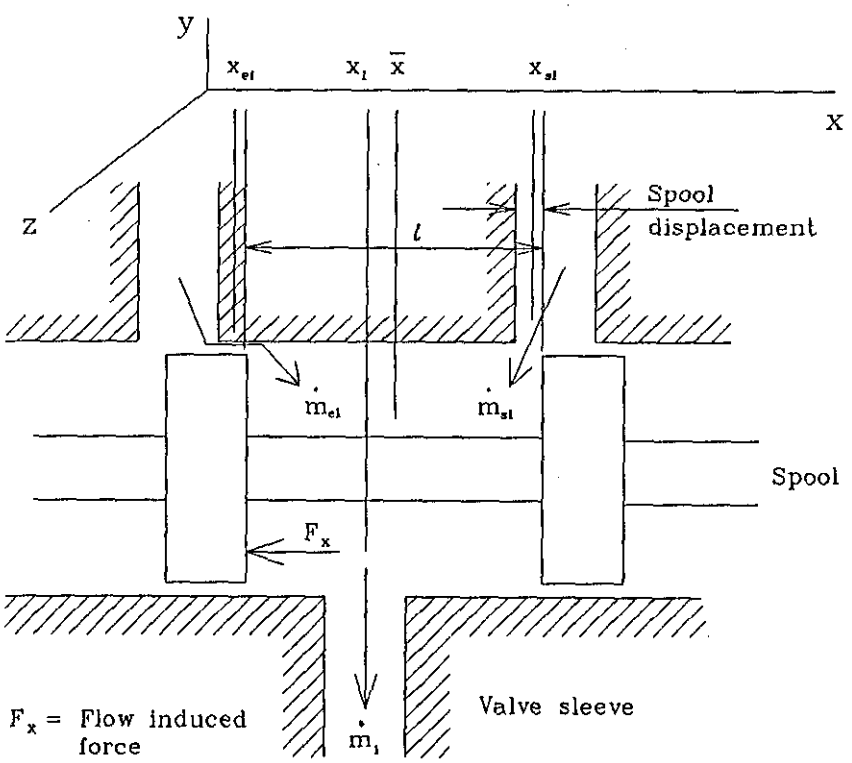

Fig. III.1 - Spatial relationship for flow induced force

APPENDIX IV

THE AREA FUNCTION

The area opened when the spool is displaced by a distance z from its normally closed position is determined by considering the conical area in Fig. 6.10,

$$\tan \phi = \frac{D_V - D_S}{2z} \qquad \text{(IV.1)}$$

$$z_S = \frac{D_S}{2 \tan \phi} \qquad \text{(IV.2)}$$

$$z_V = \frac{D_V}{2 \tan \phi} \qquad \text{(IV.3)}$$

The surface area of the cone with height z_S and base D_S is,

$$A_S = \frac{\pi D_S^2}{4 \tan \phi} . \sqrt{(1 + \tan^2 \phi)} \qquad \text{(IV.4)}$$

Similarly,

$$A_V = \frac{\pi D_V^2}{4 \tan \phi} . \sqrt{(1 + \tan^2 \phi)} \qquad \text{(IV.5)}$$

The truncated conical flow area opened for air

$$A_O = \frac{\pi}{4 \tan \phi} . (D_V^2 - D_S^2) . \sqrt{(1 + \tan^2 \phi)} \qquad \text{(VI.6)}$$

Expressing in terms of z

$$A_O = \frac{\pi (D_V + D_S)}{2} . \sqrt{[z^2 + \frac{(D_V - D_S)^2}{4}]} \qquad \text{(IV.7)}$$

If $D_V = D_S$, i.e. no manufacturing tolerance,

$$A_o = \pi . D_s . z \qquad \text{(IV.8)}$$

which is the ideal valve formula. If the spool goes in the negative direction, the passage for air will be restricted to the gap of the clearance. In other words, when $z < 0$, the area is

$$A_o = \frac{\pi (D_v + D_s)}{4} . (D_v - D_s) = \frac{\pi (D_v^2 - D_s^2)}{4} \qquad \text{(IV.9)}$$

APPENDIX V

ADIABATIC FLOW OF COMPRESSIBLE FLUID BETWEEN TWO STATIONS WITH NON-STAGNATION UPSTREAM CONDITION

Consider two stations (1) and (2) in the flow stream, and neglecting static potentials,

$$H_1 + \frac{u_1^2}{2} = H_2 + \frac{u_2^2}{2} \qquad (V.1)$$

together with the adiabatic gas equations,

$$\left(\frac{P_1}{\delta_1^n}\right) = \left(\frac{P_2}{\delta_2^n}\right) \qquad (V.2)$$

and the perfect gas law,

$$P = \delta RT \qquad (V.3)$$

The three equations can be combined to form,

$$u_2^2 = u_1^2 + \left(\frac{2n}{n-1}\right).\left(\frac{P_1}{\delta_1} - \frac{P_2}{\delta_2}\right) \qquad (V.4)$$

where n = ratio of specific heats

Dividing by nRT_2 and noting the relationships of T_1, T_2, P_1, P_2,

$$M_2^2 = \frac{M_1^2}{r^{\frac{n-1}{n}}} + \frac{2}{n-1}.\left(\frac{1}{r^{\frac{n-1}{n}}}\right).\left(1-r^{\frac{n-1}{n}}\right) \qquad (V.5)$$

where $r = \frac{P_2}{P_1}$

The mass flow rate

$$\dot{m} = A_1 \cdot \delta_1 \cdot u_1 = A_2 \cdot \delta_2 \cdot u_2 \tag{V.6}$$

Expressing in terms of conditions at (2),

$$\dot{m} = A_2 \cdot u_2 \cdot \frac{nP_2}{nRT_2} = A_2 \cdot M_2 \cdot P_2 \sqrt{\left(\frac{n}{RT_2}\right)} \tag{V.7}$$

Substituting (V.5) and (V.2) into (V.7),

$$\dot{m} = \frac{A_t P_1}{\sqrt{T_1}} \cdot \sqrt{\left(\frac{n}{R}\right)} \cdot M_2 \cdot \left(\frac{M_1^2(n-1)+2}{M_2^2(n-1)+2}\right)^{\frac{n+1}{2(n-1)}} \tag{V.8}$$

In terms of r,

$$\dot{m} = \frac{A_t P_1}{\sqrt{T_1}} \cdot r^{\frac{1}{n}} \cdot \sqrt{\left(\frac{n}{R}\right)} \cdot \sqrt{\left[M_1^2 + \frac{2}{n-1}\left(1 - r^{\frac{n-1}{n}}\right)\right]} \tag{V.9}$$

where $A_t = A_2$ = throat area

Differentiating Eqn (V.9) with respect to r and equating to zero, the critical pressure ratio

$$r_{crit} = \left(\frac{M_1^2(n-1)+2}{n+1}\right)^{\frac{n}{n-1}} \tag{V.10}$$

which corresponds to the value at $M_2 = 1$. Since the flow will resolve to shock waves when it reaches sonic condition beyond the throat, the maximum flow rate is

$$\dot{m}_{crit} = \frac{A_t P_1}{\sqrt{T_1}} \cdot \sqrt{\left(\frac{n}{R}\right)} \cdot \left(\frac{M_1^2(n-1)+2}{n+1}\right)^{\frac{n+1}{2(n-1)}} \tag{V.11}$$

If $P_2 > P_1$, the flow is reversed. The mass flow rate equation becomes:

$$\dot{m} = \frac{A_t P_2}{\sqrt{T_2}} \cdot r^{\frac{1}{n}} \cdot \sqrt{\left(\frac{n}{R}\right)} \cdot \sqrt{\left[M_2^2 + \frac{2}{n-1}\left(1 - r^{\frac{n-1}{n}}\right)\right]} \qquad \text{if } r \geq r_{crit}$$

$$\dot{m}_{crit} = \frac{A_t P_2}{\sqrt{T_2}} \cdot \sqrt{\left(\frac{n}{R}\right)} \cdot \left(\frac{M_2^2(n-1)+2}{n+1}\right)^{\frac{n+1}{2(n-1)}} \qquad \text{if } r < r_{crit}$$

(V.12)

where $A_t = A_1$ = throat area

$$r = \frac{P_1}{P_2}$$

$$r_{crit} = \left(\frac{M_2^2(n-1)+2}{n+1}\right)^{\frac{n}{n-1}}$$

Combining Eqn (V.9) - (V.12), a flow function Γ can be defined:

$$\Gamma(P_1, T_1, M_1, P_2, T_2, M_2) = \frac{\dot{m}}{A_t} \cdot \sqrt{\left(\frac{R}{n}\right)} \qquad (V.13)$$

APPENDIX VI

Derivation of Flow Node Temperature

Consider energy flow into the valve land volume in Fig. VI.1,

(a) Case : $\dot{m}_{s1} \geq 0$, $\dot{m}_1 \geq 0$ and $\dot{m}_{e1} \geq 0$

$$C_p T_s \dot{m}_{s1} + \frac{u_s^2}{2} \dot{m}_{s1} + C_p T_e \dot{m}_{e1} + \frac{u_e^2}{2} \dot{m}_{e1} = C_p T_v \dot{m}_1 + \frac{u_v^2}{2} \dot{m}_1$$

Solving for T_v and noting that $M_2 = \frac{u_2}{nRT}$, $C_p = \frac{nR}{n-1}$

$$T_v = \frac{T_s \dot{m}_{s1}(1 + \frac{n-1}{2} M_s^2) + \dot{m}_{e1} T_e (1 + \frac{n-1}{2} M_e^2)}{\dot{m}_1 (1 + \frac{n-1}{2} M_v^2)}$$

$$\approx \frac{T_s \dot{m}_{s1}(1 + \frac{n-1}{2} M_s^2) + \dot{m}_{e1} T_e (1 + \frac{n-1}{2} M_e^2)}{\dot{m}_1} \qquad \text{(VI.1)}$$

If $M_s = M_e = 0$, Eqn (VI.1) can be further simplified to

$$T_v \approx \frac{T_s \dot{m}_{s1} + \dot{m}_{e1} T_e}{\dot{m}_{s1} + \dot{m}_{e1}} \qquad \text{(VI.2)}$$

(b) Case : $\dot{m}_{s1} \geq 0,\ \dot{m}_1 \geq 0,\ \dot{m}_{e1} < 0$

$$C_p T_s \dot{m}_{s1} + \frac{u_s^2}{2}\dot{m}_{s1} = C_p T_v(-\dot{m}_{e1} + \dot{m}_1) + \frac{u_v^2}{2}(-\dot{m}_{e1} + \dot{m}_1)$$

$$T_v = \frac{\dot{m}_{s1} T_s\left(1 + \frac{n-1}{2} M_s^2\right)}{\dot{m}_1 - \dot{m}_{e1}}$$

$$= T_s\left(1 + \frac{n-1}{2} M_s^2\right) \qquad \text{(VI.3)}$$

(c) Case : $\dot{m}_{s1} \geq 0,\ \dot{m}_1 < 0,\ \dot{m}_{e1} \geq 0$

All restrictions are provided for inward flows. This is physically impossible but in mathematical formulation of the model, this is also determined to deal with occasional anomalies in the process of model evaluation or simulation of pneumatic responses. The complete mathematical model is also necessary to produce hypothetical results for extreme case validations.

$$\dot{m}_{s1} T_s\left(1 + \frac{n-1}{2} M_s^2\right) + \dot{m}_{e1} T_e\left(1 + \frac{n-1}{2} M_e^2\right) - \dot{m}_1 T_1\left(1 + \frac{n-1}{2} M_1^2\right)$$

$$= T_v(\dot{m}_{s1} + \dot{m}_{e1} - \dot{m}_1)$$

Therefore,

$$T_v = \frac{\dot{m}_{s1} T_s\left(1 + \frac{n-1}{2} M_s^2\right) + \dot{m}_{e1} T_e\left(1 + \frac{n-1}{2} M_e^2\right) - \dot{m}_1 T_1\left(1 + \frac{n-1}{2} M_1^2\right)}{\dot{m}_{s1} + \dot{m}_{e1} - \dot{m}_1} \qquad \text{(VI.4)}$$

(d) Case : $\dot{m}_{s1} \geq 0,\ \dot{m}_1 < 0,\ \dot{m}_{e1} < 0$

The service port is at high pressure such that air flows from both supply and service ports to exhaust.

$$C_p T_s \dot{m}_{s1} - \dot{m}_1 T_1 C_p + \frac{u_s^2}{2} \dot{m}_{s1} - \frac{u_1^2}{2} \dot{m}_1 = \dot{m}_{e1} C_p T_v + \dot{m}_{e1} \frac{u_v^2}{2}$$

$$T_v = \frac{\dot{m}_{s1} T_s (1 + \frac{n-1}{2} M_s^2) - \dot{m}_1 T_1 (1 + \frac{n-1}{2} M_1^2)}{\dot{m}_{s1} - \dot{m}_1} \qquad \text{(VI.5)}$$

(e) Case : $\dot{m}_{s1} < 0,\ \dot{m}_1 \geq 0,\ \dot{m}_{e1} \geq 0$

This is also physically impossible. Exhaust pressure is always less than supply pressure so that flow always goes from supply or service port to exhaust.

$$C_p T_e \dot{m}_{e1} + \frac{u_e^2}{2} \dot{m}_{e1} = C_p T_v \dot{m}_1 + \frac{u_v^2}{2} \dot{m}_1 - C_p T_v \dot{m}_{s1} - \frac{u_v^2}{2} \dot{m}_{s1}$$

$$T_v = \frac{\dot{m}_{e1} T_e \ (1 + \frac{n-1}{2} M_e^2)}{\dot{m}_{e1}}$$

$$= T_e (1 + \frac{n-1}{2} M_e^2) \qquad \text{(VI.6)}$$

(f) Case : $\dot{m}_{s1} < 0,\ \dot{m}_{e1} < 0,\ \dot{m}_1 \geq 0$

All flows go from valve land volume outwards. This is another physically impossible case. The value of T_v is independent of any of T_s, T_e, or T_1 or any combination. The temperatures of the linking volumes are averaged to produce a reasonable value

for mathematical processing

$$T_v = T_{average} = \frac{T_s + T_e + T_1}{3} \qquad \text{(VI.7)}$$

(g) Case : $\dot{m}_{s1} < 0,\ \dot{m}_1 < 0,\ \dot{m}_{e1} \geq 0$

The service port is supplying air back to the valve.

$$C_pT_v\dot{m}_{s1} + \frac{u_v^2}{2}\dot{m}_{s1} + C_pT_e\dot{m}_{e1} + \frac{u_e^2}{2}\dot{m}_{e1} = C_pT_1\dot{m}_1 + \frac{u_1^2}{2}\dot{m}_1$$

$$T_v = \frac{\dot{m}_1T_1(1 + \frac{n-1}{2}M_1^2) - \dot{m}_{e1}T_e(1 + \frac{n-1}{2}M_e^2)}{\dot{m}_1 - \dot{m}_{e1}} \qquad \text{(VI.8)}$$

(h) Case : $\dot{m}_{s1} < 0,\ \dot{m}_1 < 0,\ \dot{m}_{e1} < 0$

The service port pressure is so high that air flows from service port to both supply and exhaust.

$$C_pT_v\dot{m}_{s1} + \frac{u_v^2}{2}\dot{m}_{s1} + C_pT_v\dot{m}_{e1} + \frac{u_v^2}{2}\dot{m}_{e1} = C_pT_1\dot{m}_1 + \frac{u_1^2}{2}\dot{m}_1$$

$$T_v = \frac{\dot{m}_1T_1\ (1 + \frac{n-1}{2}M_1^2)}{\dot{m}_{s1} + \dot{m}_{e1}}$$

$$= T_1(1 + \frac{n-1}{2}M_1^2) \qquad \text{(VI.9)}$$

Combining the above 8 cases, the resultant temperature can be defined as:

$$T_V = \Omega(\dot{m}_{s1}, \dot{m}_{e1}, \dot{m}_{1v}, M_{s1}, M_{e1}, M_{1v}, T_{s1}, T_e, T_{1v}) \qquad \text{(VI.10)}$$

APPENDIX VII

CONSTANTS

Array	C Parameters (constants)		Default values
C(1)	1-D adiabatic flow constant	=	1.4
C(2)	Universal gas constant (J/kg/K)	=	286.76
C(3)	Max physical spool displacement (mm)	=	1.0
C(4)	Underlap (mm)	=	0.0
C(5)	Supply pressure (N/m^2)	=	589000.0
C(6)	Supply temperature (K)	=	294.0
C(7)	Exhaust pressure (N/m^2)	=	101300.0
C(8)	Exhaust temperature (K)	=	294.0
C(9)	Valve sleeve diameter (mm)	=	10.0
C(10)	Valve spool diameter (mm)	=	9.98
C(11)	Coefficient of discharge (supply)	=	0.8
C(12)	Coefficient of discharge (exhaust)	=	0.8
C(13)	Plastic tube diameter	=	4.0
C(14)	Cylinder length (m)	=	0.3
C(15)	Piston diameter (m)	=	0.05
C(16)	Piston rod diameter (m)	=	0.025
C(17)	Mass of load (kg)	=	1.6
C(18)	Coeff of viscous friction (Ns/m)	=	30.0
C(19)	Load in direction of piston action (N)	=	0.0
C(20)			Not used
C(21)	Proportional gain (profile not used)	=	1.0

Array	C Parameters (constants)		Default values
C(22 to 23)			Not used
C(24)	Threshold velocity (m/s)	=	0.00001
C(25)	Spool rod diameter (mm)	=	6.0
C(26)	Controller delay (s)	=	0.0005
C(27)	Position dead band (m)	=	0.0
C(28)	Slope of pressure drop in tubing	=	0.4
C(29)	Threshold percent of hysteresis	=	5.0
C(30)	Reference flow for pressure drop	=	0.00465
C(31)	Forced closed loop exit time	=	1.42
C(32)	Dither frequency (Hz)	=	50.0
C(33)	Dither amplitude (mm of spool disp)	=	0.2
C(34)	Dither phase lag (in degrees)	=	0.0
C(35)	Residual volume in chamber 1 (m^3)	=	0.00002
C(36)	Residual volume in chamber 2 (m^3)	=	0.00002
C(37)	Spool signal amplifying factor	=	1.0
C(38)	Software saturation limit (mm)	=	1.0
C(39)	Valve port diameter (mm)	=	3.3
C(40)	Start time of controller function (s)	=	0.0
C(41)	Sampling time (s)	=	0.0013
C(42)	Encoder pulse (mm of stroke/pulse)	=	0.01205
C(43)	Proportional gain on derived velocity	=	1.0
C(44)	Proportional gain on derived acc	=	1.0
C(45)	Velocity dead band	=	0.0
C(46)	Static friction (extending) (N)	=	70.0
C(47)	Coulomb friction (extending) (N)	=	40.0
C(48)	Static friction (retracting) (N)	=	40.0

Array	C Parameters (constants)		Default values
C(49)	Coulomb friction (retracting) (N)	=	11.0
C(50)	Spool coefficient K_s (s^{-2})	=	36000.0
C(51)	Spool damping coefficient K_d (s^{-1})	=	100.0
C(52)	Blind width reduction factor	=	0.5
C(53)			Not used
C(54)	Turbulence coeff. for Mach Number	=	1.0
C(55)	Leakage coeff. bet. chamber (empirical)	=	0.0
C(56)	Passage resistance (Egli's rho)	=	20.0
C(57)	Leakage passage thickness (m)	=	0.0001
C(58)	Reverse flow coeff. of discharge	=	1.0
C(59)	Temperature difference limit in FLS	=	200.0
C(62)			Working constant
C(63)	Diameter of connector (mm)	=	5.0
C(64)			Working constant
C(65)			Not used
C(66)	Stepper puls gain (mm spl disp/pulse)	=	0.0125
C(67)			Not used
C(68)	Burrows' k5 (pressure feedback)	=	12.4
C(69)			Not used
C(70)	Length of valve land (flow ind. forces)	=	0.01
C(71)			Working constant
C(72)			Not used
C(73)			Working constant
C(74 to 80)			Not used
C(81)	Solenoid force gain coefficient (N/mm)	=	25.0
C(82)	Valve spring stiffness (N/mm)	=	25.0

Array	C Parameters (constants)		Default values
C(83)	Initial valve spring compression (N)	=	25.0
C(84)	Static friction of spool (N)	=	3.0
C(85)	Coulomb friction of spool (N)	=	2.0
C(86)	Mass of spool (kg)	=	0.023
C(87)	Spool velocity threshold (mm/s)	=	0.00001
C(88)			Not used
C(89)	Region of infinite stiffness (m)	=	0.001
C(90)	Infinite stiffness at end stops (N/m)	=	1000000.0
C(91)	Infinite stiffness for spool stop (N/m)	=	100000.0
C(92 to 300)			Not used

Array	L Flags (integer indicators)		Default values
L(1)	Controller start working flag		= 0
L(2)	Spool operator indicator (solenoid)		= 1
L(3)	Loop flag	(closed)	= 1
L(4)	System identification	(discrete)	= 1
L(5)	Feedback mode	(position)	= 1
L(6)	Number of moves required		= 1
L(7)	Step counts for moves (Working integer)		= 0
L(8)	Gain profile requirement flag (used)		= 1
L(9)			Working integer
L(10)	Diagnostic flag	(off)	= 0
L(11)	Dead band exit condition flag (disabled)		= 1
L(12)			Working integer
L(13)			Working integer
L(14)	Velocity calculation mode flag (vary)		= 1
L(15)			Working integer
L(16)	Model type	(flow node)	= 1
L(17)	Coeff. of discharge flag	(Perry's)	= 1
L(18)	Actuator leakage model indicator (Egli's)		= 1
L(19)	Flag for control software kp(-ve) bug		= 0
L(20)	Max stepper motor actuator steps		= 40
L(21)	Load model flag		= 0
L(22)	Controller model flag	(Discrete)	= 1
L(23 to 50)			Not used
L(51)	Velocity calculation time		= 0
L(52)	Counting integer for velocity calculation		= 5
L(53 to 63)			Not used

Array	L Flags (integer indicators)	Default values
L(64)		Working integer
L(65)		Not used
L(66)		Not used
L(67)	Span of application of each Kp data	= 4
L(68)	Scale factor for quantised spool command	= 65536
L(69)		Not used
L(70 to 76)		Working integer
L(77)	Acceleration calculation time	= 3
L(78 to 80)		Working integer
L(81 to 98)		= Not used
L(99)	Reserved by package	= 0
L(100)	Reserved by package	= 0

APPENDIX VIII

DERIVATION OF ANALYTICAL TUBING PRESSURE DROP

The pressure at any point of compressible fluid in pipe flow with friction is given by [6.48]

$$\frac{P}{P^*} = \frac{1}{M}\sqrt{\left[\frac{n+1}{2+(n-1)M^2}\right]} \qquad \text{(VIII.1)}$$

where P = Pressure

M = Mach number

* = Condition at critical position

and the frictional effects

$$\frac{4fL^*}{D} = \frac{1-M^2}{nM^2} + \frac{n+1}{2n}\ln\left[\frac{(n+1)M^2}{2+(n-1)M^2}\right] \qquad \text{(VIII.2)}$$

Considering the tubing connecting the two sections 1 and 2, and assuming the condition at position 1 is known,

$$M_1 = \frac{\dot{m}}{A_1P_1}\sqrt{\left(\frac{RT_1}{n}\right)} \qquad \text{(VIII.3)}$$

$$\frac{4fL_1^*}{D} = \frac{1-M_1^2}{nM_1^2} + \frac{n+1}{2n}\ln\left[\frac{(n+1)M_1^2}{2+(n-1)M_1^2}\right] \qquad \text{(VIII.4)}$$

$$\frac{4fL_2^*}{D} = \frac{1-M_2^2}{nM_2^2} + \frac{n+1}{2n}\ln\left[\frac{(n+1)M_2^2}{2+(n-1)M_2^2}\right] \qquad \text{(VIII.5)}$$

where $L_1^* - L_2^* = L$, length of tubing. The values of f are tabulated in Appendix V of reference [6.49].

Substituting,

$$\frac{4fL_2^*}{D} = \frac{4fL_1^*}{D} - \frac{4fL}{D} \qquad \text{(VIII.6)}$$

into Eqn (VIII.5), M_2 can be found.

If $\dot{m}$ is negative, the flow is reversed. Eqn (VIII.6) becomes

$$\frac{4fL_2^*}{D} = \frac{4fL_1^*}{D} + \frac{4fL}{D} \qquad \text{(VIII.7)}$$

Substituting pipe sections 1 and 2 into (VIII.1),

$$\frac{P_1}{P^*} = \frac{1}{M_1}\cdot\sqrt{\left[\frac{n+1}{2+(n-1)M_1^2}\right]} \qquad \text{(VIII.8)}$$

$$\frac{P_2}{P^*} = \frac{1}{M_2}\cdot\sqrt{\left[\frac{n+1}{2+(n-1)M_2^2}\right]} \qquad \text{(VIII.9)}$$

so that,

$$P_2 = P_1\frac{M_1}{M_2}\cdot\sqrt{\left[\frac{2+(n-1)M_1^2}{2+(n-1)M_2^2}\right]} \qquad \text{(VIII.10)}$$

where M_1 and M_2 are of the same sign.

It is noted that the flow is choked when the flow Mach number is unity. In this case, the flow conditions will be altered such that the inlet conditions at section 1 will just produce a sonic condition at section 2. That is,

$$M_2 = 1 \qquad \text{(VIII.11)}$$

$$P_2 = P^* \qquad \text{(VIII.12)}$$

$$\text{where } P^* = \frac{P_1M_1}{\sqrt{\left[\frac{n+1}{2+(n-1)M_1^2}\right]}} \qquad \text{(VIII.13)}$$

On the contrary, if the downstream condition at position 2 is known, then

$$M_2 = \frac{\dot{m}}{A_2 P_2} \sqrt{\left(\frac{RT_2}{n}\right)} \qquad \text{(VIII.14)}$$

$$\frac{4fL_2^*}{D} = \frac{1-M_2^2}{nM_2^2} + \frac{n+1}{2n} \ln\left[\frac{(n+1)M_2^2}{2+(n-1)M_2^2}\right] \qquad \text{(VIII.15)}$$

Therefore,

$$\frac{4fL_1^*}{D} = \frac{4fL}{D} + \frac{4fL_2^*}{D} \qquad \text{(VIII.16)}$$

$$= \frac{1-M_1^2}{nM_1^2} + \frac{n+1}{2n} \ln\left[\frac{(n+1)M_1^2}{2+(n-1)M_1^2}\right] \qquad \text{(VIII.17)}$$

from which M_1 is solved.

Combining Eqn (VIII.7) and (VIII.8),

$$P_1 = P_2 \frac{M_2}{M_1} \sqrt{\left[\frac{2 + (n-1)M_2^2}{2 + (n-1)M_1^2}\right]} \qquad \text{(VIII.18)}$$

Similar to the previous case, the downstream Mach number M_2 must not exceed unity, otherwise, Eqn (VIII.15) is not valid.

APPENDIX IX

CONTROL ALGORITHM FOR SOLENOID OPERATED VALVE SYSTEM

The gain determination algorithm was designed based on the findings of Moore [1.8]. The parameter L_{prof} which determined the span of applicability of each gain profile element was set to 4 in the source code (to simplify data entry user interface). Only 256 elements existed in the gain profile conforming to that in the simulation programme. The default gain profile was set as follows:

$K_p(0)$ = \$2000 = 8192

$K_p(1)$ = \$1800 = 6144

$K_p(2)$ = \$1000 = 4096

$K_p(3)$ = \$0800 = 2048

$K_p(4)$ = \$0500 = 1280

$K_p(5)$ = \$0300 = 768

$K_p(6)$ = \$0200 = 512

$K_p(7)$ = \$0180 = 384

$K_p(8)$ = \$0140 = 320

$K_p(9)$ = \$0120 = 288

$K_p(10)$ - $K_p(255)$ = \$0100 = 256

The decimal values were entered into the simulation model from an ASCII file during model initialisation.

Assuming the timer on the target system has been enabled, all

the position, velocity and acceleration values were determined within the timer interrupt service routine "PTM". These information were stored in specific memory locations which could be referenced throughout the software. The steps involved in the DAC output calculation routine "GAIN" were:

(a) The position gain profile element applicable to the current position error n_p was determined.

Let i_{prof} = element number of the gain profile array
n_p = position error in hexadecimal value
n_v = velocity in hexadecimal value
n_a = acceleration in hexadecimal value
K_v = velocity gain
K_a = acceleration gain

then $i_{prof} = \min (n_p/4, 255)$

(b) An intermediate DAC value was calculated:

$$n_{DAC1} = K_p(i_{prof}) * n_p - K_v * n_v - K_a * n_a$$

where n_v, n_a = velocity and acceleration values calculated by the differential values of the position data

All values were in 32-bit binary format.

(c) Due to the limitation of 12-bit DAC, the DAC value was further reduced by

$$n_{DAC2} = n_{DAC1}/L_{DAC}$$

where L_{DAC} = 256 for solenoid valve operator, or
65536 for stepper motor valve operator

(d) Additional saturation limits were also imposed to restrict the output value to within the range appropriate to the valve operator:

For the solenoid valve operator, the final DAC output value was

$$n_{SPLCOM} = \text{sign}(n_{DAC2}) * \min(|n_{DAC2}|, 2048)$$

where $\text{sign}(n_{DAC2}) = +1$ if $n_{DAC2} > 0$

-1 if $n_{DAC2} < 0$

For the stepper motor operated valve, the DAC output was

$$n_{SPLCOM} = \text{sign}(n_{DAC2}) * \min(|n_{DAC2}|, 40)$$

REFERENCES

[1.1] WESTON R.H., MOORE P.R., THATCHER T.W. (1983)
"Design of a Family of Modular Robots", ICPR Conference, Windsor, Canada, August, 1983, Proceedings, TD5d

[1.2] MORGAN G. (1985)
"Programmable Positioning of Pneumatic Actuators", Applied Pneumatics, May, pp.16-20.

[1.3] THATCHER T.W., WESTON R.H., MOORE P.R. (1983)
"Software System for Modular Robots", Conference on Advanced Software in Robotics, Liege, Belgium, May, 1983, Proceedings pp 48-54.

[1.4] THATCHER T.W., WESTON R.H., MOORE P.R. (1983)
"Modularity in Workhandling Systems", UK Robotics Research Conference, IEE London, December, 1983, Proceedings, pp 28-34.

[1.5] MOORE P.R., WESTON R.H., THATCHER T.W. (1984)
"Control of Pneumatic Servo-drives Using Digital Compensation", IASTED International Symposium on Telecommunication and Control, Halkidiki, Greece, August, 1984, Proceedings, pp.264-268

[1.6] NAGARAJAN R., WESTON R.H. (1985)
"Front-end Control Schemes for Pneumatic Servo-driven Modules", Proc Instn Mech Engrs, Vol.199, No.B4, pp.271-277

[1.7] PU J., WESTON R.H. (1988)
"Position Control of Pneumatic Drives and the Use of Learning Methodologies", 8th International Symposium on Fluid Power, Birmingham, England, 19-21 April, 1988, Paper C2, pp.169-198

[1.8] MOORE P.R. (1986)
"Pneumatic Motion Control Systems for Modular Robots", Ph.D. Thesis, 1986, Department of Manufacturing Engineering, Loughborough University of Technology

[2.1] NARRAWAY R. (1982)
"Making a Start in CAD", Engineering Materials and Design, Pt.6, July/August, 1982, pp.15-17

[2.2] DEANE J.N.S. (1980)
"Computer Aided Design and Manufacture", the Management of Automation Conference, the British Management Data Foundation, 2-3 December, 1980, London, U.K.

[2.3] CORNELL T.R. (1985)
"Systems Integration Is a Mandatory Component in Achieving an Optimum Systems Environment", in "Computer Integrated Manufacturing Systems: Selected Readings", ed. NAZEMETZ J.W., HAMMER W.E.Jr., SADOWSKI R.P., IIE, 1985, pp.145-153

[2.4] SADOWSKI R.P. (1985)
"History of Computer Use in Manufacturing Shows Major Need Now Is for Integration", in "Computer Integrated Manufacturing Systems: Selected Readings", ed. NAZEMETZ J.W., HAMMER W.E.Jr., SADOWSKI R.P., IIE, 1985, pp.3-7

[2.5] McKENOWN P.A. (1980)
"The Place of Quality Control in Automated Manufacturing", the Management Automation Conference, British Management Data Foundation, 2-3 December, 1980, London, UK

[2.6] CLARK V.L., PEPPIATT N.A., STEEL J., SMITHS. (1987)
"Computer Integrated Manufacturing: a Case Study in the Development of the Thermoplastic Seals", Proc Instn Mech Engrs, Vol.201, No.B2. 1987, pp.107-115

[2.7] FRENCH R.L. (1985)
"Management Looking at CIMS Must Deal Effectively with These Issues and Realities", in "Computer Integrated Manufacturing Systems: Selected Readings", ed. NAZEMETZ J.W., HAMMER W.E. Jr., SADOWSKI R.P., IIE, 1985, pp.209-213

[2.8] BRAVOCO R.R. (1985)
"Planning a CIM System Using System Engineering Methods", in "A Program Guide for CIM Implementation", ed. SAVAGE C.M., SME, 1985, pp.19-38

[2.9] LEE S.E., MOSIER C.T. (1985)
"The Development of a Computer Integrated Manufacturing System: A Modern Approach", in "Computer Integrated Manufacturing Systems: Selected Readings", ed. NAZEMETZ J.W., HAMMER W.E. Jr., SADOWSKI R.P., IIE, 1985, pp.229-236

[2.10] DELONG L.W. (1985)
"A Structured Approach to Integrated Factory Automation", AUTOTECH International Conference on Industrial Automation, 7-8 March, 1985, Hong Kong

[2.11] HOLLAND J.R. (1983)
"Factory Area Networks - The Key to Successful Factory Automation Strategies", AUTOFACT Europe Conference, 13-15 September, 1983, Geneva, Switzerland, Society of Manufacturing Engineering, Paper MS83-523, pp.1-17

[2.12] YEOMANS R.W., CHOUDRY A., HAGEN P.J.W.ten (1985)
"Design Rules for a CIM System", North-Holland, 1985, Ch.1-2, pp.1-11

[2.13] MERCHANT E. (1985)
"The Importance of Flexible Manufacturing Systems to the Realisation of Full Computer-Integrated Manufacturing", in "Flexible Manufacturing Systems", ed. WARNECKE H.J., STEINHILPER R., IFS, 1985, pp.27-43

[2.14] ZYGMONT J. (1986)
"Flexible Manufacturing Systems - Curing the Cure-all", High Technology, October, 1986, pp.22-27

[2.15] KIEF H.B., OLLING G., WATERS T.F. (1986)
"Flexible Automation '87/88 - The International CNC Reference Book", Becker, Ch.23, pp.23.1-23.21, Ch.17, pp.17.1-17.15

[2.16] STUTE G. (1980)
"State of the Art of Flexible Manufacturing Systems", Management of Automation Conference, the British Management Data Foundation, 2-3 December, 1980, London, UK

[2.17] WARNECKE H.J., STEINHILPER R. (1985)
"Flexible Manufacturing Systems ", IFS, 1985, Section 5, pp.237-312

[2.18] YOSHIKAWA H. (1984)
"Flexible Manufacturing Systems in Japan", Proceedings of the 9th Triennial World Congress of IFAC, Budapest, Hungary, 2-6 July, 1984, Vol.5, pp.2239-2337

[2.19] WILKINS A. (1984)
"Computer Control in Flexible Manufacturing Systems (FMS)" in "Real-time computer control", ed. BERNETT S., LINKENS D.A., IEE Control Engineering Series 24, Ch. 7, pp.114-120

[2.20] RATHMILL K., CHAN W.W. (1985)
"What Simulation Can Do for FMS Design and Planning", in Flexible Manufacturing Systems, IFS, ed. WARNECKE H.J., STEINHILPER R., 1985, pp.105-117

[2.21] RANKY R.G. (1984)
"A Software Library for Designing and Controlling Flexible Manufacturing Systems", Proceedings of the 9th Triennial World Congress, IFAC, Budapest, Hungary, 2-6 July, 1984, Vol.5, pp.2511-2516

[2.22] HEINONEN R., RANTA J., WAHLSTROM B. (1984)
"A Conceptual Framework for the Design of Complex Automation Systems", Proceedings of the 9th Triennial World Congress, IFAC, Budapest, Hungary, 2-6 July, 1984, Vol.5, pp. 2585-2589

[2.23] NUMERICAL ENGINEERING SOCIETY (1983)
"Robots-Too Often Totally Misunderstood by Industry", in "Numerical Engineering", February/March, 1983, pp.13-16

[2.24] BRODY H. (1986)
"The Robot - Just Another Machine?", High Technology, October, 1986, pp.31-35

[2.25] MIDDLE J.E., SURY J. (1985)
"Studies to Advance the Application of Robotic Welding", in "Flexible Manufacturing - Recent Development in FMS, Robotics CAD/CAM, CIM", ed. RAOUF A., AHMAD S.I., Elsvier, pp.187-200

[2.26] INGERSOLL ENGINEERS (1980)
"Industrial Robots: The Report by Ingersoll Engineers", Vol.1, DOI/NEL

[2.27] ASTROP R. (1982)
"Robot Applications: A Trio of Success", Machinery and Production Engineering, February, 1982, pp.24-29

[2.28] SUGANO S., WAKAGAWA J., TANAKA Y., KATO I. (1984)
"Keyboard Playing by an Anthropomorphic Robot: Fingers and Arm Model and Its Control System of WAM-7R", the 5th Symposium on Theory and Practice of Robots and Manipulators, 26-29 June, 1984, Udine, Italy, pp.151-161

[2.29] BILLINGSLEY J. (1984)
"Robotics", in "Real-time computer control", ed. BERNETT S., LINKENS D.A., IEE Control Engineering Series 24, Ch.13, pp.216-226

[2.30] EDKINS M. (1983)
"Linking Industrial Robots and Machine Tools", in "Robotic Technology", IEE Control Engineering Series 23, ed. PUGH A., Peregrinus, 1983, Ch.13, pp.142-150

[2.31] LAM P.H.L. (1985)
"A Flexible Assembly System for Electronic and Toy Assembly", International Conference on Industrial Automation, 7-8 March, 1985, Hong Kong

[2.32] GOODFELLOW S.D., MUNRO N. (1985)
"An Integrated Environment for Computer Aided Control Systems Engineering", Proceedings of the 3rd IFAC/IFIP Symposium, Lyngby, Denmark, 31 July - 2 August, 1985, pp.43-46

[2.33] NAKANISHI T. (1985)
"Japan's Experience in Industrial Automation with Specific Reference to Small and Medium Manufacturing Industries", Internation Conference on Industrial Automation, 7-8 March, 1985, Hong Kong

[2.34] LEE C.S.G, CHUNG M.J., TURNEY J.L., MUDGE T.N. (1982)
"On the Control of Mechanical Manipulators", IFAC Identification and System Parameters Estimation, 1982, Washington, D.C., USA, pp.1629-1634

[2.35] PARK H.S., CHO H.S. (1981)
"An Approach to the Design of Ideal Robotic mainpulators Having Simple Dynamic Characteristics", Proc Instn Mech Engrs, Vol.201, No.B4, 1987, pp.221-228

[2.36] WESTON R.H., MOORE P.R., THATCHER T.W. (1984)
"Design of Modular Robotic Systems", Microprocessors and Microsystems, February, 1984, Vol.8, No.1, pp 16-20.

[2.37] BROWN R.A. (1983)
"Designing Custom Robots for In-Plant Use", 13th International Symposium on Industrial Robots, 1983, Chicago, USA, pp.20-45 to 20-56

[2.38] ROBER BOSCH GmbH (1983)
"Bosch Flexible Assembly Systems: Flexible Workplaces up to Flexible Assembly Lines", Product Catalogue, 1983

[2.39] MARTONAIR LIMITED (1984)
"Modular Handling Units", Publication No.S/1/138, Issue 3, 10/84

[2.40] MOORE P.R., WESTON R.H., THATCHER T.W., GASCOIGNE J.D. (1983)
"Modular Robot Systems", Proceedings, 2nd IASTED International Symposium on Robotics and Automation, Lugano, Switzerland, June, 1983, pp.165-169

[2.41] SURNIN B.N. et al (1978)
"Design Features of Modular Type Robots", Machines and Tooling, Vol.49, No.7, 1978, pp.17-20

[2.42] KING K. L. (1981)
"A Building Block Approach to Advanced Control Techniques", Control Engineering, August, 1981, pp.17-20

[2.43] THATCHER T.W., WESTON R.H., MOORE P.R. (1984)
"Software Structures for Modular Robots", International Journal of Production Research, January, 1984, Vol.22, No.1, pp.71-84

[2.44] THATCHER T.W., WESTON R.H., MOORE P.R., HARRISON R. (1985)
"Supervisory Control of Single Axis Controllers for Modular Robotic Systems Using a Serial Interface", National Conference on Production Research, Nottingham, 9-11 September, 1985

[2.45] VUKOBRATOVIC M., STOKIC D. (1984)
"Non-adaptive Dynamic Control for Manipulation Robots: Invited Survey Paper", the 5th Symposium on Theory and Practice of Robots and Manipulators, 26-29 June, 1984, Udine, Italy, pp. 109-122

[2.46] INSTITUTION OF PRODUCTION ENGINEERS (1970)
"Automated Assembling", 1970, Section 4, IProdE Code No.130.4

[2.47] TREER K.R. (1970)
"Automated Assembly", Society of Manufacturing Engineers, 1970, Ch.7, pp.215-236

[2.48] ARCHER J.R., BLENKINSOP P.T. (1983)
"Actuation for Industrial Robots", IMechE Conf. Electric versus Hydraulic Drives, 27 October, 1983, London, UK, No. C306/83, pp.85-89

[2.49] CONWAY H.G., COLLINSON E.G. (1953)
"An Introduction to Hydraulic Servo-mechanism Theory", Proc of the Conference on Hydraulic Servomechanism, Instn Mech Engrs, 13 February, 1953, pp.1-11

[2.50] NEAL T.P. (1974)
"Performance Estimation for Electrohydraulic Control Systems", the National Conference on Fluid Power, Philadelphia, Pennsylvania, November, 1974

[2.51] ROCKWELL INTERNATIONAL CORPORATION (1981)
"Space Shuttle Technical Manual - Space Shuttle Main Engine", Rocketdyne Division, Part No. RS0070001, Contract NAS8-27980, DPD No.341, DR NO. LS-090-1, January, 1981

[2.52] LEE S. Y. (1954)
"Contribution to Hydraulic Control 6 - New Valve Configuration for High Pressure Hydraulic and Pneumatic Systems", Trans of the ASME, August, 1954, pp.905-911

[2.53] KASPERBAUTER K. (1980)
"Proportional Valves and Their Fields of Application", Industrial and Production Engineering, February, 1980, pp.106-114

[2.54] KIM S.D., CHO H.S., LEE C.O. (1988)
"Stability Analysis of a Load-sensing Hydraulic System", Proc Instn Mech Engrs, Vol. 202, No. A2, 1988, pp.79-88

[2.55] ARAFA H.A., RIZK M. (1987)
"Spool Hydraulic Stiffness and Flow Force Effects in Electrohydraulic Servovalves", Proc Instn Mech Engrs, Vol.201, No.C3, pp.193-199

[2.56] EDGE K.A., DARLING J. (1986)
"Cylinder Pressure Transients in Oil Hydraulic Pumps with Sliding Plate Valve", Proc Instn Mech Engrs, Vol.200, No.B1, 1986, pp.45-54

[2.57] BURROWS C.R., MARTIN D.J. (1974)
"Measuring the Oscillating Flow from an Electro-hydraulic Servovalve Using an Indirect Method", Proc Instn Mech Engrs, Vol.188, 51/74, 1974, pp.519-526

[2.58] EDGE K.A., FIGUEREDO K.R.A. (1987)
"An Adaptively Controlled Electrohydraulic Servo-mechanism - Part 1: Adaptive Controller Design, Part 2: Implementation", Proc Instn Mech Engrs, Vol.201, No.B3, 1987, pp.175-189

[2.59] PENNINGTON K.W., POLLARD M.G. (1983)
"The Development of an Electro-Mechanical Tilt System for the Advanced passanger Train", IMechE Conf Electric versus Hydraulic Drives, No. C299/83, pp.21-28

[2.60] WALKER D.G.W. (1983)
"Electric and Hydraulic Drives for Heavy Industrial Robots", IMechE Conf. Electric Versus Hydraulic Drives, No. C298/83, pp.15-19

[2.61] L'HOTE F., KAUFFMANN J.M., ANDRE P., TAILLARD J.P. (1983)
"Robot Technology", Vol. 4, Prentice-Hall, Ch. 3-4, pp.57-156

[2.62] TAL J. (1984)
"Motion Control by Microprocessors", Galil Motion Control Inc., USA, 1984

[2.63] MASORY O. (1986)
"Improving Contouring Accuracy of NC/CNC Systems with Additional Velocity Feed Forward Loop", Tech Brief, Journal of Engineering for Industry, Trans. of the ASME, Vol.108, August, 1986, pp.227-230

[2.64] BACKE W., SAFFE P. (1986)
"Development Trends in Hydraulic and Pneumatic Technology", VDI-Z, November, 1986, Vol.128, pp.855-857 (in German)

[2.65] LARSEN W.W. (1982)
"The Evolution of Pneumatics into Robotics, Part 2: Typical Control System for a Pneumatic Pick and Place Robot", Automation and Control, New Zealand, No.1, 1982, Vol.12, pp.31-35

[2.66] ROHNER P. (1979)
"Fluid Power Logic Circuit Design", Macmillan, 1979, Pt.II, pp.43-148

[2.67] MO P.T. (1985)
"Incroporating Flexibility into Pneumatic Sequence Control with Microprocessor", Industrial Supplies, Issue 11, January, 1985, pp.56-61

[2.68] EISENBROWN B. (1988)
"Programmable Controllers Move to Systems Solutions", Manufacturing Engineering, January, 1988, pp.59-61

[2.69] PESSEN D.W. (1987)
"Using Programmable Controllers for Sequential Systems with Random Inputs", Proc Instn Mech Engrs, Vol.201, No.C4, pp.245-249

[2.70] LEUNG T.P., CHICK W.K. (1985)
"CAD for Pneumatic Circuit Design in Low Cost Automation", Proceedings of the IFAC/IFORS Symoposium, Beijing, People's Republic of China, 20-22 August, 1985, pp.237-240

[2.71] CHENG R.M.H., McKINNON G.M. (1974)
"A Simple Pneumatic Position Table", Design Engineering Conference, ASME, Design Engineering Division, 1974, pp.523-527

[2.72] DRAZAN P.J., JEFFERY M.F. (1976)
"Microprocessor Control and Pneumatic Drive of a Manipulating Arm", 3rd Conference on Industrial Robot Technology and 6th International Symposium on Industrial Robots, 24-26 March, 1976, Nottingham, England, Paper D2, pp.9-20

[2.73] DRAZAN P.J. (1983)
"Control of Robot Dynamics by Microcomputers", in "Robotic Technology", IEE Control Engineering Series 23, ed. PUGH A., Peregrinus, 1983, Ch.5, pp.38-51

[2.74] HARADA M., OYAMA O. (1984)
"Position Control with Pneumatic Piston and Microprocessor", Proceedings of the 9th Triennial World Congress, IFAC, Budapest, Hungary, 2-6 July, 1984, Vol.5, pp.2785-2790

[2.75] NORWOOD R.E. (1962)
"A Pneumatic Flapper Valve Study", Proc. 1st Int. Congress, IFAC, Moscow, 1962, pp.260-265

[2.76] HAYASHI S., MATSUI T., ITO T. (1975)
"Study of Flow and Thrust in Nozzle - Flapper Valves", Journal of Fluids Engineering, March, 1975, No. 75-FE-3, Vol.97, Trans of the ASME, pp.39-50

[2.77] PECKHAM R.G., BURROWS C.R. (1975)
"Static and Dynamic Torque Characteristics of a Pneumatic Flapper Valve", 4th International Fluid Power Symposium, 16-18 April, 1975, Sheffield, England, Paper E4, pp.61-75

[2.78] SCHWENZER R. (1984)
"Static and Dynamic Behaviour of State Controlled Pneumatic Drives", Oelhyd. and Pneum., Vol.28, Pt.3, 1984, pp.154-161 (in German)

[2.79] BACKE W. (1985)
"Application of Servo-pneumatic Drives for Flexible Robotics", Robotsysteme, pp.111-119, Vol.1, No.2, 1985 (in German) also "The Application of Servo-pneumatic Drives in Flexible Mechanical Handling Techniques", Robotics, Vol.2, No.1, March, 1986, pp.45-56

[2.80] THATCHER T.W., WESTON R.H., MOORE P.R., HARRISON R. (1985)
"Single Axis Controllers for Modular Workhandling Systems", Proceedings of IASTED International Symposium on Robotics and Automation, Lugano, Switzerland, June, 1985, pp.240-243

[2.81] WESTON R.H., MORGAN G. (1984)
"A New Family of Robot Modules and Their Industrial Application", IMechE Conf. on UK Robotics Research, Mechanical Engineering Publications, London, December, 1984

[2.82] HARRISON R., WESTON R.H., MOORE P.R., THATCHER T.W. (1985)
"The Industrial Application of Pneumatic Servo-Controlled Modular Robots", National Conference on Production Research, Nottingham, 9-11 September, 1985

[2.83] DINERSTEIN J. (1954)
"The Development of Valve Controlled Pneumatic Servomechanism", M.Sc. Thesis, Department of Electrical Engineering, M.I.T., Cambridge, Mass., U.S.A.

[2.84] REETHOF G. (1957)
"Analysis and Design of a Servomotor Operating on High-pressure Compressed Gas", Trans. of the ASME, May, 1957, pp.875-885

[2.85] KATO S., MARUI E., MATSUBAYASHI T., SUZUKI M. (1972)
"Some Considerations on Characteristics of Pneumatic Servo-mechanism", Bull. of JSME, Vol.15, Pt.80, February, 1972, pp.225-235

[2.86] MANNETJE J.J.'t (1981)
"Pneumatic Servo Design Method Improves System Bandwidth Twenty-fold", Control Engineering, June, 1981, pp.79-83

[2.87] SANDOZ D.J. (1984)
"A Survey of Computer Control", in "Real-time computer control", ed. BERNETT S., LINKENS D.A., IEE Control Engineering Series 24, Ch. 1, pp.1-17

[2.88] NGUYEN H.T., PACKNICKE E., ANDERS P. (1984)
"Servo-pneumatic Cylinder Drive for Positioning Purposes", Kolloqium, 1984, pp.137-157 (in German)

[2.89] MOORE P.R., WESTON R.H., THATCHER T.W. (1985)
"Compensation in Pneumatically Actuated Servo-Mechanisms", Trans. Instrumentation, Measurement and Control, July-September, 1985, Vol.7, Pt.4

[2.90] KERNIGHAN B.W., RITCHIE D.M. (1978)
"The C Programming Language", Bell Telephone Laboratories, Inc., Murray Hill, New Jersey, USA

[2.91] FREDERICK D.K. (1982)
"Software Summaries", Control Systems Magazine, IEEE, Vol.2, No.4, December, 1982, pp.37-44

[2.92] JACOBS O.L.R. (1985)
"Computer Aided Design of Control Systems in the United Kingdom", Proceedings of the 3rd IFAC/IFIP Symposium, Lyngby, Denmark, 31 July - 2 August, 1985, pp.75-80

[2.93] MARCOCCI L., SPELTA S. (1983)
"Computer Aided Modelling of Complex Processes: A Program Package", Proceedings of the IMACS/International Symposium, Nantes, France, 9-11 May, 1983, pp.61-66

[2.94] CHEN D.U., HUO H.Q., MA X.Q. (1985)
"Computer Aided Design of Hydraulic System", Proceedings of the IFAC/IFORS Symp., Beijing, People's Republic of China, 20-22 August, 1985, pp.233-236

[2.95] LEANEY P.G. (1982)
"Models for Use in the Design of Servo-drives", Supplementary Report to the Mechanical Engineering and Machine Tool Requirement Board, DoI, September, 1982

[3.1] WELLSTEAD P.E. (1979)
"Introduction to Physical System Modelling", Academic Press, Ch.7-8, pp.144-238

[3.2] EYKHOFF P. (1985)
"New Trends in Identification", Proceedings of the IFAC/IFORS Symp., Beijing, People's Republic of China, 20-22 August, 1985, pp.27-36

[3.3] McCLOY D. (1967-68)
"Graphical Analysis of the Step Response of Hydraulic Servomechanisms", Proc Instn Mech Engrs, Vol.182, Pt.1, No.12, 1967-68, pp.243-254

[3.4] McCLOY D., MARTIN H.R. (1973)
"Control of Fluid Power: Analysis and Design", Longman, 2/e, Ch.13-14, pp.185-273

[3.5] CLARKE D.W. (1973)
"Experimental Comparison of Identification Methods", United Kingdom Automation Council 5th Control Convention, Modelling and Simulation of Applied Control Systems, the Institute of Measurement and Control, University of Bath, 17-20 September, 1973, pp.1-9

[3.6] DRAZAN P.J., THOMAS P.B. (1978)
"Simulation of an Electro-pneumatic Manipulator System", 5th Int'l Fluid Power Symp., 13-15 September, 1978, pp.59-72

[3.7] PALM III W.V. (1986)
"Control Systems Engineering", John Wiley, 1986, Ch.1, pp.13-19

[3.8] MINORSKY N. (1922)
"Directional Stability and Automatically Steered Bodies", J. Am. Soc. Naval Engrs, Vol.34, Pt.2, May, 1922, pp.280-309

[3.9] HARPUR N.F. (1953)
"Some Design Considerations of Hydraulic Servos of Jack Type", Proc. Conf. Hydraulic Servo-mechanisms, Instn Mech Engrs, 1953

[3.10] SHEARER J.L. (1954)
"Dynamic Characteristics of Valve Controlled Hydraulic Servomotors", Trans. of the ASME, Aug, 1954 pp. 895-903

[3.11] RAUSCH R.G. (1959)
"Analysis of Valve Controlled Hydraulic Servo-mechanisms", Bell System Technical Journal, 38, 1959

[3.12] BELL R. (1970)
"The Performance of Electrohydraulic Cylinder Drives for Numerically Controlled Machine Tools", Ph.D. Thesis, UMIST, October, 1970

[3.13] WATTON J. (1984)
"The Generalised Response of Servovalve-Controlled, Single Rod, Linear Actuators and the Influence of Transmission Line Dynamics", Journal of Dynamic Systems, Measurement and Control, June, 1984, Vol.106, pp.157-162

[3.14] LIEPMANN H.W., ROSHKO A. (1957)
"Elements of Gasdynamics", John Wiley, 1957, Ch.8, pp.202-216

[3.15] BLACKBURN J.F., REETHOF G., SHEARER J.L. (1960)
"Fluid Power Control", MIT Press, Ch.15, pp.521-561

[3.16] MARIUZZO C., METO A.F.M., SOARES A.M.C., MANSOUR W.M. (1980)
"Analysis and Design of a Class of Pneumatic Positioning Servos", Sociedade Brasileira de Automatica, 16-19 September, 1980, pp.455-462

[3.17] ARAKI K. (1971)
"Compensation of a Force-Feedback Pneumatic Servo-valve", Trans. Soc. Instr. Control Eng., Vol.7., Pt.4, pp.366-375 (in Japanese)

[3.18] MARIUZZO C.L., METO A.F.M., SOARES A.M.C., MANSOUR W.M. (1980)
"Mathematical Models for Pneumatic Actuators", Congresso Brasileiro de Automatica, Rio de Janeiro, Brasil, pp.445-453

[3.19] BILLINGS S.A. (1984)
"Identification of Non-linear Systems", in "Nonlinear System Design", 1984, ed. BILLINGS S.A., GRAY J.O., OWEN D.H, Ch.2, pp.30-45, IEE Control Engineering Series 25

[3.20] PARKS P.C. (1984)
"Stability Criteria for Nonlinear Systems - A Survey", in "Non-linear System Design", ed. BILLINGS S.A., GRAY J.O., OWENS D.H., IEE Control Engineering Series 25, Ch.3, pp.30-45

[3.21] BOWNS D.E, ROLFE A.C. (1975)
"The Digital Computation of Pressures and Flows in Interconnected Fluid Volumes, Using Lumped Parameter Theory", 4th International Fluid Power Symposium, 16-18 April, 1975, Sheffield, England, Paper A1, pp.1-17

[3.22] IYENGAR S.K.R., FITCH E.C. (1975)
"A Systematic Approach to the Analysis of Complex Fluid Power Systems", 4th International Fluid Power Symposium, 16-18 April, 1975, Sheffield, England, Paper A2, pp.19-34

[3.23] DRANSFIELD P., STECKI J.S. (1974)
"Dynamic Modelling Techniques for Fluid Power Control Systems", 5th Australian Conference on Hydraulic and Fluid Mechanics, Christchurch, New Zealand, 9-13 December, 1974, pp.27-34

[3.24] ROSENBERG R.C., KARNOPP D.C. (1972)
"A Definition of the Bond graph Language", Journal of Dynamic Systems, Measurement and Control, Trans. of the ASME, September, 1972, pp. 179-182

[3.25] BOWNS D.E., ROLFE A.C. (1978)
"Computer Simulation as a First Step Towards Computer Aided Design of Fluid Power Systems", 5th Int'l Fluid Power Symp., 13-15 September, 1978, Durham, England, Paper A3, pp.29-45

[3.26] HULL S.R., BOWNS D.E. (1985)
"The Development of an Automatic Procedure for the Digital Simulation of Hydraulic Systems", Proc Instn Mech Engrs, Vol.199, No.B1, 1985, pp.51-57

[3.27] BACKE W., HOFFMANN W. (1981)
"DSH-Program System for Digital Simulation of Hydraulic Systems", 6th Int'l Fluid Power Symposium, 8-10 April, 1981, Cambridge, England, Paper C1, pp.95-114

[3.28] LEANEY P.G. (1986)
"The Modelling and Computer Aided Design of Hydraulic Servosystems", Ph.D. Thesis, 1986, Department of Manufacturing Engineering, Loughborough University of Technology

[3.29] TAN E.S.P., DRANSFIELD P. (1986)
"A Rotary Electropneumatic Servo-drive for Industrial Robots", 3rd Conference on Control Engineering, 12-14, May, 1986, Sydney, pp.1-5

[3.30] MO P.T. (1988)
"A New Technique in Pneumatic Servomechanism Modelling", 28 Nov - 2 Dec, 1988, Forum on Applications in Fluid Mechanics, Annual Meeting of the ASME, Chicago, USA

[3.31] SHEARER J.L. (1983)
"Digital Simulation of a Coulomb-Damped Hydraulic Servomechanism", Journal of Dynamic Systems, Measurement and Control, Trans. of the ASME, December, 1983, Vol.105, pp.215-221

[3.32] BENDER E., KOTSCHENREUTER P. (1980)
"Pneumatic Actuated Position Control System", Regelunstech Proax., Vol.22, Pt.9, September, 1980, pp.326-332, (in German) also "Position Control Loops with Pneumatic Actuators", Process Automation, pt.2, 1980, pp.85-90

[3.33] SCI Sub-Committee (SOFTWARE COUNCILS INC.) (1967)
"The SCi Continuous System Simulation Language (CSSL)",
Simulation, Simulation Councils, Inc, December, 1967,
pp.201-303

[3.34] LUCAS J.J., WAIT J.V. (1975)
"DARE P - a Portable CSSL-type Simulation Language",
Simulation, Simulation Councils, Inc, January, 1975,
pp.17-28

[3.35] KORN G.A. (1982)
"EARLY DESIRE: A Floating-point Equation Language
Simulation System for Minicomputer and Microcomputers",
Simulation, May, 1982, pp.151-159

[3.36] BARTHELMES M., BRESSLER P., BUND Z., GUTSCHOW K., HEEGER
J., LEMKE H.J. (1983)
"CATPAC: A Software Package for Computer aided Control
Engineering", Proceedings of the IMACS/Internation
Symposium, Nantes, France, 9-11 May, 1983, pp.73-78

[3.37] ATHERTON D.P. (1984)
"An Overview of Non-linear Systems Theory", in "Nonlinear
system Design", ed. BILLINGS S.A., GRAY J.O., OWENS D.H.,
IEE Control Engineering Series 25, Ch.1, pp.1-27

[3.38] CELLIER F.E. (1983)
"Simulation Software: Today and Tomorrow", Proceedings of
the IMACS/International Symposium, Nantes, France, 9-11
May, 1983, pp.3-19

[3.39] ARAKI M. (1985)
"Industrial Applications in Japan of Computer Aided
Design Packages for Control Systems", Proceedings of the
3rd IFAC/IFIP Symposium, Lyngby, Denmark, 31 July-2
August, 1985, pp.59-64

[3.40] BERNETT B. (1981)
"Communication Mode Simulation Package for Continuous and
Discrete Systems User's Manual", Control Systems Centre,
UMIST, 1981

[3.41] MAYERS D.F. (1961)
"Methods of Runge-Kutta Type", in "Numerical Solution of
Ordinary and Partial Differential Equations", ed. FOX L.,
1961, pp.16-27

[3.42] SUN MICROSYSTEMS INC. (1986)
"SunCore Reference Manual", Rev.G, February, 1986

[3.43] MO P.T. (1987)
"Compilation and Use of CMS-2 Package on Sun Workstations", Application Notes, Department of Manufacturing Engineering, Loughborough University of Technology, September, 1987

[3.44] EWINS D.J. (1986)
"Modal Testing: Theory and Practice", Research Studies Press, 1986, Ch.2, pp.19-86

[4.1] UNRUH D.R. (1972)
"A Standard Format for Mathematical Models of Fluid Power Systems", 28th National Conf. on Fluid Power, U.S.A., 13-15 September, 1972, pp.498-518

[4.2] FESTO DIDACTIC GmbH (1984)
"Pneumatic Application Examples", Application Notes, Festo Didactic GmbH, Postfach 6040, Ruiter Strasse 82, D-7300 Esslingen 1, West Germany

[4.3] MEIXNER H., KOBLER R. (1978)
"Introduction to Pneumatics", Esslingen, Festo Didactic GmbH, Ch.11, pp.183-199

[4.4] NORGREN MARTONAIR (1988)
"General Catalogue", Norgren Martonair Ltd., P.O. Box 22, Easter Avenue, Staffordshire WS13 6SB, UK, Form No. NMGCa 4/88

[4.5] NEUHAUS R. (1981)
"Electropneumatic Servo-drive with Closed Position Control", Oelhydraul. and Pneum., February, 1981, Vol.25, Pt.2, pp.120-125

[4.6] GOLDWATER M.H., FINCHAM A.E. (1981)
"Modelling of Gas Supply Systems", in "Modelling of Dynamical Systems", Vol.2, ed. NICHOLSON H., Peregrinus, IEE Control Engineering Series 13, pp.151-177

[4.7] CEBECI T., KELLER H.B. (1974)
"Flows in Ducts by Boundary-layer Theory", 5th Australian Conference on Hydraulics and Fluid Mechanics, Christchurch, New Zealand, 9-13 December, 1974, pp.538-545

[5.1] THATCHER T.W. (1983)
"Evaluation of KDRS Rig Fitted with Stepper Driven Servo-valve under Proportional Control", Internal Report, Department of Manufacturing Engineering, Loughborough University of Technology, June, 1983

[5.2] MARTONAIR LTD (1984)
"Modular Handling Unit", Publication No. S/1/143, Issue 1, 3/84

[5.3] THATCHER T.W. (1983)
"Martonair Designed Servo-amplifier - Mark 1 and 2", Internal Report, Department of Manufacturing Engineering, Loughborough University of Technology, April, 1983

[5.4] McLENNAN SERVO SUPPLIES LTD. (1982)
"92000 Series Digital Linear Actuators Specification", Product Catalogue, 982-12

[5.5] KUO B.C. (1974)
"Theory and Applications of Stepper Motors", West Publishing Co.

[5.6] COOKE J.R. (1988)
"Stepper Motors: Principles and Characteristics", Proc Instn Mech Engrs, Vol.202, No.D2, 1988, pp.111-117

[5.7] MOTOROLA INC. (1984)
"MVME110-1 Monoboard Microcomputer Users' Manual", 1984

[5.8] TEXAS INSTRUMENTS
"74LS2000 Advanced Information", 1984

[5.9] BURR-BROWN INC (1986)
"Burr-Brown Integrated Circuits Data Book", 1986, Section 5, pp.70-77, Section 6, pp.77-86, Section 7, pp.7-10

[5.10] MO P.T. (1988)
"Control Software for Pneumatic Servo-drive Analysis", Int'l Conf. on Computer Engineering and Education '88, Singapore, 24-25 October, 1988

[6.1] ZIEMER R.E., TRANTER W.H., FANWIN D.R. (1983)
"State Variable Techniques", in "Signals and Systems-Continuous and Discrete", MacMillan Ch.6, pp.256-267

[6.2] JEBAR H.S., LICHTAROWICZ L., ROYLANCE T.F. (1975)
"Thermodynamic Analysis of Charging Processes", 4th International Fluid Power Symposium, 16-18 April, 1975, Sheffield, England, Paper E1, pp.1-17

[6.3] SHEARER J.L. (1954)
"Continuous Control of Motion with Compressed Air", Sc.D. Thesis, Department of Mechanical Engineering, M.I.T., Cambridge, Mass., U.S.A.

[6.4] CUTLAND M.J. (1967)
"Response of a Pneumatic Servo-mechanism", MSc(Eng) Thesis, 1967, University of London

[6.5] BURROWS C.R. (1969)
"Non-linear Pneumatic Servo-mechanisms", Ph.D. Thesis, 1969, University of London

[6.6] BOWNS D.E., BALLARD R.L. (1972)
"Digital Computation for the Analysis of Pneumatic Actuator Systems", Proc Instn Mech Engrs, Vol.186, 1972, pp.881-889

[6.7] CHITTY A., LAMBERT T.H. (1976)
"Modelling a Loaded Two-way Pneumatic Actuator", Journal of Measurement and Control, Vol.9, 1976, pp.19-25

[6.8] BURROWS C.R. (1969)
"Effect of Position on the Stability of Pneumatic Servomechanism", Journal of Mechanical Engineering Science, Vol.11, No.6, 1969, pp.615-616

[6.9] SULLIVAN D.A. (1981)
"Historical Review of Real-fluid Isentropic Flow Models", Journal of Fluids Engineering, Trans. of the ASME, Vol.103, June, 1981, pp.258-267

[6.10] BLEVINS R.D. (1984)
"Applied Fluid Mechanics Handbook", Van Norstrand, 1984, Ch.6, pp.38-123

[6.11] EGLI E. (1937)
"The Leakage of Gases Through Narrow Channels", Journal of Applied Mechanics, Vol.59, June, 1937, pp.A-63 - A-67

[6.12] SHELL COMPANY OF HONG KONG LTD. (1987)
"Industrial and Automative Lubricants", 1987

[6.13] BOWNS D.E., BALLARD R.L., STILES L. (1973)
"The Effect of Seal Friction on the Dynamic Performance of Pneumatic Actuators", 3rd International Fluid Power Symposium, pp.29-48, Paper G3, 9-11 May, 1973, Turin, Italy

[6.14] CHIAPPULINI R. (1971)
"Friction and Its Effects on Linear Positional Hydraulic and Electro-hydraulic Servosystems", Annals of the C.I.R.P., Vol.XVIV, 1971, pp.125-129

[6.15] HIBBLER R.C. (1983)
"Engineering Mechanics - Statics", McMillan, Ch.8, pp.283-289

[6.16] SHEARER J.L. (1957)
"Nonlinear Analog Study of a High Pressure Pneumatic Servomechanism", Trans. of the ASME, April, 1957, Vol.79, No.3, pp.465-472

[6.17] BOTTING L.R., EYNON G.T., FOSTER K. (1969-70)
"The Response of a High Pressure Pneumatic Servo-mechanism to Step and Sinewave Inputs", Proc Instn Mech Engrs, Automatic Control Group, Vol.184, Pt.1, No.54, 1970, pp.993-1011

[6.18] FIROOZIAN R., FOSTER K. (1983)
"The Comparison of Performance of Servo Feed-drive Systems", Proc Instn Mech Engrs, C301/83, 1983, pp.41-50

[6.19] THATCHER T.W. (1983)
"Optimisation of Dither Frequency and Amplitude", Internal Report, 1983, Department of Manufacturing Engineering, Loughborough University of Technology

[6.20] BELL R., de PENNINGTON A., t'MANNETTJE J.J. (1974)
"The Modelling of Electrohydraulic Control Valves and Its Influence on the Design of Electrohydraulic Drives", Journal of Mechanical Engineering Science, Vol.16, No.3, 1974

[6.21] HATTORI M., ANNO T. (1980)
"Effect of Dither on Non-linear Characteristics of a Position Control System", Electrical Engineering in Japan, Vol.100, No.4, 1980, pp.143-149

[6.22] LOGAN E., LOUIS R.J. (1976)
"Experimental Investigation of Flow Induced Forces in Pneumatic Spool Valves", Journal of Dynamic Systems, Measurement and Control (Tech Briefs), Trans. of the ASME, September, 1976, pp.316-318

[6.23] LEE S.Y., BLACKBURN J.F. (1952)
"Contribution to Hydraulic Control:
1 - Steady State Axial Forces on Control-valve Pistons
2 - Transient-flow Forces and Valve Instability"
Trans. of the ASME, August, 1952, pp.1005-1016

[6.24] STONE K.L. (1974)
"The Effect of Servovalve Backlash on Servo System Stability", Proceedings, National Conference on Fluid Power, 1974, pp.139-152

[6.25] ARAFA H.A., RIZK M.(1987)
"Identification and Modelling of Some Electro-hydraulic Servo-valve Non-linearities", Proc. Instn Mech Engrs, Vol.201, No.C2, pp.137-144

[6.26] ANDERSEN B.W. (1976)
"The Analysis and Design of Pneumatic Systems", John Wiley, Ch.3, pp.93-95

[6.27] SHEARER J.L (1980)
"The Effects of Radial Clearance, Rounded Corners, and Underlap on Servovalve Characteristics", Proc Joint Automatic Control Group, ASME, 1980

[6.28] ARAKI K. (1981)
"Effects of Valve Configuration on a Pneumatic Servo", 6th Int'l Fluid Power Symposium, 8-10 April, 1981, Cambridge, England, Paper F2, pp.271-291

[6.29] BOWNS D.E., BALLARD R.L. (1975)
"Some Aspects of the Dynamic Behaviour of Pneumatic Actuators" 4th International Fluid Power Symposium, 16-18 April, 1975, Sheffield, England, Paper A3, pp.29-45

[6.30] SHEARER J.L. (1956)
"Study of Pneumatic Processes in the Continuous Control of Motion with Compressed Air I & II", Trans. of the ASME, February, 1956, pp.233-249

[6.31] BURROWS C.R. (1972)
"Fluid Power Servomechanisms", Van Nostrand Reinhold, Ch.5, pp.132-154

[6.32] NAZARCZUK K. (1979)
"Modelling of Pneumatic Drives", 5th World Congress on Theory of Machines and Machines, 8-13 July, 1979, New York, ASME, pp.1258-1261

[6.33] EUN T., CHO Y.J., CHO Y.S. (1982)
"Stability and Positioning Accuracy of a Pneumatic On-off Servomechanism", American Control Conference, 14-16 June, 1982, Arlington, USA, Vol. 3, Paper WP9-3:30, pp.1189-1194

[6.34] ARAKI K. (1979)
"Frequency Response of a Pneumatic Valve Controlled Cylinder with an Uneven-undevelop Four-way Valve, Part I and II", Trans. of the Soc. of Instr. Control Engrs, Japan, Vol.10, No.1, pp.57-63 and pp.41-47 (in Japanese)

[6.35] SHAPIRO A.H. (1953)
"The Dynamics and Thermodynamics of Compressible Fluid Flow", Ronald Press, 1953, Ch.4, pp.73-111

[6.36] SANVILLE F.E (1971)
"A New Method of Specifying the Flow Capacity of Pneumatic Fluid Power Valves", 2nd Int'l Fluid Power Symposium, 4-7 January, 1971, BHRA, Cranfield, England, Paper D3, pp.37-47

[6.37] ZALMANZON L.A., IVANOV N.N., LIMONOVA M.E. (1968)
"Theoretical and Experimental Investigation of Fluidic Elements", IFAC Symposium on Fluidics, 4-8 November, 1968, London, Paper A4

[6.38] KAMAL W.A., ODUKWE A.O., LIVESEY J.L. (1974)
"The Effects of 'Controlled' Inlet Conditions on the Performance of Conical Diffusers Preceeded by Normal Shock Boundary Layer Interaction", 5th Australian Conference on Hydraulics and Fluid Mechanics, 9-13 December, 1974, Christchurch, New Zealand, pp.98-107

[6.39] KAMAL W.A., ODUKWE A.O., LIVESEY J.L. (1974)
"A Perfmance Predication Method for High Subsonic Inlet Mach Number Conical Diffusers", 5th Australian Conference on Hydraulics and Fluid Mechanics, 9-13 December, 1974, Christchurch, New Zealand, pp.67-73

[6.40] HUBER R.E. (1965)
"Simplifed Analysis of a Gas Powered Servo Actuator", Proc. Aerospace Fluid Power Systems and Equipment Conference, SAE, 1965, pp.346-360

[6.41] MO P.T. (1989)
"Analysis of Compressed Air Flow Through Spool Valve", Proc Instn Mech Engrs, Vol.203, Paper C02788, accepted for publication

[6.42] NUMERICAL ALGORITHM GROUP (1976)
"C05-Zeros of One or More Transcendental Equations" NAGFLIB:1331/384, Mk5, January, 1976, pp.1-9

[6.43] INTERNATIONAL MATHEMATICAL AND SCIENCE LIBRARY (IMSL) (1982)
"IMSL Routine Manual - ZSPOW", June, 1982, pp.(ZSPOW)1-3

[6.44] POWELL J.D. (1970)
"A Hybird Method for Non-linear Equation", in "Numerical Methods for Non-linear Algebraic Equations", ed. RABINOWITZ P., Gordon and Breach, 1970, Ch.6-7, pp.87-161

[6.45] SAAD M.A. (1985)
"Compressible Fluid Flow", Ch.5, pp.191-223

[6.46] STREETER V.L. (1971)
"Fluid Mechanics", 5/e, McGraw Hill, 1971, pp.341-344

[6.47] KUNKLE J.S., WILSON S.D., COTA R.A. (1969)
"Compressed Gas Handbook", NASA, 1969, Ch.8, pp.151-179

[6.48] WARD SMITH A.J. (1971)
"Pressure Losses in Ducted Flows", Butterworths, Pt.3, pp.29-84

[6.49] ANDERSON J.D. JR. (1982)
"Modern Compressible Flow", McGraw Hill, Ch.3, pp.39-81

[7.1] TSAI D.H., SLAWSKY M.M. (1957)
"Determination and Correlation of Flow Capacities of Pneumatic Components", National Bureau of Standards Circular 588, October, 1957

[7.2] PERRY J.A.Jr. (1949)
"Critical Flow Through Sharp-Edged Orifices", Trans. of the ASME, October, 1949, pp.757-764

[7.3] STENNING A.H. (1954)
"An Experimental Study of Two-Dimensional Gas Flow Through Valve Type Orifice", The Annual Meeting of the ASME, 28 Nov - 3 Dec, 1954, New York, Paper No. 54-A-45

[7.4] LOGAN E., LOUIS R.J. (1974)
"Finding Accurate Discharge Coefficients for Pneumatic Spool Valves", Machine Design (Tech Briefs), September, 1974, Vol.46, No.21, pp.140-141

[7.5] COMPRESSED GAS ASSOCIATION INC. (1981)
"Handbook of Compressed Gases", Van Nostrand, 2nd edition, 1981, pp.255-258

[7.6] KAYE G.W.C., LABY T.H. (1973)
"Tables of Physical and Chemical Constants", 14th edition, Longman, Section 1.8, pp.101-124

[7.7] SIGNAL TECHNOLOGY INC. (1985)
"Interative Laboratory System Modules 1 & 2 V5.0 for the IBM-PC User's Guide", Reference Manual, December, 1985

[7.8] BENDAT J.S. (1974)
"Foundamental of Time Series Analysis", Paper presented at a series of seminars held in USA and Europe, 1974, sponsored by Time/Data, a GR Company

[7.9] BURROWS C.R., WEBB C.R. (1970)
"Further Study of a Low-Pressure On-off Pneumatic Servomechanism", Proc Instn Mech Engrs, Automatic Control Group, Vol.184, Pt.1, No.45, 1970, pp.849-857

[8.1] PU J. (1988)
"Advancements in the Programmable Motion Control of Pneumatic Drives for Robots and Other Flexible Machines", Ph.D. Thesis, 1988, Department of Manufacturing Engineering, Loughborough University of Technology

[8.2] PU J. (1988)
"Motion Control of Pneumatic Drives", Microprocessors and Microsystems, Vol.12, No.7, September, 1988, pp.373-382

[9.1] BURROWS C.R., WEBB C.R. (1967-68)
"Simulation of an On-off Pneumatic Servomechanism", Proc Instn Mechn Engrs, Vol.182, Pt.1, No.29, pp.631-642

[9.2] WESTON R.H., MOORE P.R., THATCHER T.W., MORGAN G. (1984) "Computer Controlled Pneumatic Servo-Drives", Proc Instn Mech Engrs, Pt.B, December, Vol.198B, No.14, pp.175-281

[9.3] CLARKE D.W. (1984) "Self tuning controller design and implementation", in "Real-time Computer Control", ed. BERNETT S., LINKENS D.A., IEE Control Engineering Series 24, Ch.3, pp.44-73

[9.4] ASTROM K.J. (1980) "A Robust Sampled Regulator for Stable Systems with Monotone Step Responses", Automatica, IFAC, Vol.16, 1980, pp.313-315

[9.5] PU J., WESTON R.H. (1988) "A New Generation of Pneumatic Servos for Industrial Robots", Robotica, August/September, 1988

[9.6] PU J., WESTON R.H. (1988) "Contouring with Pneumatic Servo Driven Industrial Robots", IEE Control Engineering Series 36, "Robot Control: Theory and Applications", Ch.14, pp.125-139

[9.7] MOORE G. (1986) "Manufacturing Automation Protocol - Mapping the Factory of the Future", Electronics and Power, IEE, April, 1986, pp.269-272